

043
RAT
15268

**GEOCHRONOLOGICAL STUDIES OF MALANI
VOLCANICS AND ASSOCIATED IGNEOUS
ROCKS OF SOUTHWEST RAJASTHAN, INDIA:
IMPLICATIONS TO CRUSTAL EVOLUTION**

**PLEASE KEEP ME CLEAN
ALSO
DO NOT DEFACE
OR MUTILATE ME**

SHAKTI SINGH RATHORE

Thesis submitted to
The Maharaja Sayajirao University of Baroda
for the Degree of

**Doctor of Philosophy
in
GEOLOGY**

पुस्तकालय THE LIBRARY
भौतिक अनुसंधान प्रयोगशाला
PHYSICAL RESEARCH LABORATORY
नवरांगपुरा, अहमदाबाद - 380009.
NAVBRANGPURA, AHMEDABAD-380009.
भारत/INDIA

July, 1994
Physical Research Laboratory
Ahmedabad - 380009, INDIA

043



B15268

043
RAT
15268

*Dedicated to
my parents and
fond memories
of my late
grand father*

CERTIFICATE

This is to certify that the thesis incorporates the results of independent investigations carried out by the candidate himself and have at no time been submitted for any other degree or diploma.



(Shakti Singh Rathore)

Candidate



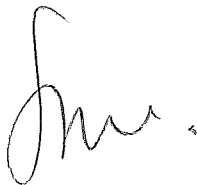
(Dr. T. R. Venkatesan)

Guide



(Prof. S. J. Desai)

Co-Guide



Prof. S. J. Desai

Head, Deptt. of Geology

M. S. University of Baroda

CONTENTS

PAGE NO.

BRIEF OUTLINE OF THE THESIS	iii
ACKNOWLEDGEMENTS	vii
LIST OF FIGURES	ix
LIST OF TABLES	xiii
CHAPTER 1. INTRODUCTION	1
CHAPTER 2. DESCRIPTION OF DIFFERENT ASSOCIATIONS OF MALANI IGNEOUS PROVINCE	12
2.1. Association I (Malani Volcanics)	12
2.2. Association II (Granites and Associated Volcanics)	20
2.3. Association III (Tavidar Volcanics)	23
2.4. Association IV (Mundwara Alkali Igneous Complex)	27
CHAPTER 3. EXPERIMENTAL TECHNIQUES	32
3.1. Potassium-Argon dating	32
3.1.1. <i>Principle</i>	32
3.1.2. <i>Age Equation</i>	35
3.2. ^{40}Ar - ^{39}Ar Dating	35
3.2.1. <i>Principle</i>	35
3.2.2. <i>Decay Factor</i>	40
3.2.3. <i>Experimental Details</i>	41
3.2.3.A. <i>Sample Preparation for Irradiation</i>	41
3.2.3.B. <i>Irradiation of Samples</i>	42
3.2.3.C. <i>Extraction and Purification of Argon</i>	43
3.3. Rubidium-Strontium Dating	51
3.3.1. <i>Principle</i>	51
3.3.2. <i>Rock Crushing</i>	54
3.3.3. <i>Rb-Sr Isotopic Studies</i>	54

3.3.3.A. Isotope Dilution	55
3.3.3.B. Ion Exchange Chromatography	56
3.3.4. Mass Spectrometry	56
3.3.5. X-ray Fluorescence Studies	59
CHAPTER 4. RESULTS AND DISCUSSION	60
4.1. Introduction	60
4.2. Association I (Malani Volcanics)	60
4.2.1. ^{40}Ar - ^{39}Ar Studies	61
4.2.2. Rb-Sr Studies	70
4.2.2.A. Basalt-Andesite-Dacite-Rhyolite Sequence	70
4.2.2.B. Ultrapotassic Rhyolites	75
4.3. Association II (Granites and Associated Volcanics)	78
4.3.1. ^{40}Ar - ^{39}Ar Studies	78
4.3.2. Rb-Sr Studies	84
4.3.2.A. Jalore Granites (Peraluminous Granites)	84
4.3.2.B. Siwana Granites (Peralkaline Granites)	87
4.3.2.C. Peralkaline Volcanics	90
4.3.2.D. Outer Rhyolites	90
4.4. Association III (Tavidar Volcanics)	95
4.4.1. K-Ar Studies	95
4.4.2. ^{40}Ar - ^{39}Ar Studies	97
4.4.3. Sr Isotopic Data	128
4.5. Association IV (Mundwara Alkali Igneous Complex)	132
4.5.1. ^{40}Ar - ^{39}Ar Studies	132
4.5.1.A. Musala Hill	132
4.5.1.B. Mer Hill	143
4.5.1.C. Toa Hill	143
4.5.2. Sr Isotopic Data	152
CHAPTER 5. SUMMARY AND CONCLUSIONS	156
REFERENCES	163

BRIEF OUTLINE OF THE THESIS

The geology of Rajasthan illustrates a classical example of rocks ranging in ages from the earliest crustal component (ca. 3300 Ma) to the recent one. The Precambrian rocks of Rajasthan evolved through three major orogenic cycles namely the Banded Gneissic Complex, the Aravalli Supergroup and the Delhi Supergroup. The Malani igneous province (*MIP*), representing the youngest Proterozoic tectonomagmatic event in southwest Rajasthan, has been suspected in recent times to represent a single magmatic cycle based on their geochemical characteristics.

This thesis describes detailed geochronological studies, of different rock units from *MIP* of southwest Rajasthan, India, using K-Ar, ^{40}Ar - ^{39}Ar and Rb-Sr dating techniques. About 20 whole rock samples were analyzed for ^{40}Ar - ^{39}Ar studies and 30 samples for Rb-Sr studies. Additionally about 10 samples were analyzed for K-Ar and 15 samples for their Sr isotopic studies.

The geochronological findings provide a new interpretation and an insight into the evolution of *MIP* of southwest Rajasthan. The description of various rock types, their geological set up, and the geochronological studies of these rocks of the *MIP* are elaborated in five chapters of the thesis. A brief summary of each chapter is given below:

Chapter I describes the regional framework of Precambrian geology of Rajasthan with specific reference to *the MIP* and objective of the thesis. The province covers an area of about 50,000 sq. km in southwest Rajasthan. The important rock types of the province are rhyolites and granites with minor occurrences of basic, intermediate, acidic and alkaline volcanics and their plutonic equivalents. The concept of *MIP* representing a single late Proterozoic tectonomagmatic event has been belied by the detailed geochemical studies carried out from different parts of the province during the last one decade by various workers. However, no chronological informations were available. The present study, therefore, was undertaken to provide precise time constraints to the various geochemically distinct associations, using K-Ar, ^{40}Ar - ^{39}Ar and Rb-Sr systematics, in order to construct an evolutionary model for the *MIP* of southwest Rajasthan.

Chapter 2 has description of different associations which were emerged out after detailed petrographic and geochemical work carried out from different parts of the *MIP* by various workers.

Chapter 3 deals with the experimental techniques employed during the course of present work. The chapter is divided into three parts. In the first two parts K-Ar and ^{40}Ar - ^{39}Ar dating techniques and their experimental details have been discussed. The third part outlines briefly the Rb-Sr dating method and the procedures for sample crushing, chemical processes for separation of Rb and Sr, mass spectrometric work for Rb and Sr isotopic analysis and XRF analysis. The XRF studies, of only a few samples, were carried out at Wadia Institute of Himalayan Geology (WIHG), Dehradun and the Rb and Sr isotopic studies were carried out at KDMIPE, ONGC, Dehradun in addition to the analyses done at PRL, Ahmedabad. The scheme of using different dating techniques was as follows:

- (i) K-Ar dating technique employed during the initial course of this work for preliminary screening of the samples.
- (ii) ^{40}Ar - ^{39}Ar dating technique for dating of younger magmatic events of mildly alkaline rocks of Tavidar and the alkaline and hyperalkaline rocks of Mundwara alkali igneous complex. The technique was also applied for dating of older rhyolites and granites from Pali and Jalore, respectively.

The samples for ^{40}Ar - ^{39}Ar studies were irradiated, for 2-3 weeks, in APSARA reactor of Bhabha Atomic Research Center (BARC), Bombay. The horizontal fluence variation, as measured by ^{50}CO activity relative to the monitor sample, was not more than 5.5%. ^{40}Ar system blanks are comparable with blanks in similar extraction systems used in other laboratories.

- (iii) Finally Rb-Sr method for dating of (a) Malani volcanics, including ultrapotassic rhyolites from Diri, Gurapratap Singh and Manihari, (b) Peraluminous (normal) and peralkaline granites from Jalore and Siwana, respectively and, (c) Associated normal and peralkaline rhyolites from Siwana ring complex.

Based on replicate analyses of calibration mixtures and a few rock samples, the errors in the mass spectrometric determinations of ^{87}Rb and ^{86}Sr are estimated to be within $\pm 0.5\%$ leading to a random error of not more than $\pm 1\%$ for their ratios and

in general 0.008% for $^{87}\text{Sr}/^{86}\text{Sr}$. ^{87}Rb and ^{86}Sr concentrations are calculated by isotope dilution technique. The $^{87}\text{Sr}/^{86}\text{Sr}$ ratios are corrected for mass fractionation assuming $^{86}\text{Sr}/^{88}\text{Sr} = 0.1194$ in the sample. The blank contribution was negligible compared to the Rb and Sr concentrations of the samples studied. The analysis of the NBS 987 standard, made during the course of this study at KDMIPE, Dehradun, gave a mean value of 0.710219 ± 0.000058 . The errors quoted in this thesis are at 2σ level.

Chapter 4 includes the Results and Discussion. The samples analyzed by Rb-Sr method have been plotted on Sr evolution diagrams to calculate the age of isotopic equilibration of a given set of related samples and the Sr isotopic composition at equilibration using the two-error least-square regression method. The samples analyzed by ^{40}Ar - ^{39}Ar method have been plotted on age spectrum diagrams as well as correlation or isochron diagrams to appraise their formation ages as well as post thermal disturbances, if any. The whole rock Rb-Sr ages illustrate distinct magmatic events at about 780, 730, 700, and 670 Ma ago. Additionally the older rocks have suffered a thermal disturbance between 500-550 Ma ago as revealed by ^{40}Ar - ^{39}Ar spectra. The region has since then, remained tectonically undisturbed until younger magmatic events which took place between 70 to 64 Ma ago as indicated by ^{40}Ar - ^{39}Ar studies of Tavidar volcanics and Mundwara igneous complex.

The data discussed provides a framework for the establishment of a reliable geochronology of the area. The major new findings are:

- (i) *The Malani igneous province of southwest Rajasthan does not represent a single magmatic event as hitherto believed and instead represents a polyphase igneous activity.*
- (ii) *Basalt-andesite-dacite-rhyolite association of Pali district are the oldest in the Malani province. These rocks were formed about 780 Ma ago from the magma generated in lower crust (excluding basalts). The basalts, though contemporary to the other associated felsic volcanics, have different source and presumably have come from much deeper level in the mantle.*
- (iii) *The Jalore and Siwana granites represent two different magmatic events and were emplaced at about 730 and 700 Ma ago, respectively. The initial Sr ratios are indistinguishable but indicate derivation of the magma from the lower crust. Further, the Siwana granites and associated peralkaline rhyolites*

(pantellerites) are coeval and cogenetic.

- (iv) *The outer rhyolites exposed south of the Siwana ring structure represent the youngest activity at Siwana about 670 Ma ago. These rocks have a very high initial $^{87}\text{Sr}/^{86}\text{Sr}$ ratio of 0.7110 due to incorporation of radiogenic ^{87}Sr in the residual magma.*
- (v) *The ultrapotassic rhyolites exposed at Manihari of Pali district have similarity in the age and initial Sr ratio with those of the outer rhyolites of Siwana, suggesting possible derivation of these rocks from the same residual magma.*
- (vi) *^{40}Ar - ^{39}Ar studies of basalt, dacite and rhyolite from Diri and Gurapratap Singh as well as of Jalore granites have indicated the existence of a thermal event around 500-550 Ma ago.*
- (vii) *^{40}Ar - ^{39}Ar studies of mildly alkaline rocks of Tavidar have indicated a span of 2 Ma from 66 to 64 Ma for the differentiated rocks, ranging in composition from andesite to potassic rhyolites. Less voluminous basic rocks (hawaiites) are contemporary to the mildly alkaline rocks but have low initial Sr ratio of 0.70441 as compared to an average of 0.70525 for the latter and indicate derivation of the magmas at different levels in the mantle.*
- (viii) *At Mundwara, the igneous activity started around 70 Ma and culminated about 64 Ma ago. The average initial Sr ratio of the complex is 0.70457, suggesting an upper mantle origin of the magma.*

Chapter 5 presents the conclusions arrived at based on the present studies and scope for future work.

ACKNOWLEDGEMENTS

I am greatly indebted to Dr. T. R. Venkatesan for introducing me to the field of geochronology and for his careful and patient guidance throughout the course of this work. I am also obliged to him for critically going through the manuscript of the thesis and making several useful suggestions. I am thankful to Prof. S. J. Desai for his constant encouragement and inspiration.

I am extremely grateful to Prof. R. K. Srivastava of Department of Geology, Udaipur for suggesting this problem, guidance in the field work as well as providing about half of the samples and several useful discussions.

I have had the good fortune to work with a number of colleagues at PRL who have helped me in numerous ways. I wish to record my sincere thanks to Dr. J. R. Trivedi who analyzed a few samples for Rb-Sr studies and to Mrs. Rashmi Jadeja, who helped me in data reduction for Ar-Ar studies. I thank Dr. Kanchan Pande for several suggestions and useful discussions which improved the thesis. Other senior members of Earth Sciences and Solar System Division, Profs. N. Bhandari, B. L. K. Somayajulu, S. Krishnaswami and Drs. S. V. S. Murty, J. N. Goswami, S. K. Bhattacharya, A. K. Singhvi, R. Ramesh, R. K. Pant, P. N. Shukla, M. M. Sarin and S. Kusumgar have always extended their assistance and encouragement. Mr Kurup and Mr Sivasankaran did excellent glass blowing work. I sincerely thank them all.

It is my pleasure to thank Prof. K. Gopalan of National Geophysical Research Institute, Hyderabad and Prof. K. K. Sharma of Wadia Institute of Himalayan Geology, Dehradun for their constructive suggestions during occasional discussions with them.

I enjoyed very much the close friendship of Gufran and Kotlia. The discussions with Shwetketu had always been inspiring and scintillating. Company of Bhusan, Naveen, Padia, Mathew, Anjan, Sarkar, Maqbool, Seema, Sarangi, Janardan, Tripathi, Birendra, Subramanian, Vijju, Supriya, Rengarajan, Ganguli, Yadav, Manohar Lal, Paulin, Nirjhari, Jyoti, Mohapatra, Clement and many others who are now no more in PRL as well as other hostellers had always been cheerful. Ravi and Rashmi helped me a lot while finalizing the thesis. Mr A. P. Gohil and his family always provided a very homely

environment. Mr D. R. Ranpura had ever been ready for help. I owe special thanks to them.

My sincere thanks are also due to Mrs. Barucha, Mrs Ghiya, Mrs. Patil and other staff members of the Library for their cooperation.

I am grateful to Prof. R. K. Varma, Director, PRL for the permission to continue my Ph. D. experiment work, even after leaving the institute. I am also thankful to ONGC management for the permission to continue the Ph. D. work. Part of this work was carried out at KDM Institute of Petroleum Exploration (KDMIPE), ONGC, Dehradun where I am presently posted. I am extremely thankful to Dr. S. K. Biswas, former Director, KDMIPE for getting my posting at KDMIPE and the permission to carry out Rb-Sr work at Geochronology Laboratory of the institute. I express my deep sense of gratitude to Mr. Kuldeep Chandra, Head, KDMIPE, Dr. Jagdish Pandey (GM, Geology), Shri K. N. Mishra (DGM, Chemistry) and Mrs. N. J. Thomas (Chief Chemist) for their sustained encouragement and support and to Shri N. K. Dutta (DGM, Geology) for providing ample freedom to carry out work at PRL during my short tenure at Ahmedabad project.

I am specially thankful to Dr. B. N. Prabhu for painstakingly going through the first draft which has substantially improved the thesis and to Dr. R. R. Singh for his constant encouragement to complete the work. I thank Dr. (Mrs). P. Rathi, Mrs. Minaxi Bansal, Dr. A. R. Vijan, S. Prasad, Pankaj and other members of Geochronology Laboratory, KDMIPE for their cheerful company and succor as and when needed.

I acknowledge the help received from Kakkad and Nambiar in neatly typing and finalizing the thesis.

I am extremely grateful to my wife Ichraj who has been the source of inspiration in all these agonizing years, and for all her involvement in my work in innumerable ways. My son master Vishal provided very tranquil environment at home by abstaining from his frolicsome activities during writing of the thesis.

Finally I wish to thank my parents and other family members for their encouragement all these years.

Shakti Singh Rathore

LIST OF FIGURES

	PAGE NO.
Fig. 1.1. Geological map of Rajasthan.	2
Fig. 1.2. Geological map of Malani igneous province, Rajasthan.	4
Fig. 1.3. Alk - SiO ₂ diagram of various rocks from the Malani igneous province.	7
Fig. 1.4. FeO - Al ₂ O ₃ +CaO diagram of rhyolitic rocks from Malani igneous province.	8
Fig. 1.5. Pre-Quaternary interpretative geological map of southwest Rajasthan.	10
Fig. 2.1. Geological map of felsic volcanics from Gurapratap Singh and Dir, Pali district, Rajasthan.	13
Fig. 2.2. Harker diagrams of Gurapratap Singh and Dir volcanics.	14
Fig. 2.3. Plot of normative Q-Or-Ab-H ₂ O of Gurapratap Singh and Dir volcanics.	16
Fig. 2.4. Variation of Rb, Sr and Ba with progressive differentiation in the felsic volcanics of Gurapratap Singh and Dir.	17
Fig. 2.5. Variation of Zn, Cr, Li, Ni and Co with progressive differentiation in the felsic volcanics of Gurapratap Singh and Dir.	18
Fig. 2.6. Variation in Ni/Co, Fe/Zn and Mg/Li with progressive differentiation in the felsic volcanics of Gurapratap Singh and Dir.	19
Fig. 2.7. Geological map of Siwana ring structure, Barmer district, Rajasthan.	21
Fig. 2.8. Geological map of Tavidar volcanics, Jalore district, Rajasthan.	24
Fig. 2.9. The Deccan volcanic province showing the distribution of plugs and alkaline intrusions.	28

Fig. 2.10.	Geological map of Mundwara alkali igneous complex, Rajasthan.	29
Fig. 3.1.	Decay scheme diagram for the branched decay of $^{40}\text{K}_{19}$ to $^{40}\text{Ar}_{18}$ by electron capture and by positron emission and to $^{40}\text{Ca}_{20}$ by emission of negative betaparticles.	33
Fig. 3.2.	Schematic of the complete mass spectrometer, gas extraction - purification system.	44
Fig. 3.3.	Section through gas extraction furnace and purifi- cation line.	45
Fig. 3.4.	Middle section of the S-S block with only one valve assembly shown.	46
Fig. 3.5.	Typical argon spectrum.	49
Fig. 4.1.	^{40}Ar - ^{39}Ar age spectrum for Dirí Basalt (D/88).	64
Fig. 4.2.	^{40}Ar - ^{39}Ar age spectrum for Dirí Dacite (D/25).	66
Fig. 4.3.	^{40}Ar - ^{39}Ar age spectrum for Dirí Rhyolite (D/174).	68
Fig. 4.4.	Rb-Sr conventional isochron diagram for Basalt-Andesite- Dacite-Rhyolite association from Dirí and Gurapratap Singh.	72
Fig. 4.5.	Rb-Sr best isochron diagram for Basalt-Andesite- Dacite-Rhyolite association from Dirí and Gurapratap Singh.	74
Fig. 4.6.	Rb-Sr conventional isochron diagram for Ultrapotassic Rhyolites from Dirí and Gurapratap Singh.	77
Fig. 4.7.	^{40}Ar - ^{39}Ar age spectrum for Jalore Granite (JR 86/15).	81
Fig. 4.8.	^{40}Ar - ^{39}Ar age spectrum for Jalore Granite (JR 86/17).	83
Fig. 4.9.	Rb-Sr conventional isochron diagram for Jalore Granite.	86
Fig. 4.10.	Rb-Sr conventional isochron diagram for Siwana Granite.	89
Fig. 4.11.	Rb-Sr conventional pooled isochron diagram for Peralkaline Granites and Peralkaline Volcanics from Siwana.	91
Fig. 4.12.	Rb-Sr conventional isochron diagram for Outer Rhyolites from south of Siwana.	93

Fig. 4.13.	Rb-Sr conventional pooled isochron diagram for Outer and Ultrapotassic Rhyolites.	94
Fig. 4.14.	^{40}Ar - ^{39}Ar age spectrum for Tavidar Andesite (VA/181).	100
Fig. 4.15.	^{40}Ar - ^{39}Ar age spectrum for Tavidar Andesite (K/67).	103
Fig. 4.16.	$^{40}\text{Ar}/^{36}\text{Ar}$ vs. $^{39}\text{Ar}/^{36}\text{Ar}$ isochron plot for Tavidar Andesite (VA/181).	104
Fig. 4.17.	$^{40}\text{Ar}/^{36}\text{Ar}$ vs. $^{39}\text{Ar}/^{36}\text{Ar}$ isochron plot for Tavidar Andesite (K/67).	105
Fig. 4.18.	^{40}Ar - ^{39}Ar age spectrum for Tavidar Trachyte (VA/58).	107
Fig. 4.19.	^{40}Ar - ^{39}Ar age spectrum for Tavidar Trachyte (K/30).	109
Fig. 4.20.	$^{40}\text{Ar}/^{36}\text{Ar}$ vs. $^{39}\text{Ar}/^{36}\text{Ar}$ isochron plot for Tavidar Trachyte (VA/58).	110
Fig. 4.21.	$^{40}\text{Ar}/^{36}\text{Ar}$ vs. $^{39}\text{Ar}/^{36}\text{Ar}$ isochron plot for Tavidar Trachyte (K/30).	111
Fig. 4.22.	^{40}Ar - ^{39}Ar age spectrum for Tavidar Rhyolite (VA/183).	115
Fig. 4.23.	$^{40}\text{Ar}/^{36}\text{Ar}$ vs. $^{39}\text{Ar}/^{36}\text{Ar}$ isochron plot for Tavidar Rhyolite (VA/183).	116
Fig. 4.24.	^{40}Ar - ^{39}Ar age spectrum for Tavidar Potassic Rhyolite (VA/168).	119
Fig. 4.25.	$^{40}\text{Ar}/^{36}\text{Ar}$ vs. $^{39}\text{Ar}/^{36}\text{Ar}$ isochron plot for Tavidar Potassic Rhyolite (VA/168).	120
Fig. 4.26.	^{40}Ar - ^{39}Ar age spectrum for Tavidar Hawaiite (VA/119).	122
Fig. 4.27.	^{40}Ar - ^{39}Ar age spectrum for Tavidar Hawaiite (K/69A).	124
Fig. 4.28.	$^{40}\text{Ar}/^{36}\text{Ar}$ vs. $^{39}\text{Ar}/^{36}\text{Ar}$ isochron plot for Tavidar Hawaiite (VA/119).	125
Fig. 4.29.	$^{40}\text{Ar}/^{36}\text{Ar}$ vs. $^{39}\text{Ar}/^{36}\text{Ar}$ isochron plot for Tavidar Hawaiite (K/69A).	126
Fig. 4.30.	Plot of initial Sr ratios Against Sr content of Tavidar volcanics.	130

Fig. 4.31.	Plot of mean initial Sr ratio of Tavidar volcanics and Mundwara igneous complex on Sr evolution diagram.	131
Fig. 4.32.	^{40}Ar - ^{39}Ar age spectrum for Musala Essexite (MR 86/1).	134
Fig. 4.33.	$^{40}\text{Ar}/^{36}\text{Ar}$ vs. $^{39}\text{Ar}/^{36}\text{Ar}$ isochron plot for Musala Essexite (MR 86/1).	135
Fig. 4.34.	^{40}Ar - ^{39}Ar age spectrum for Musala Basalt (MR 86/2).	138
Fig. 4.35.	$^{40}\text{Ar}/^{36}\text{Ar}$ vs. $^{39}\text{Ar}/^{36}\text{Ar}$ isochron plot for Musala Basalt (MR 86/2).	139
Fig. 4.36.	^{40}Ar - ^{39}Ar age spectrum for Musala Syenite (MR 86/4).	141
Fig. 4.37.	$^{40}\text{Ar}/^{36}\text{Ar}$ vs. $^{39}\text{Ar}/^{36}\text{Ar}$ isochron plot for Musala Syenite (MR 86/4).	142
Fig. 4.38.	^{40}Ar - ^{39}Ar age spectrum for Musala Syenite (MR 86/5).	145
Fig. 4.39.	^{40}Ar - ^{39}Ar age spectrum for Mer Syenite (MR 86/7).	147
Fig. 4.40.	$^{40}\text{Ar}/^{36}\text{Ar}$ vs. $^{39}\text{Ar}/^{36}\text{Ar}$ isochron plot for Mer Syenite (MR 86/7).	148
Fig. 4.41.	^{40}Ar - ^{39}Ar age spectrum for Toa Gabbro (MR 86/9).	150
Fig. 4.42.	Plot of initial Sr ratios Against Sr content of Mundwara alkali igneous complex.	154

LIST OF TABLES

	PAGE NO.
Table 3.1. Interfering nuclear reaction caused by neutron irradiation of samples.	38
Table 3.2. Results obtained on irradiated salts.	40
Table 3.3. Typical system blank contributions at various temperature steps.	50
Table 3.4. Isotopic abundances of Rb and Sr Spikes.	56
Table 3.5. $^{87}\text{Sr}/^{86}\text{Sr}$ values of NBS 987 standard measured during the course of this study.	58
Table 4.1. Step heating argon isotopic compositions and apparent ages of sample D/88 (DIRI BASALT).	63
Table 4.2. Step heating argon isotopic compositions and apparent ages of sample D/25 (DIRI DACITE).	65
Table 4.3. Step heating argon isotopic compositions and apparent ages of sample D/174 (DIRI RHYOLITE).	67
Table 4.4. Rb-Sr isotopic data of Malani volcanics from Dir, Gurapratap Singh and Manihari, Pali district.	71
Table 4.5. Rb-Sr isotopic data of ultrapotassic rhyolites from Manihari.	76
Table 4.6. Step heating argon isotopic compositions and apparent ages of sample JR 86/15 (JALORE GRANITE).	79
Table 4.7. Step heating argon isotopic compositions and apparent ages of sample JR 86/17 (JALORE GRANITE).	82
Table 4.8. Rb-Sr isotopic data of peraluminous granites from Jalore district.	85
Table 4.9. Rb-Sr isotopic data of peralkaline granites and peralkaline volcanics from Siwana, Barmer district.	88
Table 4.10. Rb-Sr isotopic data of outer rhyolites from south of Siwana.	92

Table 4.11.	Analytical data and calculated K-Ar ages of Tavidar volcanics, Jalore district.	96
Table 4.12.	Step heating argon isotopic compositions and apparent ages of sample VA/181 (TAVIDAR POTASSIC ANDESITE).	99
Table 4.13.	Step heating argon isotopic compositions and apparent ages of sample K/67 (TAVIDAR POTASSIC ANDESITE).	101
Table 4.14.	Step heating argon isotopic compositions and apparent ages of sample VA/58 (TAVIDAR TRACHYTE).	106
Table 4.15.	Step heating argon isotopic compositions and apparent ages of sample K/30 (TAVIDAR TRACHYTE).	108
Table 4.16.	Step heating argon isotopic compositions and apparent ages of sample VA/183 (TAVIDAR RHYOLITE).	113
Table 4.17.	Step heating argon isotopic compositions and apparent ages of sample VA/168 (TAVIDAR POTASSIC RHYOLITE).	117
Table 4.18.	Step heating argon isotopic compositions and apparent ages of sample VA/119 (TAVIDAR HAWAITE).	121
Table 4.19.	Step heating argon isotopic compositions and apparent ages of sample K/69A (TAVIDAR HAWAITE).	123
Table 4.20.	Summary of $^{40}\text{Ar}/^{39}\text{Ar}$ results of Tavidar volcanics.	127
Table 4.21.	Rb-Sr content and Sr isotopic ratios of Tavidar volcanics.	129
Table 4.22.	Step heating argon isotopic compositions and apparent ages of sample MR 86/1 (MUSALA ESSEXITE).	133
Table 4.23.	Step heating argon isotopic compositions and apparent ages of sample MR 86/2 (MUSALA BASALT).	137
Table 4.24.	Step heating argon isotopic compositions and apparent ages of sample MR 86/4 (MUSALA SYENITE).	140
Table 4.25.	Step heating argon isotopic compositions and apparent ages of sample MR 86/5 (MUSALA SYENITE).	144
Table 4.26.	Step heating argon isotopic compositions and apparent ages of sample MR 86/7 (MER SYENITE).	146

Table 4.27. Step heating argon isotopic compositions and apparent
ages of sample MR 86/9 (TOA GABBRO). 149

Table 4.28. Rb-Sr content and Sr isotopic ratios of Mundwara
alkali igneous complex. 153

CHAPTER I

INTRODUCTION

The geology of Rajasthan presents an excellent example encompassing rocks of all the ages right from the earliest crustal component to the recent. The four fold classification of the Precambrian rocks of Rajasthan (Heron, 1953) envisages the geological evolution through three major orogenic cycles represented by the rocks of the Banded Gneissic Complex (BGC), the Aravalli Supergroup and the Delhi Supergroup (called systems earlier), respectively (Fig. 1.1). This sequence remains the basic framework of reference despite certain revisions in the local stratigraphic sequence and regional correlation due to later investigations.

There have been mainly five periods of acid magmatism in Rajasthan as summarized by Choudhary et al. (1984). These periods have been placed at (1) 3000-2900 Ma, (2) 2600-2500 Ma, (3) 2000-1900 Ma, (4) 1700-1500 Ma, and (5) 850-750 Ma.

The Banded Gneissic Complex (BGC) marks the basement in Rajasthan which must predate 3000 Ma as one of the intrusives in it, i.e. Untala granite, east of Udaipur, has been dated as 2950 ± 150 Ma by Choudhary et al. (1984). Further, Gopalan et al. (1990) have found Sm-Nd evidence of 3307 ± 65 Ma old biotite gneiss, Mewar Gneiss, from Jhamarkotra SE of Udaipur. Very recently Widenbeck and Goswami (1994) have also obtained high precision $^{207}\text{Pb}/^{206}\text{Pb}$ zircon age of 3281 ± 3 Ma for the orthogneiss from the same area. The base of Aravalli Supergroup has been indicated at 2000 Ma. The original Delhi rocks of Heron (1953) have recorded two magmatic events widely separated in space and time. While the earliest granitic activity at 1600 Ma has been recorded only in the Alwar basin in the northeast Rajasthan, the younger activity between 850- 750 Ma has been wide spread, as shown by the nearly concordant ages of '*Erinpura type*' granites along the Aravalli mountain range and the Malani rhyolites in the western plains of the Aravalli range (Choudhary et al., 1984).

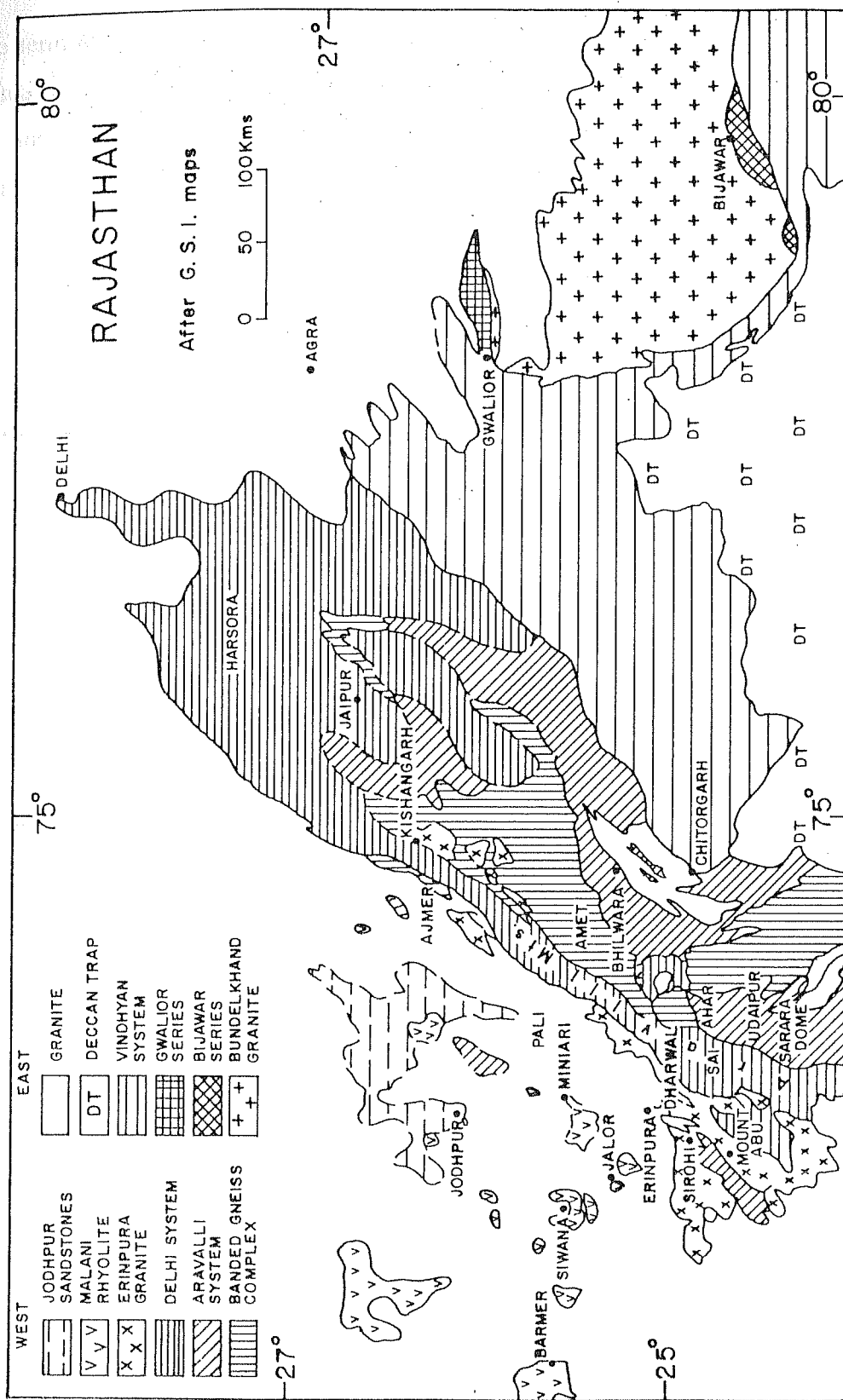
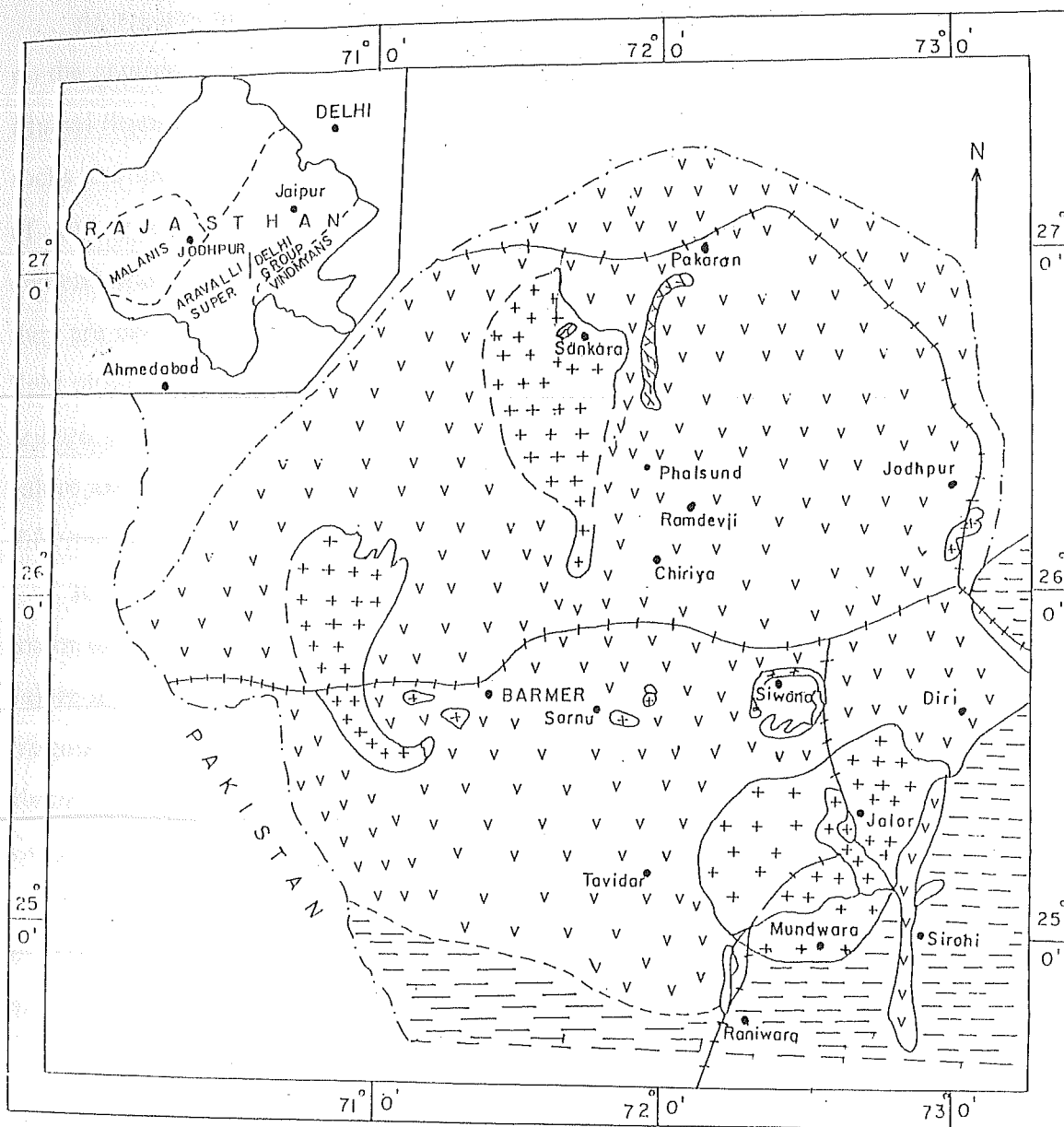


Fig. 1.1. Geological Map of Rajasthan (After G.S.I. Maps).

The term *Malani* was first introduced by Blanford (1877) for a group of volcanic rocks spread in parts of western Rajasthan, after Malani district of former Barmer State. The first and the only detailed account of Malani was given by La Touche (1902) who made detailed geological traverses in Pali, Jalore and Jodhpur districts of Rajasthan and provided petrographic description of the rocks. La Touche (1902) called it as '*Malani Igneous Suite*'. Coulson (1933) extended the limits of Malani to the State of Sirohi and named it as '*Malani System*' consisting of plutonic, hypabyssal, volcanic and tuffaceous rocks of varying composition. Pascoe (1960) retained the name given by La Touche. In recent times the term has rather been used loosely and various workers have used different connotations. Kochhar (1984) has continued the term *Malani Igneous Suite* while Srivastava (1988) has used *Malani Volcanic Province*. Bhusan (1991) called it as *Malani Igneous Complex*. However, we prefer to use the term Malani Igneous Province (*MIP*), which has also been used by Chandrasekaran and Srivastava (1992), to cover all the igneous rocks (volcanic as well as plutonic) of varying composition from the area and the same terminology will be followed throughout the text.

The *MIP* marks the youngest Proterozoic tectonomagmatic event covering an area of about 50,000 sq. km in western and southwestern Rajasthan and perhaps continues in the Sind province of Pakistan. The Malani represents one of the largest volcanisms in India, second only to Deccan Traps, and the area covered extends from south of Sirohi to north of Pokaran and from east of Jodhpur to Pakistan International Boundary (Fig. 1.2). Contemporaneous volcanism has also been reported in Churu and Jhunjhunu districts of northeastern Rajasthan extending upto Tosham in Haryana (Kochhar et al. 1985).

The province consists dominantly of felsic volcanics (rhyolites) and their plutonic equivalents with minor occurrences of alkaline, basic, intermediate and peralkaline acid volcanics and plutonites. The rocks occur as inselbergs, tors and residual hill ranges from near east of Jodhpur upto the edge of the Thar desert of India covering a width of approximately 240 km. Since the volcanic rocks occur in parts of the Thar desert, most of the area remains blanketed by thick sand cover leaving only small exposed outcrops. The Malani volcanics overlie Proterozoic metamorphics of uncertain age (pre-Delhi or Delhi Supergroup) at many places in Pali and Sirohi districts and underlie the



INDEX

- | | | | |
|--|------------------------------------|--|-----------------------------------|
| | ACID AND BASIC DYKES | | OBSERVED CONTACT |
| | ANDESITIC AGGLOMERATE AND RHYOLITE | | PROBABLE CONTACT |
| | GRANITE | | CONCEALED BELOW YOUNGER SEDIMENTS |
| | RHYOLITE | | INTERNATIONAL BOUNDARY |
| | BASALT, ANDESITE | | RAILWAY LINE |
| | ARAVALLI/DELHI SUPER GROUP | | |

Fig. 1.2 Geological Map of Malani Igneous Province, Rajasthan
(After Bhushan, 1985).

Trans-Aravalli Vindhya.

As regards the stratigraphic position of the province, Heron (1917), in his memoir on the geology of northeastern Rajputana, had suggested that the magmatic stocks of the Malani rhyolites are the batholithic granite (the Erinpura granite) intrusive into the Delhi rocks and that they were the product of fissure eruptions which inaugurated the uprising of the Aravalli chain. He, further, reported that the Malani rhyolites were contemporaneous with the upper most Delhis, since in Kirana hill (Sargoda, Pakistan), they are interstratified with sedimentaries of the Ajabgarh type. But subsequently, in the light of the work of Coulson (1933) and earlier work of La Touche (1902), Heron (1953) revised his opinion and suggested that the parent stocks of the Malani rhyolite were the Jalore and Siwana granite which also intrude Erinpura type of granite and that all the different igneous rocks of the province belong to a single Proterozoic magmatic event.

Regarding age of the *MIP*, work of Crawford and Compston (1970) remains the major one. They dated the Malani rhyolites and related granites from Barmer, Pali and Jalore districts and gave Rb-Sr isochron age of 745 ± 10 Ma, thus, indicating a single magmatic event around 745 Ma ago. This was supported in recent years by Pareek (1981), Kochhar (1984) and Bhusan (1985, 1989). Further, two samples dated by Crawford and Compston (1970), one rhyolite and other granite, gave much younger model ages of 526 and 428 Ma, respectively. Based on this, they also suggested the possibility of existence of some younger flows and granites. The Tosham volcanics and associated granites have also given Rb-Sr isochron age of 745 ± 20 Ma (Kochhar et al., 1985).

It is noteworthy to mention here that the heterogeneous suite of '*Erinpura type*' granite, traditionally distinguished from the Malani rhyolites and associated high level granites (Heron, 1953), were however considered, despite their chemical incoherence, of the same age of about 740 Ma by Crawford and Compston (1970) and Crawford (1975). Further, the studies of Choudhary et al. (1984) demonstrated that the Erinpura proper granite and the suite of intrusive granites, all along the axial zone of Aravallis from Sendra in the north and Sai in the south, have ages in the time band of 800 ± 50 Ma. Jhunjhunu and Ambaji granites in the northeast and south Rajasthan are also of this generation. Though these ages are in the order of the Malani igneous province, a slightly

earlier time of formation of Erinpura granite is not ruled out (Choudhary et al., 1984).

However, the contention of *MIP* representing a single magmatic event is belied by the detailed petrographic and geochemical work done in the last decade by Srivastava and his co-workers from different parts of the Malani province, namely, Diri (25°37':73°02'), Gurapratap Singh (25°37':73°09') and Manihari (25°40':73°08') in Pali district, Tavidar and Karara (24°51': 72°09'; 24°54': 72°10') in Jalore district, Siwana (25°39': 72°25'), Sarnu-Dandali (25°45': 71°45') and west of Barmer town in Barmer district, and Mundwara (24°50': 72°33') in Sirohi district of Rajasthan (Fig. 1.2). The alkali vs. silica diagram (Fig. 1.3) and total iron vs. alumina plus calcium diagram (Fig. 1.4) of various rocks from these areas reveal that rocks from these localities plot along different trends belonging to four different associations (Srivastava, 1988). These associations are:

1. *Basalt-andesite-dacite-rhyolite association of Diri, Gurapratap Singh and Manihari (Pali district) (Fig. 1.3 and 1.4). Besides the normal rhyolites and rhyolitic tuffs, there are also some ultrapotassic rhyolites in the area which do not correspond to the main trend but plot alongwith some of the potassic rhyolites belonging to the association (3) which will be described below. Analyses of normal rhyolites from Barmer and Siwana and of Tosham volcanics given by Pareek (1986) also plot along this trend.*
2. *Comendite-pantellerite, sodatrachytes and associated peralkaline granites of Barmer and Siwana (Barmer district). These rocks show a steady increase in iron with decreasing alumina plus calcium or increasing peralkalinity, in contrast to the rocks belonging to association (1), which show a decrease in total iron with decreasing alumina and lime (Fig. 1.4).*
3. *Mildly alkaline trachy basalt-trachy andesite-trachyte-alkali rhyolite of Tavidar and Karara (Jalore district). These rocks are characterized by relatively high K₂O (Fig. 1.3). The dominant rock types of this association are the trachytes, quartz trachytes and the potassic rhyolites. The amount of the associated potassic andesites, hawaiites and mugearites is relatively small. Some of the mugearites post date the main phase of eruption.*
4. *Alkaline and hyperalkaline rocks including alkali pyroxenites, micro-melteigites,*

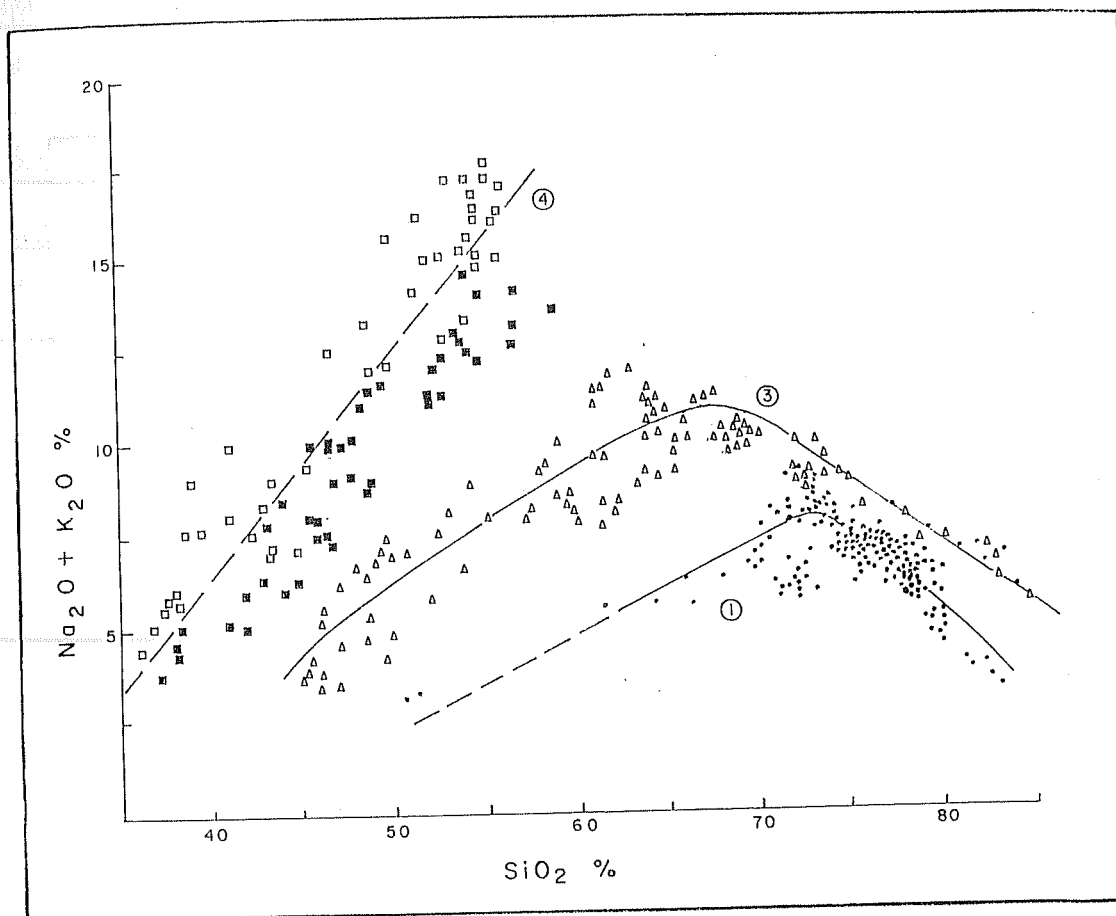


Fig. 1.3. AlK - SiO₂ Diagram of Various Rocks from the Malani Igneous Province (After Srivastava, 1988). Solid Circles : Basalt-Andesite-Dacite-Rhyolite from Gurapratap Singh and Dir (Pali District); Open Triangles : Trachyandesite-Trachyte-Alkali Rhyolite from Tavidar (Jalore District); Open and Solid Squares : Alkaline Rocks from Sarnu-Dandali (Barmer District) and Mundwara (Sirohi District), respectively.

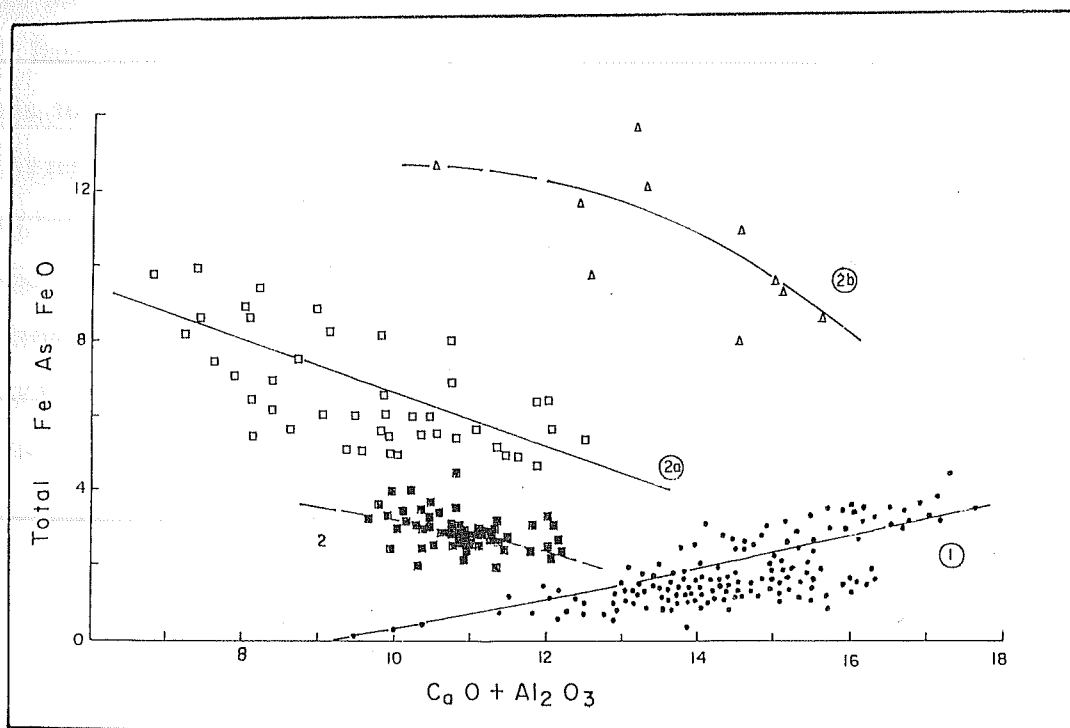


Fig. 1.4. FeO - Al₂O₃+CaO Diagram of Rhyolitic Rocks from Malani Igneous Province (After Srivastava, 1988). Solid Circles : Normal Rhyolites, Rhyodacites and Dacites from Pali, Barmer and South of Siwana; Solid Squares : Comendites from SE of Barmer town; Open Squares : Pantellerites and Peralkaline Granites from Siwana; Open Triangles : Soda Trachytes from Siwana.

ijolites, essexites, various foidal syenites, basanites, nephelinites, phonolites and carbonatites of Mundwara (Sirohi district), Sarnu-Dandali and west of Barmer town (Barmer district) (Fig. 1.3).

Bhusan and Sengupta (1979) have also reported four phases of Malani activity from Sankara, Jaisalmer. The first phase is represented by rhyolites and porphyry flows, while the second phase is a coarse grained biotite granite intruding into the first phase. The third phase includes both extrusive and intrusive rocks of acid and intermediate composition and the last phase is of intrusive basic rocks. Recently Chandrasekaran and Srivastava (1992) have also reported polyphase igneous activity, based on multivariate statistical analysis, for the *MIP*.

As regards the time framework of various associations of Srivastava (1988), no work has yet been done. However, he has postulated that association (1) is oldest and coeval with the Erinpura granite phase. It overlies the pre-Delhi or Delhi Supergroup of rocks and extends from east of Jodhpur to the edge of Thar desert in the form of roughly NE-SW or NNE-SSW trending hills. The Jalore and Siwana type granites and the associated comendites and pantellerites of association (2), which occur in the areas of basement uplift and crustal upwarps (marked by Sarnu high and Therad high) (Fig. 1.5), represent younger sub-volcanic ring complexes typical of the areas of epeirogenic doming. The fact that they intrude the volcanics of association (1), and the presence of a strong thermal event between 500-550 Ma in resetting the mineral assemblages of the Erinpura type granites (Choudhary, 1984) and younger model Rb-Sr ages of 526 and 428 Ma for a rhyolite and granite from Barmer and Jalore, respectively (Crawford and Compston, 1970), taken together suggest that these granites represent a Palaeozoic event unrelated to Erinpura granites or the rhyolites of association (1).

The Tavidar and Karara rocks as well as the mildly alkaline rocks of the Sarnu-Dandali belonging to association (3), situated at the edge of the Sanchor basin and the Barmer graben respectively (Fig. 1.5), have been correlated to epeirogenic movements which started in the early Jurassic time and continued upto the end of Cretaceous. These epeirogenic movements led to subsidence and formation of the Kutch and Sanchor basins in the south and Jaisalmer basin in the central part of Rajasthan. The alkaline rocks

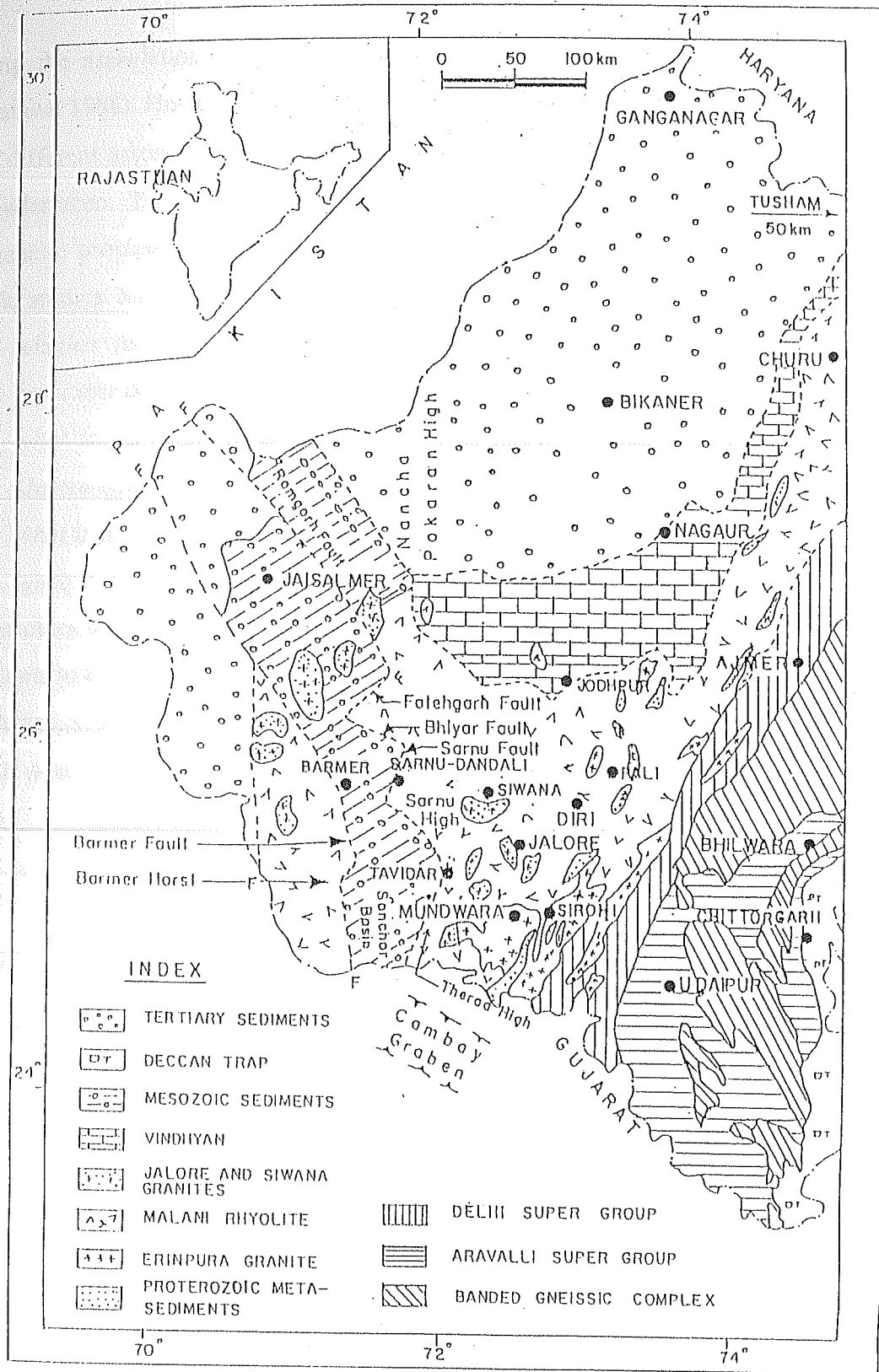


Fig. 1.5. Pre-Quaternary Interpretative Geological Map of Southwest Rajasthan (After Srivastava, 1988 : Superimposed on Structures of Dasgupta and Chandra, 1978).

marking the association (4) are the youngest and belong to a post-Cretaceous event (Srivastava, 1988). However, in the absence of any radiometric dates, the time framework to the different associations remain speculative. Keeping this in view the present study was undertaken. The present study is aimed at seeking answers to evolutionary and petrogenetic problems of the Malani igneous province of southwest Rajasthan through isotopic studies. Some of the pertinent questions that need to be answered are:

- (a) *whether the different associations belong to a single magmatic cycle or they represent different magmatic episodes as envisaged by Srivastava (1988),*
- (b) *what is the relationship between peralkaline (Siwana type) and peraluminous (Jalore type) granites/rhyolites and finally,*
- (c) *what is the position of various magmatic episodes in the evolution of the Malani igneous province ?*

In other words, the main objective of the present study, is to provide precise time constraints to the various associations referred to above, using K-Ar, ^{40}Ar - ^{39}Ar and Rb-Sr systematics, in order to construct an evolutionary model for the Malani igneous province of southwest Rajasthan.

CHAPTER II

DESCRIPTION OF DIFFERENT ASSOCIATIONS OF MALANI IGNEOUS PROVINCE

2.1. ASSOCIATION I (*MALANI VOLCANICS*)

The felsic volcanics of Gurapratap Singh and Dirī belong to andesite-dacite-rhyolite association and are part of the Malani igneous province (*MIP*) of Rajasthan. These volcanics have been referred to as Malani volcanics (Srivastava, 1988). The area under study lies 30 km southwest of Pali, between North latitudes $25^{\circ}35'$ - $25^{\circ}40'$ and East longitudes 73° - $73^{\circ}10'$ (Fig. 1.5). The volcanics are confined to hill ranges running NE-SW to NNE-SSW in semi arcuate fashion and have been extruded on a basement of mica schist and shale/slate belonging to the Aravalli or the Delhi Supergroup. Most of the rocks are aphyric to sparsely phyrīc with an obsidian like look. Flows generally have a dip 10° to 15° to NW.

The distribution of various rock types in the area is shown in Fig. (2.1). The main rock types include dacite, rhyodacite and rhyolite with minor occurrences of basalt and andesite. The rhyolites occupy lower ground while high silica rhyolites are seen on the top of hills. A very small isolated occurrence of basalt was found in the plains to the NE of village Bhavnagar. The field disposition of the basalt i.e. whether occurring in the form of a dyke or as a flow, could not be ascertained. The rhyolites are cut by numerous dykes of rhyolite porphyries and rarely by dolerite (Srivastava et al., 1989a).

Srivastava et al. (1989a,b) carried out detailed geochemical study (major and trace elements) of these volcanics. The chemical data of different rock types plotted on the Harker diagrams (Fig. 2.2) revealed a systematic variation in all major elements with the

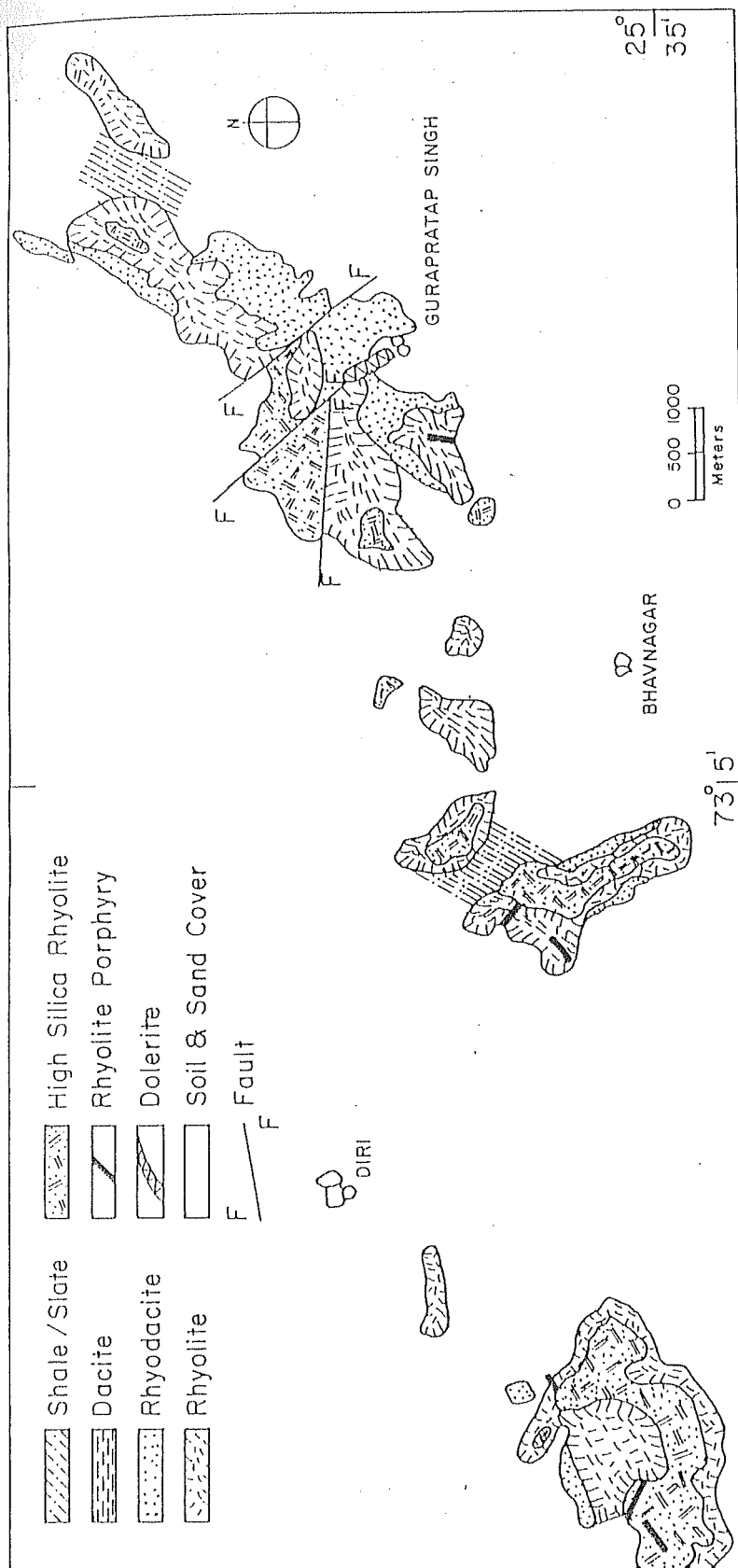


Fig. 2.1. Geological Map of Gurupratap Singh and Dir, Pali District, Rajasthan (After Srivastava et al., 1989a)

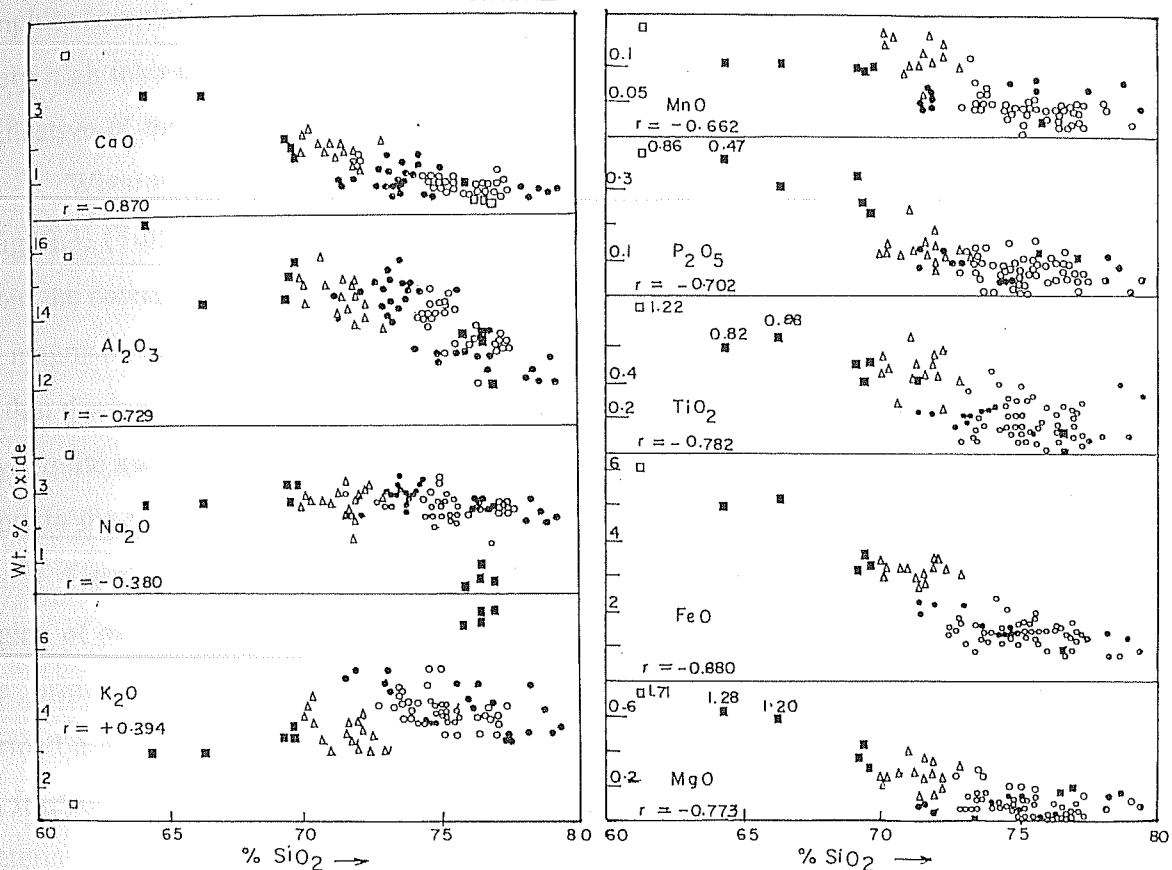


Fig. 2.2. Harker Diagrams of Gurapratap Singh and Dirri Volcanics (After Srivastava et al., 1989a). Symbols : Open Square-Andesite; Solid Square-Dacite; Triangle-Rhyodacite, Solid Circle-Rhyolite; Open Circle-High Silica Rhyolite, Diagonally Filled Square-Ultrapotassic Rhyolite and Half Filled Circle-Rhyolite Porphyry.

progress of differentiation suggesting that the entire sequence except the ultrapotassic rhyolites is cogenetic and that the changes have been controlled by some sort of fractional crystallization mechanism. Srivastava et al. (1989a), further, carried out Principal Components Analysis (PCA) (Le Maitre, 1968, 1982; Till and Colley, 1973) of the data which revealed that in the early stages the fractionating phase was soda-lime plagioclase, amphibole and/or iron oxide but in the later stages, K-feldspar became a dominant phase. Very high inter-chemical correlations have been observed by these authors which is also indicative of the cogenetic nature of these rocks and a single process evolution.

When the compositions of these rocks are projected in the system Ab-Or-Q-H₂O (Fig. 2.3) (Tuttle and Bowen, 1958), majority of the rocks plot in the quartz field away from the cotectic minima at $pH_2O = 500 \text{ kg/cm}^2$ and outside the low temperature 'valley' of magmatic crystallization. Only a small number of samples plot close to the minima within the low temperature valley. Further, ultrapotassic rhyolites plot in a field of their own, quite away from the main field framed by majority of data points, and the andesite plots in the field of sodic feldspar close to the 3000 kg/cm^2 cotectic line.

Carmichael (1963) and Barth (1966) have pointed out that while the plots in the region of primary plagioclase represent the product of magmatic crystallization, plots in the primary field of quartz and K-feldspar do not appear to represent a residual liquid formed under conditions of equilibrium crystallization. These could either be a product of fractional crystallization of magma or the product of partial melting of crustal material. The role of fractional crystallization in developing the cogenetic sequence of andesite-dacite-rhyodacite-high silica rhyolite has also been supported by Harker diagrams and Principal components analysis of major elements.

Further, the behaviour of trace elements e.g. Rb, Sr and Ba (Fig. 2.4) and Zn, Cr, Li, Ni and Co (Fig. 2.5) as well as that of elemental ratios e.g. Ni/Co, Fe/Zn and Mg/Li (Fig. 2.6) is also in keeping with a model of fractional crystallization (Srivastava et al., 1989b). The K/Rb relationship is most important in elucidating the evolutionary model of a cogenetic sequence. Gast (1968) and Shimizu (1964) have pointed out the usefulness of K/Rb ratio to distinguish the fractional crystallization from a batch of partial melting. According to Gast (1968), during fractional crystallization the K/Rb ratio

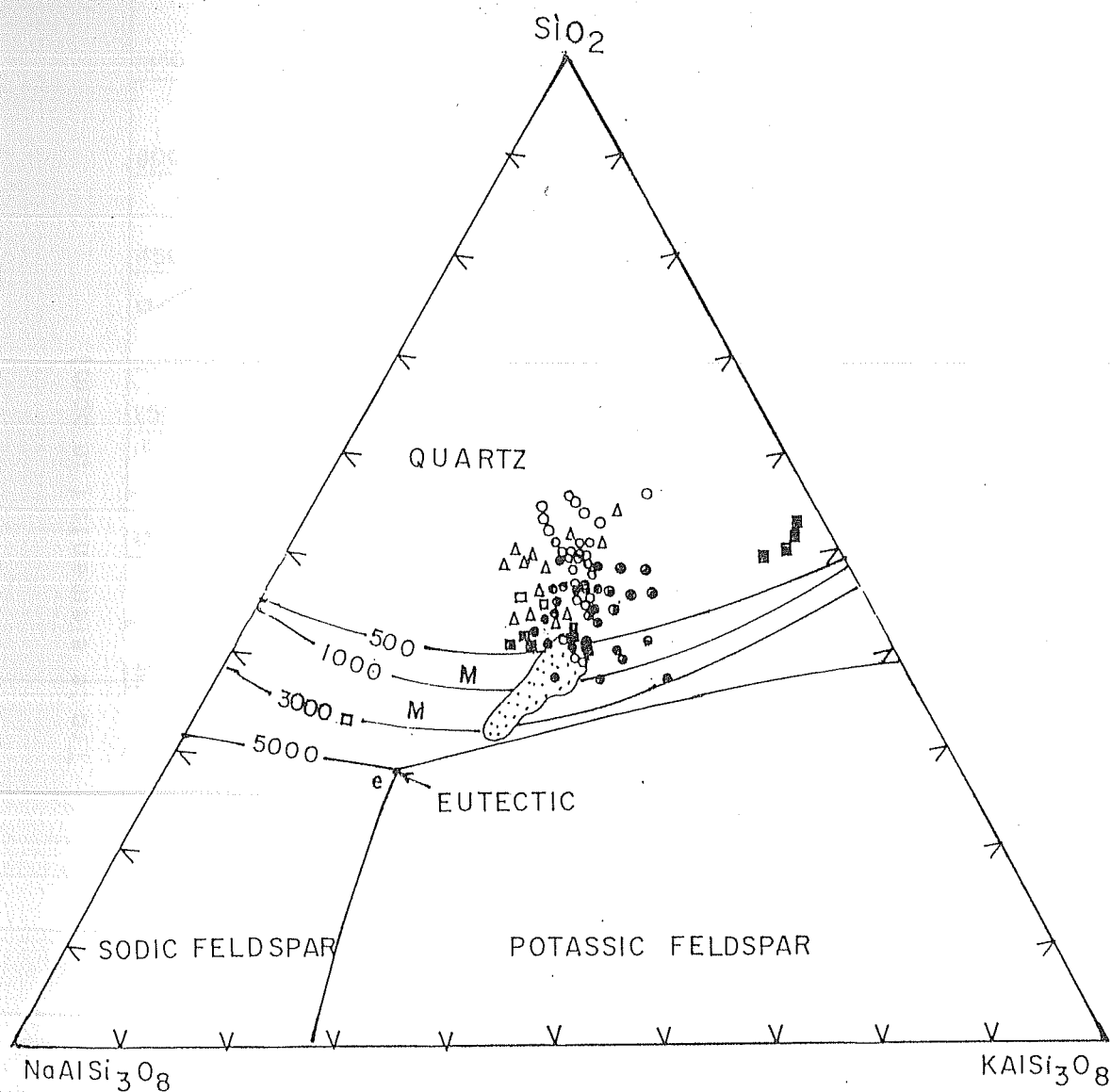


Fig. 2.3. Plot of Normative Q-Or-Ab-H₂O of Gurapratap Singh and Dirri Volcanics (After Srivastava et al., 1989a) Symbols as in Fig. 2.2.

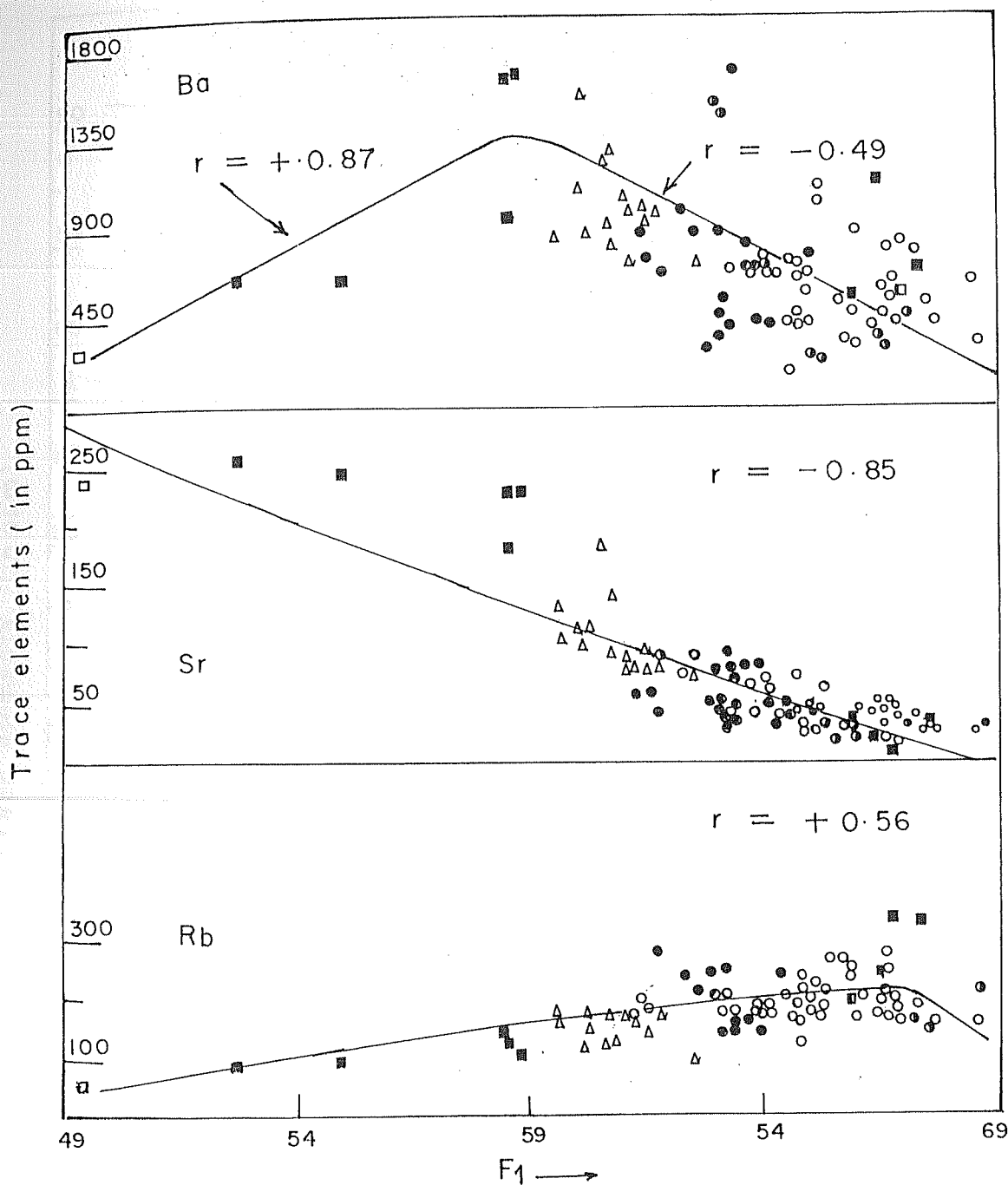


Fig. 2.4. Variation of Rb, Sr and Ba with Progressive Differentiation in the Felsic Volcanics of Gurapratap Singh and Dirri (After Srivastava et al., 1989b). Symbols: Open Square-Andesite; Solid Square-Dacite; Triangle-Rhyodacite, Solid Circle-Rhyolite; Open Circle-High Silica Rhyolite, Diagonally Filled Square-Ultrapotassic Rhyolite and Half Filled Circle-Rhyolite Porphyry.

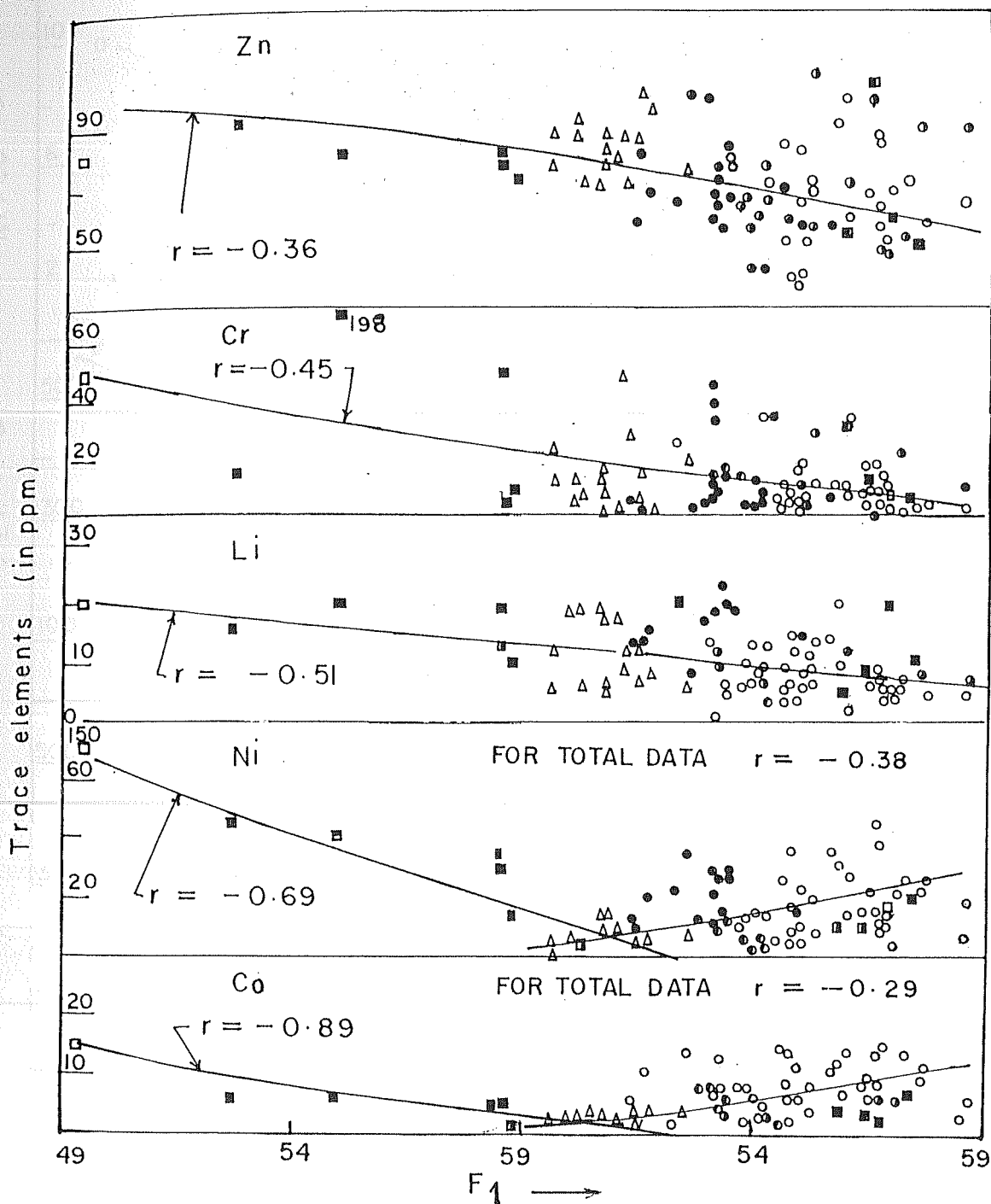


Fig. 2.5. Variation of Zn, Cr, Li, Ni and Co with Progressive Differentiation in the Felsic Volcanics of Gurapratap Singh and Dir (After Srivastava et al., 1989b). Symbols: Open Square-Andesite; Solid Square-Dacite; Triangle-Rhyodacite, Solid Circle-Rhyolite; Open Circle-High Silica Rhyolite, Diagonally Filled Square-Ultrapotassic Rhyolite and Half Filled Circle-Rhyolite Porphyry.

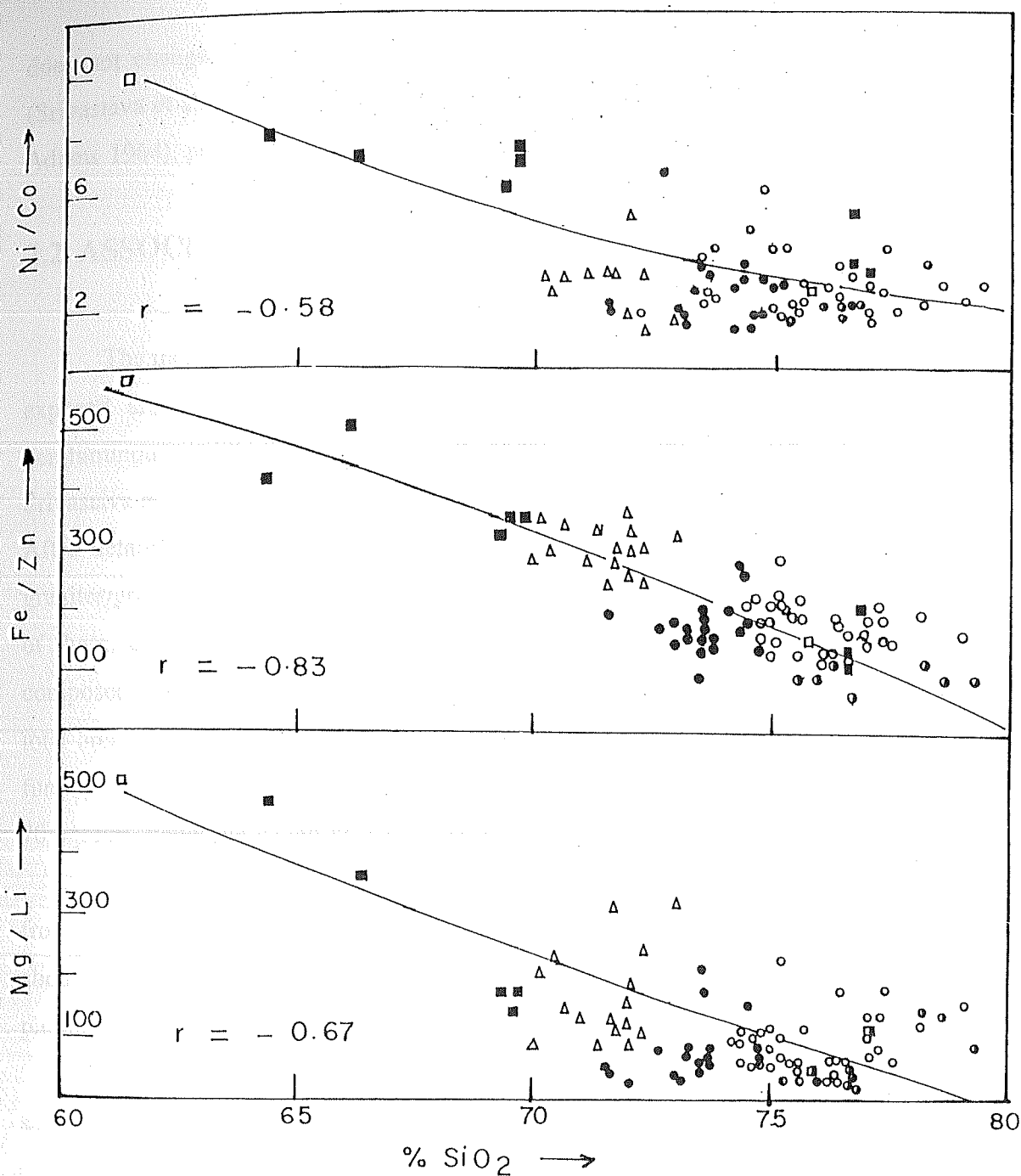


Fig. 2.6. Variation in Ni/Co, Fe/Zn and Mg/Li with Progressive Differentiation in the Felsic Volcanics of Gurapratap Singh and Diri (After Srivastava et al., 1989b). Symbols: Open Square-Andesite; Solid Square-Dacite; Triangle-Rhyodacite, Solid Circle-Rhyolite; Open Circle-High Silica Rhyolite, Diagonally Filled Square-Ultrapotassic Rhyolite and Half Filled Circle-Rhyolite Porphyry.

does not change. The K/Rb ratio of all the rocks of the present area is 202 ± 40 (Srivastava et al., 1989b) which is similar to median value of crustal rocks (Heier and Adams 1964), pointing to the crustal nature of the source for these rocks.

2.2. ASSOCIATION II (GRANITES AND ASSOCIATED VOLCANICS)

The most important rock types of *MIP* are the granites. These granites are mainly exposed around Jalore and Siwana area of the province. The Jalore Granite is peraluminous, while the Siwana Granite is peralkaline in nature. Kochhar (1984) and Srivastava et al. (1988) have considered these granites as anorogenic or A-type granites. After detailed field work in the area, Bhusan (1991) identified fifteen plutons of granites/granitoids in the *MIP* covering cumulatively an area of about 8800 sq. km. Out of these, six ring dykes and a pluton, covering an area of about 1100 sq. km, are composed of riebeckite/aegirine granite (Siwana Granite) and seven plutons, covering a total area of about 7600 sq. km, are of biotite granite (Jalore Granite). Bhusan (1991), further, identified two small plutons of hornblende granite, covering an area of about 70 sq. km, which he called as Malani Granite.

The Jalore Granite is conspicuous by its pink colour and range in composition from pegmatite granite to granodiorite. The Sankara pluton is the largest with an area of about 3700 sq. km (Fig. 1.2) followed by Jalore pluton covering 3300 sq. km. The other plutons range between 50 to 250 sq. km.

Discontinuous outcrops of the Siwana Granite occur as an elliptical pattern (ring shaped) around Siwana, covering an area of about 290 sq. km (Fig. 2.7). The continuous exposures on the southern periphery provide a thickness of about 8 km from outer to inner contact with the rhyolites.

The peralkaline magmatism has attracted attention of the earth scientists world over for a variety of reasons. The most important amongst them are their tectonic significance and mode of occurrence. Normally, peralkaline volcanics have been associated with the peralkaline granites. The peralkaline silicic rocks are commonly found in non-orogenic continental regions which have been subjected to crustal swelling

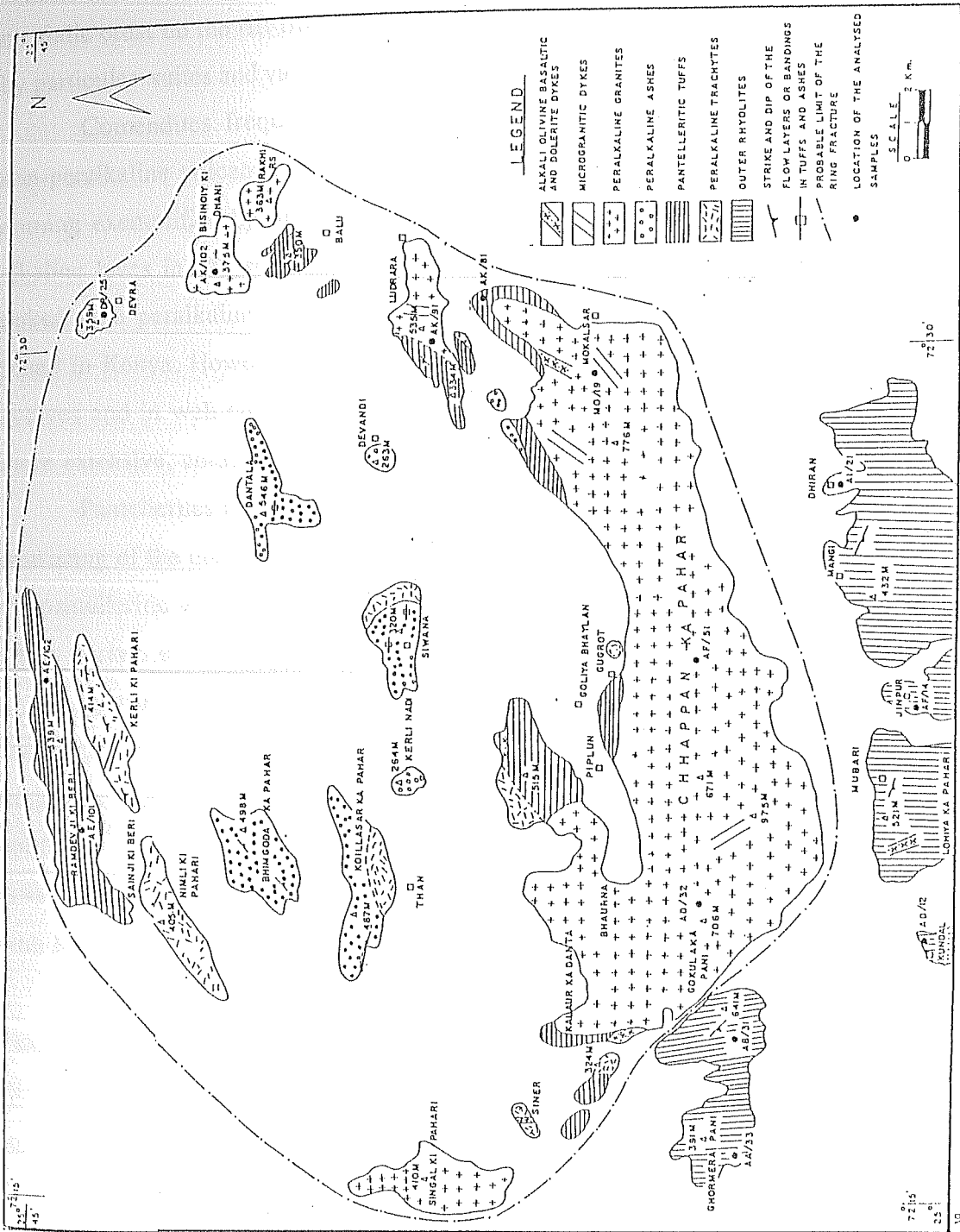


Fig. 2.7. GEOLOGICAL MAP OF SIWANA GRANITES AND ASSOCIATED VOLCANICS (AFTER YADAV, 1988)

and rifting (Le Bas, 1971). Peralkaline magmatism can occur during pre-rifting (e.g. epeirogenic doming), initial rifting (development of linear fractures and beginning of crustal attenuation) and continued rifting (extensive crustal attenuation leaving little or no sialic crust on the rift floor) (Bowden, 1974). Each event appears to be characterized by particular suites and varying proportions of peralkaline siliceous and associated rocks.

Comendites frequently occur in sub-volcanic ring complexes associated with non-peralkaline volcanics. Comenditic associations are typical products of epeirogenic doming exemplified by the elevated domes of vitreous to granophyric peralkaline and alkaline lavas in Tibesti (Vincent, 1970). In rift valleys, comendites are more closely linked with peralkaline trachytes and pantellerites. Examples of these associations are found in Kenya. However, the proportion of comendite becomes diminished as the rift evolves and in well developed rift systems (e.g. Ethiopia), where crustal attenuation is more extensive, comendites are virtually absent (Mohr, 1970).

Pantellerites are related to the development of rifting. The Ethiopian rift system consisting of the main Ethiopian rift and the Danakil depression provides good example of pantelleritic volcanism and its relationship with the extent of rifting (Tazieff et al., 1969; Barberi et al., 1970).

Further, Bowden (1974) suggested that the Peralkaline granites are common on continental regions of epeirogenic doming (Pre-rift tectonic environment) and are frequently displayed as sub-volcanic ring structures. Bailey (1974) considered regional uplift and alkaline magmatism as characteristic feature of continental rifts. Greenburg (1981) concluded that the younger granites of Egypt represent magmatism associated with the rift mechanism.

The intrusive nature of Siwana granite was first indicated by La Touche (1902) and Coulson (1933). Subsequently, various theories have been put forward for the ring structure and emplacement of the peralkaline granites. Mukherjee (1958) suggested a doubly plunging syncline for a subsidence structure. Pascoe (1960) speculated that the circular plan at Siwana has a connection with the roots of a volcano. Murthy (1962) for the first time interpreted this as a feature of cauldron subsidence, having a similarity to the Nigerian ring complex. Narayan Das et al. (1978) related the alkali magmatism of

trans-Aravalli region to crustal dislocations. Bhusan (1984) also suggested that the alkaline granites of Siwana and Barmer have been emplaced as ring dykes due to cauldron subsidence. Kochhar (1984) attributed this structure to an intra-cratonic hot spot activity. Sinha Roy (1984) suggested that the Malani acid and calc-alkaline volcanics and associated plutonic episodes are possibly the result of low angle subtraction of the south Delhi oceanic crust beneath the ancient crustal block. Bhusan and Mohanty (1988) suggested that the Siwana granite has intruded along a collapse structure as a low-angle cone intrusion. Further, they envisaged that the peralkaline granites and associated trachytes and rhyolites at Siwana indicate the zone of active rifting in a distinct late Proterozoic crustal regime. Srivastava (1988) correlated sub-volcanic ring complexes to a period of crustal upwarping before the commencement of Gondwana rifting.

2.3. ASSOCIATION III (*TAVIDAR VOLCANICS*)

The mildly alkaline rocks from Tavidar and Karara (Jalore district) and Sarnu-Dandali (Barmer district) have been grouped together in association 3 (Fig. 1.3). These volcanic rocks have been considered to belong to Malani igneous province (Coulson, 1933). In the present study, only the rocks from Tavidar have been selected for geochronological and Sr isotopic studies. The area lies 35 km SW of the Bhinmal town of Jalore district between North latitudes $24^{\circ}46'10''$ - $24^{\circ}54'10''$ and East longitudes $72^{\circ}05'40''$ - $72^{\circ}10'29''$ and cover an area of approximately 70 sq. km. The volcanics have their northern limit near the village Chatwara and extend 15 km to the south upto the villages Pal and Jalerakurd (Fig. 2.8). The region consists of a number of hills trending NE-SW and are surrounded by vast arid desertic plains. Most of the hills have heights between 300 to 330 m. The chain of hills appear in two rings, one to the north of the village Tavidar and the other to its south. The northern ring is breached in the east but the southern ring is more or less complete. The central part of the southern ring is filled with sand and alluvium. The distribution of various rock types occurring in the area is given in Fig. (2.8). Dashora (1981) and Ranawat and Dashora (1984) have given preliminary account of the rocks occurring in the north of the village Tavidar and have

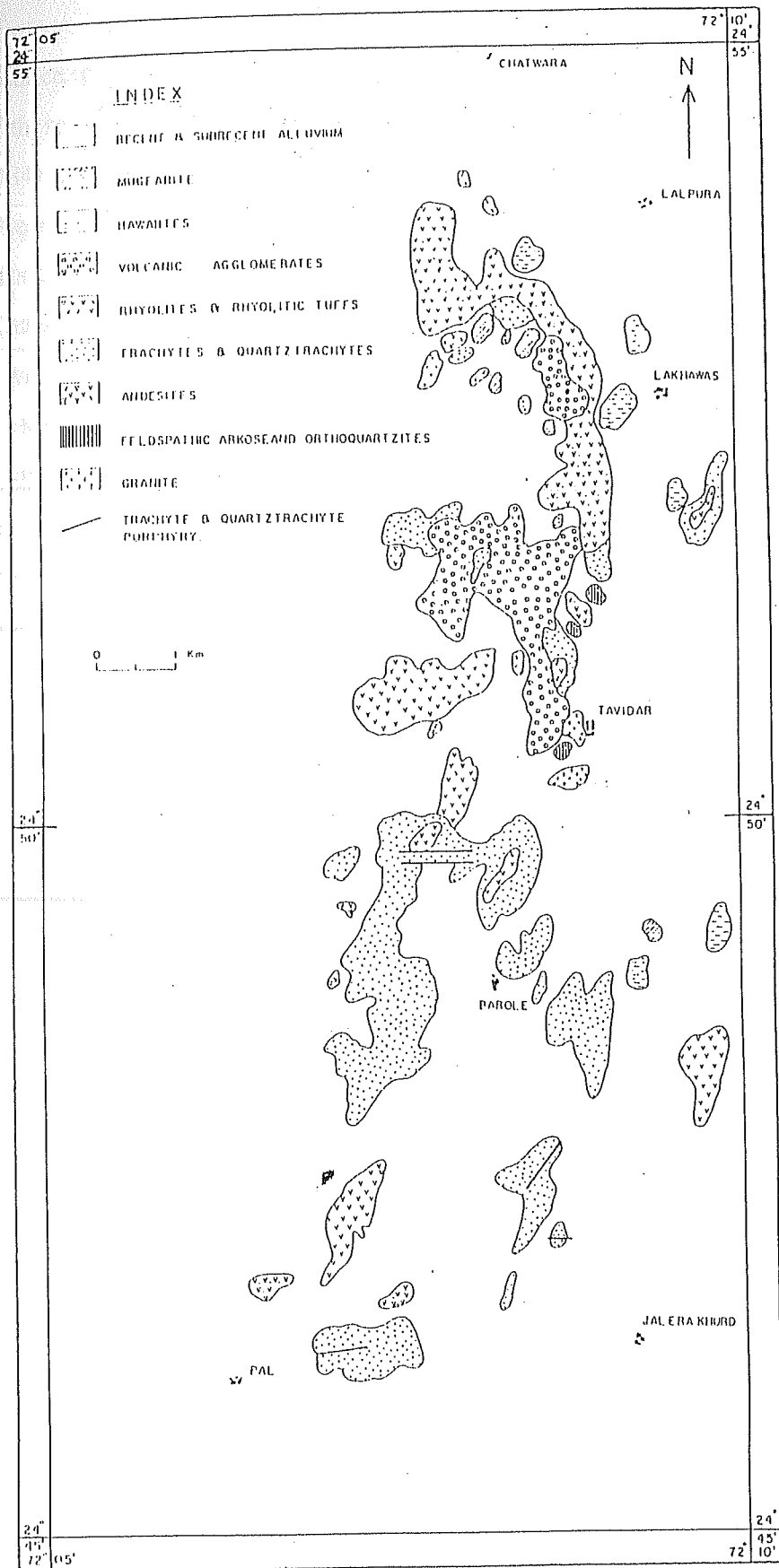


Fig. 2.8. Geological Map of Tavidar Volcanics, Jalore District, Rajasthan (After Agrawal, 1984).

reported presence of basalts, andesites, trachytes and rhyolites besides pyroclastic rocks. The work of these authors was mainly on the fluorite mineralization found in these rocks. Agrawal (1984) has carried out extensive field mapping, petrographic and geochemical studies of these rocks with a view to understand the genetic process or processes responsible for the development of different rock types in this area. He observed that the basic rocks (hawaiites and mugearites) occur in very small proportion and also their field relationship with other rocks of the area is not clear, as they occur in isolated patches.

With the introduction of modern methods of chemical data analysis like multivariate statistical analysis (Davis, 1973; Le Maitre 1968, 1982; Till and Colley, 1973), it has become possible to evaluate very efficiently the available chemical data for classifying and understanding the genesis of the rocks. In the conventional methods of classification it is difficult to deal with vast quantity of data e.g. the variation diagrams, which utilize a few oxides at a time, in effect, ignore the correlation of these oxides with other oxides, leading to under utilization of the informations contained in the data. Further, petrologists normally apply variation diagrams using two or more variables at a time to study qualitatively the inter-relationship between various components. The relationship between various oxides can also be studied by using the linear correlation coefficient (r) which is a quantitative measure of the same (Chayes, 1960; Le Maitre, 1982). Upadhyaya et al. (1988) have determined correlation coefficients between all possible pairs of elements for the data with and without basalts. They found that SiO_2 correlates negatively with all the elements except K. High correlation found in the Tavidar rocks are indicative of their cogenetic nature and of the operativeness of a single stage process during the evolution of these rocks. These authors have also presented the application of various statistical methods to Tavidar volcanics for better understanding of the classification and genesis of these rocks from chemical analysis alone. By applying the clustering method based on distance coefficient (Davis, 1973; Le Maitre, 1982), the rocks have been classified as belonging to basalts, andesites, trachytes and rhyolites. The splitting of trachytic rocks into three sub-clusters, indicate considerable variation in the trachytic rocks of the area.

The host rock of these volcanics is generally not seen, but in the village Tavidar

and in a nala immediately to its south, exposures of granites are seen (Fig. 2.8). Similar granitic rocks are also found in the north of Raniwara town which is about 15 km SE of Tavidar. The Raniwara granite is supposed to be a part of Jalore granite (Agrawal, 1984).

Besides the granite, in the Tavidar village and in the nala to its south, there are three small occurrences of sedimentaries also, comprising feldspathic arkose and ortho quartzites. One outcrop of feldspathic arkose is found almost above the granite near Tavidar and other outcrop is in the plains to the north of the village. The orthoquartzite is confined to low ground and is visible even from distance as a shining white rounded patch. The field relationship as it appears is that the granites are overlain by the feldspathic arkose and orthoquartzites, which in turn have been intruded by the volcanics. The succession, as it appears in the area, is as follows (after Agrawal, 1984).

Volcanic agglomerates

Rhyolites and rhyolitic tuffs

Trachytes, quartz-trachytes and their porphyries

Andesites

Orthoquartzites and feldspathic arkose (probably of Cretaceous age)

Granites (probably equivalent to Jalore Granites)

The feldspathic arkose and orthoquartzite are lithologically very similar to Barmer sandstone and orthoquartzite of the lower Cretaceous age (Agrawal, 1984). If the present orthoquartzites and arkose are of the same age, then the volcanics cannot belong to the Malani volcanic activity as has been hitherto believed and instead, they may have an age similar to Mundwara alkaline complex (Srivastava, 1983). However, in the absence of any radiometric date, or definite correlation between the Barmer sandstone and the orthoquartzites and the present occurrences, the question of the age of the Tavidar volcanics remains uncertain.

2.4. ASSOCIATION IV (*MUNDWARA ALKALI IGNEOUS COMPLEX*)

The Mundwara alkali igneous complex constitute the association 4. The complex first reported by Coulson (1933), occupying an area of 12 sq. km, is one of the plug like bodies occurring in the western and north western part of the Indian shield in the Deccan volcanic province. In conformity to the other alkaline occurrences, this complex also occurs as ring shaped and plug like intrusion within the Erinpura granite terrain and is situated about 35 km NW of Mount Abu in the neighborhood of Mer-Mundwara village (24°50':72°33') in the Sirohi district of Rajasthan.

The Mundwara complex along with a few other alkaline occurrences e.g. Kadi, Panwad, Netrang and Jawahar etc. (Fig. 2.9) fall along the N-S trending Rajasthan-Gujarat rift and west coast rift in contrast to the majority of the other similar occurrences which fall along the E-W trending Narmada lineament and its easterly extension (Bose, 1980). The distribution of the plugs define belts of alkaline magmatism which are intersecting near the gulf of Cambay (Khambhat). Bose (1980) attributed plume generated fracture zones responsible for the alkaline magmatism.

The various rock types of the complex are distributed in three distinct physiographic units viz. Toa (max. height 436 m), Mer (max. height 584 m) and Musala (max. height 509 m) hills (Fig. 2.10) and each of them contain undisturbed and complete suite of mafic to felsic derivatives. While, Toa and Mer are circular chains of hills, Musala is an isolated hill of conical shape rising precipitously from the plains. These hillocks are denuded relics of laccolith like bodies and are riddled profusely by radial and concentric dikes (Sharma, 1967) ranging in composition from hawaiites, through mugearites to phonolites. In fact, this suite of rocks is a field museum of igneous petrology and contains an abundant variety of rocks ranging from ultrabasic to alkalic and acidic (Subrahmanyam and Rao, 1972).

Studies on petrology and geochemistry of the complex have earlier been carried out by various workers viz. Bose and Das Gupta (1973), Chakraborty and Bose (1978), Chakraborty (1979, 1984), Das Gupta (1974, 1975), Lebas and Srivastava (1989), Sharma (1967), Srivastava (1989), Subrahmanyam (1986), Subrahmanyam and

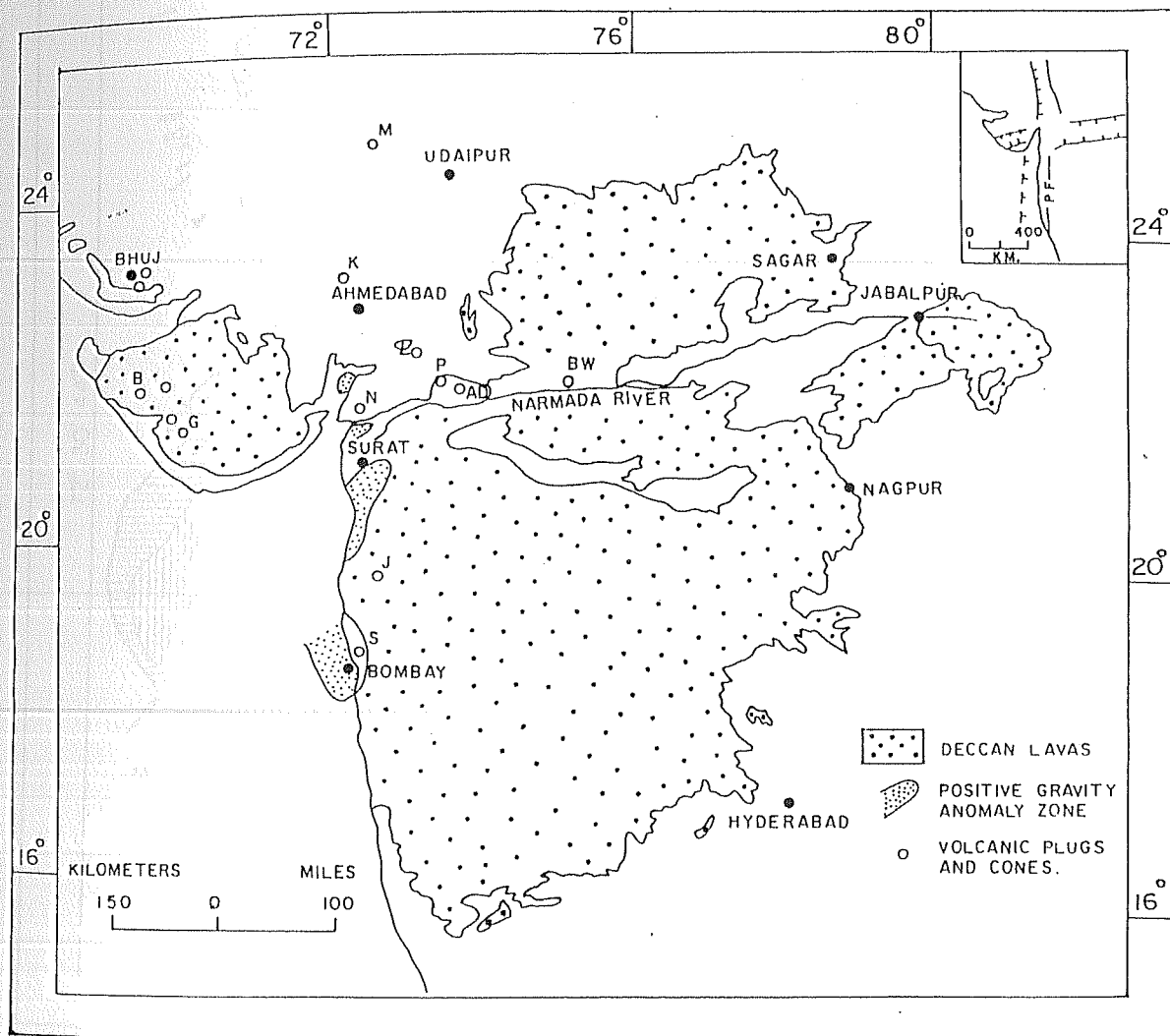


Fig. 2.9. The Deccan Volcanic Province Showing the Distribution of Plugs and Alkaline Intrusions (open circles). AD = Amba Dongar, B = Barda, BW = Barwaha, G = Girnar, J = Jawahar, K = Kadi, M = Mundwara, N = Netrang, P = Panwad, PV = Pavagad, S = Salsette. Inset shows the alignment of Plume generated rift zones controlling the tectonic setting for alkaline magmatism. PF = Panvel Flexure (After Bose, 1980).

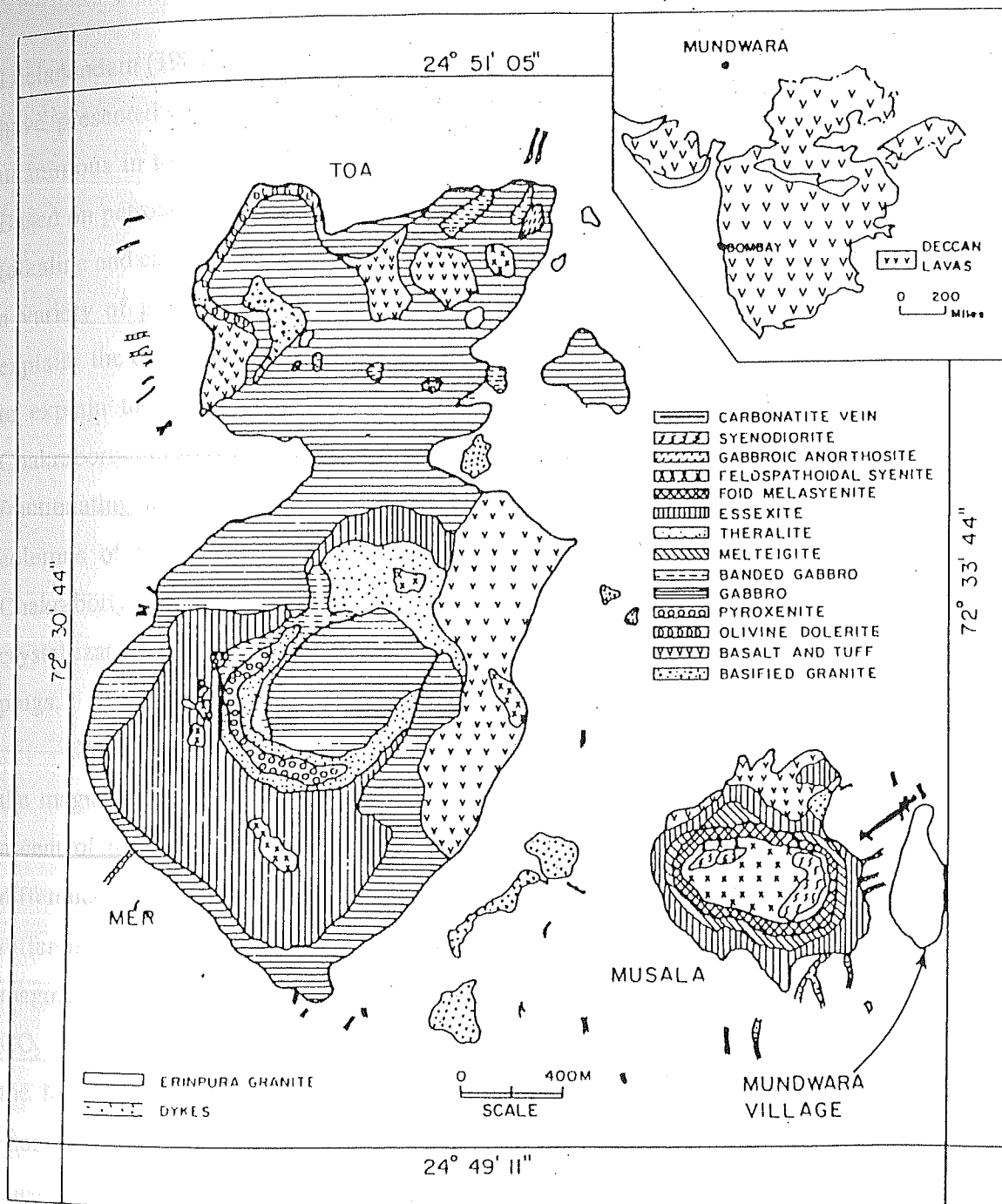


Fig. 2.10. Geological Map of Mundwara Alkali Igneous Complex, Rajasthan (After Subrahmanyam and Leelanandan, 1989).

Leelanandam (1989, 1991) and Upadhyaya and Srivastava (1987). These authors, though have presented different models to explain the genesis of the diverse rock types, are unanimous in their view about alkali basalt being the parental source for these rocks. Based on petrochemical studies of the complex, Sharma (1969) has discerned two trends (alkaline and calc-alkaline) of differentiation. Yadava and Karkare (1976) have envisaged a variety of processes such as differentiation, assimilation and mixing of magma to explain the diversity of rock types in this complex. Chakraborty and Bose (1978) tried to explain the origin of different rock types by subsidiary trends of differentiation. Chakraborty (1984) considered that the plugs may represent successive channels of a fractionating magma at depth or they may manifest different levels of differentiating columns of the magma in synchronous plugs with different degree of subsidence. Chakraborty (1984), however, also concedes that the three plutons may represent separate crystallization columns with normal fractionation processes operative in the individual plugs.

Petrological studies by Subrahmanyam (1986) indicate that the emplacement of the magma took place in three pulses and was spurred by volatiles released during the ascent of the magma. Subrahmanyam and Leelanandam (1989), further, suggest that differences in the volatile contents of the magma in the three plutons are responsible for different trends of differentiation. Due to differential solubility of CO_2 and H_2O in the magma, the earliest pulse, emplaced at Musala, predominantly contained the less soluble CO_2 . The last pulse of magma containing more soluble water was emplaced at Toa with the Mer pluton being formed from the intermediate pulse of the magma containing moderate amounts of both CO_2 and H_2O . Variable volatile contents of the magma in the three plutons have brought about three different trends of differentiation and, hence three distinct suites of rocks.

High water content in the magma of the Toa pluton has resulted in a cumulo porphyric suite of rocks. High CO_2 content in the magma of the Musala pluton has induced immiscibility in the parental magma and the two immiscible liquids, one hawaiitic liquid and the other phonolitic, subsequently followed independent courses of fractional crystallization resulting in the formation of essexites, hawaiites, mugearites,

melteigites and phonolites, feldspathoidal syenites, respectively. Moderate and approximately equal amount of water and CO_2 in the magma of the Mer pluton have brought out a calc-alkaline trend of differentiation under high oxygen fugacity conditions and the residual carbon thermal solutions have given rise to carbonatite veins. Srivastava (1989) attribute fractional crystallization of primary hydrous basanitic liquid responsible for different rock types.

CHAPTER III

EXPERIMENTAL TECHNIQUES

This chapter describes the experimental techniques and methodology employed during the course of this work. The chapter is divided into three parts. In the first two parts K-Ar and ^{40}Ar - ^{39}Ar dating techniques and their experimental details are discussed. The third part outlines briefly Rb-Sr dating method and the procedures for sample crushing, chemical processes for separation of Rb and Sr, mass spectrometric work for Rb and Sr isotopic analysis and XRF analysis. The XRF studies were carried out at Wadia Institute of Himalayan Geology (WIHG), Dehradun and the Rb and Sr isotopic studies were carried out at KDM Institute of Petroleum Exploration (KDMIPE), ONGC, Dehradun in addition to the analysis done at Physical Research Laboratory (PRL), Ahmedabad.

3.1. POTASSIUM-ARGON DATING

3.1.1. PRINCIPLE

Potassium in nature consists of three isotopes, viz. ^{39}K , ^{40}K and ^{41}K with abundances of 93.2581%, 0.01167% and 6.7302%, respectively. Of these ^{40}K is radioactive, decaying to ^{40}Ar (half life 1.25×10^9 years) by electron capture and to ^{40}Ca by β^{-1} decay (Fig. 3.1). The branch yielding radioactive argon ($^{40}\text{Ar}^*$) as daughter product provides the basis for the K-Ar dating technique through its accumulation over geological time.

In the simplest case of an igneous rock, the K-Ar method normally yields an age that is equal to the time that has elapsed since its eruption and cooling. The argon being an inert gas do not make any crystal lattice bonding and instead simply stay in the crystal lattices as neutral atoms. Any thermal shock at any time after its accumulation will cause diffusion of argon from the lattices. Thus, rocks that have experienced elevated

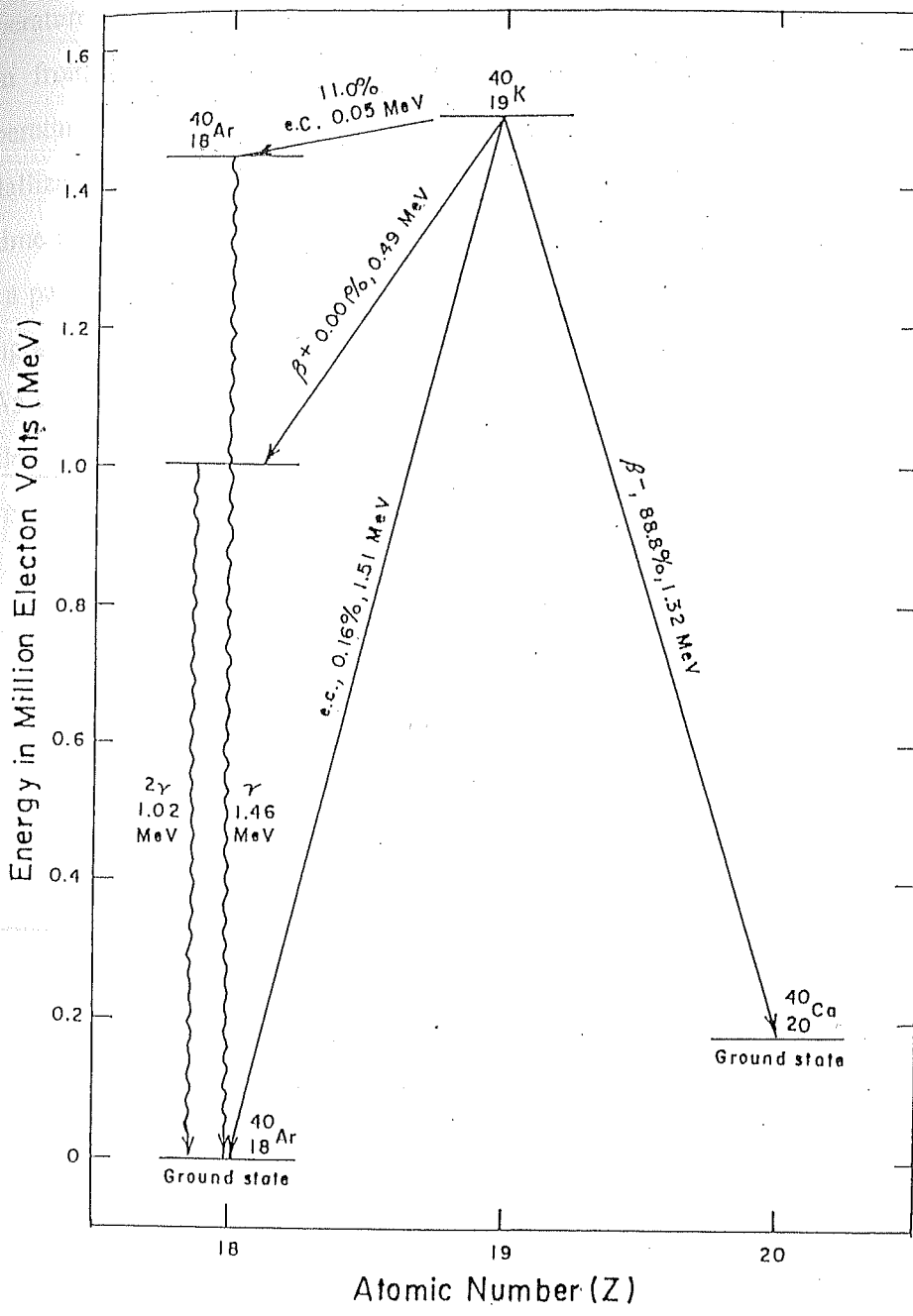


Fig. 3.1. Decay Scheme Diagram for the Branched Decay of $^{40}\text{K}_{19}$ to $^{40}\text{Ar}_{18}$ by Electron Capture and by Positron Emission and to $^{40}\text{Ca}_{20}$ by Emission of Negative Beta Particles.

temperature after crystallization may partially or completely lose accumulated radiogenic argon from their constituent minerals, depending upon the diffusion behavior, the temperature and the time involved. A K-Ar age, therefore, may register the time since crystallization and cooling below a critical temperature (which blocks argon diffusion), the time since cooling after a metamorphic event or an intermediate age that does not date a particular event, but simply reflects partial loss of radiogenic argon by diffusion during a metamorphic event.

As with all isotopic dating methods, there are number of assumptions that must be fulfilled for a K-Ar age to be related to any geological event. The most important assumptions are:

1. *The radiogenic argon measured in a sample is produced by in-situ decay of ^{40}K in the interval since the rock crystallized or is recrystallized.*
2. *Corrections can be made for non-radiogenic ^{40}Ar present in the rock being dated. For terrestrial rocks the assumption generally is made that all such argon is atmospheric in composition with $(^{40}\text{Ar}/^{36}\text{Ar})_{\text{atm}} = 295.5$.*
3. *Potassium is homogeneously distributed in the sample.*
4. *The sample must have remained in a closed system since the event being dated. Thus, there should have been no loss or gain of potassium or ^{40}Ar , other than by radiogenic decay of ^{40}K .*

In the K-Ar dating method, the potassium and argon are measured on two separate portions of the sample. Potassium is measured as total potassium and the amount of total ^{40}K is calculated from the known present day isotopic composition of potassium (Steiger and Jager, 1977). The most commonly used techniques of potassium measurement are flame-photometry, atomic absorption spectro-photometry and isotope dilution mass spectrometry. Argon normally is determined by isotope dilution technique. Following purification of the argon, isotopic analysis is carried out by means of mass spectrometry, from which the content of ^{40}Ar can be calculated. Since, in the present work provision for isotope dilution is not available, sensitivity of the mass spectrometer for ^{40}Ar measurement is experimentally determined using a known age standard (e.g. MMhb-1 of 520.4 ± 1.7 Ma, Samson and Alexander, 1987).

3.1.2. AGE EQUATION

If $^{40}\text{Ar}^*$ is the radiogenic daughter accumulated by spontaneous decay of ^{40}K in a rock of age 't', then

$$^{40}\text{Ar}^* = (\lambda_e/\lambda) \times ^{40}\text{K} (e^{\lambda t} - 1) \quad \text{---- (1)}$$

$$\text{or } t = (1/\lambda) \times \ln [(\lambda \cdot ^{40}\text{Ar}^*/\lambda_e \cdot ^{40}\text{K}) + 1]$$

where,

λ_e = decay constant of electron capture ($0.581 \times 10^{-10}/\text{a}$)

λ_β = decay constant of β^{-1} decay ($4.962 \times 10^{-10}/\text{a}$)

$\lambda_e + \lambda_\beta = \lambda$ = Total decay constant ($5.543 \times 10^{-10}/\text{a}$)

$^{40}\text{K}/\text{K} = 0.0001167$ (Steiger and Jager, 1977)

3.2. ^{40}Ar - ^{39}Ar DATING

3.2.1. PRINCIPLE

To overcome some of the shortcomings of the K-Ar method viz. potassium inhomogeneity in the sample, the loss of argon due to thermal event or the presence of excess argon etc., which bring uncertainty in the age interpretation, a new method i.e. ^{40}Ar - ^{39}Ar method was developed (Merrihue and Turner, 1966) which is an analytical conversion of the conventional K-Ar method.

In the ^{40}Ar - ^{39}Ar method, the sample to be dated is first irradiated in a nuclear reactor to transform a portion of the ^{39}K to ^{39}Ar by the fast neutron reaction i.e. $^{39}\text{K}(n,p)^{39}\text{Ar}$, which has a threshold neutron energy of 1.2 Mev. After irradiation, the sample is placed in an ultra-high vacuum system and the argon extracted from it by fusion is purified and analyzed isotopically in a mass spectrometer.

The amount of ^{39}Ar produced, due to irradiation with fast neutrons, is given by:

$$^{39}\text{Ar}_K = ^{39}\text{K} \Delta t \int \phi(\epsilon) \sigma(\epsilon) d(\epsilon) \quad \text{---- (2)}$$

where Δt is the irradiation time, $\phi(\epsilon)$ is the neutron flux at energy ϵ and $\sigma(\epsilon)$ is the neutron capture cross section at energy ϵ for $^{39}\text{K}(n,p)^{39}\text{Ar}$ reaction. The integration is for over all energies of the incident neutrons.

Combining eqn. (1) and (2) will give:

$$\frac{^{40}\text{Ar}^*}{^{39}\text{Ar}_K} = \frac{^{40}\text{K} (e^{\lambda t} - 1)}{^{39}\text{K} \Delta t \int \phi(\epsilon) \sigma(\epsilon) d(\epsilon)} \quad \text{---- (3)}$$

It is convenient to define a dimensionless irradiation parameter "J" as follows:

$$J = \frac{^{39}\text{K} \Delta t \int \phi(\epsilon) \sigma(\epsilon) d(\epsilon)}{^{40}\text{K}} \quad \text{---- (4)}$$

substituting eqn. (4) in (3) gives:

$$\frac{^{40}\text{Ar}^*}{^{39}\text{Ar}_K} = \frac{e^{\lambda t} - 1}{J}$$

which, upon rearrangement allows calculation of the age "t" of the sample as follows:

$$t = \frac{1}{\lambda} \ln (1 + J \ ^{40}\text{Ar}^*/^{39}\text{Ar}_K) \quad \text{---- (5)}$$

where $^{40}\text{Ar}/^{39}\text{Ar}$ = the ratio of radiogenic ^{40}Ar to the potassium derived ^{39}Ar by neutron irradiation of the sample.

From eqn. (5) age of the sample can be calculated provided the irradiation parameter

"J" is known, which is dependent upon the duration of the irradiation, the neutron flux and the reaction cross section. Because of the difficulties encountered in accurately determining the relevant integrated fast neutron fluence that a sample has received, a monitor or standard sample, whose age is precisely known, is irradiated along with the unknown samples to monitor the fluence.

In the case of monitor sample, rearrangement of eqn. (5) will give:

$$J = \frac{(e^{\lambda t_m} - 1)}{(^{40}\text{Ar}^*/^{39}\text{Ar}_K)_m} \quad \text{--- (6)}$$

Since age of the monitor sample (t_m) is known, so by simply measuring the $(^{40}\text{Ar}^*/^{39}\text{Ar}_K)_m$ in the gas extracted from the monitor sample after irradiation, the parameter "J" can be determined.

This value of J is then used in eqn. (5), together with the $(^{40}\text{Ar}^*/^{39}\text{Ar}_K)$ ratio measured on the unknown sample irradiated at the same time, to calculate its age "t".

When a rock is irradiated with fast neutrons, many reactions produce interfering argon isotopes. These sources of interference have been discussed in detail by Mitchell (1968), Brereton (1970), Dalrymple and Lanphere (1971), Turner (1971), Tetley et al. (1980) and Dalrymple et al. (1981). Out of the various possible reactions (Table 3.1), the following four reactions produce significant interferences:



The measured concentrations of different argon isotopes represent the cumulative effect of various interferences as shown below:

$$^{36}\text{Ar}_m = ^{36}\text{Ar}_{\text{atm}} + ^{36}\text{Ar}_{\text{Ca}}$$

$$^{37}\text{Ar}_m = ^{37}\text{Ar}_{\text{Ca}}$$

$$^{39}\text{Ar}_m = ^{39}\text{Ar}_{\text{K}} + ^{39}\text{Ar}_{\text{Ca}}$$

$$^{40}\text{Ar}_m = ^{40}\text{Ar}_{\text{atm}} + ^{40}\text{Ar}_{\text{K}} + ^{40}\text{Ar}^*$$

where subscript **m** stands for measured, **Ca** for calcium derived, **K** for potassium derived, **atm** for trapped initial component and superscript ***** for radiogenic argon component.

Therefore, to determine $(^{40}\text{Ar}^*/^{39}\text{Ar})_{\text{K}}$ ratio to be used in the age calculation, the $^{40}\text{Ar}/^{39}\text{Ar}$ ratio measured in the mass spectrometer needs to be corrected for atmospheric, calcium and potassium derived interfering isotopes.

Table 3.1. Interfering nuclear reactions caused by neutron irradiations of samples (Brereton, 1970)

Argon Isotope Produced	Calcium	Potassium	Argon	Chlorine
^{36}Ar	$^{40}\text{Ca}(\text{n}, \text{n}\alpha)$	-	-	-
^{37}Ar	$^{40}\text{Ca}(\text{n}, \alpha)$	$^{39}\text{K}(\text{n}, \text{nd})$	$^{36}\text{Ar}(\text{n}, \alpha)$	-
^{38}Ar	$^{42}\text{Ca}(\text{n}, \text{n}\alpha)$	$^{39}\text{K}(\text{n}, \text{d})$ $^{41}\text{K}(\text{n}, \alpha, \beta^-)$	$^{40}\text{Ar}(\text{n}, \text{nd}, \beta^-)$	$^{37}\text{Cl}(\text{n}, \gamma, \beta^-)$
^{39}Ar	$^{42}\text{Ca}(\text{n}, \alpha)$ $^{43}\text{Ca}(\text{n}, \text{n}\alpha)$	$^{39}\text{K}(\text{n}, \text{p})^{\text{a}}$ $^{40}\text{K}(\text{n}, \text{d})$	$^{38}\text{Ar}(\text{n}, \gamma)$ $^{40}\text{Ar}(\text{n}, \text{d}, \beta^-)$	-
^{40}Ar	$^{43}\text{Ca}(\text{n}, \alpha)$ $^{44}\text{Ca}(\text{n}, \text{n}\alpha)$	$^{40}\text{K}(\text{n}, \text{p})$ $^{41}\text{K}(\text{n}, \text{d})$	-	-

^aThis is the principal reaction on which the ^{40}Ar - ^{39}Ar method is based.

Significant amount of ^{36}Ar and ^{39}Ar are produced from calcium during neutron irradiation, and unless proper corrections are made, erroneous ^{40}Ar - ^{39}Ar ages will be obtained. The atmospheric ^{40}Ar is corrected by means of ^{36}Ar . Clearly, if the ^{36}Ar produced from ^{40}Ca during irradiation is not taken into account, there will be over correction for atmospheric ^{40}Ar , resulting in low apparent ages. ^{37}Ar is solely derived from ^{40}Ca and can be used to correct for both reactor induced ^{36}Ar and ^{39}Ar derived from calcium (Brereton, 1970). The correction factor, $(^{36}\text{Ar}/^{37}\text{Ar})_{\text{Ca}}$ and $(^{39}\text{Ar}/^{37}\text{Ar})_{\text{Ca}}$ are determined by measuring the relative production rates of these isotopes in pure calcium salt i.e. CaF_2 after neutron irradiation. Similarly, correction is also made for neutron induced ^{40}Ar produced from potassium. The correction factor $(^{40}\text{Ar}/^{39}\text{Ar})_{\text{K}}$ is determined by measuring the relative production rates of these isotopes in the pure potassium salt i.e. K_2SO_4 after the irradiation. After incorporating these corrections the expression for $(^{40}\text{Ar}^*/^{39}\text{Ar}_{\text{K}})$ becomes:

$$\frac{^{40}\text{Ar}^*}{^{39}\text{Ar}_{\text{K}}} = \frac{\left(\frac{^{40}\text{Ar}}{^{39}\text{Ar}}\right)_{\text{m}} - 295.5 \left(\frac{^{36}\text{Ar}}{^{39}\text{Ar}}\right)_{\text{m}} - \left(\frac{^{36}\text{Ar}}{^{37}\text{Ar}}\right)_{\text{Ca}} \times \left(\frac{^{37}\text{Ar}}{^{39}\text{Ar}}\right)_{\text{m}}}{1 - \left(\frac{^{39}\text{Ar}}{^{37}\text{Ar}}\right)_{\text{Ca}} \times \left(\frac{^{37}\text{Ar}}{^{39}\text{Ar}}\right)_{\text{m}}} - \left(\frac{^{40}\text{Ar}}{^{39}\text{Ar}}\right)_{\text{K}}$$

where $(^{40}\text{Ar}/^{39}\text{Ar})_{\text{m}}$, $(^{36}\text{Ar}/^{39}\text{Ar})_{\text{m}}$ and $(^{37}\text{Ar}/^{39}\text{Ar})_{\text{m}}$ are the measured ratio of these isotopes and $(^{36}\text{Ar}/^{37}\text{Ar})_{\text{Ca}}$, $(^{39}\text{Ar}/^{37}\text{Ar})_{\text{Ca}}$ and $(^{40}\text{Ar}/^{39}\text{Ar})_{\text{K}}$ are the neutron induced correction factors for calcium and potassium. The correction factors used to correct the effects of calcium and potassium interfering isotopes are given in Table 3.2.

The variation in Ca produced $(^{36}\text{Ar}/^{37}\text{Ar})_{\text{Ca}}$ and $(^{39}\text{Ar}/^{37}\text{Ar})_{\text{Ca}}$ ratios in the two irradiations is about 23% and 21%, respectively, while that in K produced $(^{40}\text{Ar}/^{39}\text{Ar})_{\text{K}}$ the variation is quite large (about 41%). The larger variation in K produced $(^{40}\text{Ar}/^{39}\text{Ar})_{\text{K}}$ ratio is probably due to large variations in the thermal neutron flux (Tetley et al., 1980).

Table 3.2. Results obtained on irradiated salts (these ratios are used to correct interfering isotopes; ^{37}Ar is corrected for decay).

Salt	$(^{40}\text{Ar}/^{39}\text{Ar})_{\text{K}}$ $\times 10^{-2}$	$(^{39}\text{Ar}/^{37}\text{Ar})_{\text{Ca}}$ $\times 10^{-4}$	$(^{36}\text{Ar}/^{37}\text{Ar})_{\text{Ca}}$ $\times 10^{-4}$	Irradiation No.
K_2SO_4	7.5780	-	-	IRRN # 13
K_2SO_4	4.4807	-	-	IRRN # 16,17
CaF_2	-	9.058	1.488	IRRN # 13
CaF_2	-	7.115	1.150	IRRN # 16,17

3.2.2. DECAY FACTOR

As both ^{37}Ar and ^{39}Ar are radioactive, it is important to correct for their decay during and subsequent to irradiation. As the half life for ^{39}Ar is 269 ± 3 yrs (Stoenner et al., 1965) and the sample is analyzed within few weeks/months after the irradiation, the correction will always be negligible. In contrast, the half life of ^{37}Ar is only 35.1 days (Stoenner et al., 1965), significant decay will occur during irradiation, and in the interval between the end of the irradiation and analysis. Therefore, proper allowance for its decay must be made, more so because ^{37}Ar is used as the reference isotope to enable corrections to ^{36}Ar and ^{39}Ar produced from calcium during irradiation. Following Brereton (1970) and Dalrymple et al. (1981), the relevant general equation for the decay factor is:

$$\text{Decay Factor} = \lambda t e^{\lambda t} / (1 - e^{-\lambda t}) \quad \text{---- (7)}$$

where t is the irradiation time and t' is the time elapsed between the end of the irradiation and analysis.

Further, because of operational requirements of the reactor, or for other reasons, irradiation may be done in a number of discrete intervals or segments. As given by Wijbrans (1985) and Pande et al. (1988), the generalized form of decay factor used for segmented irradiation is given by:

$$\text{Decay Factor} = \lambda \sum_{i=1}^n t_i / \sum_{i=1}^n [(1 - e^{-\lambda t_i}) / e^{-\lambda t'}] \quad \text{----- (8)}$$

where t_i is the duration of irradiation of segment i . t_i' is the time elapsed between the end of the irradiation segment i and analysis of the sample, n is the total number of irradiation segments and λ is the decay constant for ^{37}Ar .

The most important advantage of ^{40}Ar - ^{39}Ar method is the graphical depiction of the analytical data. The sample is normally heated in incremental temperature steps until fusion and at each temperature step isotopic ratio i.e ($^{40}\text{Ar}^*/^{39}\text{Ar}_K$) is measured, which should be identical if the sample has not been disturbed after formation. In this case both $^{40}\text{Ar}^*$ and $^{39}\text{Ar}_K$ belong to the same lattice sites occupied originally by ^{40}K . Hence the ratio of $^{40}\text{Ar}^*/^{39}\text{Ar}_K$ will remain constant. When these ratios (or apparent ages calculated using these ratios) are plotted against temperature (or more commonly cumulative % of ^{39}Ar) they define a spectrum of ages which are essentially parallel to the X axis. The age obtained from different temperature steps, which mutually agree (within experimental errors), is called as a plateau age and the diagram is known as the age spectrum diagram. However, if the sample has been affected by secondary thermal processes, then it would give a disturbed spectrum from which also useful information can be construed.

3.2.3. EXPERIMENTAL DETAILS

3.2.3.A. SAMPLE PREPARATION FOR IRRADIATION

Fresh whole rock samples, powdered to 20 to 80 mesh size by a stainless steel mortar

and pestle, were used in all the studies. About 600-700 mg of homogenized powder of each sample was used for irradiation. The 520.4 ± 1.7 Ma old Minnesota Hornblende (MMhb-1) (Samson and Alexander, 1987) was used as a monitor.

The whole rock powder samples and monitor alongwith pure CaF_2 and K_2SO_4 were filled in cleaned quartz vials. Two type of vials were used for irradiation viz. 6-7 mm diam. vials for rock samples and 2-3 mm diam. vials for K_2SO_4 , CaF_2 and monitor. To minimize the effects of the vertical flux gradient, all the vials were filled to the same height.

To determine the fluence received by each sample relative to that of the monitor pure Ni wire was included in each sample vial. These vials were sealed at atmospheric pressure and packed in an aluminium reactor can. The reactor can was sealed and irradiated for about 20 days in the APSARA reactor of Bhabha Atomic Research Center (BARC), Bombay.

3.2.3.B. IRRADIATION OF SAMPLES

The samples were irradiated in two batches in APSARA reactor of BARC, Bombay. This is a light water moderated reactor with neutron flux of about 10^{12} neutron/cm²/sec with the fast flux representing about 50-60% of the total. The samples were irradiated in D4 (core) position of the reactor which receives maximum flux with minimum variation. The irradiation was done for 73 and 75 hours at 1 MW power level in 12 and 15 discrete steps spreading over 20 and 25 days, respectively. The maximum and minimum duration of the irradiation in a step was of seven and one hour, respectively. The total flux received by the samples was about 2.6×10^{17} neutron/cm². The vertical variation in the fluence was not measured but the horizontal fluence variation as measured by ⁵⁸Co activity was found to be about 5.5 and 3.8%, respectively.

After irradiation, the samples were stored in a separate room for about a month to allow the high level, short lived radioisotopes to decay. Samples were then split into aliquots, weighed and wrapped in aluminium foils and loaded in the sample holder of the argon extraction system.

3.2.3.C. EXTRACTION AND PURIFICATION OF ARGON

A brief description of the technique employed in argon extraction and purification is given here. The approaches used in for both the conventional K-Ar and ^{40}Ar - ^{39}Ar dating methods are similar. The major differences are that in K-Ar dating the sample is fused directly, while in ^{40}Ar - ^{39}Ar dating the sample is heated in incremental steps until it is fused completely.

An argon extraction and purification system is illustrated schematically in Fig. 3.2. It consists essentially of a high vacuum line with appropriate pumping facilities, a furnace assembly in which a sample can be heated in a controlled manner to release argon, getter systems for purification of the released gases, isolation valves and activated charcoal trap cooled at -196°C for moving gas from one part of the line to another.

The furnace of the extraction unit is an all metal, compact and indigenously made resistance heater (Fig. 3.3). It consists of a molybdenum crucible with a plug forming its base into which a thermocouple is inserted. The crucible is electrically heated by a concentric tantalum filament which in turn is surrounded by tantalum heat shield in a stainless steel vacuum chamber. Power for the heater, derived from a variac controlled low voltage, high current transformer, is delivered by means of a copper feed-through. The temperature of the crucible is measured with a 95% Pt + 5% Rh - 80% Pt + 20% Rh thermocouple, which has been calibrated earlier by optical pyrometry. The temperatures are estimated to be accurate to $\pm 50^\circ\text{C}$. The outer SS jacket of furnace is connected to chilled water supply for cooling purpose. Samples are dropped into the crucible from a glass sample holder connected to the top flange.

The gas purification system consists of five valves (V_1 - V_4 and V_9) and five getters (Fig. 3.2). The valves V_1 - V_4 are interconnected and fitted on a single rectangular stainless steel block. The middle section of this block is shown in Fig. 3.4.

The sample gas released from the crucible, first comes in contact with Ti-Zr getter connected between valve V_2 and V_3 . The Ti-Zr getter is kept hot at around 800°C when most of the active gases will either chemically combine with or be absorbed by the getter. Further, on cooling to room temperature this getter will adsorb hydrogen present

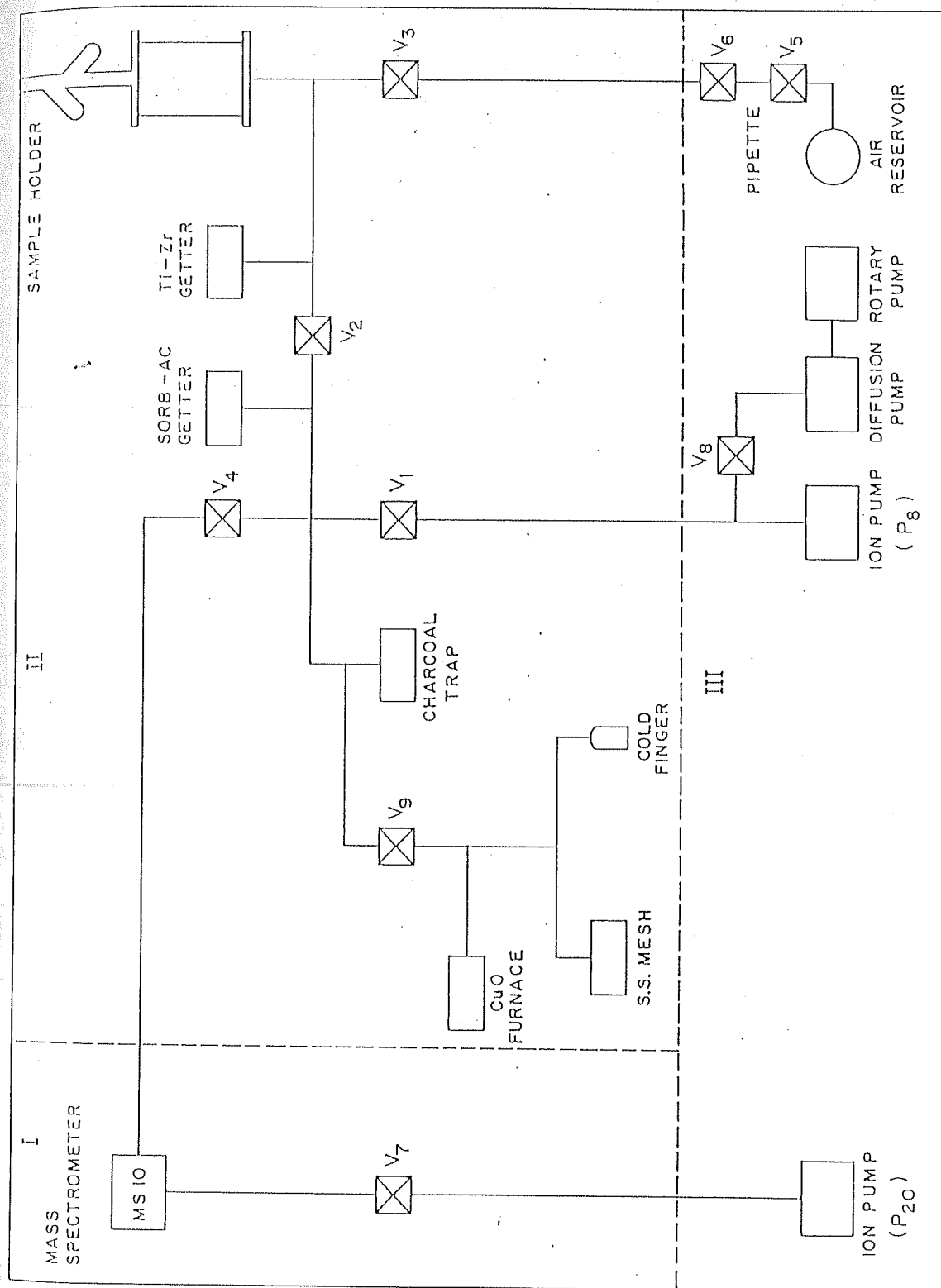


Fig. 3.2. Schematic of the Complete Mass Spectrometer, Gas Extraction - Purification System.

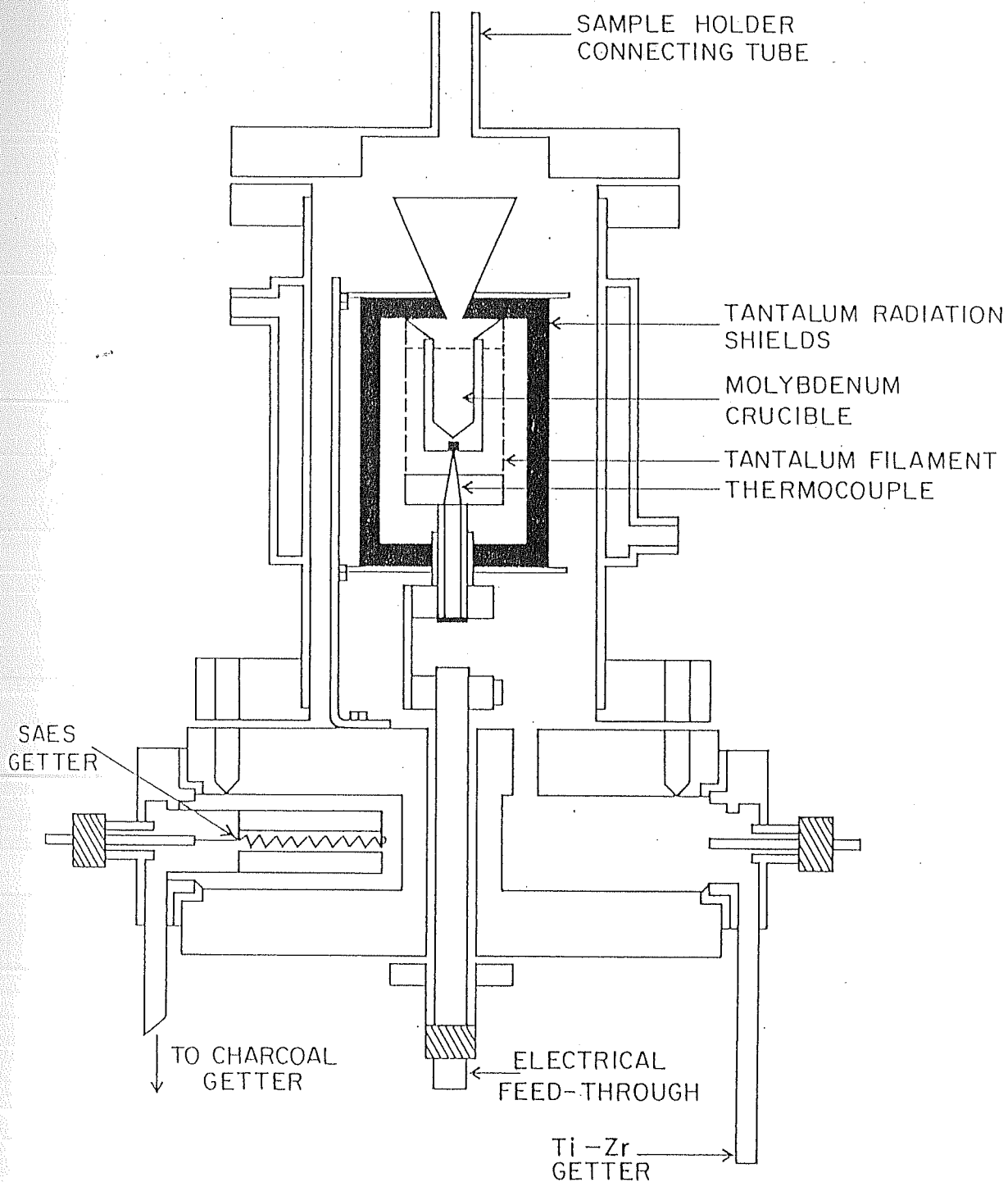


Fig. 3.3. Section through Gas Extraction Furnace and Purification Line.

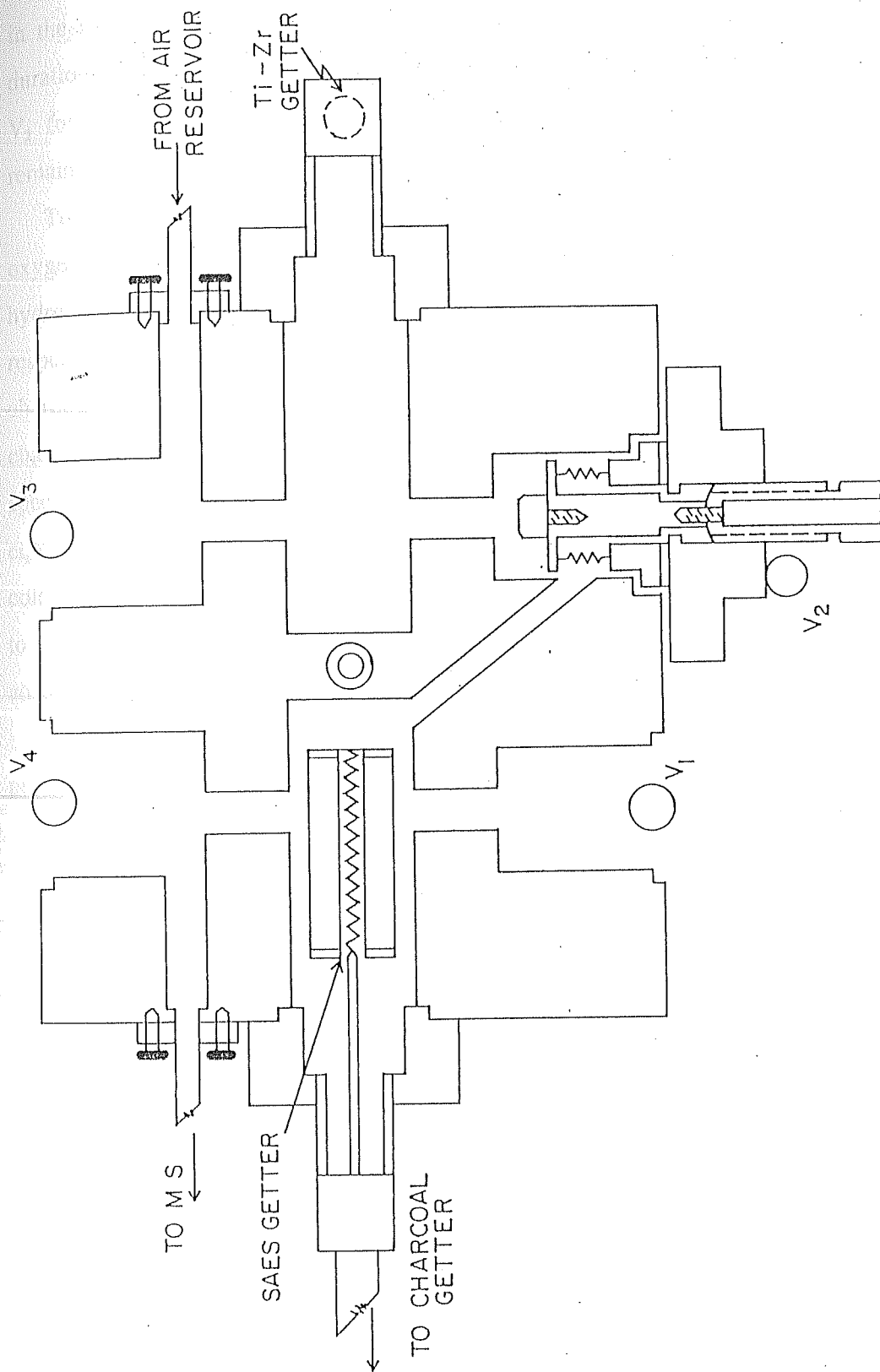


Fig. 3.4. Middle Section of the S-S Block with Only One Valve Assembly

in the sample gas. Thus, the cleaned gas, accumulated for about 50 minutes (typical duration of a temperature step) is allowed to react with SAES getter by opening valve V_2 for further purification. The water vapour is adsorbed on cold finger and the remaining gas is taken on stainless steel mesh kept at liquid nitrogen temperature.

The second round of cleaning is done by oxidation reactions in CuO furnace. The oxygen released from CuO furnace (kept at around 800°C) react with the hydrogen and hydrocarbons present in the sample gas and form water molecules and carbon dioxide, respectively, which are retained on the cold finger. The CuO furnace is isolated from charcoal finger by the valve V_9 . The purified gas thus left with argon is adsorbed on the charcoal cooled at liquid nitrogen temperature. It is then admitted into the mass spectrometer after 10 minutes through valve V_4 for isotopic analysis. After the gas is equilibrated in the mass spectrometer, (say 2 minutes) V_4 is closed. The charcoal finger, cold finger and s.s. mesh are connected to ion pump (P_8) by opening valve V_9 and V_1 to pump out the remaining gas. The similar procedure is adopted for cleaning up and adsorption etc. in all the successive steps.

The procedure normally followed in a temperature step for the extraction and purification of argon can be described as follows:

00⁰⁰ Cl V_3 , V_2 , F \uparrow , Ti \uparrow , Water on to cool furnace wall

00²⁰ Ti \downarrow

00⁴⁵ SSM \downarrow , Ch \downarrow

00⁵³ Cl V_1 , Op V_2 , LN₂ on CF, F \downarrow

00⁵⁵ LN₂ on SSM

01¹⁵ Cl V_9 , LN₂ on Ch, SSM \uparrow , CF \uparrow , CuO \uparrow

01²³ Cl V_7 , Op V_4 , F (residual)

01²⁵ Cl V_4 , Cl V_2 , Ti \uparrow , Ch \uparrow , F \uparrow (next step)

01³⁰ CuO \downarrow

01⁴³ Op V_9 , LN₂ on CF

01⁴⁵ LN₂ on Ch

01⁵⁵ Cl V_9 , Ch \uparrow , Cl V_7 , MSBG, SSM \uparrow (heater), CF \uparrow

02⁰⁵ Check V_7 Cl, Op V_4 , Let in gas into MS

02⁰⁷ Cl V₄, Op V₁, V₉, Ch↑ (heater)

02³² Op V₇

The abbreviations used are:

Cl = Close, F = Furnace, Ti = Ti-Zr getter, SSM = Stain less Steel Mesh, Ch = Charcoal, LN₂ = Liquid Nitrogen, CF = Cold Finger, MSBG = Mass Spectrometer Back Ground, ↑ = Up, and ↓ = Down.

In the **K-Ar** studies, the samples were heated in a single temperature step to about 1500°C. At this temperature most of the rock-forming minerals melt away, while in the ⁴⁰Ar-³⁹Ar studies, the samples were degassed in steps, normally sixteen, of successively higher temperature, starting from 400°C until fusion at about 1500°C. The K₂SO₄, CaF₂ and monitor sample (MMhb-1) were, however, degassed in single temperature (1500°C) step. The gas in each temperature step was purified following the procedure described earlier in this section and then admitted into the MS10S (180° deflection, 5 cm radius) mass spectrometer having permanent magnet of 1.8 kilo gauss. The mass spectrometer was operated in the static mode. By voltage scanning, the ions of masses 40, 39, 38, 37, and 36 were collected on a Faraday cup and the ion currents measured sequentially in picco amperes (pa) were recorded on a chart recorder Fig 3.5.

In case of **K-Ar** method, since there was no production of ³⁹Ar and ³⁷Ar, ion currents corresponding to ⁴⁰Ar, ³⁸Ar and ³⁶Ar were recorded. The peak heights and the corresponding time of peak measurements from the time 't₀' i.e. the time of admission of the gas into the mass spectrometer, measured manually, were used for the best fit (Bevington, 1969) to compute the required isotopic abundances and ratios.

The system blanks were measured at different temperatures before and after each sample. The blank measurement consisted of measuring the argon concentration by following the same procedure as for the sample but without having any sample in the crucible. Since the actual blank contribution during each heating step was not known, therefore, the blank correction at each temperature step was calculated using the graph made by plotting the measured blank against the temperature. The mean ⁴⁰Ar blank at 500°C was 4.4 x 10⁻⁹ cc STP, rising to 1.9 x 10⁻⁸ cc STP at 1500°C. Thus, the blank contribution to the sample gas were very small varying from 2-4% upto 1300°C

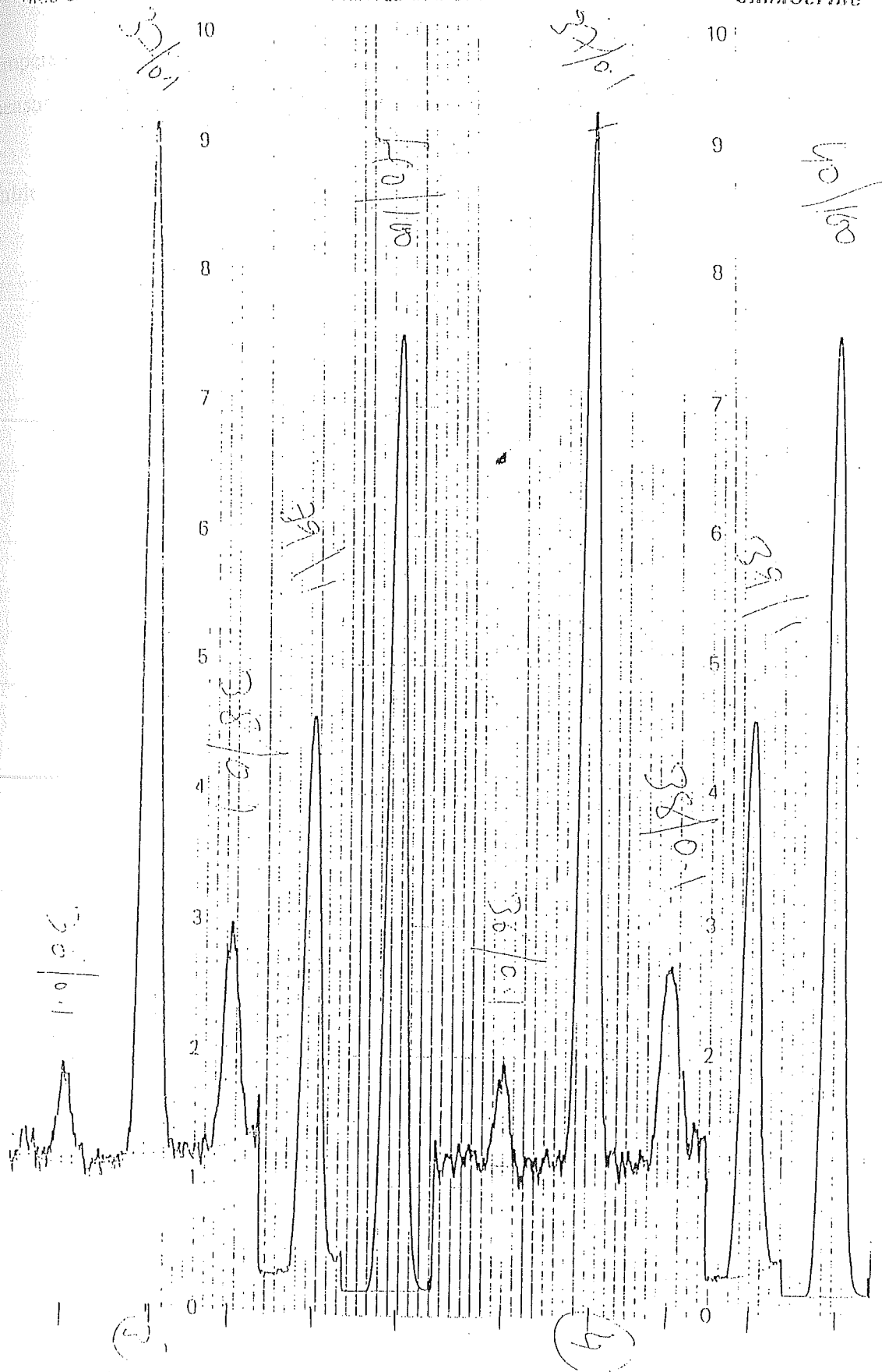


Fig. 3.5. Typical Argon Spectrum.

temperature but increased to about 10-20% in the fusion step. Typical blank contributions measured for the sample VA/181 at various temperature steps are given in Table 3.3.

Table 3.3. Percentage of system blanks calculated for different temperature steps in sample VA/181.

Temperature °C	Argon Isotopes			
	^{36}Ar	^{37}Ar	^{39}Ar	^{40}Ar
450	4.53	-	-	2.59
500	5.22	-	-	2.74
550	9.60	-	-	1.02
750	5.85	-	-	0.22
800	18.20	-	-	0.50
900	13.31	-	-	0.67
1000	4.02	-	-	0.36
1050	5.36	-	-	0.59
1150	10.17	-	-	1.08
1250	11.91	-	-	1.75
1350	26.40	-	-	3.81
1500	56.09	-	-	14.69

Mass discrimination (MD) corrections were done by analyzing atmospheric argon (AIR SPIKE) introduced from a pipette system. Each sample was followed and preceded by Air Spike analysis and an average of the pre and the post analysis was used for the MD correction. The measured atmospheric $^{40}\text{Ar}/^{36}\text{Ar}$ ratios fell randomly in the range of

308-312 and did not show any relation with the filament life. Mass spectrometer sensitivity was estimated from repeated measurement of the monitor sample (MMhb-1) and was typically in the range of $1.2-1.4 \times 10^{-8}$ cc STP/pa. Errors were computed by quadratically propagating the errors in the measured ratios, blanks and interfering isotopes. An error of $\pm 25\%$ in the atmospheric argon blank was also applied. The error quoted on the apparent and integrated ages include the error in J but the error boxes in age spectra plots do not include the error in J. All the errors are quoted at 2σ level. Isochron ages have been computed using the two error regression method outlined by York (1969) of data points corresponding to the plateau steps. The plateau ages are weighted means of the apparent ages of steps forming the plateau. The total-gas or integrated ages have been computed by appropriate weighting of the apparent ages with $1/\sigma_i^2$. A plateau is considered defined if the ages recorded by 4 or more contiguous temperature steps, each representing $>5\%$ of the total ^{39}Ar evolved and together constituting $>50\%$ of the total ^{39}Ar evolved, are mutually concordant within 2σ uncertainty. If any of the steps in between do not agree with the other steps or the total ^{39}Ar constituting the plateau is less than 50%, we call it as a pseudo plateau.

3.3. RUBIDIUM-STRONTIUM DATING

3.3.1. PRINCIPLE

For Rb-Sr dating, the $^{87}\text{Rb}/^{86}\text{Sr}$ ratios measured for a set of whole rock or mineral separates are plotted against $^{87}\text{Rb}/^{86}\text{Sr}$ ratios which conform to a straight line on Sr-evolution diagram, provided all the samples had commenced with the same $^{87}\text{Sr}/^{86}\text{Sr}$ ratio and have remained in a chemically closed system since the time 't' of its formation (Nicolaysen, 1961; Lanphere et al., 1964). Such a straight line, called an isochron, is defined by the equation :

$$(^{87}\text{Sr}/^{86}\text{Sr})_m = (^{87}\text{Sr}/^{86}\text{Sr})_i + (^{87}\text{Rb}/^{86}\text{Sr}) (e^{\lambda t} - 1) \quad \text{---- (9)}$$

where, λ is the decay constant of ^{87}Rb .

The slope of this isochron gives the time since the sample remained closed and the intercept on the ordinate directly gives the initial $^{87}\text{Sr}/^{86}\text{Sr}$ composition. In cases where there is independent geological and chemical evidence that the samples are cogenetic, it can be interpreted as the time elapsed since the whole rock samples last became closed to Rb and Sr. It can be seen from the eqn. (9) that the samples with poor radiogenic Sr enrichment closely determine the intercept while those with high radiogenic enrichment constrain the slope. Therefore, a good dispersion in the Rb/Sr ratios is desirable so as to have good control on the isochron.

Since the data points are subject to analytical errors, they do not strictly align on a straight line. This leads to the problem of determination of the slope and intercept for a given set of experimental points. The best fit line obtained by simple regression techniques, in which one of the co-ordinates is assumed to be free of errors, is not satisfactorily valid. Murthy and Compston (1965) and York (1966) developed a procedure in which allowance is made for errors in both the co-ordinates. The procedure assumes that the errors are uncorrelated and normally distributed. Individual weighting factors are assigned to each point. These are commonly the inverse square of experimental errors.

York (1966) gave somewhat simplified expressions for uncertainties in slope and intercept. However, he did not specify any criterion to test the goodness of fit of the straight line to the data. Mc Intyre et al. (1966) gave a slightly different weighting method and gave exact expressions for variances of slope and intercept and also specified that the goodness of fit can be judged by computing a quantity called 'mean square of weighted deviates (MSWD)' given by:

$$\text{MSWD} = \frac{1}{N-2} \left[\sum_{i=1}^N W_i (a + bx_i - Y_i)^2 \right] \quad \text{---- (10)}$$

Where W_i is a function of $W(X_i)$, $W(Y_i)$ and slope (b). The quantity under the bracket is distributed as χ^2 and has an expectation of $N-2$. MSWD should, therefore, be

close to unity. If the MSWD significantly exceeds unity, it implies that either (a) the measurements are less accurate than supposed in the calculation of weights or, (b) various assumptions underlying the expectation of a linear isochron plot have not been satisfied. In other words (a) some of the samples may have been in open system with respect to Rb and/or Sr, (b) the samples may not have commenced with the same initial $^{87}\text{Sr}/^{86}\text{Sr}$ ratio, and/or, (c) the samples may not be of the same age. In such cases, where MSWD greatly exceeds 1, the authors call the isochron an 'errorchron' and suggest various models for weighting the data in such a way as to make MSWD close to unity. Slope is recalculated with new weights. The underlying assumption is that the scatter of data in such cases is due to geological processes over and above the analytical errors. Brooks et al. (1968) recommended yet another weighting procedure. York (1969) gave a method for correlated errors. The relative merits of all these methods have been reviewed by Brooks et al. (1972). Williamson (1968), adopting a similar weighting technique as York (1966), showed that the least squares cubic is redundant and can be reduced to a linear equation. He also gave an exact expression for variance in the slope and intercept and also criteria for testing the goodness of fit by performing χ^2 test on the expression within the parenthesis in eqn. (10). However, York (1969) method has been followed for regression of the data presented in this study.

For the present study, only representative samples with good spread in Rb/Sr ratios were selected. The cut off value for MSWD has been fixed at 2. The uncertainty in the slope and intercept has been quoted at 2σ level. The ages have been calculated using the decay constant of ^{87}Rb as $1.42 \times 10^{-11} \text{ yr}^{-1}$ as recommended by IUGC Subcommittee on Geochronology (Steiger and Jager, 1977). For petrogenesis purposes, $(^{87}\text{Sr}/^{86}\text{Sr})_i$ ratios are calculated using $(^{87}\text{Sr}/^{86}\text{Sr})_m$ and an appropriate age. The $(^{87}\text{Sr}/^{86}\text{Sr})_i$, thus, calculated is the model value. The errors in the model $(^{87}\text{Sr}/^{86}\text{Sr})_i$ ratios have been calculated by quadratically compounding the errors in $^{87}\text{Rb}/^{86}\text{Sr}$ ratios and $(^{87}\text{Sr}/^{86}\text{Sr})_m$ using the following equation:

$$\sigma_{Ri}^2 = \sigma_{Rm}^2 + AR^2 \cdot \lambda^2 \cdot (e^{\lambda t})^2 \cdot \sigma_t^2 + (e^{\lambda t} - 1)^2 \cdot \sigma AR^2 \quad \text{---- (11)}$$

where,

$$\sigma_{\text{Ri}} = \sigma(^{87}\text{Sr}/^{86}\text{Sr})_{\text{i}}, \sigma_{\text{Rm}} = \sigma(^{87}\text{Sr}/^{86}\text{Sr})_{\text{m}}$$

$$\text{AR} = (^{87}\text{Rb}/^{86}\text{Sr}) \text{ and } \sigma_{\text{AR}} = \sigma(^{87}\text{Rb}/^{86}\text{Sr})$$

Various processes involved in chemical and Rb-Sr isotopic studies are discussed below:

3.3.2. ROCK CRUSHING

Fresh samples each weighing about 10-15 kg were cleaned with brush and distilled water to remove surface contamination, if any. The samples were broken into small pieces using a hammer. Sample pieces containing mineral veins and inclusions were discarded and the residual pieces were then crushed to <3-5 mm size using a jaw crusher (Fritz pulverizer). The crushing surfaces of the pulverizer were cleaned before and after each sample with a high pressure air blast and preconditioned with a small amount of the sample being processed. Crushed samples were thoroughly mixed to ensure homogenization and then poured onto a clean paper for coning quartering. The opposite quarters were collected, which were further quartered to draw about 2-3 kg of the representative coarse fractions. About 1 kg of the coarse fraction was preserved in a polythene bag for further use, if required. The residual coarse fractions were further reduced to 1 mm size using again the jaw crusher and finally about 200-300 g of the representative sample was collected by coning quartering.

This sample fraction (<1 mm size) was powdered to <200 mesh size using a TEMA swing mill and stored in a pre-cleaned and conditioned polythene/plastic bottles. This fraction, which is a homogeneous representative of the whole rock sample, was used for Rb-Sr isotopic studies. Maximum care was taken to prevent any cross contamination.

3.3.3. Rb and Sr ISOTOPIC STUDIES

For dating as well as petrogenesis purpose only whole rock analysis was done. Rb and Sr isotopic studies were carried out at two places i.e. at Physical Research

Laboratory (PRL), Ahmedabad and Keshava Deva Malaviya Institute of Petroleum Exploration (KDMIPE), ONGC, Dehradun.

However, as majority of the samples were analyzed at KDMIPE, the details of various procedures followed at KDMIPE are discussed here. The procedures followed at PRL are given in Trivedi (1990). All chemical operations were carried in a clean HEFA filter laboratory. All labwares were either of teflon or quartz. The procedures for sample dissolution, spike addition and ion exchange chromatography, are given below:

About 150-200 mg of representative powder samples were weighed in a Mettler balance (AE 240) in a 25 ml teflon beaker and were moistened with a few drops of high purity double distilled water. Mixture of acids (4 ml HF + 2 ml HNO₃ + 2 ml HClO₄) were added in the samples and kept in pressure digestion bomb at 150°C for 16 hours. Samples were then evaporated to dryness at 90°C and one more acid treatment (HF + HNO₃) was given to ensure complete digestion. After evaporation of the acid mixtures, the residues were dissolved in about 5 cc of 6N HCl and dried before finally making the solutions in 3 cc of 2.5 N HCl.

3.3.3.A. ISOTOPE DILUTION

The ⁸⁷Rb and ⁸⁴Sr spikes of high purity were used for isotope dilution analysis. The isotopic abundances of the Rb and Sr spikes are given in Table 3.4. The spike concentrations were calibrated against standard solutions of normal Rb and Sr. Working (dilute) Rb and Sr spike solutions having concentrations of about 34 and 5 ppm, respectively, were prepared from mother (concentrate) spike solutions for day to day use. The exact spike concentrations were known only after applying dilution/correction factor. The spike solutions were added by weight before digestion of the samples to ensure complete mixing.

Table 3.4: Isotopic ratios of Rubidium and strontium spikes.

Strontium (^{84}Sr spike)	(Natural ratios*)
$^{86}\text{Sr}/^{84}\text{Sr} = 0.057052$	17.6728
$^{87}\text{Sr}/^{84}\text{Sr} = 0.022779$	
$^{88}\text{Sr}/^{84}\text{Sr} = 0.181299$	148.0137
Rubidium (^{87}Rb spike)	
$^{85}\text{Rb}/^{87}\text{Rb} = 0.009107$	2.5927

*As per Steiger and Jager (1977)

3.3.3.B. ION EXCHANGE CHROMATOGRAPHY

Ion exchange chromatography was used to separate Rb and Sr from the whole rocks. The ion exchange columns were made from quartz tube (I.D. 8 mm) and filled with Dowex 50 X 8% DVB (200-400 mesh) cation exchange resin to a height of 18 cm. 100 ml of 2.5 N HCl was used as eluent.

The sample solutions were centrifuged for 20 minutes in clean polypropylene centrifuge tubes and sucked in 5 ml weight burettes. The samples were then loaded onto the resin bed. The Rb and Sr fractions (28 to 36 and 54 to 72 ml fractions, respectively) were collected in separate beakers, evaporated to dryness and stored for mass spectrometric analysis. The columns were regenerated by passing 50 ml 6N HCl through column bed followed by 50 ml double distilled water and then 50 ml 2.5N HCl.

3.3.4. MASS SPECTROMETRY

At PRL, Ahmedabad, Rb and Sr isotopic studies were carried out on a 23 cm radius 60° sector magnetic field single focussing custom made mass spectrometer. The mass spectrometer is fitted with a thin lens ion source and a faraday cup for collection of ions. The filament holder with source slit is removable so that a new filament could be spot welded, degassed and loaded with sample. Tantalum filaments ($0.030'' \times 0.001''$) of more

than 99.99% purity were outgassed in a separate vacuum system at a temperature higher than that required for efficient ionization of Sr. Samples were taken in a precleaned disposable teflon pipette and evaporated directly on the centre of a predegassed filament. The mass spectrometer is pumped by two ion pumps, 30 l/sec pump for the analyzer tube and 80 l/sec pump for the source region. The source was initially pumped down to a pressure of 10^{-3} torr with a rotary and a sorption pump. It was then isolated from these pumps and gradually opened to the 80 l/sec ion pump. A working pressure of $\approx 10^{-7}$ torr in the source chamber was obtained within an hour after introducing a new sample. The ion acceleration potential used was 4500 V. Ion currents were measured on recently upgraded semi automated data collection system using an IBM PC/XT (Trivedi, 1990). This system controls the mass spectrometer in the peak switching mode, measures the ion currents digitally and computes isotopic ratios. Rb data were taken at 0.1-0.3 V signal level for ^{87}Rb whereas Sr data at 1-3 V level for ^{88}Sr . It was ensured that no residual Rb was left in the sample during Sr isotopic analysis.

At KDMIPE, Rb and Sr isotopic studies were carried out on VG 354 thermal ionization mass spectrometer (270 cm radius, 60° deflection and single focussing) (Fig. 3.6). The mass spectrometer is fitted with a faraday cup as well as a photo multiplier for collection of ions but the multiplier (Daly knob) was not used for Rb and Sr isotopic analysis. The sample turret has a housing of sixteen beads (filaments) which are degassed separately in a degassing unit before loading of the samples. The elements pumping the source housing of the mass spectrometer are the 110 l/sec ion pump, the source titanium sublimation pump and the source cold trap while the analyzer is pumped by means of a 30 l/sec ion pump and a titanium sublimation pump. Rough pumping of the mass spectrometer is done by means of an Edwards E2M5 two stage rotary pump through a zeolite trap and an additional liquid nitrogen cold trap. A working pressure of $\approx 10^{-7}$ torr in the source chamber is achieved within 2 hours after loading a new sample turret. The ion acceleration potential used was 8000 V with internal resistance of 10^{11} ohms. Rb and Sr isotopic measurements were done on an on line HP 9836 data acquisition system using General Peak Jumping (GPJ) software provided by V.G. Isotopes. Rb isotopic measurements were made in the range of 0.3-0.5 V corresponding to ^{87}Rb while those

of Sr were made in the range of 0.5-2 V corresponding to ^{88}Sr . Mean of 45 and 150 cycles were taken for Rb and Sr analysis, respectively.

Based on replicate analyses of calibration mixtures and a few rock samples, the errors in the mass spectrometric determinations of ^{87}Rb and ^{86}Sr are estimated to be within $\pm 0.5\%$ leading to a random error of not more than $\pm 1\%$ for their ratios. ^{87}Rb and ^{86}Sr concentrations were calculated by isotope dilution technique. The $^{87}\text{Sr}/^{86}\text{Sr}$ ratios were corrected for mass fractionation assuming $^{86}\text{Sr}/^{88}\text{Sr} = 0.1194$ in the sample. The analysis of the NBS 987 standard, made during the course of this study at KDMIPE, Dehradun, gave a mean value of 0.710219 ± 0.000058 as given in Table 3.5.

Table 3.5. $^{87}\text{Sr}/^{86}\text{Sr}$ values of NBS 987 standard measured during the course of this study

Sl. No.	Date	$^{87}\text{Sr}/^{86}\text{Sr}$
1	25.09.1992	0.710016 ± 0.000064
2	30.09.1992	0.710162 ± 0.000043
3	30.09.1992	0.710253 ± 0.000057
4	01.10.1992	0.710184 ± 0.000057
5	05.10.1992	0.710287 ± 0.000064
6	18.02.1993	0.710239 ± 0.000064
7	23.02.1994	0.710244 ± 0.000057

All measurements are normalised to $(^{86}\text{Sr}/^{88}\text{Sr}) = 0.1194$
Reference NBS 987 value is 0.710248 ± 0.000044
Errors quoted are at 2σ level
Decay constant $\lambda (^{87}\text{Rb}) = 1.42 \times 10^{-11} \text{ yr}^{-1}$

3.3.5. X-RAY FLUORESCENCE STUDIES

Rb and Sr measurements for Tavidar volcanics and Mundwara igneous complex were carried out, on an energy dispersive XRF system (EDAX Philips Exam Six in combination with PV 9100), at Wadia Institute of Himalyan Geology, Dehradun, India.

Precision of these measurements as determined from replicate analysis of standards is 5%.

CHAPTER IV

RESULTS AND DISCUSSION

4.1. INTRODUCTION

To understand the evolution of Malani igneous province (MIP), temporal status of various associations must be established. Keeping this in view, systematic dating of each association was undertaken using K-Ar, ^{40}Ar - ^{39}Ar and Rb-Sr methods. The K-Ar method was employed only in the initial phase of the work for preliminary screening of the samples while ^{40}Ar - ^{39}Ar and/or Rb-Sr methods were used in subsequent studies, depending upon suitability of the technique for eliciting chronological informations. The samples dated by ^{40}Ar - ^{39}Ar method were also studied for Sr isotopic composition, in order to know their petrogenesis.

About half of the samples under investigation were provided by Prof. R. K. Srivastava of Department of Geology, M. L. Sukhadia University, Udaipur, Rajasthan. Most of these samples were collected by his students working for their doctoral thesis from different parts of the Malani province (Maheswari, 1983; Agrawal, 1984; Gaur, 1984; Yadav, 1988; Yadav, 1991). The remaining samples were collected during a field trip to Rajasthan in 1986.

4.2. ASSOCIATION I (*MALANI VOLCANICS*)

The felsic volcanics of Gurapratap Singh and Dirri of Pali district (Fig. 1.3), commonly referred to as Malani volcanics, have been grouped in this association. The analytical results of ^{40}Ar - ^{39}Ar and Rb-Sr studies are discussed below.

4.2.1. ^{40}Ar - ^{39}Ar STUDIES

Three samples were analyzed from basalt-andesite-dacite-rhyolite association of Dir and Gurapratap Singh, Pali district, for ^{40}Ar - ^{39}Ar studies. The dated samples include a basalt (D/88), a dacite (D/25) and a rhyolite (D/174).

The samples were irradiated in two batches. The minimum and maximum value of J was 0.00224 ± 0.00002 and 0.00275 ± 0.00004 for D/88 and D/25, respectively.

Analytical results of the $^{40}\text{Ar}/^{39}\text{Ar}$ analysis of these samples are presented in Tables 4.1 to 4.3. The values are corrected for K- and Ca-derived Ar isotopes. After correction for Ca-derived ^{36}Ar , the ^{36}Ar is used to correct for trapped ^{40}Ar on the assumption that the $^{40}\text{Ar}/^{36}\text{Ar}$ ratios of the trapped argon has the modern atmospheric value of 295.5. Minnesota hornblende (MMhb-1), with an age of 520.4 ± 1.7 Ma (Samson and Alexander, 1987), has been used as monitor for all the samples. The total or integrated ages are calculated by adding the isotopic abundances of all the temperature steps. The errors have been computed by quadratically propagating the errors in the measured ratios, blanks and interfering isotopes. The error quoted on the apparent and integrated ages include the error in J but the error boxes in age spectra plots do not include the error in J . All the errors quoted here after are at 2σ level.

The age spectra are plotted in Fig. 4.1 to 4.3, which exhibit a step-wise age increase in all the samples with increasing temperature. Similar patterns, normally interpreted as resulting from argon loss by diffusion, have been obtained for slowly cooled rocks and for rocks that have been reheated subsequent to the time of their formation (Hanson et al., 1975; Berger and York, 1981; Harrison and McDougall, 1981 and Zeitler, 1987).

The apparent ages for the initially released gas in each sample provide an estimate of the time of reheating or the time since the rock began to retain argon quantitatively owing to cooling below the blocking temperature of different rock forming minerals (Frank and Stettler, 1979). Also shape of the release spectra will vary depending upon the grain size, the amount of argon loss and the conditions of episodic heating (Turner, 1968, 1969; Gillespie et al., 1982)

In the sample D/88 (basalt) four temperature steps (550 to 700°C; 28.4% ^{39}Ar

Notes for tables:

1. Radiogenic ^{40}Ar as percentage of total ^{40}Ar .
2. All data are corrected for blank, mass discrimination and interference.
3. ^{37}Ar and ^{39}Ar are corrected for decay and error quoted for age includes error in J.
4. Errors quoted are at 2σ level.
5. Errors on $^{87}\text{Rb}/^{86}\text{Sr}$ ratios are 2% at 2σ level.

Table 4.1. Step heating argon isotopic compositions and apparent ages of sample D/88 (DIRI BASALT)
 $J=0.00224 \pm 0.00002$

Temp. (°C)	$^{36}\text{Ar}/^{39}\text{Ar}$	$^{37}\text{Ar}/^{39}\text{Ar}$	$^{40}\text{Ar}/^{39}\text{Ar}$	Age (Ma)	^{39}Ar (%)	$^{40}\text{Ar}^*$ (%)
400	0.1347 ± 0.0041	3.3566 ± 0.0679	183.80 ± 1.50	503 ± 11	1.1	78.3
450	0.0405 0.0010	3.1229 0.0063	130.44 0.88	424 6	4.2	90.8
500	0.0154 0.0013	2.6167 0.0052	135.24 0.87	462 7	4.9	96.6
550	0.0158 0.0007	3.9964 0.0079	142.72 0.87	485 6	6.4	96.7
600	0.0143 0.0007	3.7099 0.0074	144.64 0.89	493 6	6.1	97.1
650	0.0122 0.0005	2.6369 0.0075	145.02 0.86	496 6	8.5	97.5
700	0.0069 0.0006	1.9187 0.0066	143.06 0.86	494 6	7.4	98.6
750	0.0079 0.0005	2.1446 0.0042	149.53 0.89	513 6	8.9	98.4
800	0.0057 0.0002	3.0859 0.0061	160.84 0.93	549 6	18.6	98.9
850	0.0066 0.0003	3.1620 0.0063	152.98 0.89	525 6	16.6	98.7
900	0.0178 0.0005	4.7422 0.0094	168.17 0.99	560 7	8.3	96.9
1000	0.0523 0.0009	20.6720 0.0413	221.50 1.30	684 8	4.5	93.6
1100	0.0702 0.0012	42.7900 0.0855	236.10 1.50	709 9	3.5	91.2
1250	0.1211 0.0073	21.9300 0.0438	240.30 2.20	679 17	1.1	85.1
TOTAL	0.0178 0.0002	5.5509 0.0042	158.30 0.30	531 4	100.0	96.7

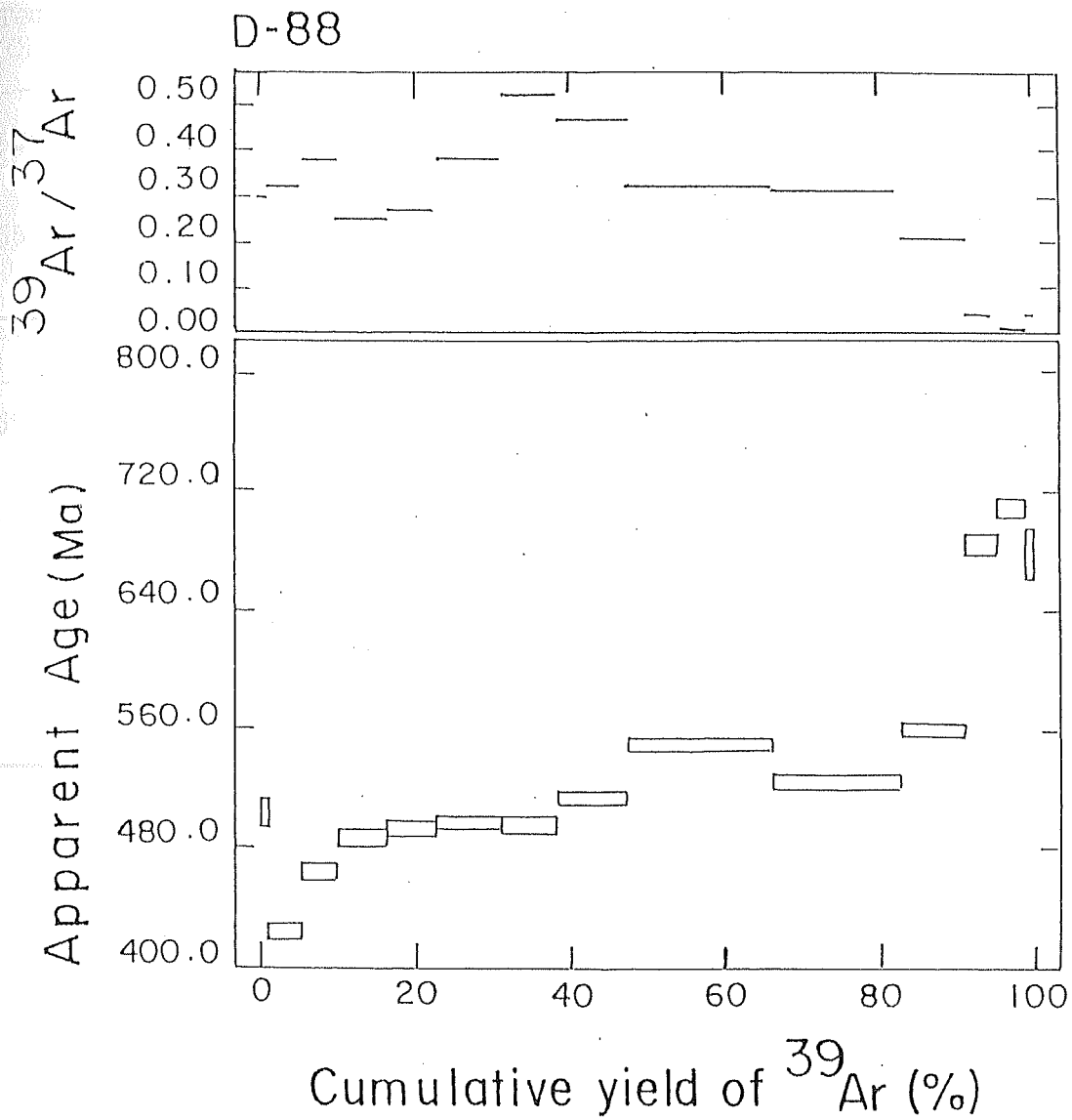


Fig. 4.1. ^{40}Ar - ^{39}Ar Age Spectrum for Diri Basalt (D/88).

Table 4.2. Step heating argon isotopic compositions and apparent ages of sample
D/25 (DIRI DACITE)
 $J=0.00275 \pm 0.00004$

Temp. (°C)	$^{36}\text{Ar}/^{39}\text{Ar}$	$^{37}\text{Ar}/^{39}\text{Ar}$	$^{40}\text{Ar}/^{39}\text{Ar}$	Age (Ma)	^{39}Ar (%)	$^{40}\text{Ar}^*$ (%)
500	0.0799 ± 0.0028	1.1334 ± 0.0147	134.31 ± 0.91	479 ± 11	1.4	82.4
550	0.0408 0.0012	0.6650 0.0320	122.75 0.74	479 8	3.1	90.2
600	0.0389 0.0008	0.3688 0.0165	132.27 0.77	517 8	5.1	91.3
650	0.0166 0.0006	0.2680 0.0027	125.10 1.30	515 8	8.9	96.1
700	0.0059 0.0003	0.2239 0.0037	120.62 0.70	510 8	12.0	98.5
750	0.0044 0.0004	0.4216 0.0034	116.07 0.67	495 8	10.8	98.9
800	0.0042 0.0003	0.6351 0.0041	118.40 0.76	504 8	14.9	98.9
850	0.0073 0.0002	1.7925 0.0099	127.00 1.80	532 9	20.9	98.3
900	0.0065 0.0004	1.8422 0.0229	144.86 0.95	598 9	12.6	98.7
950	0.0231 0.0012	4.7171 0.0094	234.20 1.40	876 13	5.0	97.0
1000	0.0336 0.0042	7.7124 0.0154	376.60 2.40	1258 17	1.6	97.4
1050	0.0493 0.0073	10.6501 0.0213	458.40 3.30	1439 20	1.0	97.0
1200	0.0809 0.0189	10.1821 0.1581	468.00 3.49	1440 32	1.0	95.0
1500	0.1440 0.0351	9.4665 0.0208	473.30 6.90	1410 58	2.0	91.0
TOTAL	0.0158 0.0012	1.5885 0.0041	148.30 8.90	600 8	100.0	96.9

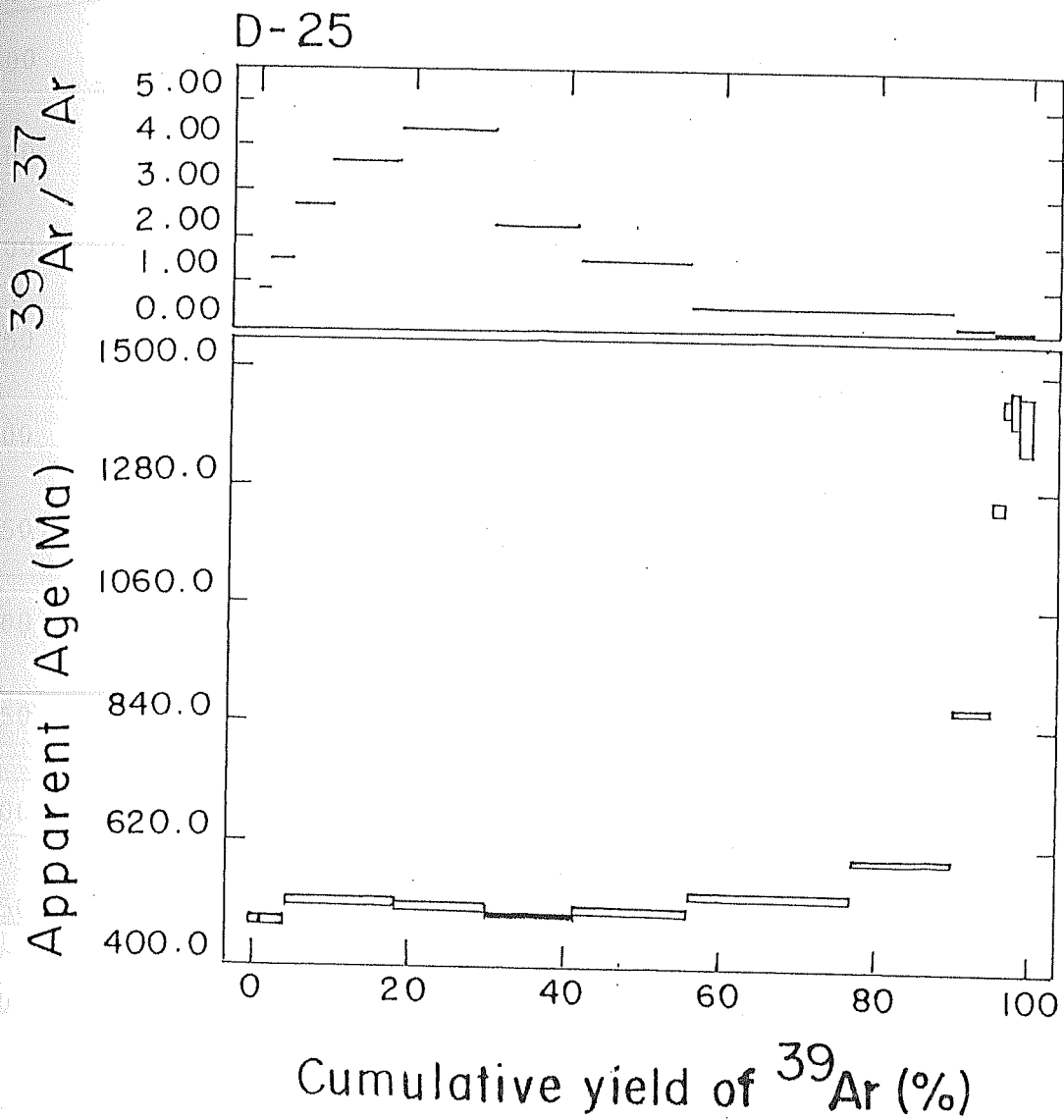


Fig. 4.2. ^{40}Ar - ^{39}Ar Age Spectrum for Diri Dacite (D/25).

Table 4.3. Step heating argon isotopic compositions and apparent ages of sample D/174 (DIRI RHYOLITE)
J=0.00269 ± 0.00004

Temp. (°C)	$^{36}\text{Ar}/^{39}\text{Ar}$	$^{37}\text{Ar}/^{39}\text{Ar}$	$^{40}\text{Ar}/^{39}\text{Ar}$	Age (Ma)	^{39}Ar (%)	$^{40}\text{Ar}^*$ (%)
500	0.0246 ±0.0009	-	143.22 ±0.83	562 ±9	2.1	94.9
550	0.0047 0.0002	0.0758 0.0022	124.80 0.72	517 8	3.5	98.9
600	0.0024 0.0001	-	126.41 0.73	523 8	10.7	99.4
650	0.0011 0.0001	-	124.65 0.74	520 8	11.5	99.8
700	0.0006 0.0001	-	132.40 1.00	549 8	12.2	99.8
750	0.0019 0.0001	-	146.95 0.84	598 9	13.7	99.6
800	0.0035 0.0001	-	183.80 1.60	721 11	14.8	99.4
850	0.0029 0.0002	0.0843 0.0025	161.25 0.93	646 10	14.4	99.5
900	0.0031 0.0001	-	200.50 1.60	774 11	7.6	99.5
950	0.0050 0.0005	0.1458 0.0091	240.40 1.40	895 13	3.5	99.4
1200	0.0130 0.0008	-	319.30 4.00	1107 15	3.7	98.8
1500	0.0145 0.0086	-	362.80 2.50	1217 22	2.0	99.0
TOTAL	0.0036 0.0002	0.0198 0.0004	166.13 0.38	662 8	100.0	99.4

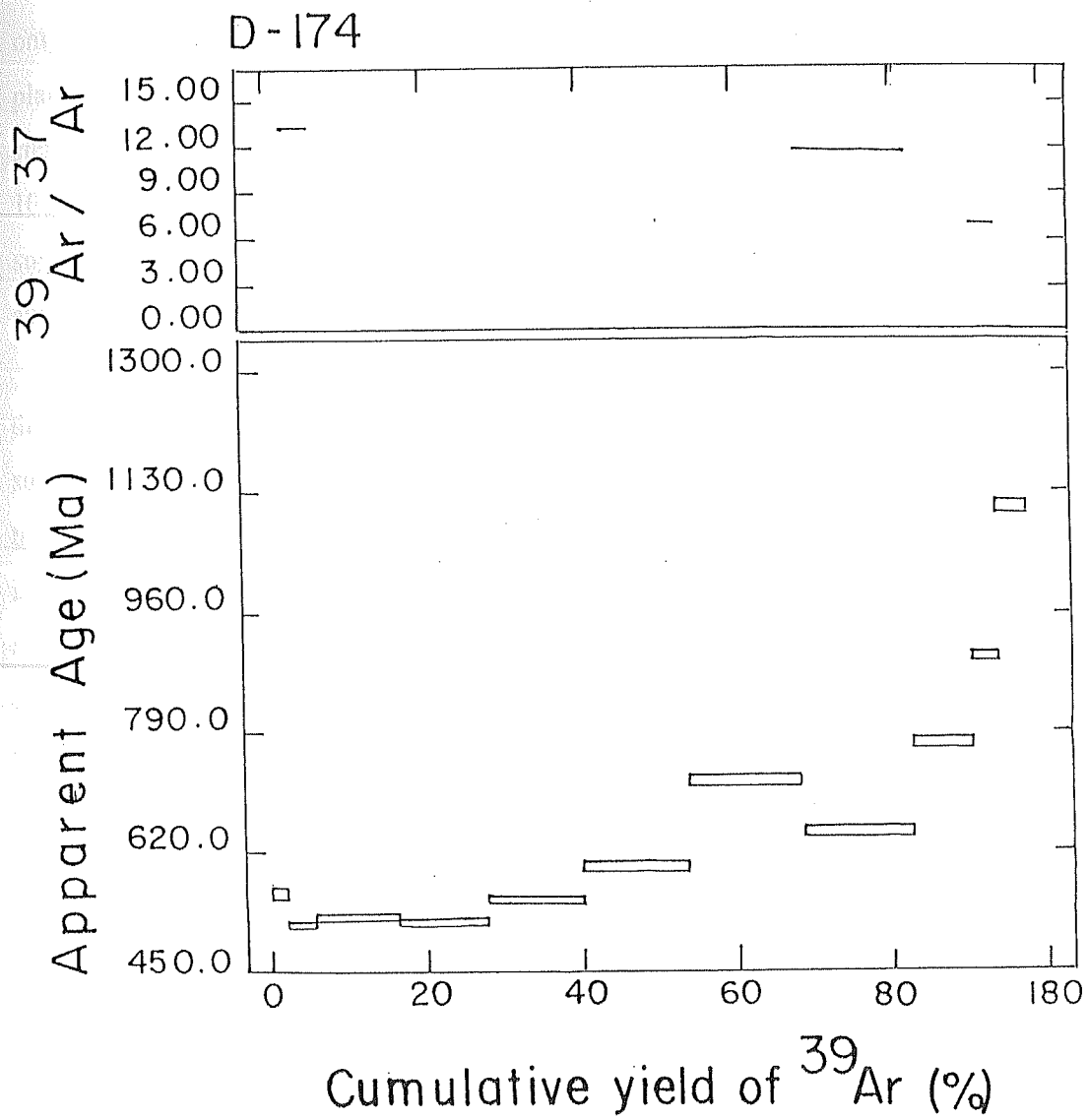


Fig. 4.3. ^{40}Ar - ^{39}Ar Age Spectrum for Diri Rhyolite (D/174).

release) exhibit apparent ages which are mutually similar and give a pseudo plateau age of 492.0 ± 4.7 Ma (Fig. 4.1). The higher temperature steps give successively higher ages. The total age is 530.9 ± 4.4 Ma. Sample D/25 (dacite) defines plateau of five intermediate temperature steps (600 to 800°C) with 51.7% of total ^{39}Ar released forming the pseudo plateau at 507.8 ± 8.2 Ma (Fig. 4.2). While in the sample D/174 (rhyolite) only three temperature steps (550 to 650°C , 25.7%, ^{39}Ar release) constitute a pseudo plateau at 520.5 ± 9.6 Ma (Fig. 4.3). The latter two samples have higher temperature steps exhibiting apparent ages which are well above of their formation age of 779 ± 10 Ma as obtained by Rb-Sr studies (discussed in Rb-Sr study part of this section), suggesting presence of excess argon. The total ages for these samples are 600.7 ± 8.0 Ma and 662.2 ± 8.4 Ma, respectively.

Where excess ^{40}Ar is known to be present, two different age patterns have been distinguished. The first is a 'saddle-shaped' spectrum where the apparent age of successive gas increments decreases systematically to a minimum and then increases for the remaining ^{39}Ar release (Lanphere and Dalrymple, 1971). The minimum apparent age is greater than the known age of the sample. This pattern occurs in whole rocks as well as mineral separates like biotite, pyroxene and plagioclase from a number of geological environments but in general tends to be associated with the crystallization of igneous rocks (Lanphere and Dalrymple, 1976; Kaneoka, 1974; Stettler and Bochsler, 1979)

The second pattern is associated with the metamorphism of pre-existing rocks. In this case the age spectra either rise steeply to a relatively flat plateau over most of the ^{39}Ar release or show step-wise age increase with increasing temperature, with apparent ages well in excess of the metamorphic and/or formation age and in some cases older than the age of the earth. This type of pattern has been demonstrated in biotites from Greenland by Pankhurst et al. (1973) and for Alpine biotites by Roddick et al. (1980).

A third pattern (Seidemann, 1976) which may show excess ^{40}Ar in the low-temperature steps but approximates the correct cooling age in the high-temperature release. However, as both Seidemann (1976) and Lanphere and Dalrymple (1977) indicate that this effect does not apply to the common rock forming minerals.

The release spectra of samples D/25 and D/174 exhibit the second pattern

mentioned above, and the anomalously high age is attributed to the presence of excess radiogenic argon, a portion of which was lost by diffusion during cooling after a thermal event around 500-550 Ma ago. Similar release curves have been obtained by Phillips and Onstotte (1986) also for the phlogopites from southern African Kimberlites.

It is clear from above that none of the three samples analyzed gave a perfect plateau but showed the spectra typical of rocks which have been reheated at about 500-550 Ma ago subsequent to their formation. Earlier Rb-Sr mineral ages determined on different granite bodies from Sendra, Sadri-Ranakpur and Sai have also indicated thermal event to reset mineral ages around 500-550 Ma ago, which otherwise have the whole rock pooled Rb-Sr age of 800 ± 50 Ma (Choudhary, 1984).

The $^{40}\text{Ar}/^{39}\text{Ar}$ studies of volcanics from Pali district have, thus, indicated the existence of this thermal event in the rocks exposed further west of Aravalli range in Rajasthan.

4.2.2. Rb-Sr STUDIES

4.2.2.A. BASALT-ANDESITE-DACITE-RHYOLITE SEQUENCE

As the ^{40}Ar - ^{39}Ar studies could not reveal the time of formation, Rb-Sr whole rock dating was employed to elucidate the time of primary crystallization of felsic volcanics from Diri, Gura pratap Singh and Manihari, Pali district.

Five samples, ranging in composition from basalt to rhyolite, were selected for Rb-Sr isotopic studies. The selected samples showed good spread in Rb/Sr ratios (0.1 to 7). The analytical data are given in Table 4.4. All the errors quoted are at 2σ level and the errors on $^{87}\text{Rb}/^{86}\text{Sr}$ ratios are 2%. When these data points are plotted on a Rb-Sr evolution diagram (Fig. 4.4) they define a best fit line corresponding to an age of 786 ± 11 Ma with an initial Sr isotopic ratio of 0.70559 ± 0.00043 . The MSWD is 2.26. However, when the sample D/88 (basalt) is omitted from the calculation, the remaining four samples define an isochron age of 779 ± 10 Ma with an initial Sr isotopic ratio of 0.70612 ± 0.00046 . The MSWD reduces to 0.29 from 2.26 which indicates that the fit

Table 4.4. Rb-Sr isotopic data of Malani volcanics from Dirí,
Gurapratap Singh and Manihari, Pali district.

Sample No.	^{87}Rb (ppm)	^{86}Sr (ppm)	$^{87}\text{Rb}/^{86}\text{Sr}$ (atomic)	$^{87}\text{Sr}/^{86}\text{Sr}$ (atomic)
D/88	13.184	33.996	0.383	0.70804 ± 0.00084
D/10	41.320	26.329	1.551	0.72336 ± 0.00012
D/117	70.509	7.607	9.163	0.80929 ± 0.00011
D/5	84.519	7.068	11.820	0.83694 ± 0.00018
GM/219	70.691	3.463	20.1778	0.92887 ± 0.00035

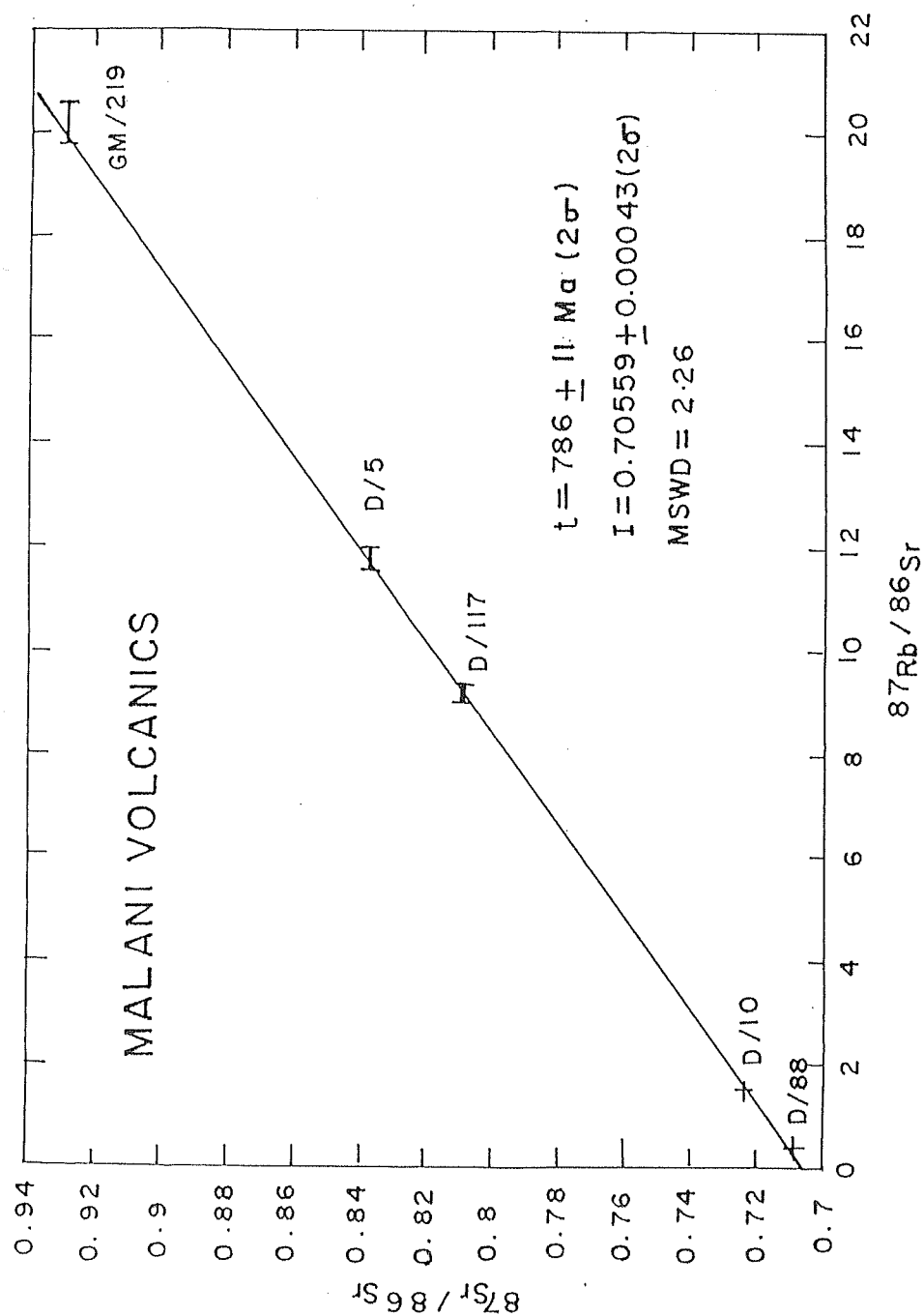


Fig. 4.4. Rb-Sr Conventional Isochron Diagram for Basalt-Andesite-Dacite-Rhyolite Association from Dirri and Gurapratap Singh.

is very good and that the samples have evolved as closed systems after their crystallization. The initial Sr ratio is indicative of crustal origin of the magma.

Further, if D/88 (basalt) is substituted for D/10 (dacite) in the calculation then the data points define an isochron age of 792 ± 11 Ma with MSWD 0.66, which is not different from the age obtained when D/88 is excluded from the calculation, suggesting contemporaneity of D/88 with the other rocks. However, the initial Sr ratio comes down to 0.70385 ± 0.00062 from 0.70612 ± 0.00046 which is quite different. This exercise, thus, suggests that though D/88 (basalt) has also crystallized at the same time, but belongs to a different, upper mantle, source. This conviction becomes more pronounced when the data points are plotted on best isochron diagram (Fig. 4.5) as developed by Provost (1990).

Recently Provost (1990) has evolved a new graphical means of displaying the data points. He named this as a best isochron diagram (BID) which has certain advantages over the conventional isochron diagram (CID) like:

- (1) *Unlike the CID, the initial ratios in BID is at a scale where its precision can be easily seen.*
- (2) *Unlike the CID, the BID displays the radiometric age as an intercept (on the right-hand border), again on an appropriate scale.*
- (3) *On the BID, highly radiogenic samples are not unduly emphasized and there is no need for inserts nor enlargements.*
- (4) *The whole height of the BID is available for displaying the analytical errors and deviations from the (nearly horizontal) isochron and there is no need for a Papanastassiou-Wasserburg insert (Papanastassiou and Wasserburg, 1971).*

Due to these optimal properties, the BID allows one to simultaneously visualize the experimental data and their analytical precision, to judge the quality of the linear fit, to appraise the accuracy of the age and initial ratio results, and to quantitatively appreciate the influence of any existing or expected datum. From the Fig. 4.5 it can be seen that the sample D/88 (basalt) is falling distinctly away (below) on the best isochron diagram indicating a different source though it is contemporaneous with the other volcanics i.e. andesite, dacite and rhyolite from Diri, Gurapratap Singh and Manihari of

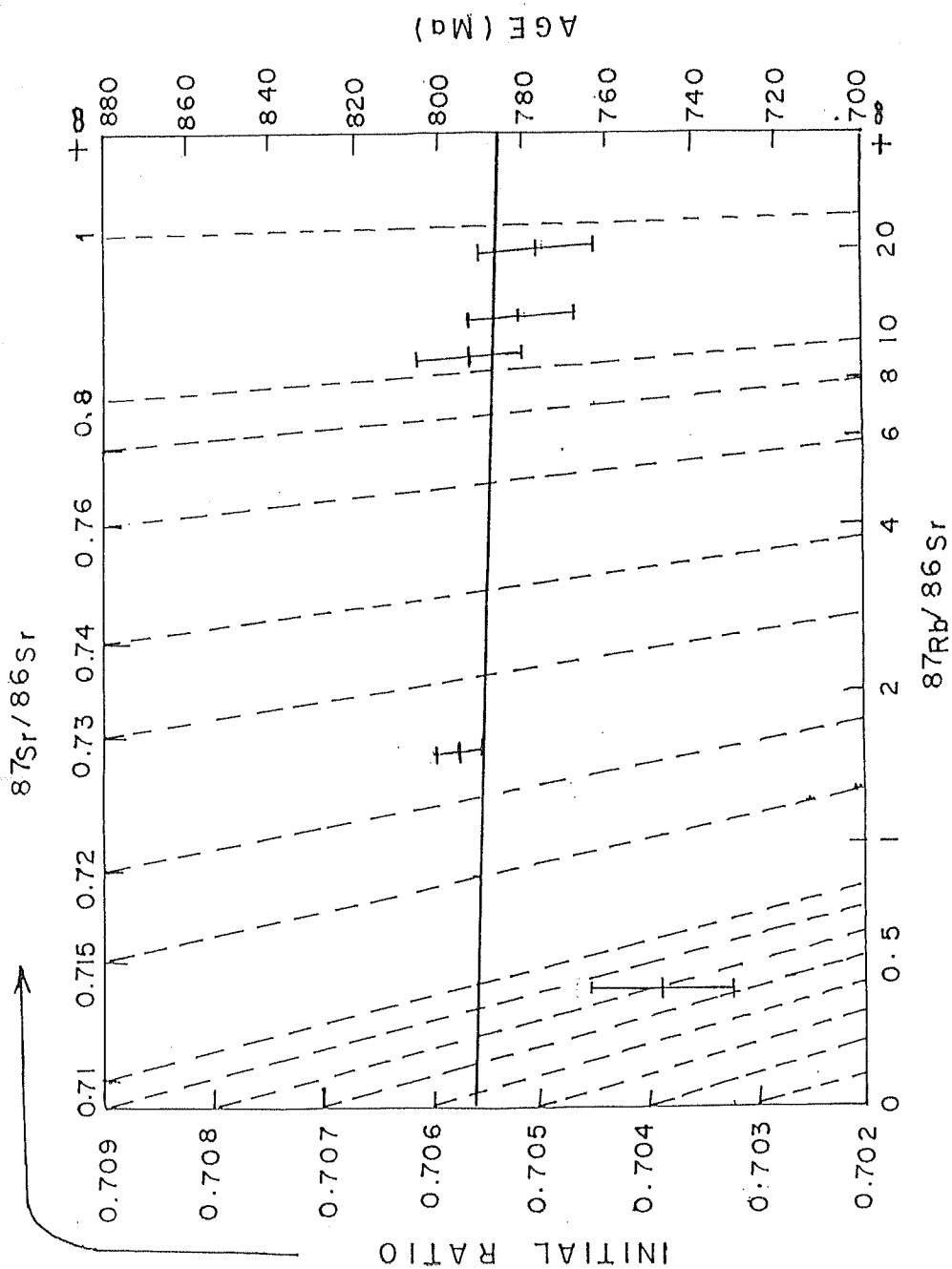


Fig. 4.5. Rb-Sr Best Isochron Diagram for Basalt - Andesite - Dacite - Rhyolite Association from Dirri and Gurapratap Singh.

Pali district. It is interesting to note here that Srivastava et al. (1989a) also reported that the field disposition of the basalt whether in the form of dyke or a flow could not be ascertained which further props up the present conviction.

4.2.2.B. ULTRAPOTASSIC RHYOLITES

A few flows of ultrapotassic rhyolites are also found at Diri, Gurapratap Singh and Manihari along with the other felsic volcanics (andesite, dacite and rhyolite etc.). These ultrapotassic rhyolites are different in their chemical behavior from the associated felsic volcanics (Fig. 2.3) and presumably mark a different phase of magmatic activity.

Five samples of ultrapotassic rhyolites from Manihari were selected for Rb-Sr studies in order to know their exact relationship with the associated felsic volcanics. The Rb/Sr ratios of the selected samples range from 3.3 to 14.6. The analytical data are given in Table 4.5. Excluding one sample (GM/31), others conform to a linear array corresponding to an age of 681 ± 15 Ma (Fig. 4.6) with an initial Sr ratio of 0.7135 ± 0.0025 . The MSWD of the fit is 1.75. The discrepancy of GM/31 may be due to either small size of the sample or slight alteration.

The primary crystallization age of 681 ± 15 Ma obtained for ultrapotassic rhyolites is about 100 Ma (at least 73 Ma) less than the age of 779 ± 10 Ma obtained for other associated felsic volcanics from Diri, Gurapratap Singh and Manihari, indicating a different magmatic episode. Further, the initial $^{87}\text{Sr}/^{86}\text{Sr}$ ratio of ultrapotassic rhyolites is much higher (0.7135 ± 0.0025) than that of the associated andesite-dacite-rhyolite association (0.70612 ± 0.00046). The high initial Sr ratio of ultrapotassic rhyolites is due to incorporation of radiogenic ^{87}Sr from the country rock, by assimilation or fusion, into the residual fraction of the magma in the crust which gave rise to other differentiated rocks of the association.

Table 4.5. Rb-Sr isotopic data of ultrapotassic rhyolites from Manihari, Pali district.

Sample No.	^{87}Rb (ppm)	^{86}Sr (ppm)	$^{87}\text{Rb}/^{86}\text{Sr}$ (atomic)	$^{87}\text{Sr}/^{86}\text{Sr}$ (atomic)
GM/62	60.522	7.178	8.335	0.79639 ± 0.00016
GM/32	63.407	6.455	9.710	0.80579 ± 0.00011
GM/31*	95.384	6.821	13.823	0.85709 ± 0.00026
GM/350	95.186	5.014	18.766	0.89310 ± 0.00009
GM/396	79.964	1.799	43.923	1.14558 ± 0.00038

* Not included in calculation

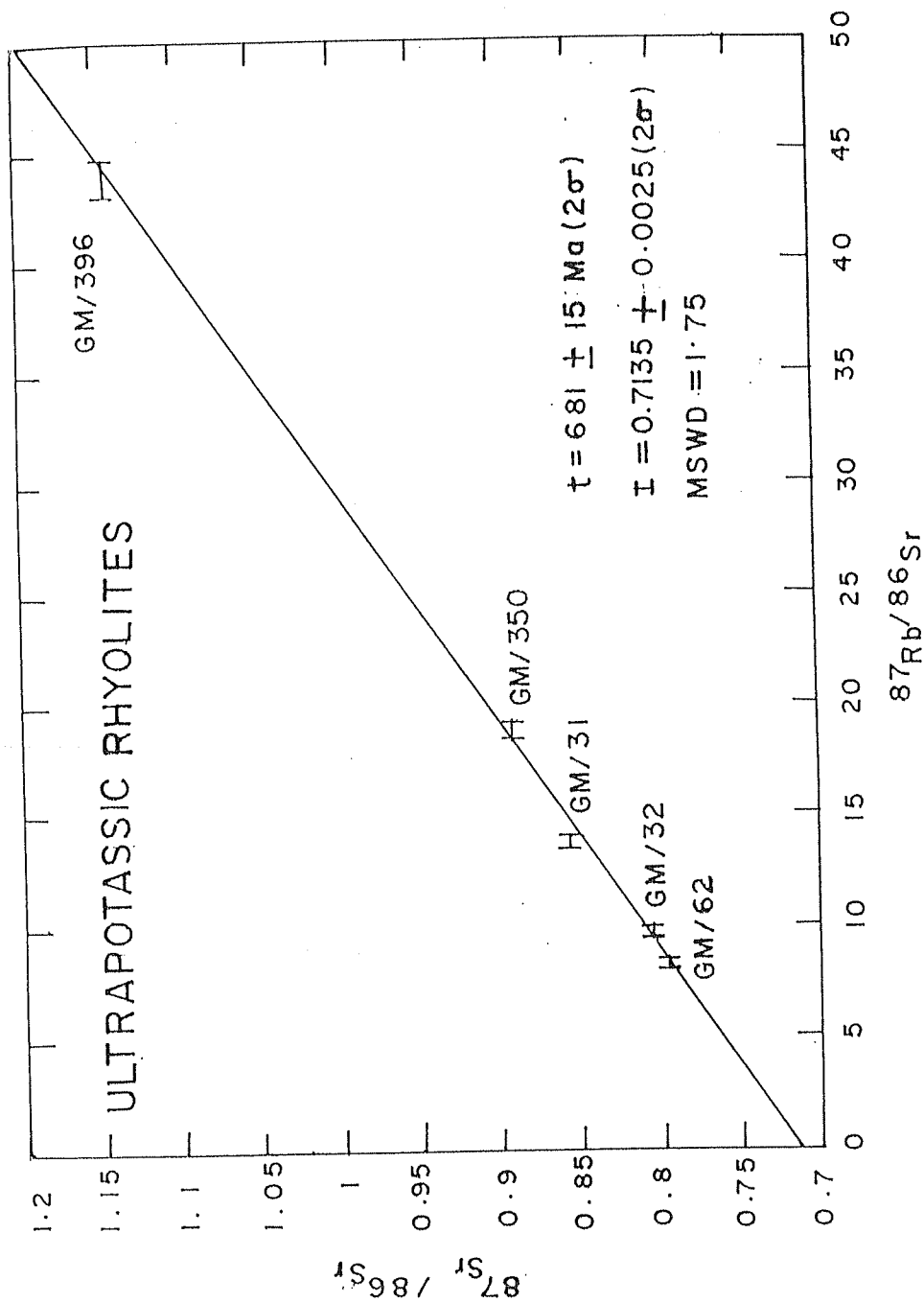


Fig. 4.6. Rb-Sr Conventional Isochron Diagram for Ultrapotassic Rhyolites from Dirri and Gurapratap Singh.

4.3 ASSOCIATION II (GRANITES AND ASSOCIATED VOLCANICS)

As mentioned earlier the granites and associated volcanics constitute the most important rock types of the province. These rocks are mainly exposed in and around Jalore and Siwana area. The granites are divided into two groups i.e. peraluminous or normal granites (Jalore granite) and peralkaline granites (Siwana granite). The peralkaline granites occur in a ring structure along with the associated peralkaline volcanics as well as normal rhyolites (Fig. 2.7). These normal rhyolites have been named as outer rhyolites.

The petrology and geochemistry of these rocks have been studied by various workers (Murthy, 1962; Venkataraman et al., 1964; Bhusan and Yagi, 1981; Bhusan and Mohanty, 1988; Yadav 1988; Kochhar, 1989; Bhusan, 1991 and Yadav, 1991). However, the geochronological studies are very limited and the work is confined to only one isochron of Crawford and Compston (1970), which has yielded an age of 745 ± 10 Ma. These authors got the isochron from the rocks which were not only differing in their chemical compositions but also their field relationship was not known. Therefore, it is very important to study individual rock groups which are supposed to be cogenetic. In the present study, an attempt is made to date Jalore and Siwana granites as well as associated peralkaline volcanics and normal (outer) rhyolites separately to know their mutual relationship and understand, ultimately, the evolution of these granites and volcanics.

4.3.1. ^{40}Ar - ^{39}Ar STUDIES

Two granite samples viz. JR/15 and JR/17 were analyzed for ^{40}Ar - ^{39}Ar studies. The analytical results are given in Tables 4.6 and 4.7 and the age spectra are shown in Fig. 4.7 and 4.8. Both the samples have experienced secondary thermal disturbance. The age spectrum of JR/15 (Fig. 4.7) is more complicated owing to the presence of excess argon as has been indicated by U-shaped release curve. The minima of the spectrum is at 515 ± 6 Ma. In the successive higher temperature steps the age increases up to 924 ± 13 Ma

Table 4.6. Step heating argon isotopic compositions and apparent ages of sample
JR 86/15 (JALORE GRANITE)
 $J=0.00237 \pm 0.00002$

Temp. (°C)	$^{36}\text{Ar}/^{39}\text{Ar}$	$^{37}\text{Ar}/^{39}\text{Ar}$	$^{40}\text{Ar}/^{39}\text{Ar}$	Age (Ma)	^{39}Ar (%)	$^{40}\text{Ar}^*$ (%)
400	0.0266 ± 0.0002	0.0399 ± 0.0011	226.00 ± 1.30	751 ± 8	3.4	96.5
450	0.0107 0.0000	0.0614 0.0005	155.59 0.89	556 6	3.1	97.9
500	0.0072 0.0001	0.0679 0.0013	161.34 0.93	577 7	1.5	98.7
550	0.0072 0.0001	0.0760 0.0016	157.42 0.91	565 6	2.1	98.6
600	0.0057 0.0002	0.1277 0.0016	156.75 0.91	564 6	1.0	98.9
650	0.0066 0.0002	0.1453 0.0017	158.71 0.92	570 6	1.1	98.8
700	0.0081 0.0001	0.1312 0.0041	167.87 0.97	597 7	1.8	98.6
750	0.0078 0.0001	0.1224 0.0011	172.12 0.99	610 7	3.0	98.6
800	0.0071 0.0003	0.0745 0.0001	148.77 0.86	538 6	5.7	98.6
850	0.0079 0.0001	0.0518 0.0001	141.82 0.82	515 6	13.1	98.3
900	0.0083 0.0001	0.0379 0.0001	160.34 0.92	573 6	39.1	98.5
1000	0.0096 0.0001	0.0381 0.0004	170.13 0.98	602 7	23.1	98.3
1050	0.0369 0.0017	0.3389 0.0051	212.10 1.20	703 8	0.7	94.9
1100	0.0512 0.0035	0.6645 0.0034	273.80 1.60	862 11	0.3	94.5

contd.

Table 4.6. (contd.)

Temp. (°C)	$^{36}\text{Ar}/^{39}\text{Ar}$	$^{37}\text{Ar}/^{39}\text{Ar}$	$^{40}\text{Ar}/^{39}\text{Ar}$	Age (Ma)	^{39}Ar (%)	$^{40}\text{Ar}^*$ (%)
1150	0.0794 ± 0.0081	1.0291 ± 0.0251	288.50 ± 2.00	879 ± 17	0.1	91.9
1200	0.1201 0.0141	1.5870 0.0951	309.00 3.30	901 26	0.1	88.0
1250	0.1021 0.0072	0.9600 0.0211	301.90 2.20	897 16	0.2	90.0
1500	0.1555 0.0045	0.8910 0.0111	328.30 2.50	924 13	0.4	86.0
TOTAL	0.0104 0.0001	0.0627 0.0001	164.03 0.45	583 5	100.0	98.1

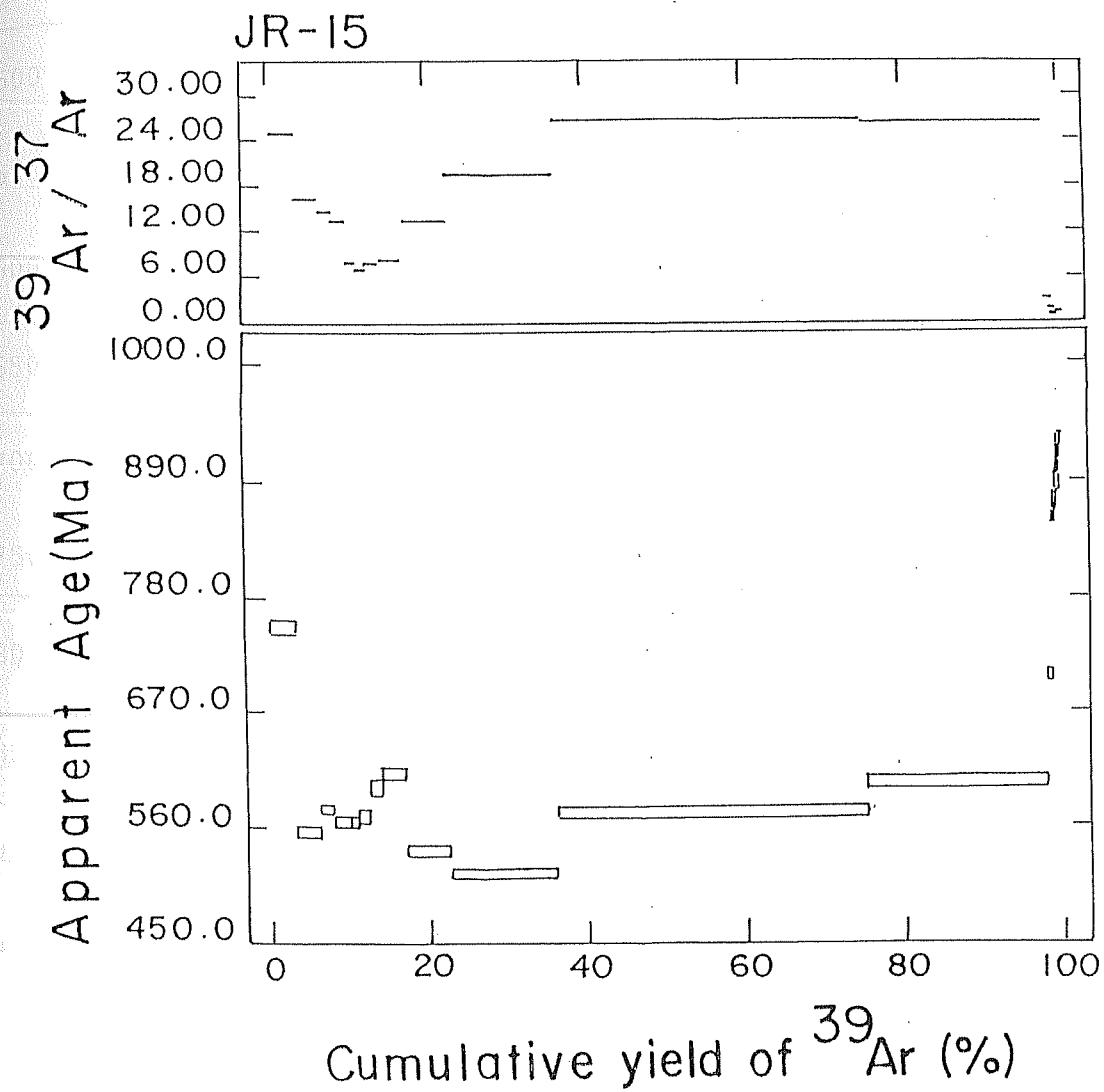


Fig. 4.7. ^{40}Ar - ^{39}Ar Age Spectrum for Jalore Granite (JR 86/15).

Table 4.7. Step heating argon isotopic compositions and apparent ages of sample
JR 86/17 (JALORE GRANITE)
 $J=0.00238 \pm 0.00005$

Temp. (°C)	$^{36}\text{Ar}/^{39}\text{Ar}$	$^{37}\text{Ar}/^{39}\text{Ar}$	$^{40}\text{Ar}/^{39}\text{Ar}$	Age (Ma)	^{39}Ar (%)	$^{40}\text{Ar}^*$ (%)
500	0.0192 ± 0.0007	0.0938 0.0053	134.52 ± 0.68	482 12	3.2	95.8
550	0.0069 0.0004	-	128.53 0.65	475 11	4.3	98.4
600	0.0083 0.0008	0.1331 0.0077	146.06 0.74	530 13	2.3	98.3
650	0.0076 0.0047	-	161.02 0.83	578 16	1.6	98.6
700	0.0058 0.0013	0.1506 0.0038	170.94 0.88	611 14	1.7	99.0
750	0.0073 0.0013	0.1252 0.0010	181.68 0.93	642 15	1.6	98.8
800	0.0079 0.0009	0.1461 0.0003	184.72 0.94	650 15	2.4	98.7
850	0.0068 0.0005	0.1457 0.0036	152.39 0.77	552 13	5.1	98.7
900	0.0054 0.0002	0.0602 0.0017	147.60 1.30	538 14	9.3	98.9
950	0.0065 0.0001	-	148.76 0.74	541 13	15.1	98.7
1000	0.0062 0.0001	0.0525 0.0004	153.52 0.77	556 13	25.0	98.8
1050	0.0081 0.0001	-	152.51 0.76	551 13	22.9	98.4
1100	0.0308 0.0002	0.1585 0.0027	175.02 0.97	600 14	1.4	94.8
1500	0.0256 0.0073	0.1424 0.0046	170.72 1.50	592 21	4.1	95.6
TOTAL	0.0083 0.0003	0.0484 0.0004	152.75 0.32	552 12	100.0	98.4

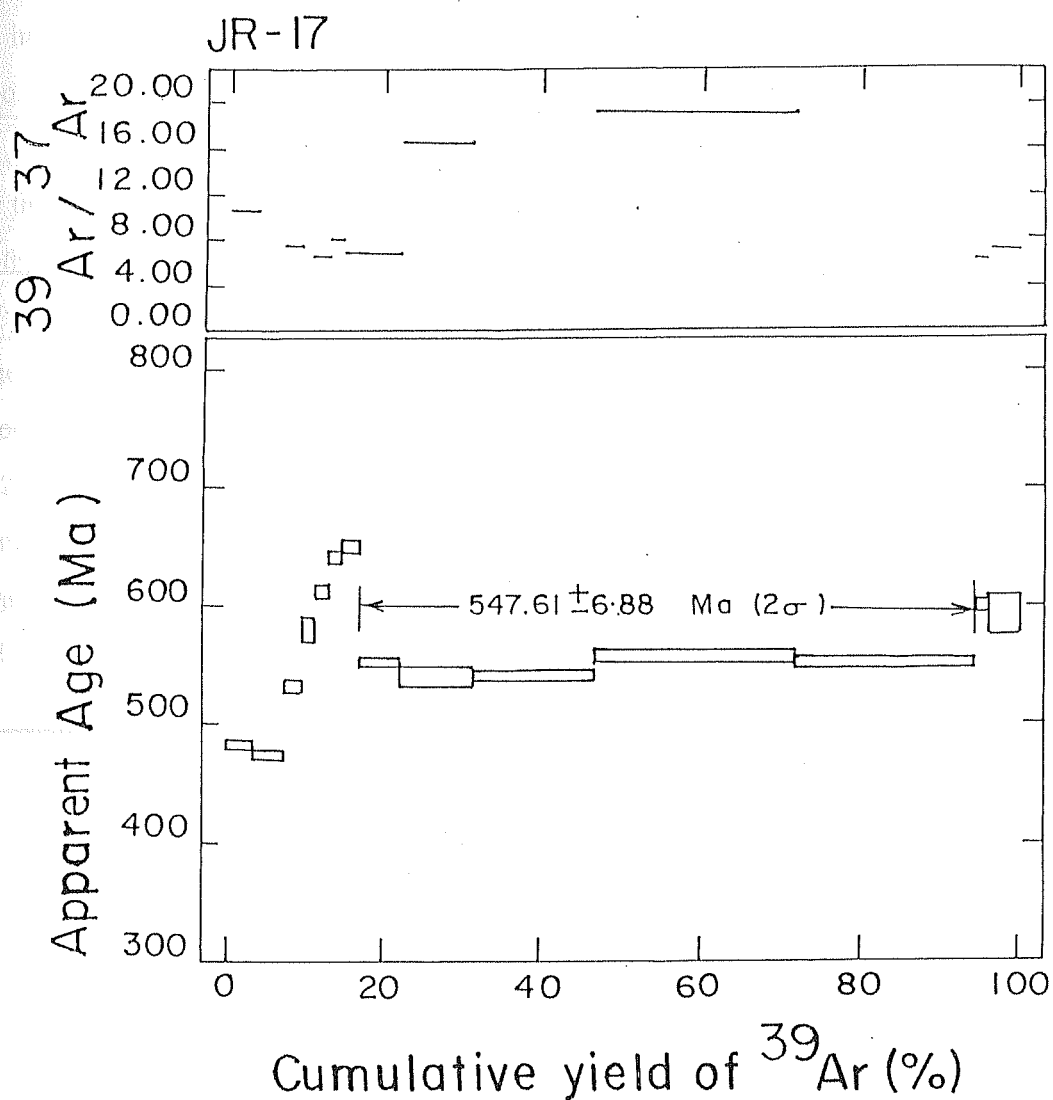


Fig. 4.8. ^{40}Ar - ^{39}Ar Age Spectrum for Jalore Granite (JR 86/17).

though the last six temperature steps amount only 1.7% of total ^{39}Ar release. The total age is 583 ± 5 Ma.

As the emplacement time of the Jalore granites have been inferred at about 730 Ma ago by Rb-Sr studies (discussed in Rb-Sr studies part) the release spectrum of JR/15 can be interpreted as to indicate the time of secondary thermal disturbance at about 500 Ma ago.

The sample JR/17 shows more or less complete isotopic reequilibration as indicated by the straight/simple release spectrum (Fig. 4.8). However, the disturbance observed in both the samples, in initial seven temperature steps, have been from low temperature mineral phases which has been substantiated by $^{39}\text{Ar}/^{37}\text{Ar}$ plots also (Fig. 4.7 and 4.8). The intermediate five temperature steps (850 to 1050°C) of JR/17 apparently form a pseudo plateau at 548 ± 7 Ma amounting 77.4% of total ^{39}Ar release. The total age is 552 ± 12 Ma, which is not different from the plateau age, suggesting that the sample was completely reequilibrated at about 550 Ma ago. Thus, the ^{40}Ar - ^{39}Ar studies of Jalore granites have also indicated the presence of secondary thermal disturbance between 500-550 Ma ago as has been witnessed by the felsic volcanics of Pali district.

4.3.2. Rb-Sr STUDIES

Here also, as the ^{40}Ar - ^{39}Ar studies could not reveal the time of formation due to secondary thermal event, Rb-Sr whole rock dating was employed to infer the emplacement time of Jalore and Siwana granites as well as associated volcanics. In the following sections individual isochrons are described in detail.

4.3.2.A. JALORE GRANITES (PERALUMINOUS GRANITES)

Seven whole rock samples of peraluminous granites were analyzed for Rb-Sr isotopic studies. The analytical data are given in Table 4.8 and plotted on a Sr evolution diagram shown in Fig. 4.9. The dispersion in Rb/Sr ratio among the samples is good ranging from 0.3 to 19.9. As can be seen all the samples except one (JR/15) conform

Table 4.8. Rb-Sr isotopic data of peraluminous granites from Jalore district.

Sample No.	^{87}Rb (ppm)	^{86}Sr (ppm)	$^{87}\text{Rb}/^{86}\text{Sr}$ (atomic)	$^{87}\text{Sr}/^{86}\text{Sr}$ (atomic)
SR/10	23.159	24.930	0.918	0.71520 ± 0.00030
JH/165	51.959	17.249	2.978	0.73608 ± 0.00035
TR/12	80.369	7.659	10.372	0.81620 ± 0.00152
JH/158	95.554	5.066	18.645	0.89636 ± 0.00014
JR/14	96.923	5.072	18.890	0.90022 ± 0.00013
JR/15*	129.702	2.729	46.973	1.25289 ± 0.00011
JR/17	127.699	2.060	61.278	1.34798 ± 0.00212

* - Not included in calculation

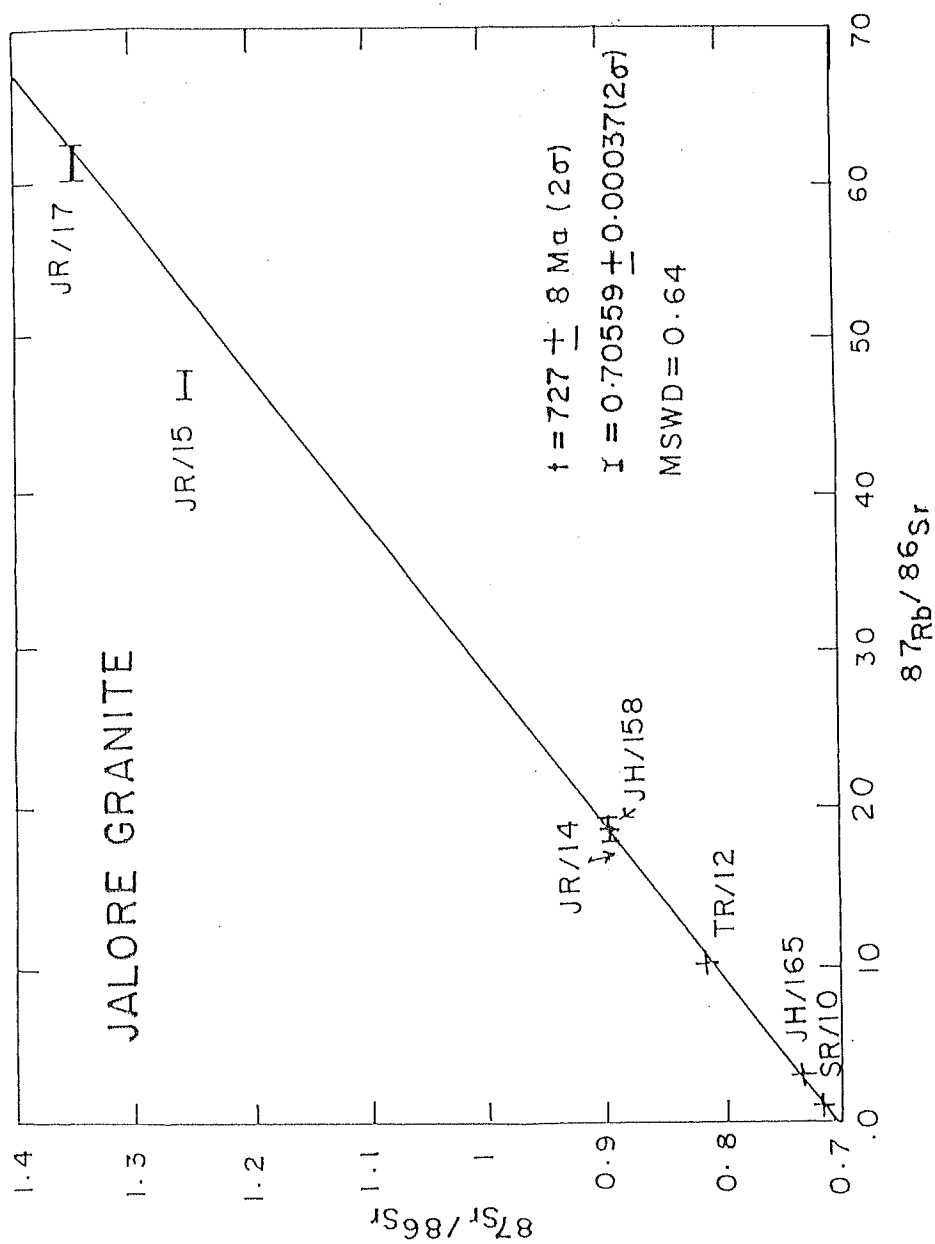


Fig. 4.9. Rb-Sr Conventional Isochron Diagram for Jalore Granite.

closely and evenly to a linear array. While the more radiogenic sample (JR/17) defines the slope within narrow limits, the least radiogenic samples (SR/10 and JH/165) constrains the intercept very closely. Two error regression of the six data points yields an isochron corresponding to an age of 727 ± 8 Ma and an intercept at 0.70559 ± 0.00037 . The fit of the data points to a straight line is very good as indicated by very low MSWD of 0.69. This shows that all the analyzed samples have evolved as closed system from a common Sr composition about 730 Ma ago. The initial Sr isotopic ratio suggest lower crustal derivation of the magma. The age of 730 Ma represents the emplacement or primary crystallization time of the Jalore granites. Out of the seven samples analyzed three (i.e. JH/150, JH/165 and JR/14) were from main Jalore pluton while two samples i.e. SR/10 and TR/12 were from Sanphara and Tikhi, respectively. Sample JR/15 was from RSMDC mine (Kala Ghata) while JR/17 was from back of Jalore fort hill.

4.3.2.B. SIWANA GRANITES (PERALKALINE GRANITES)

Six whole rock samples of peralkaline granites were analyzed for Rb-Sr studies. Out of these four samples viz. A/D/32, A/F/41, A/K/91 and A/K/102 were collected from main Siwana granite pluton while the remaining two samples i.e. DR/25 and MO/19 were collected from Dewra and Mokalsar, respectively (Fig. 2.7). The analytical data are given in Table 4.9. The samples show good radiogenic enrichment and mutual spread in Rb/Sr ratios. A well defined isochron (Fig. 4.10) can be obtained from the data points which gives an age of 698 ± 10 Ma with an initial Sr ratio of 0.7067 ± 0.0041 . The fit of the data to a straight line is excellent with the MSWD of 0.85.

From the foregoing discussion it is clear that Siwana granites are certainly younger, by atleast 11 Ma, than that of the Jalore (Peraluminous) granites. Therefore, these two type of granites i.e. peraluminous (Jalore type) and peralkaline (Siwana type) granites represent two different magmatic activities at short interval. The initial Sr ratios, however, could not be distinguished and suggest lower crustal origin of the magmas.

Table 4.9. Rb-Sr isotopic data of peralkaline granites and peralkaline volcanics from Siwana, Barmer district.

Sample	^{87}Rb	^{86}Sr	$^{87}\text{Rb}/^{86}\text{Sr}$	$^{87}\text{Sr}/^{86}\text{Sr}$
No.	(ppm)	(ppm)	(atomic)	(atomic)
A/D/32	44.21	3.05	13.68	0.84110 ± 0.00021
DR/25	83.054	2.980	27.548	0.99030 ± 0.00140
MO/19	46.674	1.550	29.762	1.00100 ± 0.00200
A/E/101 ^v	102.19	1.599	63.187	1.33903 ± 0.00072
A/K/91	111.4	1.673	65.81	1.36050 ± 0.00004
A/K/102	71.57	0.803	88.10	1.57990 ± 0.00066
A/E/102 ^v	145.46	1.578	91.111	1.58591 ± 0.00059
A/F/51	129.11	1.38	92.48	1.61820 ± 0.00074

^v peralkaline volcanics

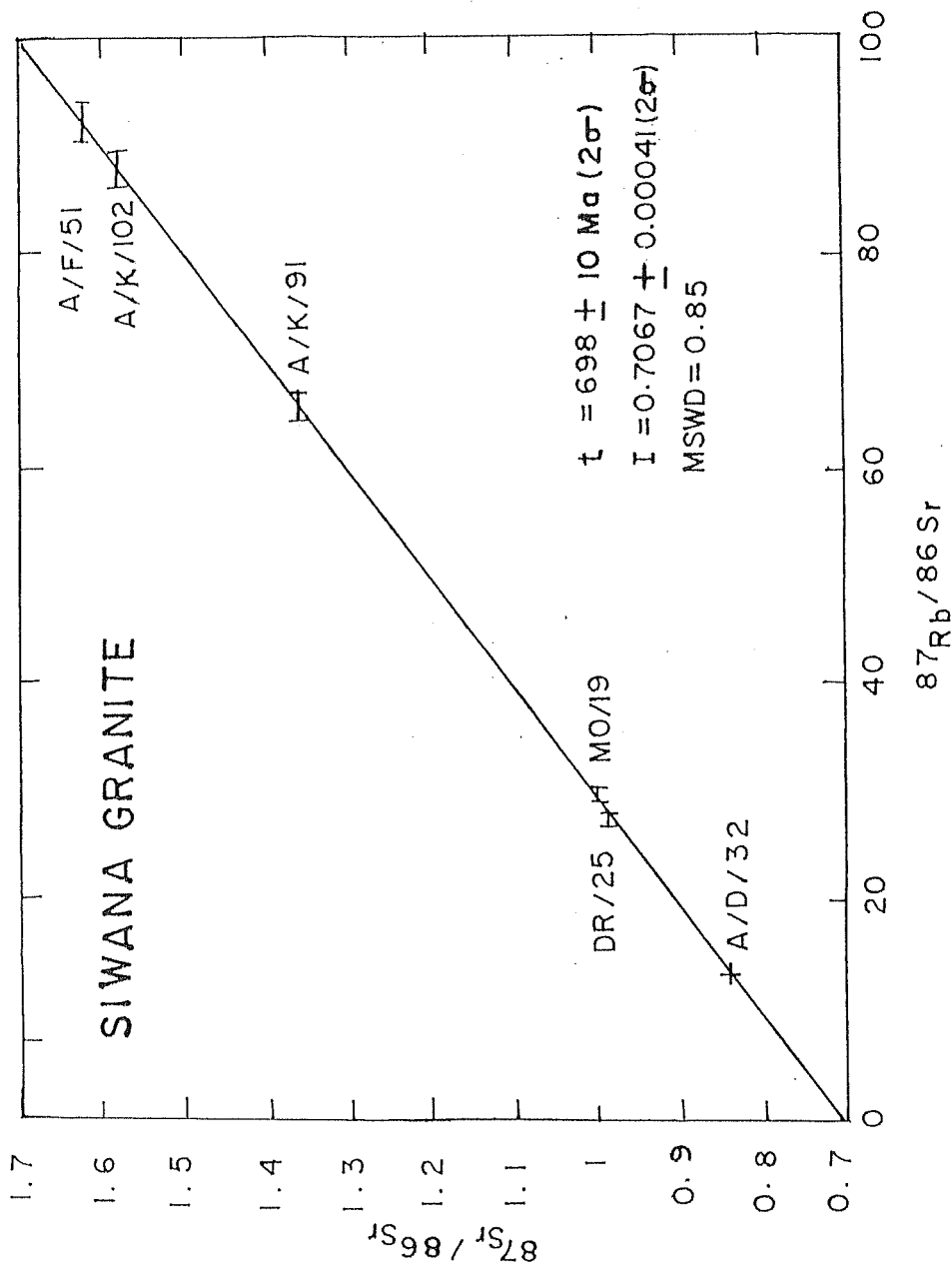


Fig. 4.10. Rb-Sr Conventional Isochron Diagram for Siwana Granite.

4.3.2.C. PERALKALINE VOLCANICS

The peralkaline volcanics i.e. soda-trachytes and pantellerites occur in association with the peralkaline granites (Fig. 2.7). To understand their temporal and genetic relationship with the peralkaline granites, two pantellerites (i.e. A/E/101 and A/E/102) were analyzed for Rb-Sr studies. The analytical data are given in Table 4.9. When these samples are regressed with the Siwana granites, the pooled isochron define an age of 693 ± 8 Ma with an initial Sr ratio of 0.7079 ± 0.0038 (Fig. 4.11). The MSWD of the fit is excellent at 0.92. This age and initial ratio is not different from the age and initial ratio of granites alone, thus, suggesting contemporaneity and cogenetic nature of these volcanics with that of the granites.

4.3.2.D. OUTER RHYOLITES

In addition to peralkaline granites and volcanics, normal rhyolites are also present at Siwana. These rhyolites occur at the southern extremity of the Siwana ring structure (Fig. 2.7) and have been named as outer rhyolites. In order to know their relationship with the peralkaline rocks, a set of five samples were selected which ranged in Rb/Sr ratio from 5.1 to 20.1. The analytical data are given in Table 4.10. One sample A/A/33 was excluded from the calculation as it was falling off from the best fit line. The line fitted to remaining four data points (Fig. 4.12) corresponds to an age of 674 ± 25 Ma with initial Sr ratio of 0.7110 ± 0.0066 . The MSWD is 2.27 indicating that the fit of the straight line is reasonably good.

Though the age of the outer rhyolites cannot be distinguished from that of the associated peralkaline granites and volcanics, the Sr isotopic ratio is relatively high (0.7110) compared to the associated peralkaline rocks (0.7067 to 0.7079). Further, the age as well as initial Sr isotopic ratio of the outer rhyolites are remarkably similar to that of the ultrapotassic rhyolites of Manihari (681 ± 15 Ma, 0.7135 ± 0.0025), Pali district. This similarity got further bolstered from the fact that when the outer rhyolites and the ultrapotassic rhyolites are plotted together on the Sr evolution diagram. The eight data

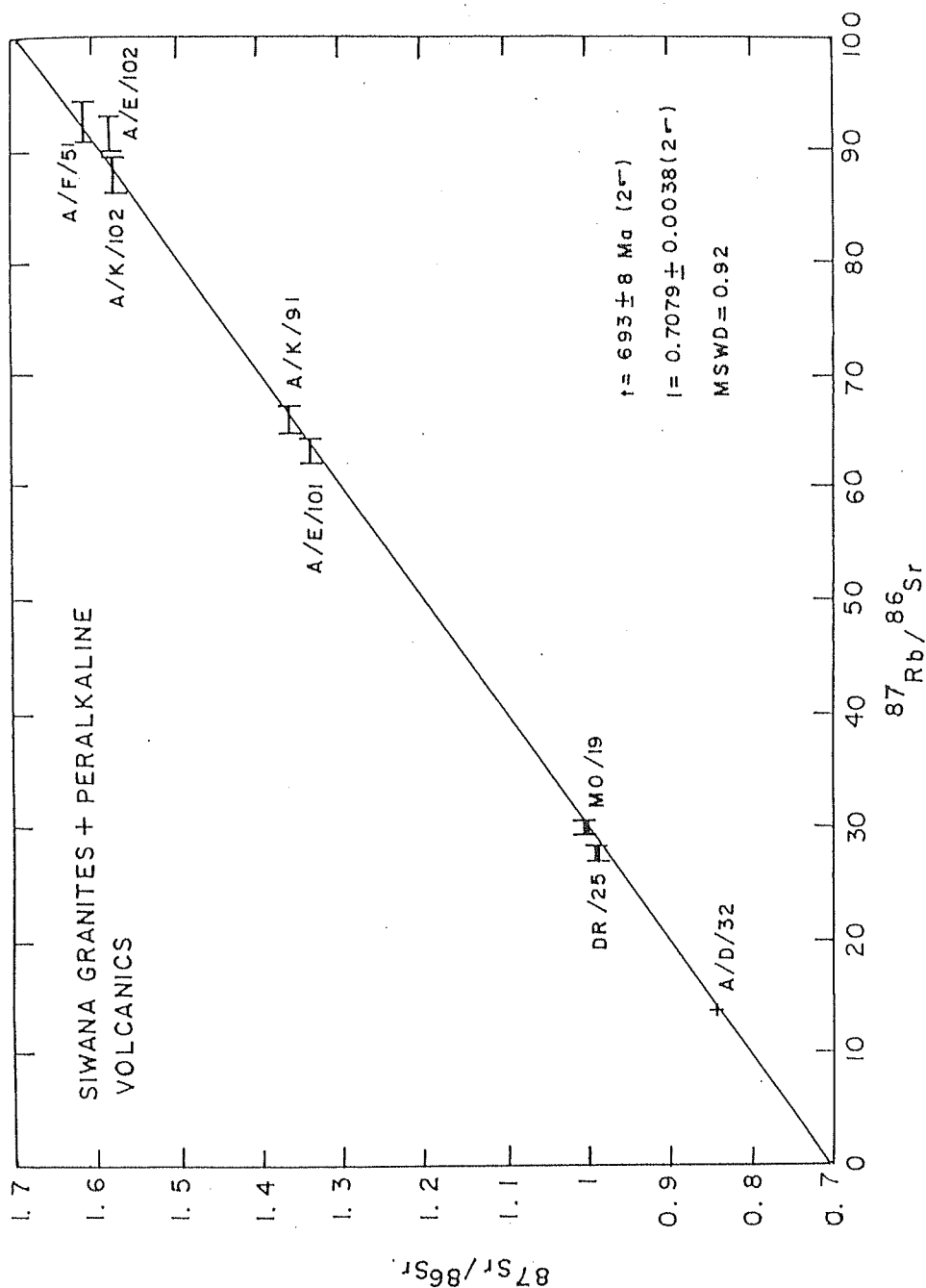


Fig. 4.11. Rb-Sr Conventional Pooled Isochron Diagram for Peralkaline Granites and Peralkaline Volcanics from Sivana.

Table 4.10. Rb-Sr isotopic data of outer rhyolites from South of Siwana,
Barmer district.

Sample No.	^{87}Rb (ppm)	^{86}Sr (ppm)	$^{87}\text{Rb}/^{86}\text{Sr}$ (atomic)	$^{87}\text{Sr}/^{86}\text{Sr}$ (atomic)
A/D/12	44.316	2.940	14.899	0.85690 ± 0.00019
A/F/14	47.352	2.893	16.182	0.86641 ± 0.00016
A/I/21	58.121	2.459	23.369	0.92849 ± 0.00059
A/B/31*	52.582	1.663	31.259	1.01824 ± 0.00031
A/A/33	65.653	1.046	62.052	1.38111 ± 0.00053

* - Not included in calculation

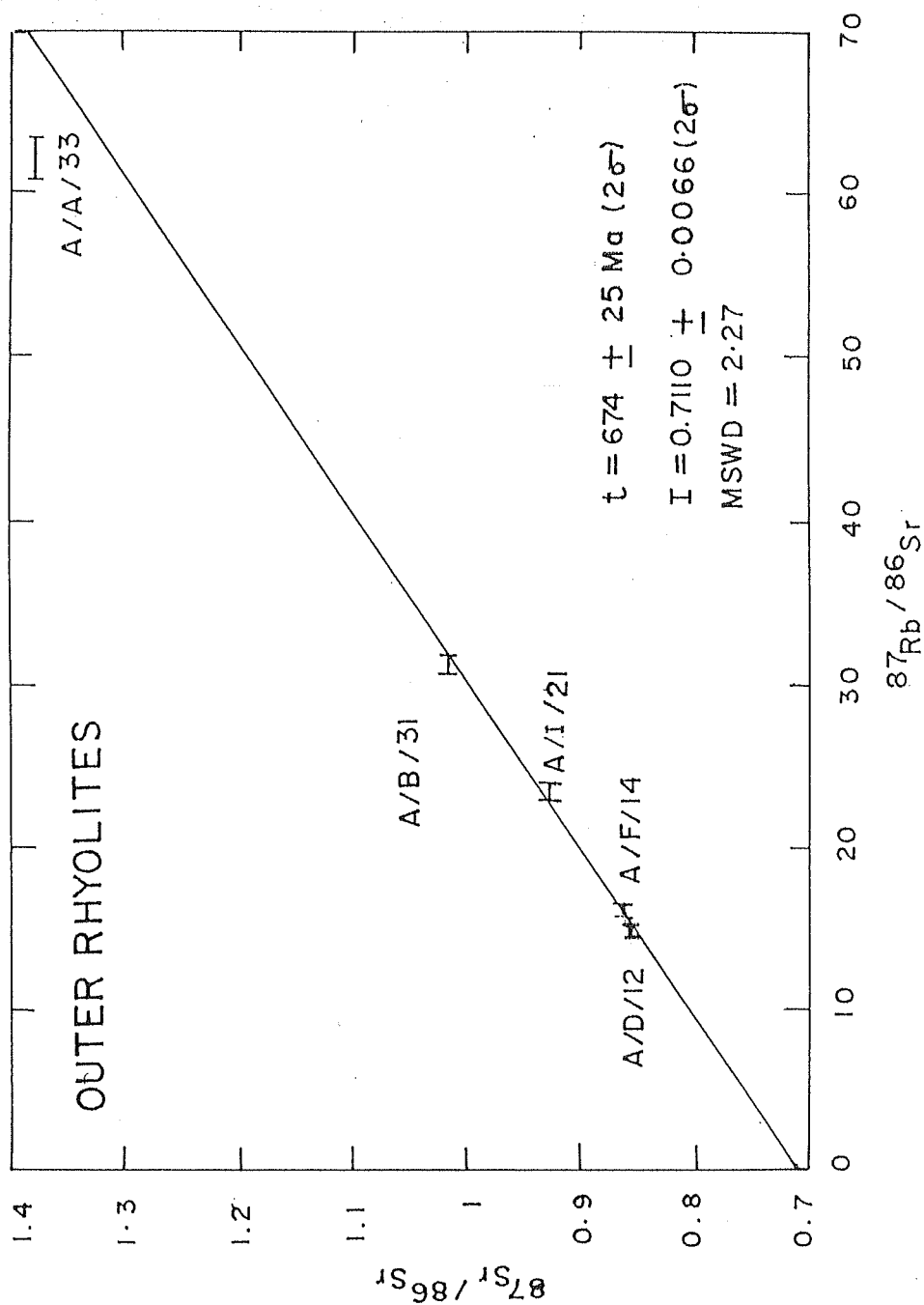


Fig. 4.12. Rb-Sr Conventional Isochron Diagram for Outer Rhyolites from Siwana.

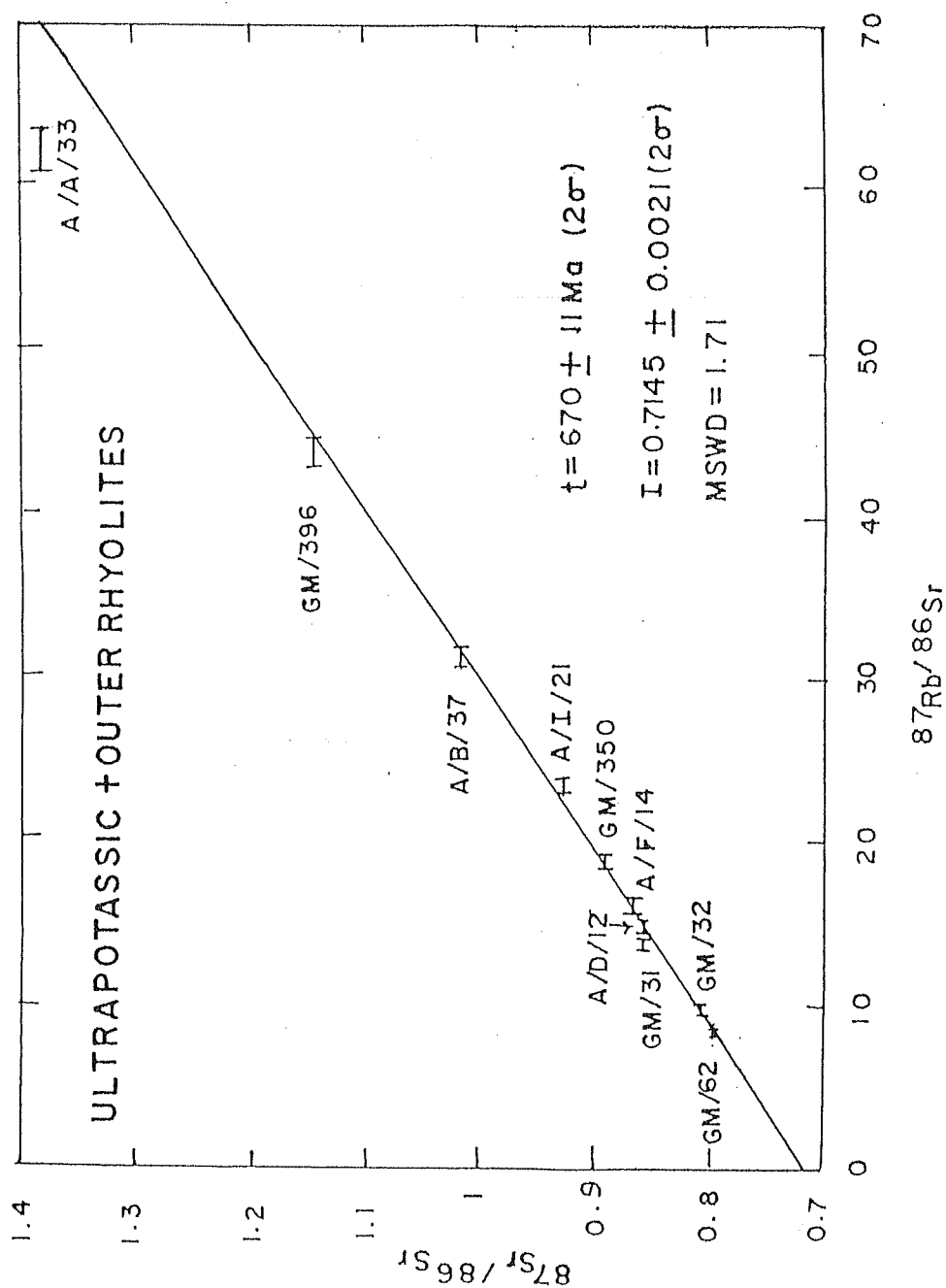


Fig. 4.13. Rb-Sr Conventional Pooled Isochron Diagram for Outer and Ultrapotassic Rhyolite.

points (excluding GM/31 and A/A/33) gave an isochron age of 670 ± 11 Ma (Fig. 4.13) with an initial Sr isotopic ratio of 0.7145 ± 0.0021 . This age and initial Sr isotopic ratio is similar to the age and initial ratio obtained for ultrapotassic and outer rhyolites separately. Further, the MSWD comes down to 1.71 from 1.75 and 2.27, respectively.

This exercise, thus, indicates that the outer rhyolites and ultrapotassic rhyolites are probably derived from the same magma and crystallized at about 670 Ma ago. It may also be possible that the outer rhyolites are cogenetic with the peralkaline rocks and probably represent the end phase of the peralkaline activity, as suggested by Jacobson et al. (1958) and Bowden and Kinnaïrd (1978) for the Nigerian younger granitic province. According to these authors the peralkaline magma at the start of the magmatic cycle may turn to metaluminous to peraluminous at the end, giving rise to a close association of both metaluminous and peralkaline rocks within a single ring complex, the situation as observed at Siwana.

However, in either of the cases, the high initial ratio of the outer as well as ultrapotassic rhyolites is attributed to incorporation of radiogenic Sr in the residual crustal magma.

4.4. ASSOCIATION III (*TAVIDAR VOLCANICS*)

Agrawal (1984) has carried out detailed petrographic and geochemical studies of the mildly alkaline rocks of Tavidar volcanics. The various rocks from Tavidar belong to trachy basalt-trachy andesite-trachyte and rhyolite association (Fig. 1.3).

4.4.1. *K-Ar STUDIES*

In the initial phase of the work, seven samples were dated by K-Ar method and the results are given in Table 4.11. As the K-Ar ages showed wide scatter, ranging from 45 to 75 Ma, ^{40}Ar - ^{39}Ar studies were carried out on the same samples. Out of the seven samples dated by K-Ar method, the ages of five samples were in agreement with ^{40}Ar - ^{39}Ar ages within the experimental errors.

Table 4.11. Analytical data and calculated K-Ar ages of Tavidar volcanics, Jalore district.

Sample No. (Rock type)	K (wt%)	Total ^{40}Ar (10^{-6} cc STPg $^{-1}$)	Rad ^{40}Ar	Age (Ma)
VA/181 (K-Andesite)	2.83	10.90	8.58	76.4 ± 3.2
VA/181(D) (K-Andesite)	2.83	9.22	8.35	74.4 ± 3.8
VA/181(T) (K-Andesite)	2.83	9.67	8.48	75.5 ± 3.2
K/67 (K-Andesite)	3.08	22.45	5.42	44.7 ± 1.8
VA/58 (Trachyte)	3.69	13.83	10.01	68.3 ± 3.0
VA/A (Qtz-Trachyte)	4.72	19.07	12.05	64.5 ± 2.6
VA/168 (K-Rhyolite)	7.12	44.43	17.78	63.1 ± 2.6
VA/119 (Hawaiite)	1.68	5.61	4.51	67.9 ± 2.6
K/69A (Hawaiite)	0.85	3.24	2.12	63.0 ± 4.5

D - Duplicate and **T** - Triplicate analysis

However, two samples viz. K/67 and VA/181, both potassic andesites, gave very discordant K-Ar ages. The sample K/67 gave a K-Ar age of about 45 Ma which is quite low as compared to its ^{40}Ar - ^{39}Ar age of 65 Ma. Sample VA/181 which was analyzed in triplicate, gave consistently higher K-Ar age of about 75 Ma, while its plateau age by ^{40}Ar - ^{39}Ar method was 66 Ma. The anomalous but consistent higher K-Ar age of this sample as well as low age of other sample (K/67) could probably be due to K inhomogeneity in the samples.

4.4.2. ^{40}Ar - ^{39}Ar STUDIES

To assign precisely the formation time to the Tavidar volcanics, in all eight samples were analyzed by ^{40}Ar - ^{39}Ar method. Out of the eight samples analyzed, two were potassic andesites (VA/181 and K/67), two trachytes (VA/58 and K/30), one rhyolite (VA/183), one potassic rhyolite (VA/168) and two hawaiites (VA/119 and K/69A). The samples were irradiated in two batches. The J factor varied from 0.00222 ± 0.00002 to 0.00234 ± 0.00005 . The minimum and maximum values of J were those obtained for samples VA/181 and K/67, respectively.

The argon isotopic composition and abundances of these samples are given in Tables 4.12 to 4.19. Their age spectra and correlation diagrams are shown in Fig. 4.14 to 4.29. A summary of ^{40}Ar - ^{39}Ar results is given in Table 4.20.

Interpretation of the results of ^{40}Ar - ^{39}Ar incremental heating experiments is strongly influenced by graphical methods of presentation. Age spectrum diagrams are widely used and there is general agreement on the interpretation of the shape of age spectra. Isotope correlation plots of $^{40}\text{Ar}/^{39}\text{Ar}$ vs. $^{39}\text{Ar}/^{36}\text{Ar}$ (using data pertaining to the plateau steps), commonly referred to as isochron diagrams, have been used to present ^{40}Ar - ^{39}Ar data, ever since the technique was first developed by Merrihue and Turner (1966). In this diagram the slope of the correlation line (isochron) is proportional to the age of the sample. The intercept on the $^{40}\text{Ar}/^{36}\text{Ar}$ axis is the isotopic composition of non-radiogenic argon in the sample, which is also called as '*initial or trapped argon*'. It is generally assumed that the trapped argon in a sample and any background contribution

from laboratory extraction apparatus is atmospheric in composition. This assumption is quite reasonable for the Tavidar volcanics, as all the samples have the intercept value of atmospheric composition i.e. $^{40}\text{Ar}/^{36}\text{Ar} = 295.5$ (Table 4.20) within the 2σ errors. Thus, the points that define an isochron are mixtures of radiogenic and atmospheric argon. The correlation lines for all the samples are well fitted with all values of MSWD less than 1 at 2σ level except for one sample VA/168, which has given MSWD of 1.2.

The age spectra for potassic andesites viz. VA/181 and K/67 (Fig. 4.14 and 4.15) define good plateaus, comprising 94% and 65.8% of ^{39}Ar released, with plateau ages of 65.9 ± 0.5 Ma and 64.6 ± 0.9 Ma, respectively. Their isochron ages (Fig. 4.16 and 4.17) are 65.5 ± 0.9 Ma and 63.5 ± 1.8 Ma, respectively. There is good agreement between the plateau and isochron ages of potassic andesites, within the experimental error, indicating that these samples have not lost any significant amount of radiogenic argon during their history. The undisturbed nature of these samples is reflected in the integrated or total ages also which are 66.6 ± 0.7 Ma and 65.7 ± 1.7 Ma for VA/181 and K/67, respectively.

The concordance of plateau, isochron and integrated ages for these two samples and considering somewhat disturbed nature of sample K/67, as inferred from its age spectrum diagram, the formation age of potassic andesites is taken as 65.9 Ma.

The release curve for two trachytes viz. VA/58 and K/30 define excellent plateaus (Fig. 4.18 and 4.19), comprising 80.4% and 100% of ^{39}Ar released and yielding plateau ages of 67.2 ± 0.4 Ma and 65.5 ± 0.6 Ma, respectively. The isochron ages (Fig. 4.20 and 4.21) for these samples are 67.6 ± 1.1 Ma and 65.5 ± 1.7 Ma, respectively. The plateau and isochron age of VA/58 is slightly higher than that of K/30.

However, the total ages of these samples are 65.6 ± 0.7 Ma and 65.6 ± 1.7 Ma, respectively, which are in excellent agreement with the plateau and isochron ages of K/30. Taking this fact into account, together with the straightforward interpretation of the perfect plateau of K/30 (100% ^{39}Ar release), it is believed that the trachytes were formed about 65.5 Ma ago. This age is indistinguishable from the age of andesites which were formed 65.9 Ma ago.

Sample VA/183 (rhyolite) has given an excellent plateau at 65.0 ± 0.4 Ma (Fig.

Table 4.12. Step heating argon isotopic compositions and apparent ages of sample
VA/181 (TAVIDAR POTASSIC ANDESITE)
 $J=0.00222 \pm 0.00002$

Temp. (°C)	$^{36}\text{Ar}/^{39}\text{Ar}$	$^{37}\text{Ar}/^{39}\text{Ar}$	$^{40}\text{Ar}/^{39}\text{Ar}$	Age (Ma)	^{39}Ar (%)	$^{40}\text{Ar}^*$ (%)
450	0.3164 ± 0.0078	1.7664 ± 0.0137	112.88 0.96	75.8 19.0	0.40	17.20
500	0.2154 0.0061	1.6199 0.0062	82.79 0.74	74.9 14.8	0.50	23.10
550	0.0115 0.0006	0.5221 0.0038	22.26 0.14	73.7 1.8	5.13	84.62
750	0.0033 0.0001	0.3061 0.0026	17.79 0.10	65.9 0.9	30.61	94.53
800	0.0020 0.0000	0.1244 0.0006	17.25 0.10	65.3 0.9	13.95	96.53
900	0.0044 0.0001	0.0945 0.0019	18.01 0.11	65.5 0.9	10.13	92.64
1000	0.0095 0.0004	0.1117 0.0014	20.03 0.12	67.4 1.4	16.82	85.86
1050	0.0108 0.0003	0.2175 0.0007	20.17 0.12	66.5 1.3	10.28	84.07
1150	0.0108 0.0006	0.8969 0.0024	20.24 0.13	66.8 1.9	5.24	84.16
1250	0.0123 0.0004	3.0455 0.0065	20.05 0.14	64.4 1.6	3.64	81.85
1350	0.0094 0.0014	2.8513 0.0057	19.78 0.22	66.7 3.8	2.30	86.00
1500	0.0089 0.0018	2.2713 0.0141	19.65 0.34	66.7 4.8	0.90	86.60
TOTAL	0.0088 0.0001	0.4500 0.0009	19.61 0.05	66.6 0.7	100.00	86.63

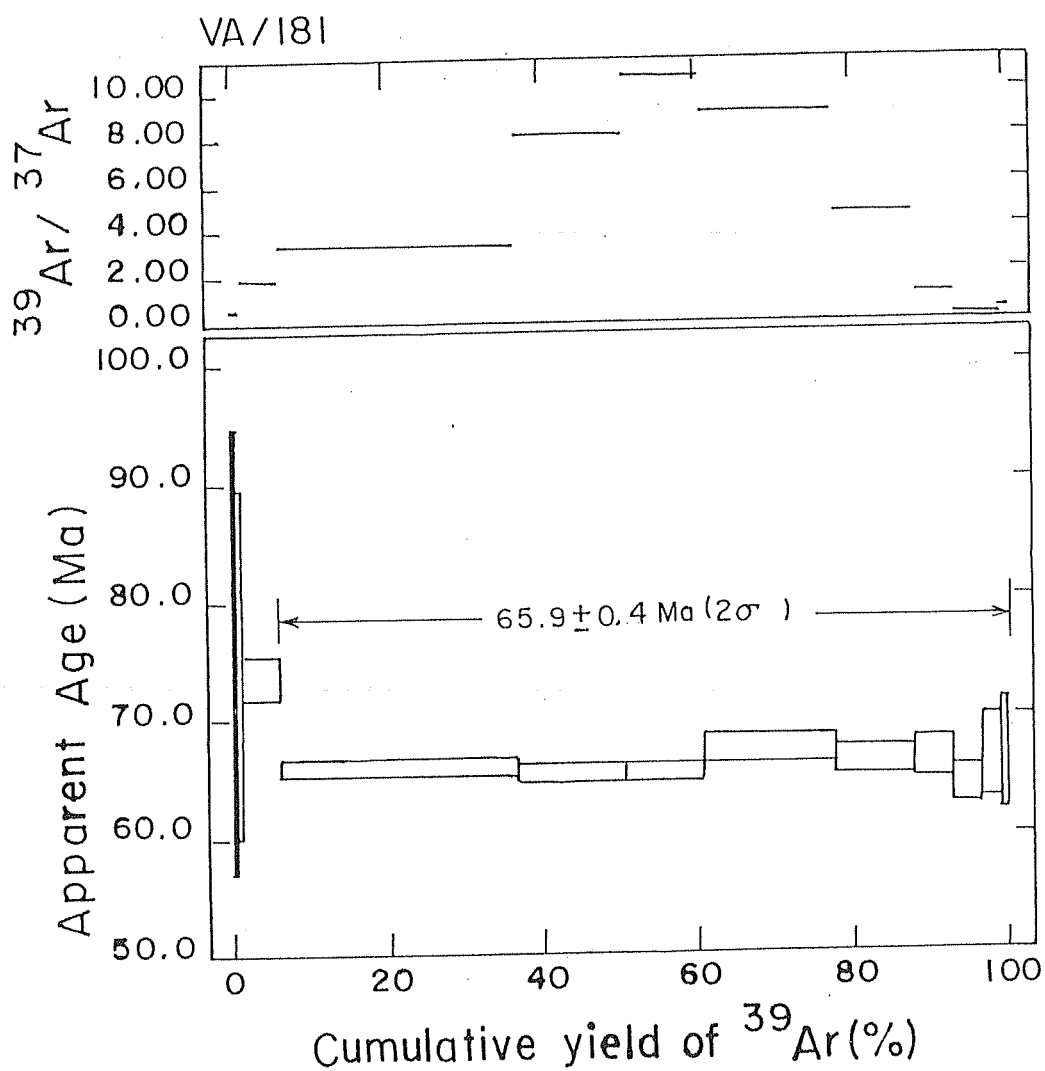


Fig. 4.14. ^{40}Ar - ^{39}Ar Age Spectrum for Tavidar Andesite (VA/181).

Table 4.13. Step heating argon isotopic compositions and apparent ages of sample
K/67 (TAVIDAR POTASSIC ANDESITE)
 $J=0.00234 \pm 0.00005$

Temp. (°C)	$^{36}\text{Ar}/^{39}\text{Ar}$	$^{37}\text{Ar}/^{39}\text{Ar}$	$^{40}\text{Ar}/^{39}\text{Ar}$	Age (Ma)	^{39}Ar (%)	$^{40}\text{Ar}^*$ (%)
500	0.0961 ± 0.0006	0.5864 ± 0.0016	43.07 ± 0.25	60.9 ± 1.8	3.90	34.00
550	0.0124 0.0003	0.5168 0.0042	19.46 0.12	65.4 2.0	4.00	81.10
600	0.0141 0.0002	0.3891 0.0012	20.87 0.14	69.2 2.2	4.50	80.10
650	0.0222 0.0002	0.2991 0.0008	23.84 0.14	71.4 2.2	6.00	72.40
700	0.0173 0.0002	0.2921 0.0005	22.05 0.13	70.1 2.0	5.70	76.70
750	0.0151 0.0001	0.2728 0.0014	20.93 0.12	68.3 1.9	10.02	78.77
800	0.0083 0.0001	0.2666 0.0007	18.18 0.11	65.2 1.8	14.16	86.42
850	0.0101 0.0001	0.3057 0.0009	18.40 0.11	63.9 1.8	13.78	83.78
900	0.0152 0.0001	0.4167 0.0023	19.73 0.11	63.2 1.8	17.65	77.15
950	0.0145 0.0002	1.0283 0.0021	19.62 0.12	63.6 1.9	7.90	78.14
1000	0.0356 0.0006	1.4046 0.0028	26.20 0.18	64.9 2.6	2.70	59.80
1050	0.0350 0.0007	1.3061 0.0026	26.60 0.17	67.3 2.8	4.40	61.00
1100	0.0321 0.0018	1.2877 0.0046	26.70 0.37	71.3 5.4	1.00	64.50

contd.

Table 4.13. (contd.)

Temp. (°C)	$^{36}\text{Ar}/^{39}\text{Ar}$	$^{37}\text{Ar}/^{39}\text{Ar}$	$^{40}\text{Ar}/^{39}\text{Ar}$	Age (Ma)	^{39}Ar (%)	$^{40}\text{Ar}^*$ (%)
1200	0.0373 0.0006	1.3794 0.0028	26.88 0.24	65.7 3.0	3.30	59.00
1500	0.0011 ± 0.0024	1.5901 ± 0.0401	17.00 ± 2.20	69.0 ± 19.0	0.90	98.10
TOTAL	0.0192 0.0001	0.5262 0.0006	21.53 0.04	65.7 1.7	100.00	73.63

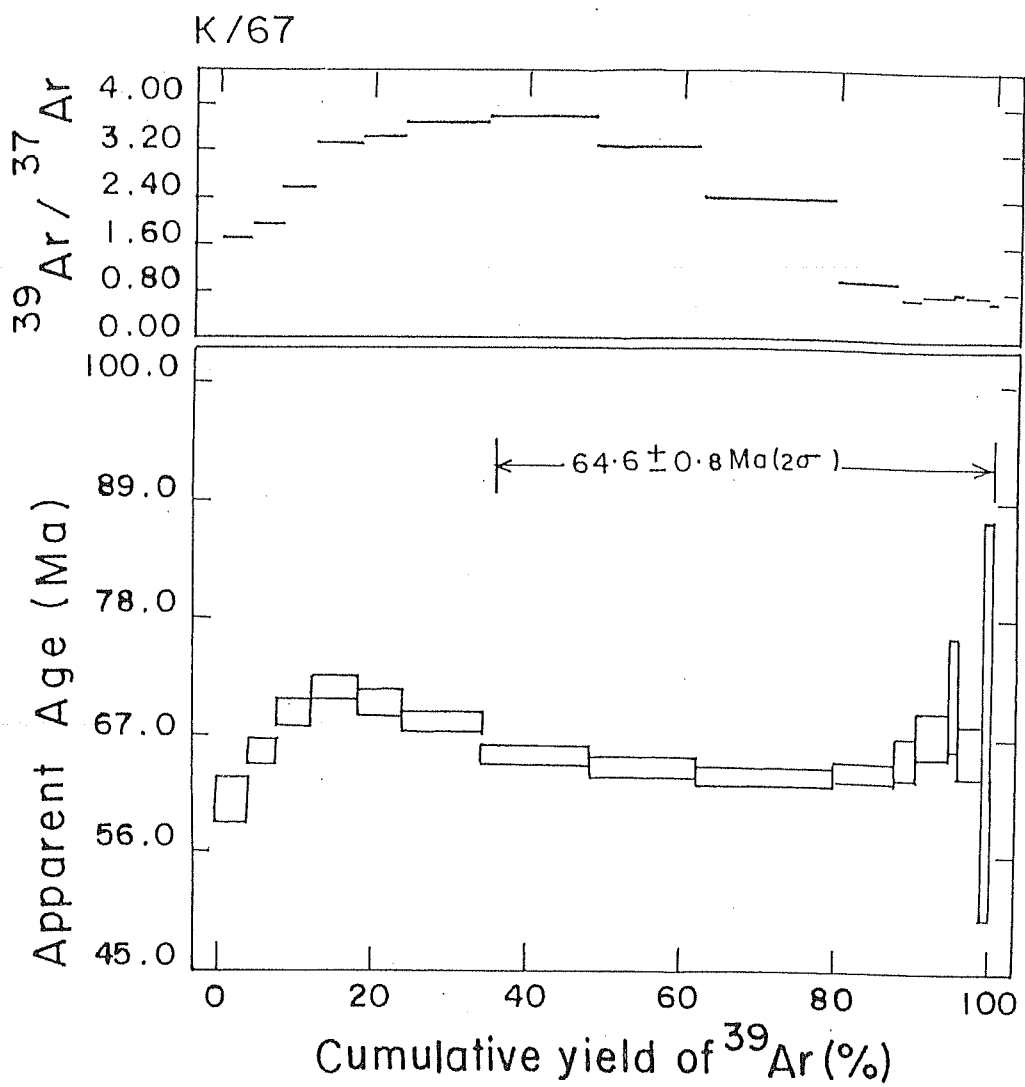


Fig. 4.15. ^{40}Ar - ^{39}Ar Age Spectrum for Tavidar Andesite (K/67).

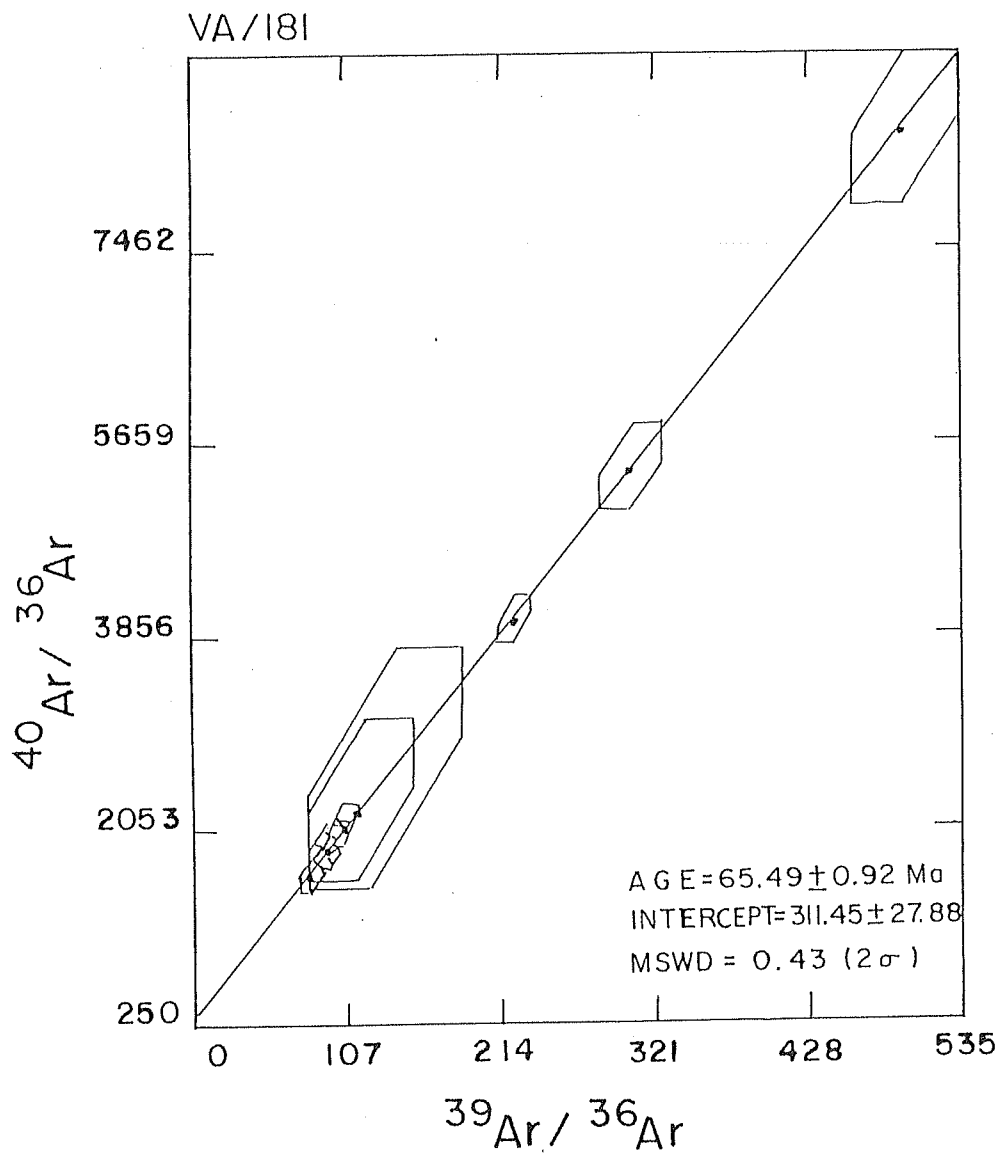


Fig. 4.16. $^{40}\text{Ar}/^{36}\text{Ar}$ vs. $^{39}\text{Ar}/^{36}\text{Ar}$ Isochron Plot for Tavidar Andesite (VA/181).

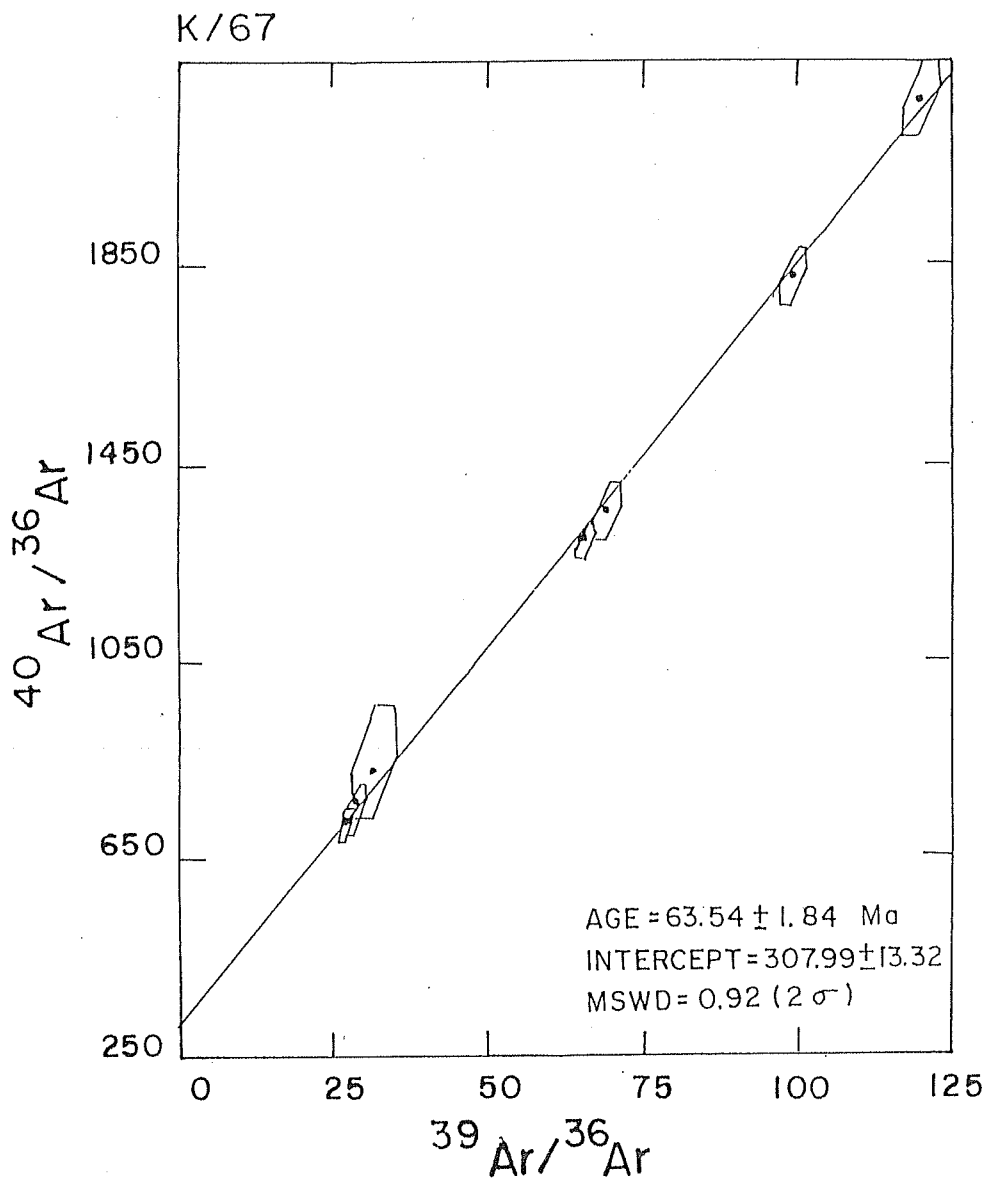


Fig. 4.17. $^{40}\text{Ar}/^{36}\text{Ar}$ vs. $^{39}\text{Ar}/^{36}\text{Ar}$ Isochron Plot for Tavidar Andesite (K/67).

Table 4.14. Step heating argon isotopic compositions and apparent ages of sample
 VA/58 (TAVIDAR TRACHYTE)
 $J=0.00224 \pm 0.00002$

Temp. (°C)	$^{36}\text{Ar}/^{39}\text{Ar}$	$^{37}\text{Ar}/^{39}\text{Ar}$	$^{40}\text{Ar}/^{39}\text{Ar}$	Age (Ma)	^{39}Ar (%)	$^{40}\text{Ar}^*$ (%)
350	0.0703 ±0.0003	0.3186 ±0.0009	33.74 0.20	51.7 1.7	6.23	38.41
500	0.0229 0.0003	0.3195 0.0014	22.42 0.13	62.2 1.4	9.28	69.75
550	0.0204 0.0004	0.6114 0.0074	21.65 0.15	62.1 1.6	4.12	72.14
700	0.0135 0.0004	0.9025 0.0021	20.55 0.15	65.7 1.6	4.09	80.54
750	0.0112 0.0001	0.2259 0.0036	20.49 0.14	68.1 1.2	5.10	83.76
800	0.0109 0.0004	0.1126 0.0006	20.08 0.14	66.8 1.5	4.70	83.82
900	0.0088 0.0001	0.0993 0.0003	19.83 0.12	68.3 1.0	19.01	86.75
1000	0.0109 0.0001	0.1265 0.0005	20.15 0.12	67.2 1.0	19.44	83.91
1100	0.0216 0.0001	0.2748 0.0007	22.92 0.13	65.6 1.1	20.50	72.04
1250	0.0414 0.0003	0.4363 0.0008	29.32 0.21	67.8 1.8	5.24	58.26
1350	0.0441 0.0024	0.4698 0.0015	31.07 0.69	71.5 7.8	1.50	58.00
1500	0.0874 0.0098	0.5459 0.0201	46.06 0.92	79.9 23.6	1.00	43.90
TOTAL	0.0207 0.0001	0.2624 0.0004	22.65 0.05	165.6 0.7	100.00	72.90

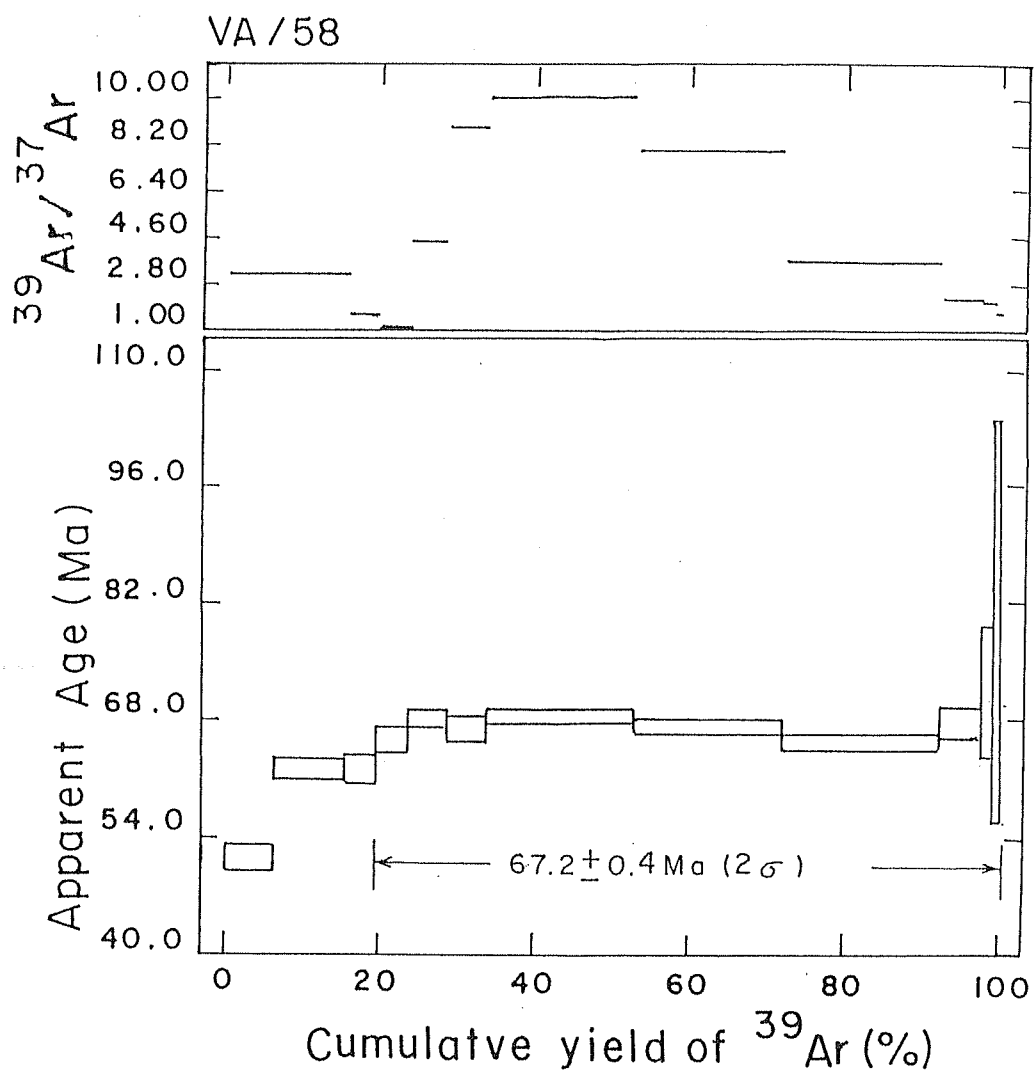


Fig. 4.18. ^{40}Ar - ^{39}Ar Age Spectrum for Tavidar Trachyte (VA/58).

Table 4.15. Step heating argon isotopic compositions and apparent ages of sample K/30 (TAVIDAR TRACHYTE)
J=0.00233 ± 0.00005

Temp. (°C)	³⁶ Ar/ ³⁹ Ar	³⁷ Ar/ ³⁹ Ar	⁴⁰ Ar/ ³⁹ Ar	Age (Ma)	³⁹ Ar (%)	⁴⁰ Ar* (%)
500	0.2653 ±0.0011	0.2505 ±0.0005	94.57 0.68	66.6 5.6	1.70	17.10
550	0.0458 0.0003	0.2568 0.0013	29.75 0.18	66.7 2.2	2.40	54.50
600	0.0248 0.0001	0.4799 0.0009	23.60 0.14	67.0 1.9	5.26	68.95
650	0.0668 0.0002	0.6632 0.0026	35.61 0.21	65.4 2.2	6.30	44.60
700	0.0019 0.0001	0.0708 0.0005	16.62 0.01	66.1 1.8	20.70	96.53
750	0.0029 0.0001	0.0486 0.0001	16.84 0.01	65.8 1.8	8.99	94.85
800	0.0063 0.0001	0.0647 0.0006	17.70 0.10	65.2 1.8	6.15	89.35
850	0.0093 0.0001	0.0608 0.0016	18.52 0.11	64.9 1.8	7.60	85.03
900	0.0106 0.0001	0.0648 0.0014	18.89 0.11	64.9 1.8	9.13	83.35
950	0.0144 0.0001	0.0832 0.0001	20.26 0.12	65.9 1.9	11.85	78.90
1000	0.0199 0.0001	0.1011 0.0007	21.58 0.13	64.6 1.9	7.56	72.67
1050	0.0217 0.0002	0.1788 0.0004	22.33 0.13	65.6 2.0	4.70	71.30
1100	0.0206 0.0002	0.2253 0.0004	22.12 0.13	65.9 1.9	4.79	72.42
1200	0.0216 0.0004	0.2632 0.0005	21.93 0.17	64.1 2.2	2.80	70.90
TOTAL	0.0197 0.0001	0.1551 0.0002	21.76 0.04	65.6 1.7	100.00	73.20

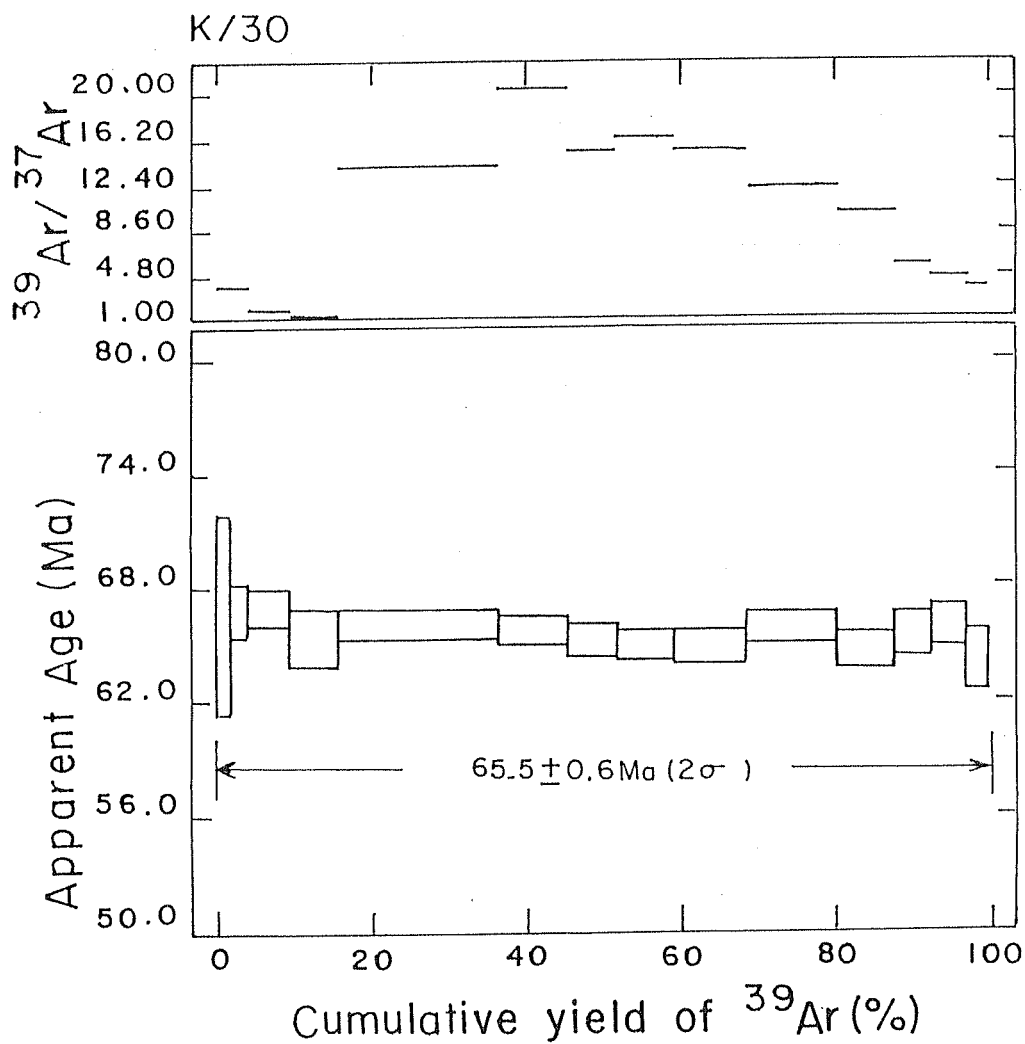


Fig. 4.19. ^{40}Ar - ^{39}Ar Age Spectrum for Tavidar Trachyte (K/30).

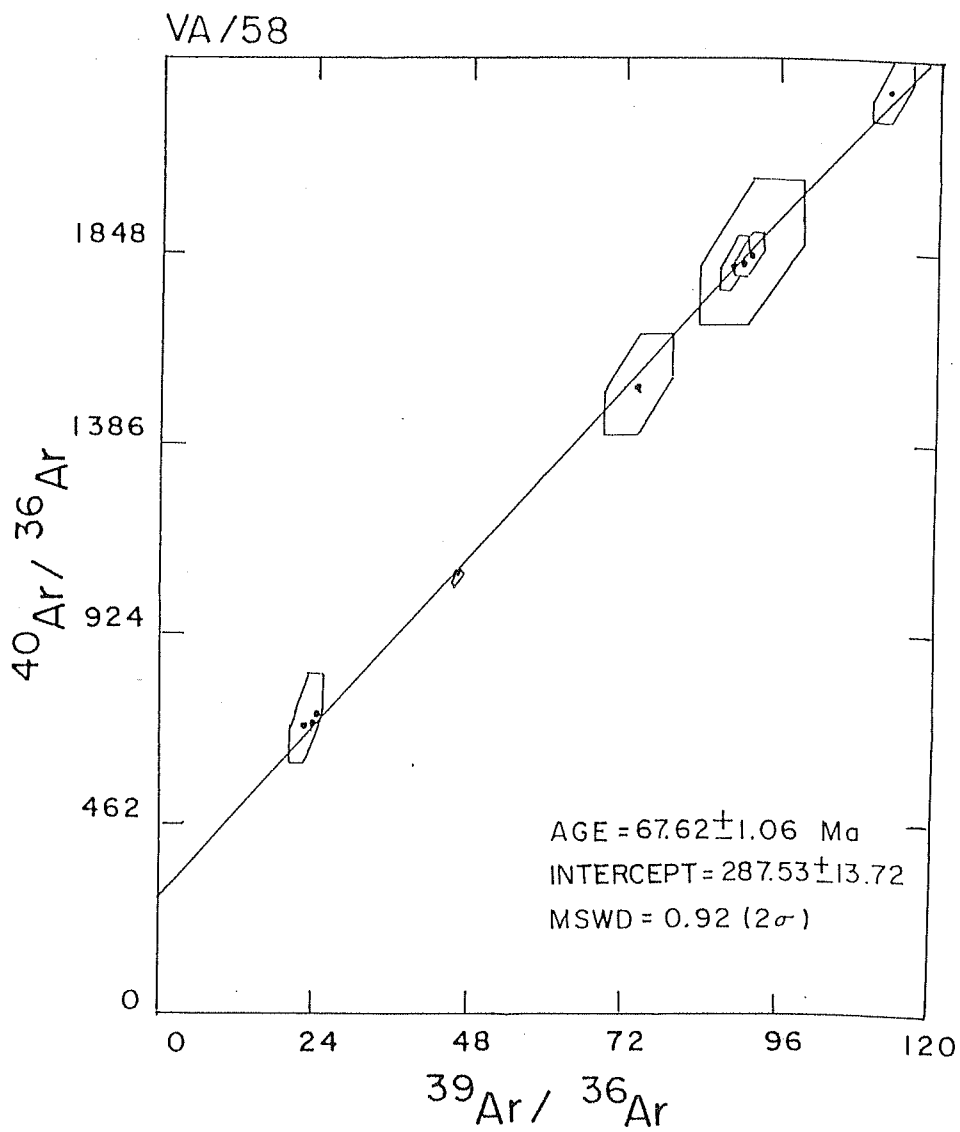


Fig. 4.20. $^{40}\text{Ar}/^{36}\text{Ar}$ vs. $^{39}\text{Ar}/^{36}\text{Ar}$ Isochron Plot for Tavidar Trachyte (VA/58).

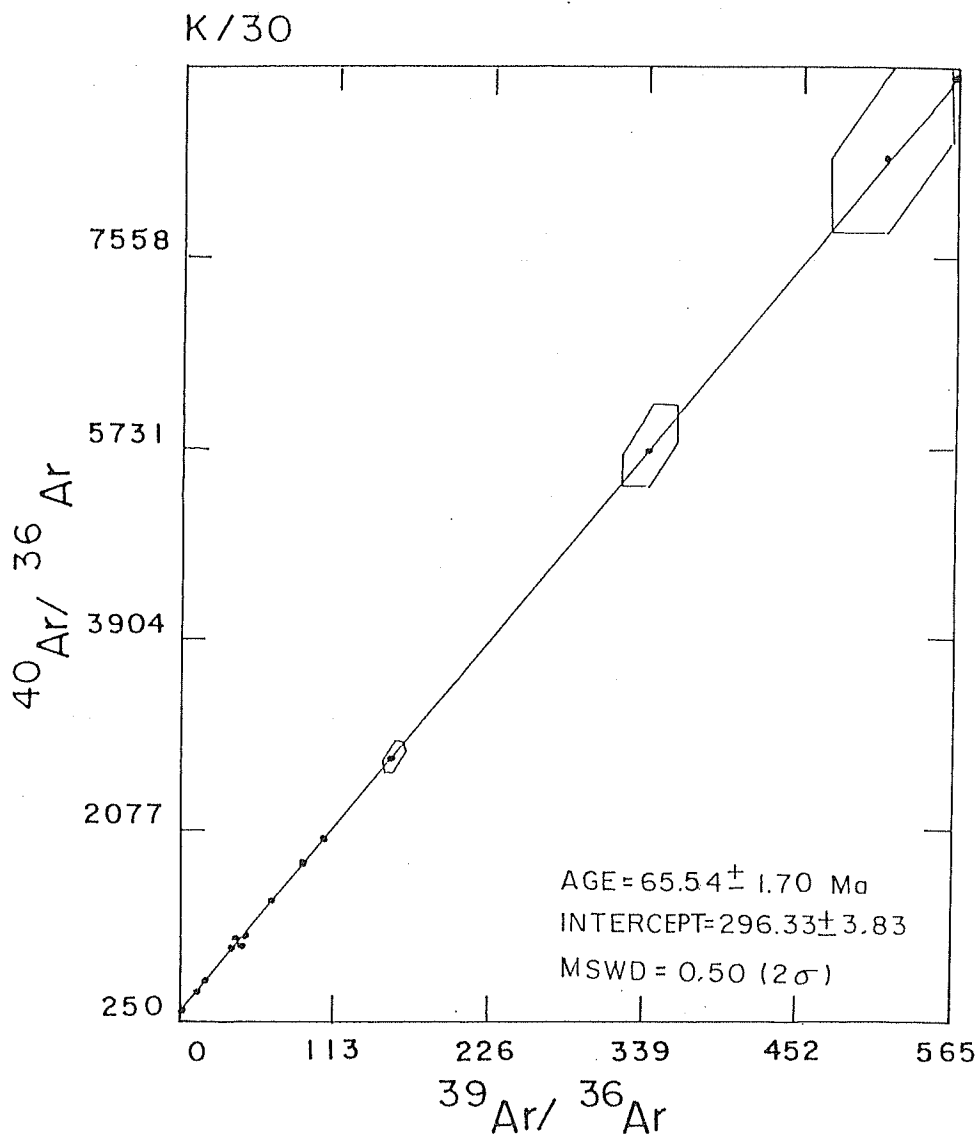


Fig. 4.21. $^{40}\text{Ar}/^{36}\text{Ar}$ vs. $^{39}\text{Ar}/^{36}\text{Ar}$ Isochron Plot for Tavidar Trachyte (K/30).

4.22) consisting of 100% ^{39}Ar released. The isochron (Fig. 4.23) and total ages for this sample are 64.5 ± 0.8 Ma and 65.1 ± 0.6 Ma, respectively. The concordance of plateau, isochron and total ages of VA/183 suggest that the rhyolite was formed 65 Ma ago.

One potassic rhyolite (VA/168) has been analyzed. In this sample comparatively less amount of ^{39}Ar release exhibit the plateau. The sample apparently shows a bi-modal ^{39}Ar release pattern (Fig. 4.24). The initial four temperature steps (excluding first step), comprising about 24% of total ^{39}Ar released, display a stair case pattern with progressively decreasing apparant ages, while the higher eight temperature steps (900° to fusion), comprising 59.5% of total ^{39}Ar released, form the plateau at 63.8 ± 0.8 Ma. However, no relation is reflected in the K/Ca ratio diagram. Thus, the stair case pattern observed in the initial temperature steps could be due to some experimental errors/recoil effect of ^{39}Ar during irradiation which may result either in loss of ^{39}Ar or increase of ^{39}Ar in slightly higher activation sites.

The isochron (Fig. 4.25) and total age of this sample are 62.8 ± 2.9 Ma and 63.3 ± 1.0 Ma, respectively. The conformity of plateau, isochron and total age of this sample suggest that there has not been any loss of argon after its formation and the age obtained from this sample infact indicates the time of its formation. Thus, the potassic rhyolite (VA/168) was formed 63.8 Ma ago.

In addition to the differentiated rocks, two hawaiites (VA/119 and K/69A) have also been dated. These samples have yielded good plateaus (Fig. 4.26 and 4.27) at 63.8 ± 0.8 Ma and 64.9 ± 0.8 Ma, comprising 84.7% and 67.7% of total ^{39}Ar released, respectively. The isochron ages (Fig. 4.28 and 4.29) for these samples are 64.2 ± 1.7 Ma and 65.3 ± 2.9 Ma, while the total ages are 64.5 ± 1.7 Ma and 61.7 ± 1.7 Ma, respectively. The total age of K/69A is slightly discordant from the total, plateau and isochron ages of VA/119 as well as plateau and isochron ages of K/69A itself. This discordance in the total age of K/69A is due to loss of argon in the initial as well as in the last three temperature steps, as is evident from the Fig. 4.27, resulting in lowering the total age of this sample. However, mutual similarity of plateau and isochron ages of these hawaiites indicate their emplacement about 64 Ma ago.

The plateau ages of Tavidar mildly alkaline rocks (see Table 4.20 for summary)

Table 4.16. Step heating argon isotopic compositions and apparent ages of sample
VA/183 (TAVIDAR RHYOLITE)
 $J=0.00227 \pm 0.00002$

Temp. (°C)	$^{36}\text{Ar}/^{39}\text{Ar}$	$^{37}\text{Ar}/^{39}\text{Ar}$	$^{40}\text{Ar}/^{39}\text{Ar}$	Age (Ma)	^{39}Ar (%)	$^{40}\text{Ar}^*$ (%)
450	0.0366 ± 0.0006	0.0581 ± 0.0008	27.44 ± 0.17	66.9 ± 2.0	2.50	60.60
500	0.0114 0.0001	0.0476 0.0007	19.41 0.11	64.5 1.0	7.29	82.50
550	0.0104 0.0001	0.0591 0.0023	19.21 0.11	64.8 1.0	6.55	83.86
600	0.0123 0.0001	0.0293 0.0007	19.57 0.12	64.1 1.0	8.37	81.31
650	0.0059 0.0001	0.0154 0.0003	17.65 0.11	64.0 0.9	7.02	90.07
700	0.0059 0.0001	0.2162 0.0004	17.92 0.11	65.0 1.0	4.15	90.19
750	0.0076 0.0001	0.0321 0.0003	18.45 0.11	65.1 0.9	5.64	87.72
800	0.0092 0.0001	0.0211 0.0001	18.99 0.11	65.4 0.9	11.61	85.53
900	0.0123 0.0001	0.0246 0.0008	19.89 0.12	65.4 1.0	9.60	81.72
1000	0.0151 0.0001	0.0213 0.0007	20.78 0.12	65.6 1.0	10.69	78.43
1050	0.0204 0.0001	0.0301 0.0001	22.27 0.14	65.4 1.2	8.13	72.93
1150	0.0251 0.0001	0.2287 0.0016	23.74 0.14	65.6 1.1	12.13	68.68
1250	0.0370 0.0004	0.0404 0.0008	27.32 0.22	65.9 1.9	2.47	59.92

contd.

Table 4.16. (contd.)

Temp. (°C)	$^{36}\text{Ar}/^{39}\text{Ar}$	$^{37}\text{Ar}/^{39}\text{Ar}$	$^{40}\text{Ar}/^{39}\text{Ar}$	Age (Ma)	^{39}Ar (%)	$^{40}\text{Ar}^*$ (%)
1300	0.0372 ± 0.0007	0.0878 ± 0.0078	27.36 ± 0.32	65.8 ± 3.0	1.40	59.97
1350	0.0436 0.0008	0.0970 0.0047	28.75 0.35	63.8 3.4	1.20	55.10
1500	0.0359 0.0017	0.1044 0.0051	26.95 0.49	65.7 5.6	1.20	60.60
TOTAL	0.0155 0.0000	0.0651 0.0003	20.78 0.04	65.1 0.6	100.00	77.86

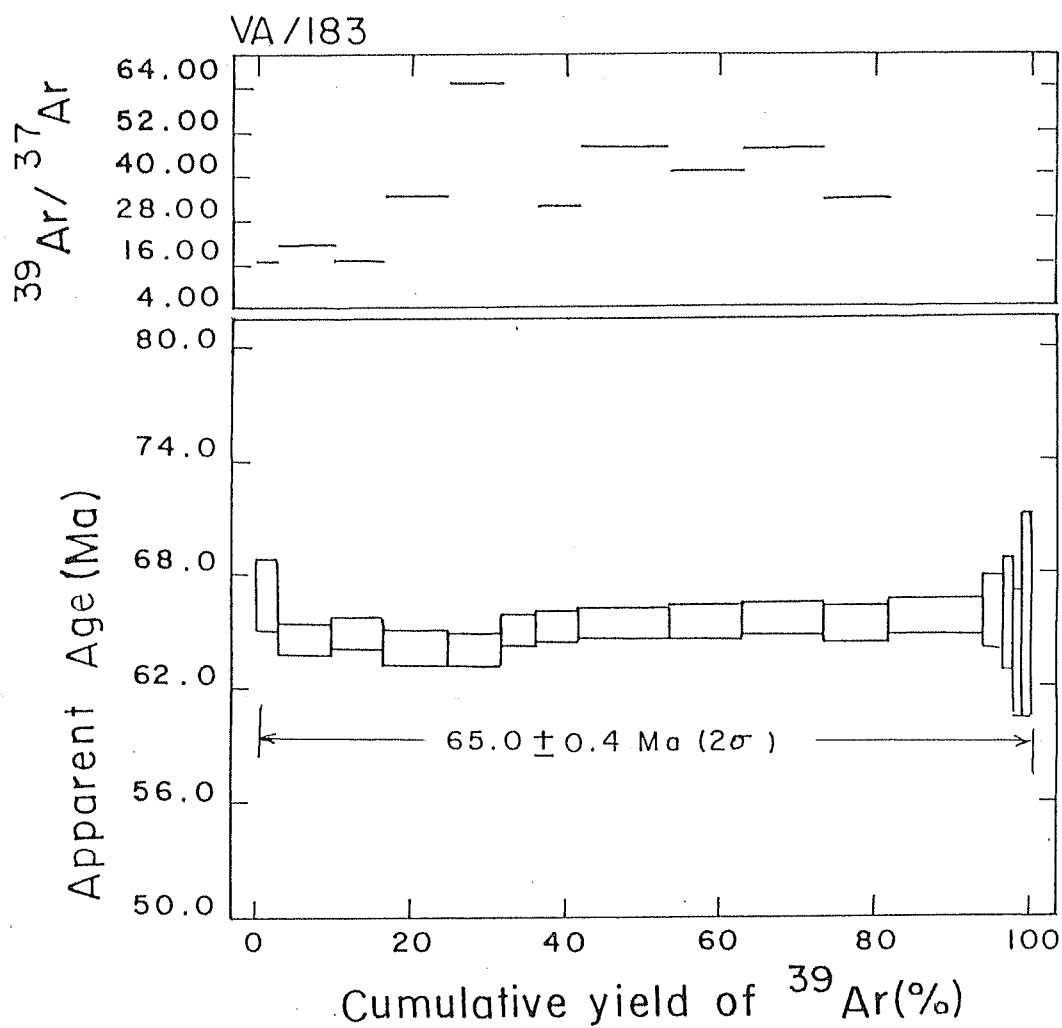


Fig. 4.22. ^{40}Ar - ^{39}Ar Age Spectrum for Tavidar Rhyolite (VA/183).

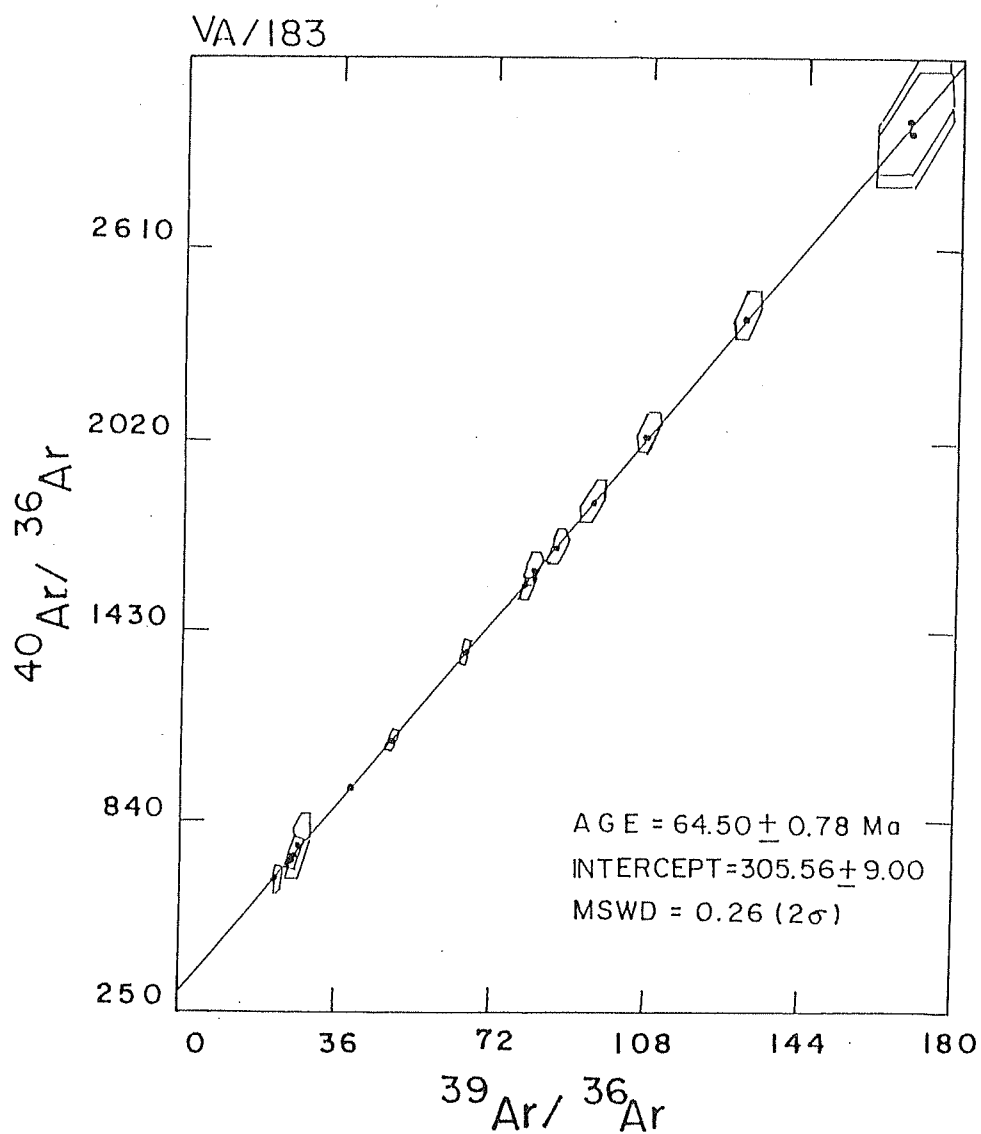


Fig. 4.23. $^{40}\text{Ar}/^{36}\text{Ar}$ vs. $^{39}\text{Ar}/^{36}\text{Ar}$ Isochron Plot for Tavidar Rhyolite (VA/183).

**Table 4.17. Step heating argon isotopic compositions and apparent ages of sample
VA/168 (TAVIDAR POTASSIC RHYOLITE)
 $J=0.00233 \pm 0.00003$**

Temp. (°C)	$^{36}\text{Ar}/^{39}\text{Ar}$	$^{37}\text{Ar}/^{39}\text{Ar}$	$^{40}\text{Ar}/^{39}\text{Ar}$	Age (Ma)	^{39}Ar (%)	$^{40}\text{Ar}^*$ (%)
450	1.0385 ± 0.0036	0.0326 ± 0.0047	314.10 1.80	30.0 14.0	1.60	2.30
500	0.2599 0.0009	0.0132 0.0013	93.08 0.54	67.0 4.2	4.20	17.50
550	0.1235 0.0004	0.0078 0.0006	51.74 0.30	62.8 2.4	7.10	29.40
600	0.1101 0.0004	0.0079 0.0006	47.02 0.27	59.8 2.2	6.80	30.80
650	0.0602 0.0002	0.0154 0.0008	31.58 0.18	57.0 1.5	5.73	43.65
700	0.0469 0.0002	0.0158 0.0001	30.66 0.18	69.2 1.6	4.72	54.78
750	0.0417 0.0002	0.0121 0.0004	28.88 0.17	68.1 1.5	5.29	57.24
800	0.0417 0.0002	0.0121 0.0004	28.73 0.17	67.6 1.5	5.06	57.09
900	0.0504 0.0002	0.0000 0.0000	30.47 0.18	64.2 1.6	6.95	51.07
1000	0.0683 0.0002	0.0068 0.0003	34.99 0.20	61.1 1.7	9.38	42.30
1050	0.0924 0.0003	0.0038 0.0001	42.63 0.25	63.2 1.9	14.63	35.92
1150	0.1085 0.0003	0.0074 0.0001	48.10 0.28	66.1 2.2	9.80	33.30
1250	0.1207 0.0004	0.0054 0.0007	50.84 0.29	62.5 2.2	15.10	29.80
1350	0.0802 0.0008	0.0366 0.0002	39.90 0.24	66.8 2.8	2.40	40.60

contd.

Table 4.17 (contd.)

Temp. (°C)	$^{36}\text{Ar}/^{39}\text{Ar}$	$^{37}\text{Ar}/^{39}\text{Ar}$	$^{40}\text{Ar}/^{39}\text{Ar}$	Age (Ma)	^{39}Ar (%)	$^{40}\text{Ar}^*$ (%)
1400	0.0825 ± 0.0012	0.1354 ± 0.0002	41.04 0.50	68.7 5.0	0.60	40.60
1500	0.0818 0.0023	0.1236 0.0002	41.59 0.66	71.7 7.6	0.60	41.90
TOTAL	0.1086 0.0001	0.0102 0.0001	47.43 0.08	63.2 1.0	100.00	32.30

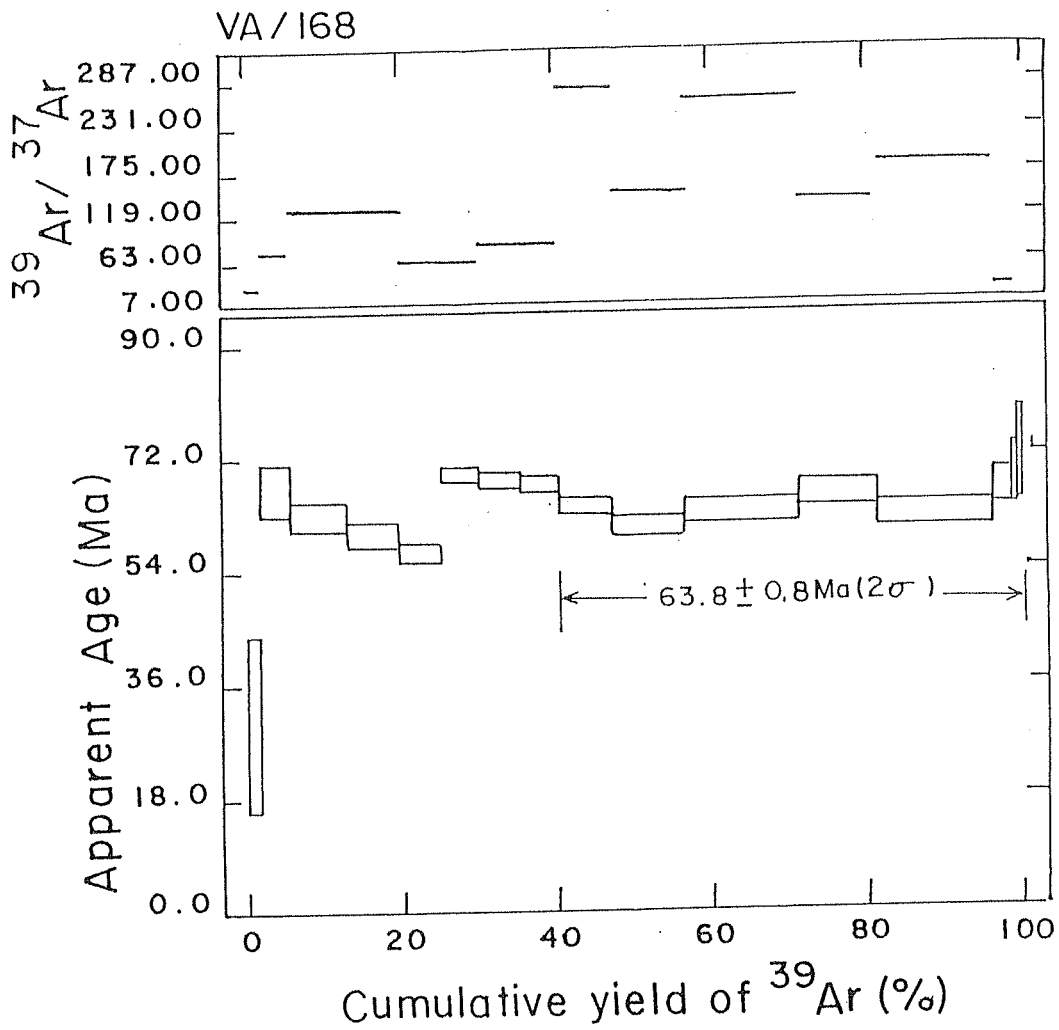


Fig. 4.24. ^{40}Ar - ^{39}Ar Age Spectrum for Tavidar Potassic Rhyolite (VA/168).

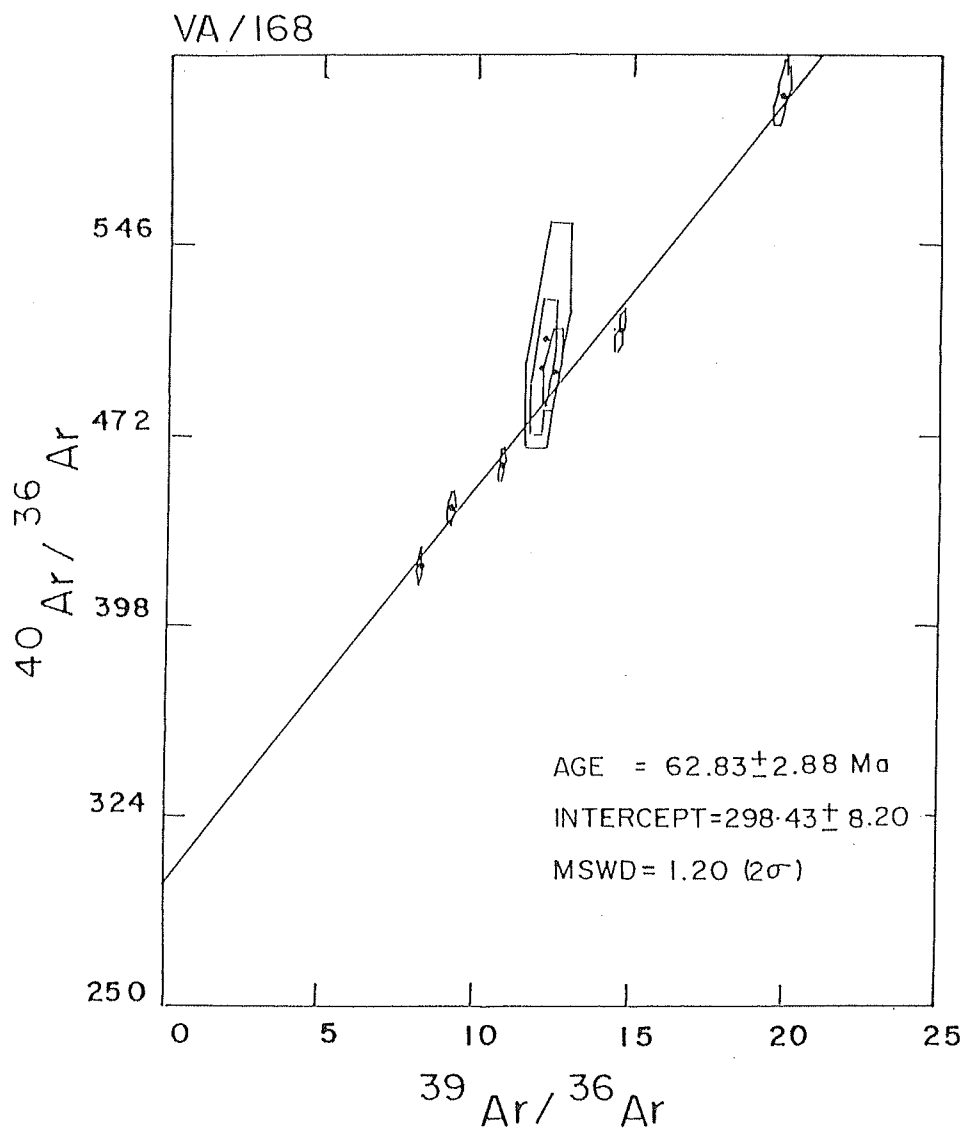


Fig. 4.25. $^{40}\text{Ar}/^{36}\text{Ar}$ vs. $^{39}\text{Ar}/^{36}\text{Ar}$ Isochron Plot for Tavidar Potassic Rhyolite (VA/168).

Table 4.18. Step heating argon isotopic compositions and apparent ages of sample
VA/119 (TAVIDAR HAWAIIITE)
 $J=0.00234 \pm 0.00005$

Temp. (°C)	$^{36}\text{Ar}/^{39}\text{Ar}$	$^{37}\text{Ar}/^{39}\text{Ar}$	$^{40}\text{Ar}/^{39}\text{Ar}$	Age (Ma)	^{39}Ar (%)	$^{40}\text{Ar}^*$ (%)
500	0.0741 ± 0.0004	1.1012 ± 0.0022	36.67 ± 0.25	61.3 ± 2.6	2.90	40.30
550	0.0411 0.0004	1.3066 0.0026	27.23 0.19	62.4 2.4	3.60	55.30
600	0.0461 0.0003	1.3351 0.0027	30.38 0.20	69.3 2.4	4.20	55.10
650	0.0452 0.0003	1.8148 0.0036	31.07 0.20	73.1 2.4	4.60	56.90
700	0.0678 0.0006	3.1631 0.0063	35.48 0.23	64.0 2.8	3.80	43.50
750	0.0531 0.0007	5.0971 0.0011	31.19 0.19	64.1 2.8	5.40	49.60
800	0.0077 0.0002	1.5023 0.0031	17.85 0.11	64.4 1.9	7.81	87.16
850	0.0064 0.0001	0.8309 0.0027	17.53 0.11	64.7 1.9	9.29	89.14
900	0.0073 0.0001	0.6767 0.0014	17.83 0.10	64.9 1.8	21.79	87.90
950	0.0097 0.0001	0.8911 0.0018	18.28 0.11	63.7 1.8	22.96	84.16
1000	0.0143 0.0003	3.6797 0.0074	19.25 0.13	62.2 2.0	5.64	77.98
1050	0.0218 0.0004	4.0811 0.0011	21.27 0.14	61.4 2.2	5.80	69.60
1100	0.0261 0.0008	4.0936 0.0082	23.24 0.28	64.3 5.4	2.20	66.80
TOTAL	0.0207 0.0001	1.6958 0.0012	21.72 0.04	64.5 1.7	100.00	71.70

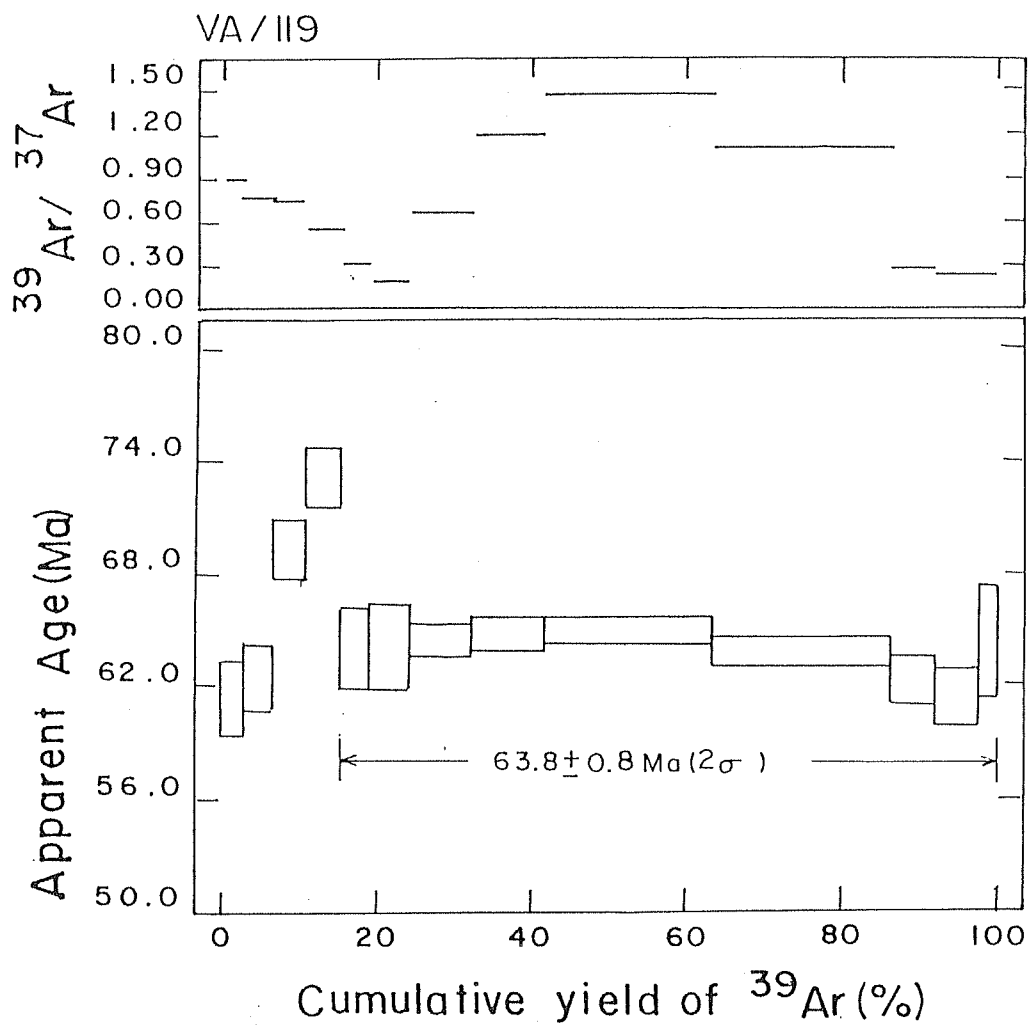


Fig. 4.26. ^{40}Ar - ^{39}Ar Age Spectrum for Tavidar Hawaiiite (VA/119).

Table 4.19. Step heating argon isotopic compositions and apparent ages of sample K/69A (TAVIDAR HAWAIIITE)
 $J=0.00229 \pm 0.00005$

Temp. (°C)	$^{36}\text{Ar}/^{39}\text{Ar}$	$^{37}\text{Ar}/^{39}\text{Ar}$	$^{40}\text{Ar}/^{39}\text{Ar}$	Age (Ma)	^{39}Ar (%)	$^{40}\text{Ar}^*$ (%)
500	0.2179 ±0.0008	1.7071 ±0.0241	76.80 ±0.45	50.5 ±3.6	5.80	16.10
550	0.0261 0.0003	1.4125 0.0034	23.59 0.14	64.5 2.2	12.10	67.30
600	0.0132 0.0006	0.9035 0.0257	20.09 0.13	65.7 2.6	10.20	80.60
650	0.0171 0.0002	1.0231 0.0026	20.92 0.13	64.4 1.9	9.74	75.88
700	0.0167 0.0003	1.2161 0.0024	20.95 0.15	64.9 2.2	6.40	76.30
750	0.0143 0.0003	1.0053 0.0053	19.84 0.16	63.4 2.2	6.10	78.70
800	0.0142 0.0002	0.7575 0.0015	20.29 0.13	65.3 2.0	10.10	79.30
850	0.0164 0.0002	0.8767 0.0021	21.08 0.13	65.8 2.0	13.06	76.92
900	0.0248 0.0002	1.4801 0.0029	22.31 0.14	60.9 1.9	13.89	67.13
950	0.0581 0.0004	6.9947 0.0141	31.03 0.21	56.4 2.4	8.10	44.70
1050	0.2630 0.0015	39.4270 0.0788	86.85 0.54	37.3 5.0	4.50	10.50
TOTAL	0.0443 0.0001	3.3299 0.0048	28.28 0.06	61.7 1.7	100.00	53.66

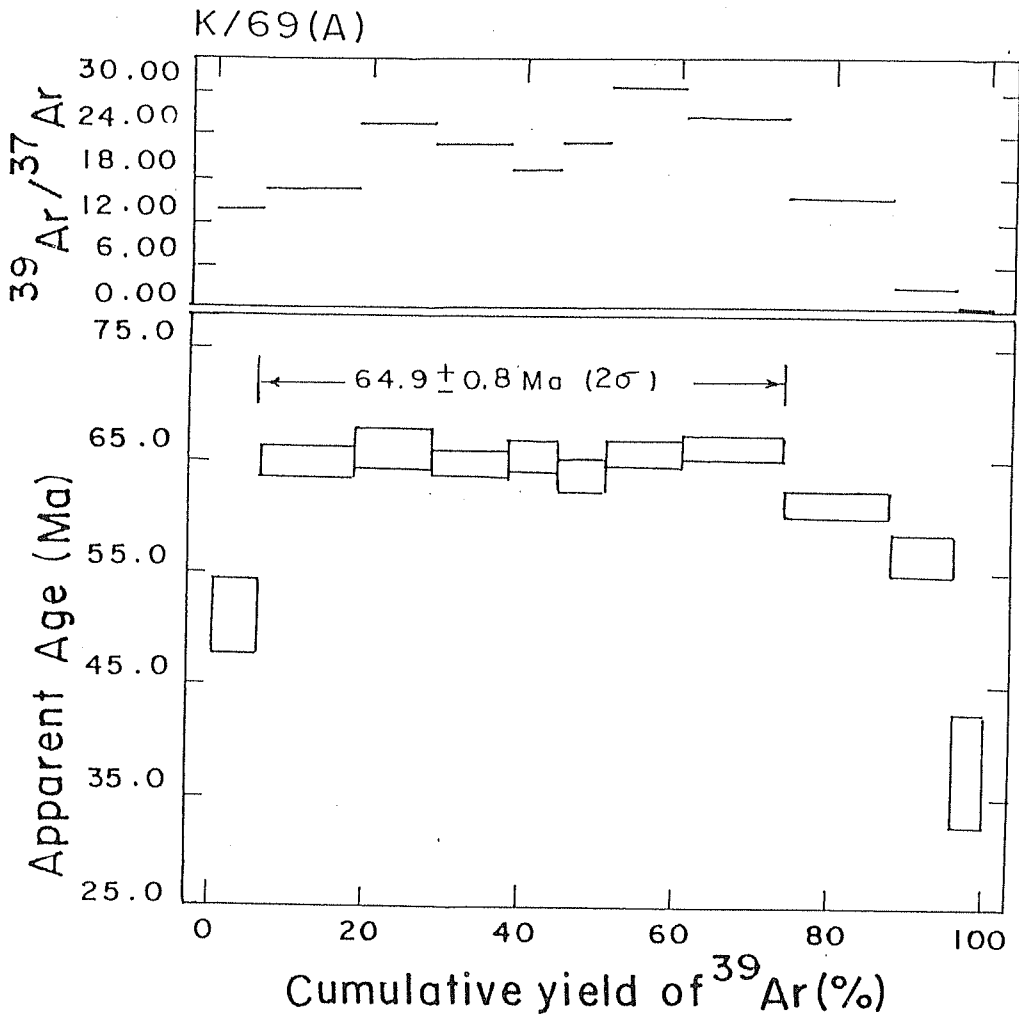


Fig. 4.27. ^{40}Ar - ^{39}Ar Age Spectrum for Tavidar Hawaiiite (K/69A).

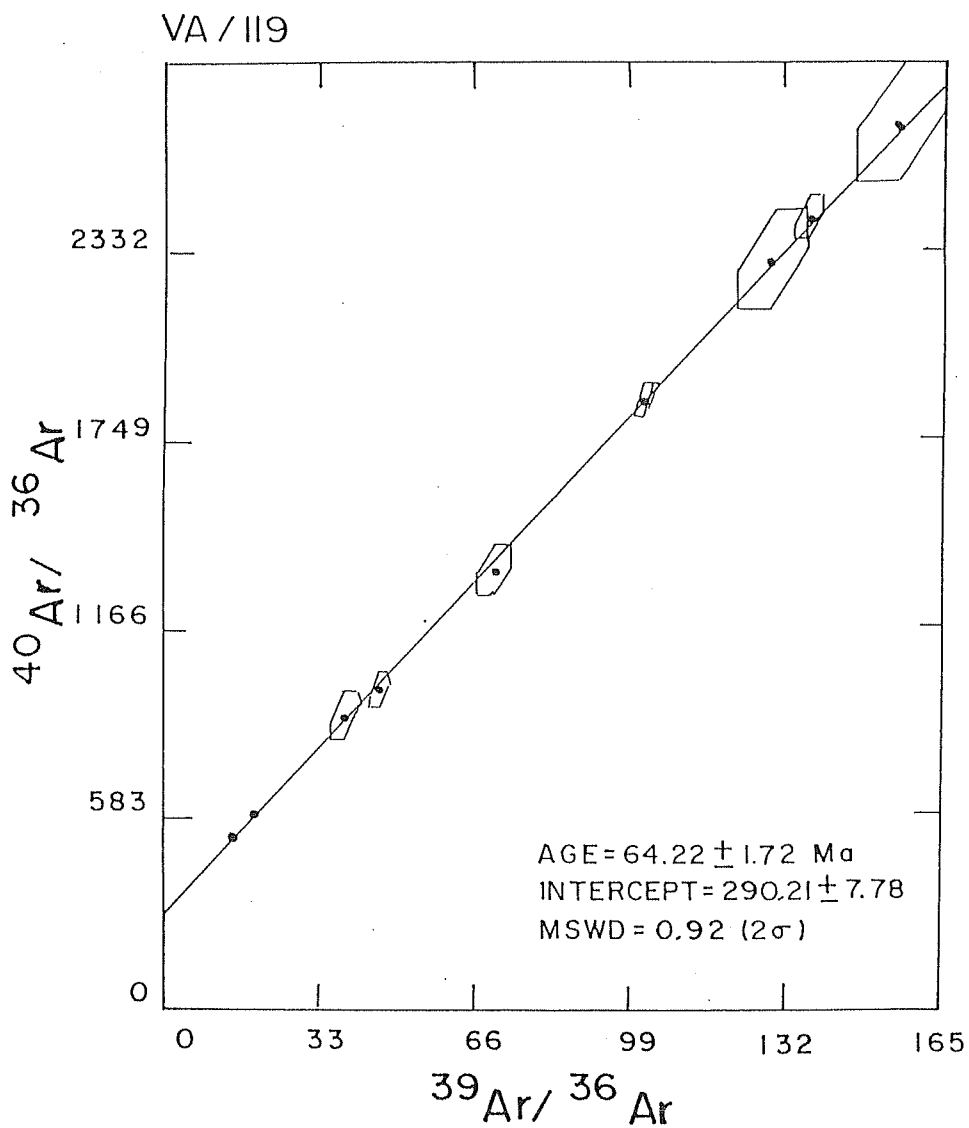


Fig. 4.28. $^{40}\text{Ar}/^{36}\text{Ar}$ vs. $^{39}\text{Ar}/^{36}\text{Ar}$ Isochron Plot for Tavidar Hawaiiite (VA/119).

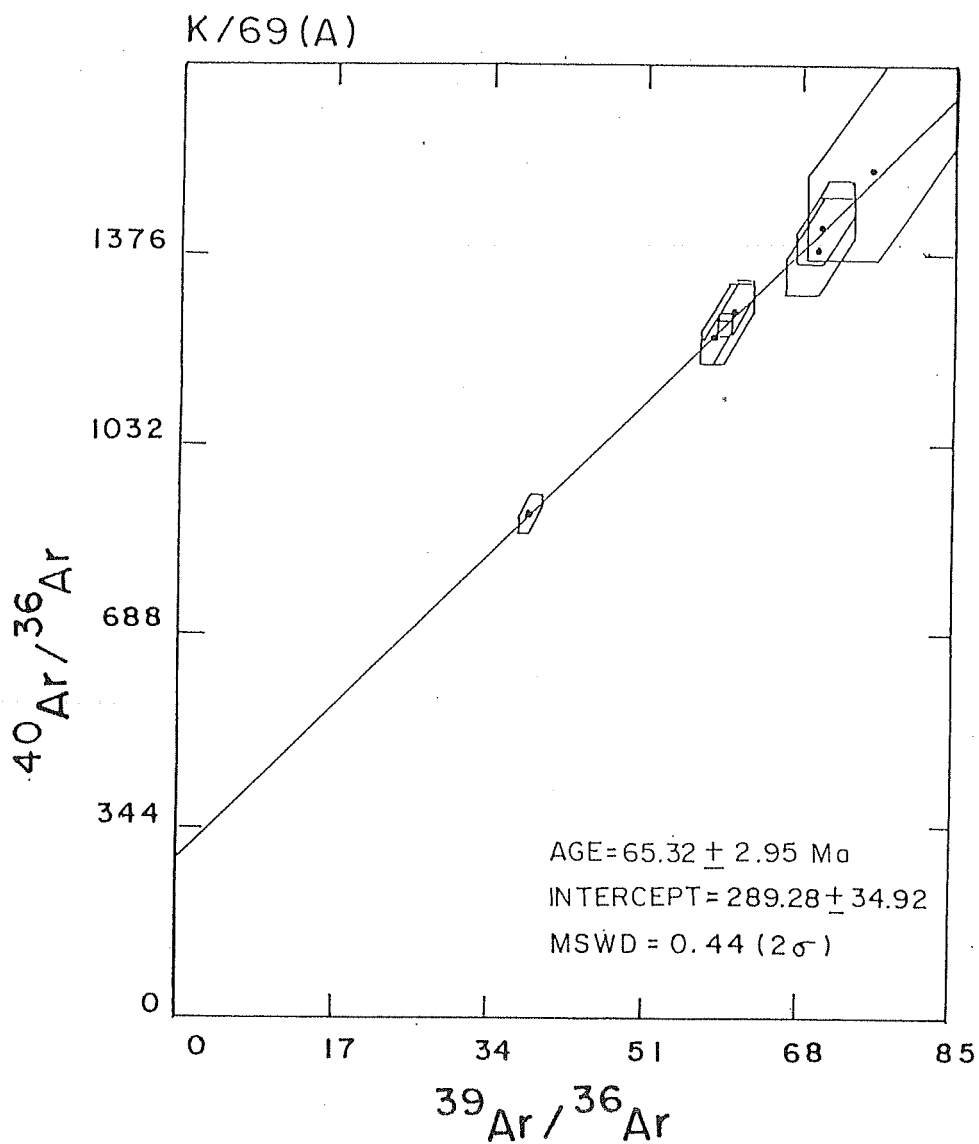


Fig. 4.29. $^{40}\text{Ar}/^{36}\text{Ar}$ vs. $^{39}\text{Ar}/^{36}\text{Ar}$ Isochron Plot for Tavidar Hawaiiite (K/69A).

Table 4.20. Summary of ⁴⁰Ar/³⁹Ar results from Tavidar volcanics, Jalore district, Rajasthan.

Sample No.	Rock type	Temp. steps (°C)	Plateau age (Ma)			Total Age, Ma (±2σ)	Correlation diagram	
			% ³⁹ Ar included	Weighted mean age, Ma (±2σ)	⁴⁰ Ar/ ³⁶ Ar vs. ³⁹ Ar/ ³⁶ Ar		MSWD (2σ)	
								Age, Ma (±2σ)
VA/181	K-Andesite	750-Fusion	94.0	65.9±0.4	66.6±0.7	65.5±0.9	311±28	0.43
K/67	K-Andesite	800-Fusion	65.9	64.6±0.8	65.7±1.7	63.5±1.8	308±13	0.92
VA/58	Trachyte	700-Fusion	80.4	67.2±0.4	65.6±0.7	67.6±1.1	288±14	0.92
K/30	Trachyte	500-Fusion	100.0	65.5±0.6	65.6±1.7	65.5±1.7	296±04	0.50
VA/183	Rhyolite	450-Fusion	100.0	65.0±0.4	65.1±0.6	64.5±0.8	306±09	0.26
VA/168	K-Rhyolite	900-Fusion	59.5	63.8±0.8	63.2±1.0	62.8±2.9	298±08	1.20
VA/119	Hawaiite	700-Fusion	84.7	63.8±0.8	64.5±1.7	64.2±1.7	290±08	0.92
K/69A	Hawaiite	550-850	67.7	64.9±0.8	61.7±1.7	65.3±2.9	289±35	0.44

are consistent with the progress of fractional crystallization model resulting in the formation of different rock types. The earliest differentiated rock i.e. andesite was formed about 66 Ma ago, while the end member of the differentiated sequence i.e. K-rhyolite was last formed about 64 Ma ago. These results, thus, demonstrate that at Tavidar the igneous activity (i.e. differentiation) continued for about 2 Ma starting from 66 to 64 Ma ago, resulting in the formation of a cogenetic suite of mildly alkaline rocks of andesite-trachyte-rhyolite-K-rhyolite. Further the hawaiites, which occur in very small proportion, were emplaced about 64 Ma ago, suggesting their contemporaneity with the mildly alkaline rocks of Tavidar.

4.4.3. Sr ISOTOPIC DATA

To understand the petrogenesis of Tavidar volcanics Sr isotopic studies were carried out at KDMIPE, ONGC, Dehradun. The initial Sr ratios have been calculated assuming an average age of 65 Ma for the Tavidar volcanics (Table 4.21). Though the initial ratios of the differentiated rocks and the hawaiites cannot be distinguished mainly because of the high errors associated with the initial ratios, due to very low abundances of Sr, of K-rhyolites (Table 4.21).

However, the mean initial $^{87}\text{Sr}/^{86}\text{Sr}$ ratio for the differentiated rocks (0.70525) is different from that of the hawaiites (0.70441), suggesting a different source for the hawaiites. It is worth mentioning here that Upadhyaya et al. (1988) have also postulated, based on correlation coefficient studies (Chayes, 1960; Le Maitre, 1982) and principal components analysis (PCA) (Le Maitre, 1968; Till and Colley, 1973), that the basalts are not cogenetic with the rest of the rocks.

When the initial $^{87}\text{Sr}/^{86}\text{Sr}$ ratios are plotted against Sr content (Fig. 4.30) they fall in a field of continental volcanics (felsic as well as basaltic) rocks as defined by Faure and Powell (1972). The mean of initial $^{87}\text{Sr}/^{86}\text{Sr}$ ratios of Tavidar volcanics lie just below the '*source region of basalt*' boundary on the Sr evolution diagram (Faure and Hurley, 1963), suggesting generation of magma from top of upper mantle (Fig. 4.31). Further, as Faure and Powell (1972) suggested that there is a decrease in the initial

Table 4.21. Rb-Sr content and Sr isotopic ratios of samples from Tavidar volcanics, Jalore district.

Sample No.	Rock Type	Rb (ppm)	Sr	K/Rb	Rb/Sr	$^{87}\text{Sr}/^{86}\text{Sr}$ (normalized)	$^{87}\text{Sr}/^{86}\text{Sr}$ (initial)
VA/181	K-Andesite	68	428	494.12	0.159	0.70634	0.70592 ± 0.00013
K/67	K-Andesite	58	317	639.66	0.183	0.70635	0.70586 ± 0.00013
VA/58	Trachyte	74	195	464.89	0.379	0.70620	0.70519 ± 0.00019
K/30	Trachyte	76	106	700.00	0.717	0.70674	0.70482 ± 0.00031
VA/168	K-Rhyolite	359	22	238.10	16.318	0.74866	0.70488 ± 0.0063
VA/183	K-Rhyolite	168	14	347.02	12.0	0.73699	0.70483 ± 0.00466
VA/119	Hawaiite	75	290	269.33	0.259	0.70528	0.70459 ± 0.00015
K/69A	Hawaiite	56	460	183.93	0.122	0.70456	0.70423 ± 0.00012

Notes to Table: (a) Initial $^{87}\text{Sr}/^{86}\text{Sr}$ ratios have been calculated assuming an average age of 65 ± 1.0 Ma as indicated by ^{40}Ar - ^{39}Ar studies. (b) Rb and Sr concentrations are determined by XRF with an accuracy of $\pm 5\%$. (c) $^{87}\text{Sr}/^{86}\text{Sr}$ ratios are normalized with $^{86}\text{Sr}/^{88}\text{Sr} = 0.1194$. (d) Errors on mass spectrometric $^{87}\text{Sr}/^{86}\text{Sr}$ measurements are taken maximum as 0.008% . (e) Errors on $(^{87}\text{Sr}/^{86}\text{Sr})_i$ are calculated using eqn. (11) given in Chapter 3. (f) Errors are quoted at 2σ level.

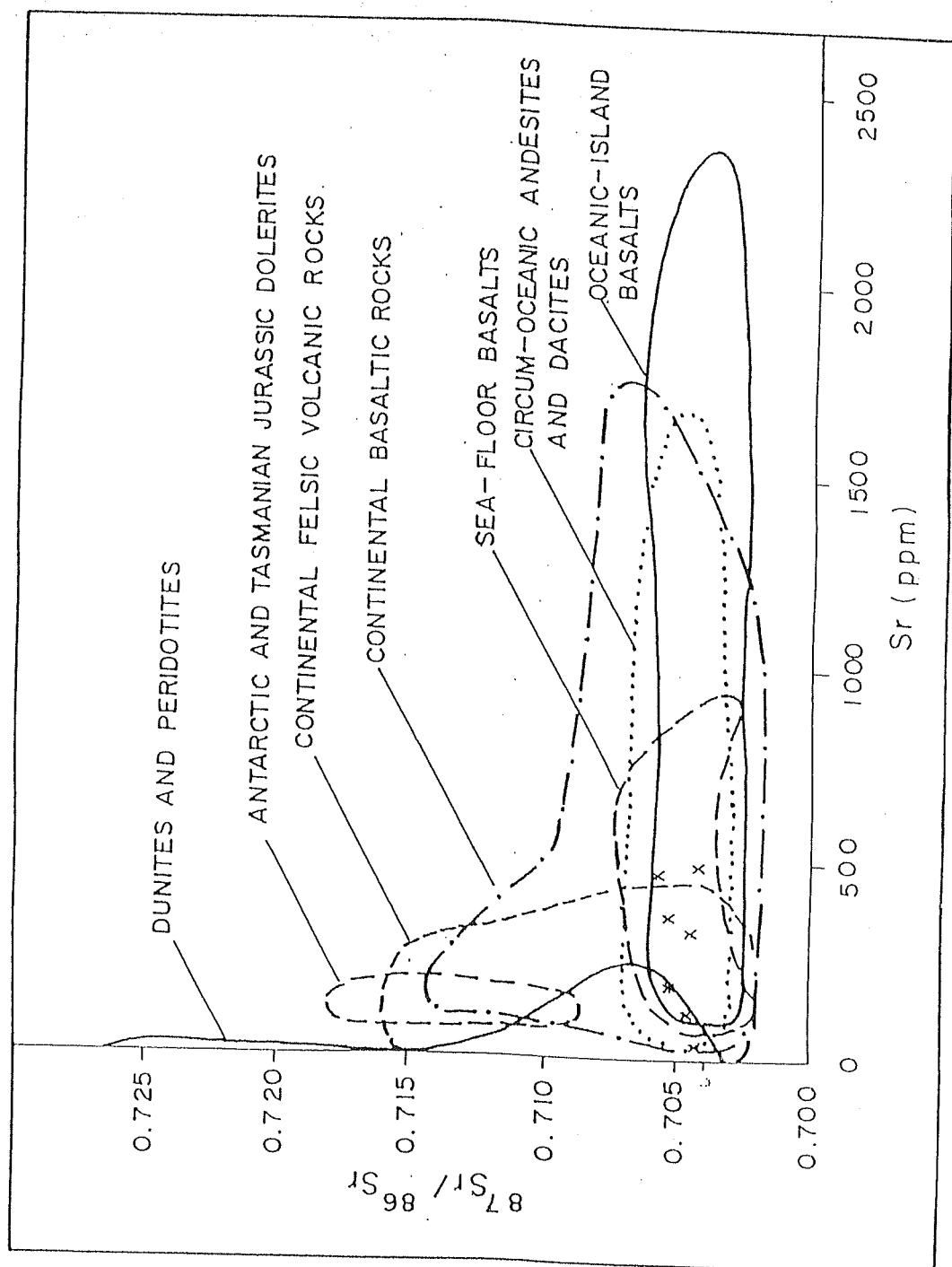


Fig. 4.30. Plot of Initial Sr Ratios Against Sr Content of Tavidar Volcanics (after Faure and Powell, 1972).

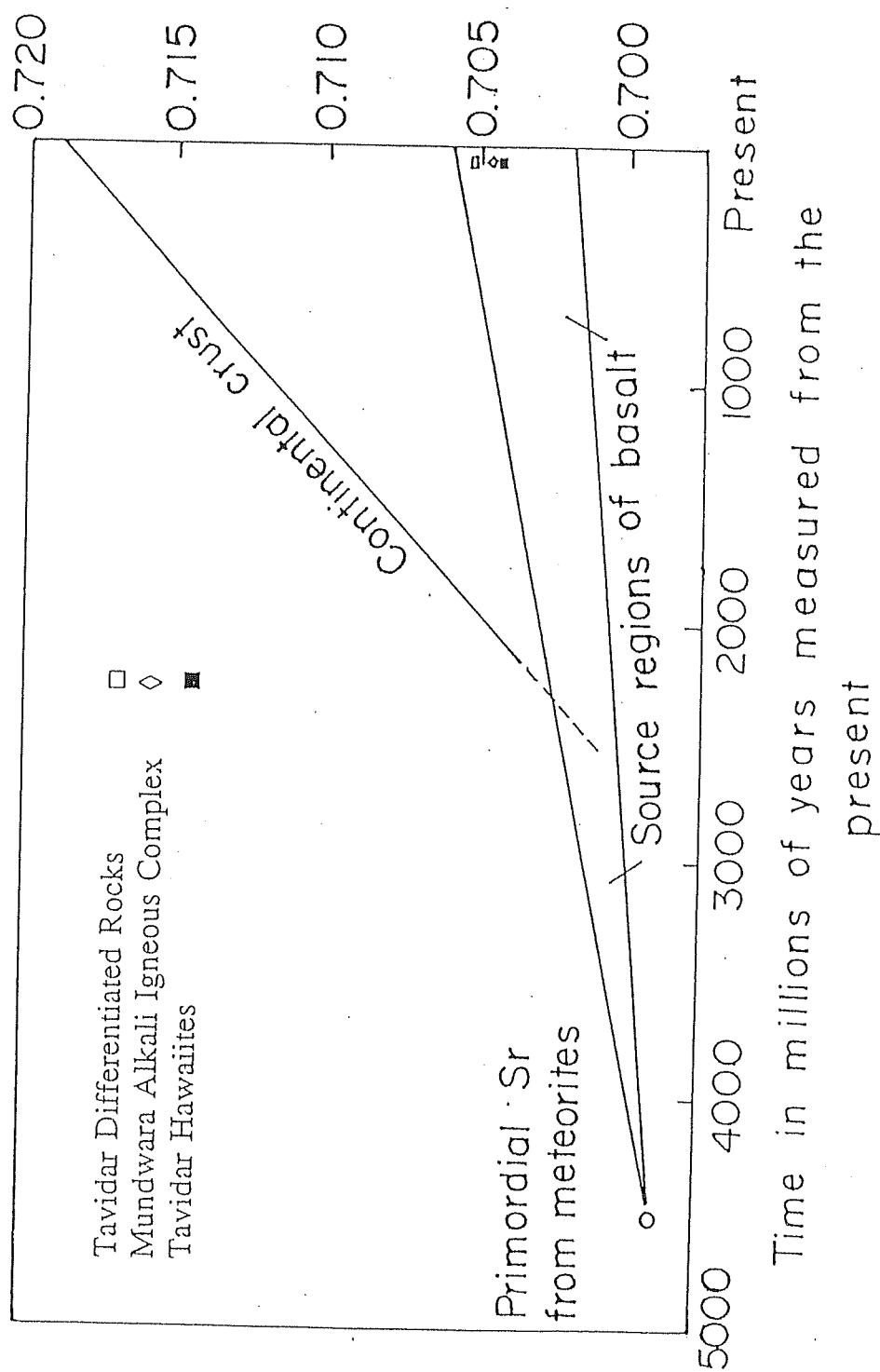


Fig. 4.31. Plot of Mean initial Sr Ratio of Tavidar Volcanics and Mundwara Alkali Igneous Complex on Sr Evolution Diagram (After Faure and Hurley, 1963).

$^{87}\text{Sr}/^{86}\text{Sr}$ ratio with an increase in the depth, therefore the hawaiites, having a mean initial ratio of 0.70441, have probably been derived from the magma generated still at deeper level in the upper mantle.

4.5. ASSOCIATION IV (*MUNDWARA ALKALI IGNEOUS COMPLEX*)

4.5.1. ^{40}Ar - ^{39}Ar STUDIES

Six whole rock samples were dated by ^{40}Ar - ^{39}Ar method to assign the emplacement time to the Mundwara alkali igneous complex, Rajasthan, India (Fig. 2.10). The dated samples include four from Musala (MR 86/1, MR 86/2, MR 86/4 and MR 86/5) hill and one each from Mer (MR 86/7) and Toa (MR 86/9) hills of the complex.

The samples were irradiated in two batches. The J factor varied from 0.00220 ± 0.00002 to 0.00237 ± 0.00005 . The minimum and maximum values of J were those obtained for samples MR 86/1 and MR 86/7, respectively.

The argon isotopic composition and abundances of these samples are given in Tables 4.22 to 4.27. Their age spectra and correlation diagrams are shown in Fig. (4.32 to 4.41).

4.5.1.A. *MUSALA HILL*

The dated rocks consist of an essexite, a basalt and two syenites. The samples were collected during a field trip to Rajasthan in 1986.

Sample MR 86/1: This is an essexite collected from the base of Musala hill, and forms the dominant rock type of the hillock. The sample shows a saddle shaped spectrum (Fig. 4.32) with intermediate five steps forming a pseudo plateau between 600-850°C temperature. The pseudo plateau steps constitute 48.6% of the total ^{39}Ar evolved and corresponds to an age of 74.8 ± 1.0 Ma. Such saddle shaped spectra have been considered diagnostic of excess argon (Lanphere and Dalrymple, 1976) with its minima marking the upper limit to the time of formation. The last two high temperature

Table 4.22. Step heating argon isotopic compositions and apparent ages of sample
MR 86/1 (MUNDWARA ESSEXITE)
 $J=0.00220 \pm 0.00002$

Temp. (°C)	$^{36}\text{Ar}/^{39}\text{Ar}$	$^{37}\text{Ar}/^{39}\text{Ar}$	$^{40}\text{Ar}/^{39}\text{Ar}$	Age (Ma)	^{39}Ar (%)	$^{40}\text{Ar}^*$ (%)
400	0.0482 ± 0.0006	0.9826 ± 0.0211	25.98 ± 0.26	46.1 ± 2.4	1.00	45.20
450	0.0093 0.0001	0.8179 0.0028	21.01 0.14	71.1 1.2	3.20	86.91
500	0.0031 0.0001	0.5065 0.0048	22.09 0.14	82.3 1.2	6.73	95.94
550	0.0017 0.0001	0.3605 0.0007	20.65 0.12	78.3 1.1	7.79	97.55
600	0.0019 0.0001	0.3303 0.0014	19.92 0.12	75.3 1.1	7.63	97.12
650	0.0046 0.0001	0.3854 0.0011	20.45 0.13	74.3 1.1	4.71	93.31
700	0.0071 0.0001	0.5235 0.0011	21.01 0.13	73.5 1.2	3.83	89.91
750	0.0045 0.0002	0.5736 0.0012	21.08 0.13	76.8 1.3	11.27	93.67
850	0.0041 0.0001	1.2051 0.0024	20.31 0.12	74.4 1.0	21.11	94.13
900	0.0051 0.0002	2.4258 0.0048	23.56 0.14	85.5 1.3	16.20	93.61
1000	0.0231 0.0001	8.2266 0.0164	33.42 0.20	103 2	15.34	79.63
1100	0.09082 0.0025	0.5341 0.0473	77.79 0.72	192 7	1.00	65.50
1200	0.1151 0.0101	19.4451 0.0909	69.60 2.40	136 28	1.00	51.00
TOTAL	0.0086 0.0001	2.3875 0.0027	23.83 0.05	82.6 0.8	100.00	89.31

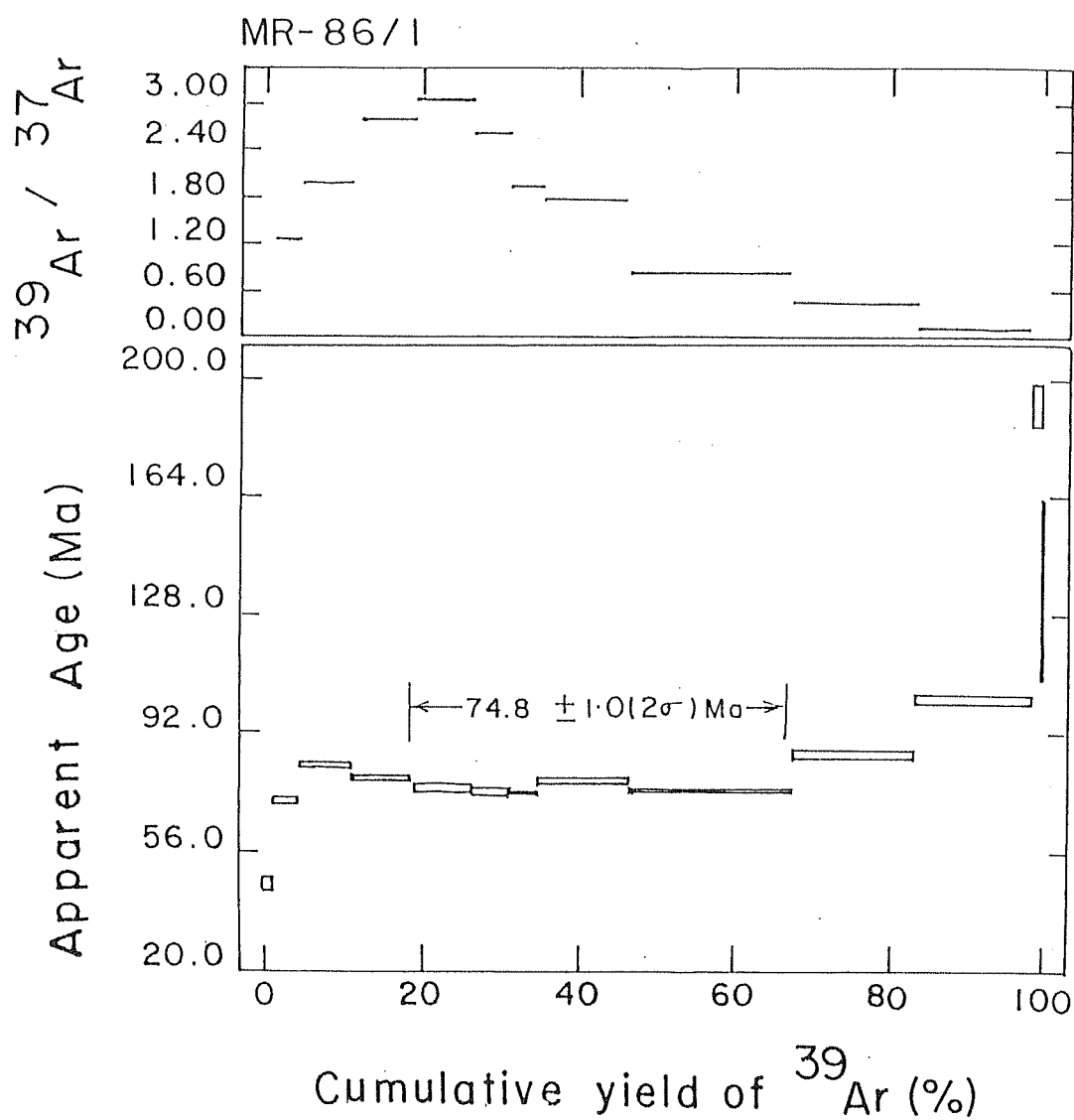


Fig. 4.32. ^{40}Ar - ^{39}Ar Age Spectrum for Musala Essexite (MR 86/1).

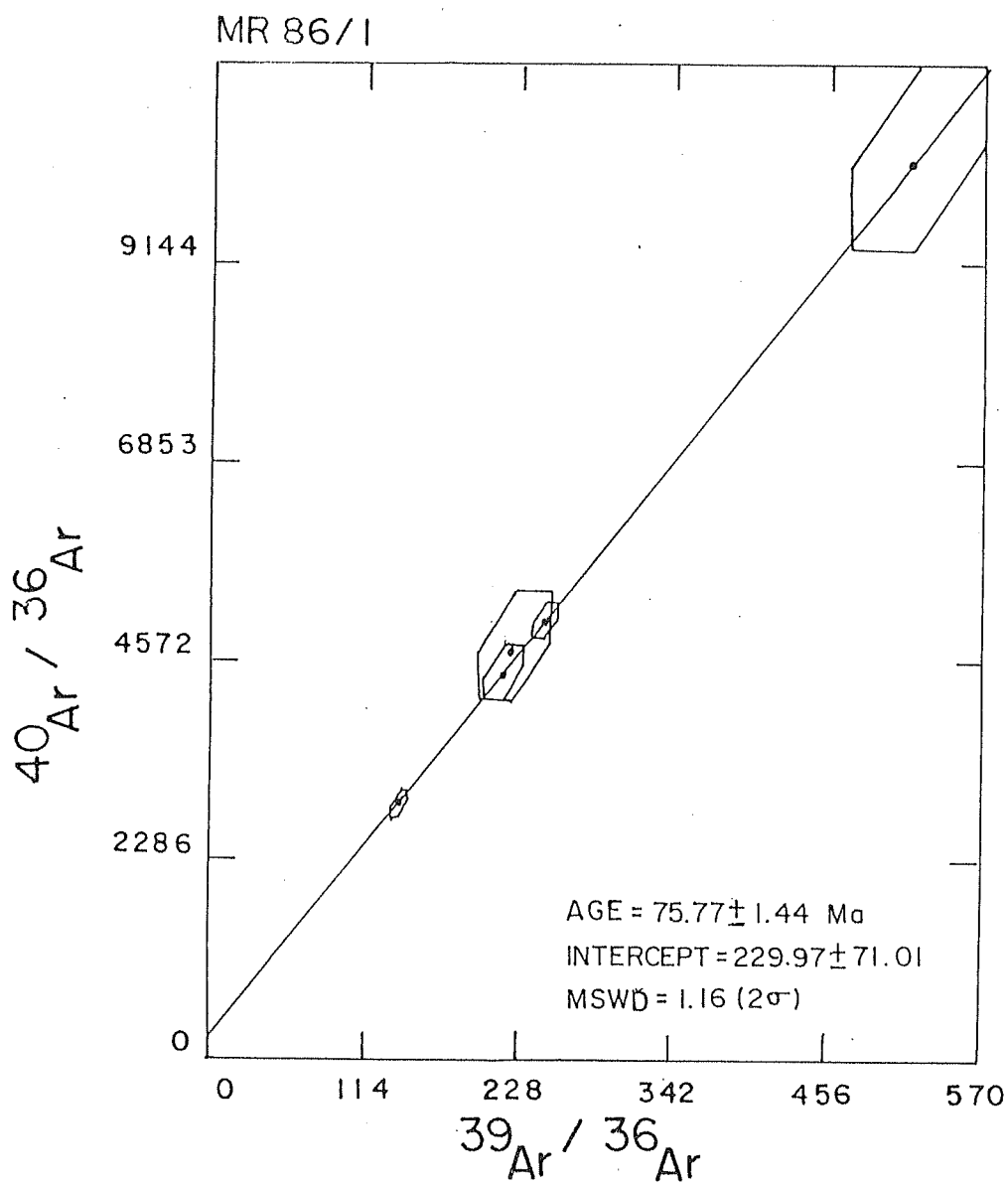


Fig. 4.33. $^{40}\text{Ar}/^{36}\text{Ar}$ vs. $^{39}\text{Ar}/^{36}\text{Ar}$ Isochron Plot for Musala Essexite (MR 86/1).

increments (1100 and 1200°C) record anomalously old apparent ages but together comprise 1% of the total ^{39}Ar evolved from the sample.

The apparent K/Ca ratio varies systematically over the experiment. The increase in $^{39}\text{Ar}/^{37}\text{Ar}$ ratio during the initial five temperature steps (i.e. up to 600°C) indicates that the argon is released from K-dominant phase, while in the remaining steps it is released from Ca-rich phase, resulting in continuous lowering of $^{39}\text{Ar}/^{37}\text{Ar}$ ratio. The isochron (Fig. 4.33) age is 75.8 ± 1.4 Ma.

Sample MR 86/2: This is a basalt occurring above the essexite body. This sample also shows a saddle shaped spectrum (Fig. 4.34) typical of sample containing excess argon. The pseudo plateau consisting of intermediate five temperature steps (i.e. 630 to 820°C) contain 45.9% of the released ^{39}Ar and yields an age of 73.9 ± 0.4 Ma. One temperature step (i.e. 770°C) gives a slightly discordant age but as it occurs in between, it has been included in the pseudo plateau.

The apparent K/Ca ratio remains almost uniform up to 770°C, followed by increase in the ratio in the next three steps, but beyond this temperature more and more argon is released from the Ca-dominant phase resulting in the continuous lowering of $^{39}\text{Ar}/^{37}\text{Ar}$ ratio. The isochron age is 71.8 ± 1.5 Ma (Fig. 4.35). However, when all the data points (steps) are used in $^{40}\text{Ar}/^{36}\text{Ar}$ vs. $^{39}\text{Ar}/^{36}\text{Ar}$ regression analysis, the slope of regression line corresponds to an age of 69.7 ± 0.8 Ma which can be considered as the formation age of the basalt.

Sample MR 86/4: This is a syenite occurring above the basalt and represents the chilled margin of the syenite body. The sample shows a perfect plateau (Fig. 4.36) consisting of all the thirteen temperature steps (100% ^{39}Ar release). The plateau age is 64.1 ± 0.6 Ma while its isochron (Fig. 4.37) and total ages are 64.5 ± 1.7 Ma and 63.8 ± 1.7 Ma, respectively.

There is good agreement between the plateau, isochron and total ages of this sample, within the experimental error, indicating that this syenite sample has not lost any radiogenic argon during its history. The concordance of plateau, isochron and total ages of this sample suggest that the syenite was emplaced about 64 Ma ago.

Sample MR 86/5: This is again a syenite collected from centre of the syenite body on

Table 4.23. Step heating argon isotopic compositions and apparent ages of sample
MR 86/2 (MUSALA BASALT)
 $J=0.00223 \pm 0.00002$

Temp. (°C)	$^{36}\text{Ar}/^{39}\text{Ar}$	$^{37}\text{Ar}/^{39}\text{Ar}$	$^{40}\text{Ar}/^{39}\text{Ar}$	Age (Ma)	^{39}Ar (%)	$^{40}\text{Ar}^*$ (%)
500	0.0209 ± 0.0002	0.2363 ± 0.0007	36.04 ± 0.21	116 ± 2	2.37	82.84
550	0.0084 0.0001	0.2901 0.0012	23.86 0.14	84.0 1.2	6.60	89.56
600	0.0035 0.0000	0.3015 0.0006	20.92 0.12	78.2 1.1	7.72	94.98
630	0.0027 0.0001	0.2864 0.0005	19.78 0.11	74.7 1.0	11.21	95.83
670	0.0021 0.0001	0.3324 0.0006	19.44 0.11	74.1 1.0	11.47	96.74
750	0.0025 0.0001	0.2978 0.0005	19.50 0.11	73.9 1.0	9.38	96.14
770	0.0026 0.0003	0.2381 0.0006	18.89 0.11	71.4 1.3	5.97	95.82
820	0.0043 0.0001	0.1891 0.0004	20.14 0.12	74.3 1.0	7.87	93.55
880	0.0036 0.0001	0.1745 0.0003	20.53 0.12	76.7 1.1	6.95	94.77
950	0.0035 0.0001	0.2481 0.0005	22.59 0.13	84.7 1.2	7.83	95.34
1000	0.0058 0.0001	0.8636 0.0017	23.17 0.13	84.2 1.2	9.18	92.48
1080	0.0081 0.0001	6.4496 0.0128	24.47 0.14	86.6 1.2	11.31	90.12
1120	0.0184 0.0004	22.8721 0.0773	27.28 0.20	85.8 1.9	1.72	80.00
1210	0.01681 0.0023	8.1831 0.0363	26.11 0.70	83.2 7.4	0.40	81.00
TOTAL	0.0051 0.0003	1.4991 0.002	21.70 0.04	79.6 0.7	100.00	93.17

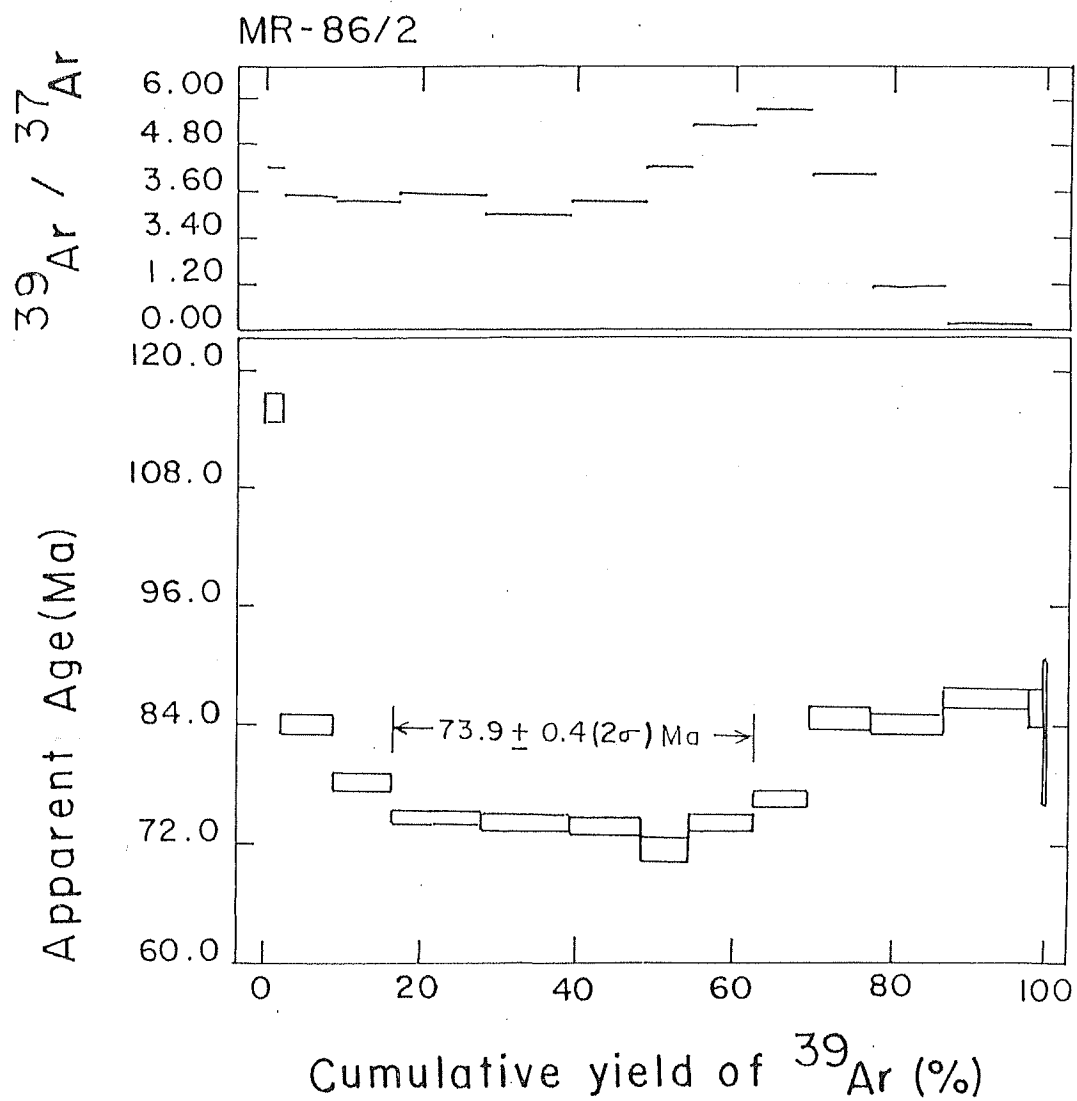


Fig. 4.34. ^{40}Ar - ^{39}Ar Age Spectrum for Musala Basalt (MR 86/2).

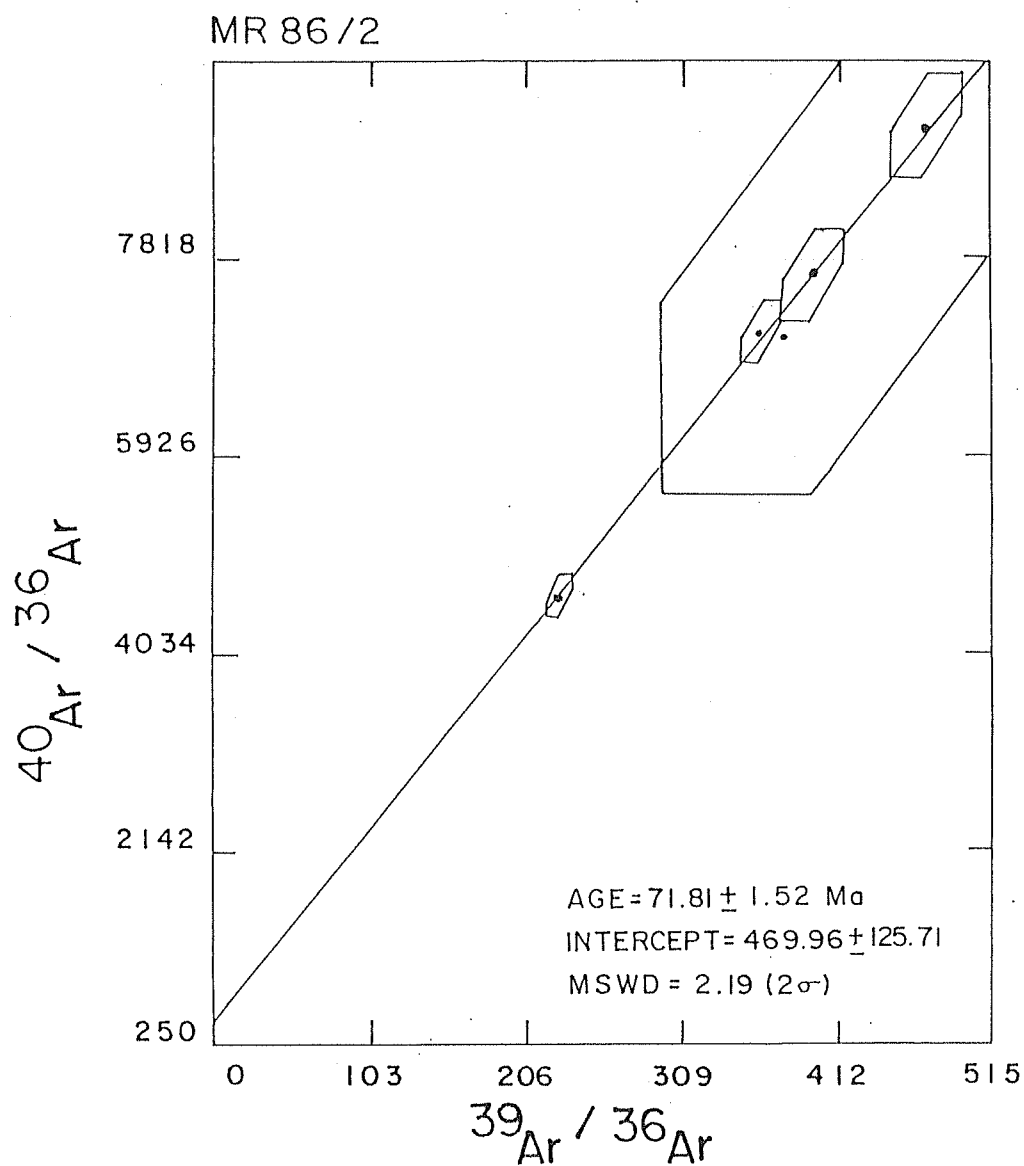


Fig. 4.35. $^{40}\text{Ar}/^{36}\text{Ar}$ vs. $^{39}\text{Ar}/^{36}\text{Ar}$ Isochron Plot for Musala Basalt (MR 86/2).

Table 4.24. Step heating argon isotopic compositions and apparent ages of sample
MR 86/4 (MUSALA SYENITE)
 $J=0.00233 \pm 0.00005$

Temp. (°C)	$^{36}\text{Ar}/^{39}\text{Ar}$	$^{37}\text{Ar}/^{39}\text{Ar}$	$^{40}\text{Ar}/^{39}\text{Ar}$	Age (Ma)	^{39}Ar (%)	$^{40}\text{Ar}^*$ (%)
500	0.1453 ± 0.0018	-	57.44 ± 0.33	60.0 ± 5.2	6.40	25.30
550	0.0265 0.0011	-	22.83 0.14	61.9 3.2	4.50	65.60
600	0.0157 0.0001	0.0521 ± 0.0027	19.89 0.12	62.9 1.9	6.16	76.60
650	0.0128 0.0001	0.0396 0.0003	19.42 0.11	64.5 1.9	8.20	80.43
700	0.0084 0.0003	-	18.20 0.11	64.8 1.9	9.51	86.30
750	0.0096 0.0003	-	18.39 0.11	64.2 2.0	9.30	84.50
800	0.0144 0.0002	-	19.65 0.15	63.6 1.9	6.31	78.32
850	0.0149 0.0002	0.0452 0.0007	19.89 0.17	63.9 1.9	7.45	77.86
900	0.0127 0.0002	0.1364 0.0039	19.36 0.11	64.4 1.9	9.86	80.54
950	0.0127 0.0002	0.3088 0.0013	19.02 0.11	62.9 1.8	14.29	80.14
1000	0.0127 0.0002	0.7446 0.0019	19.39 0.11	64.5 1.9	10.05	80.56
1050	0.0108 0.0004	1.7833 0.0036	19.28 0.14	66.4 2.2	4.30	83.40
1200	0.0154 0.0015	4.9281 0.0098	21.30 0.43	69.0 5.2	1.60	78.60
TOTAL	0.0215 0.0001	0.3134 0.0005	21.83 0.04	63.8 1.7	100.00	70.81

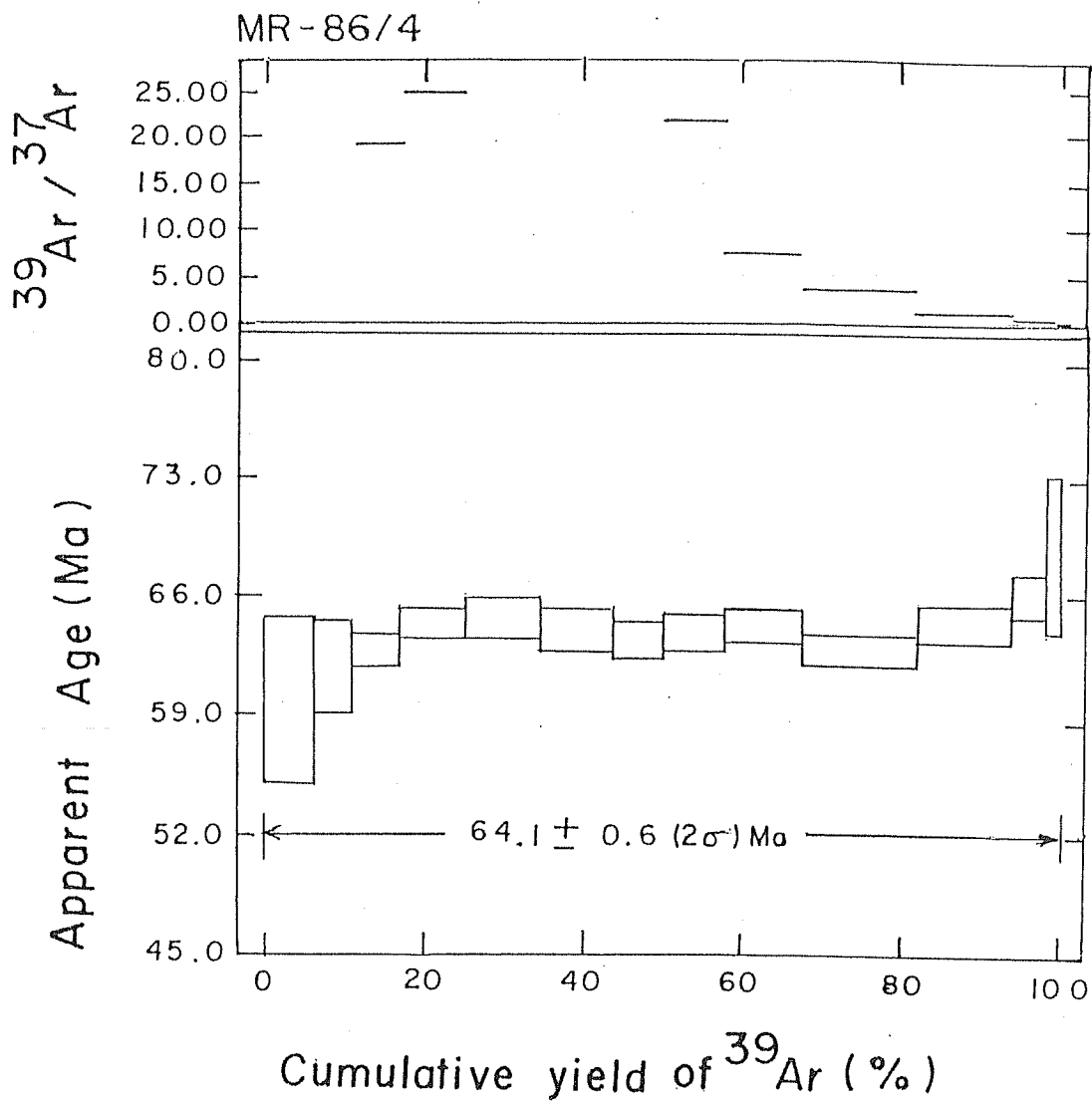


Fig. 4.36. ^{40}Ar - ^{39}Ar Age Spectrum for Musala Syenite (MR 86/4).

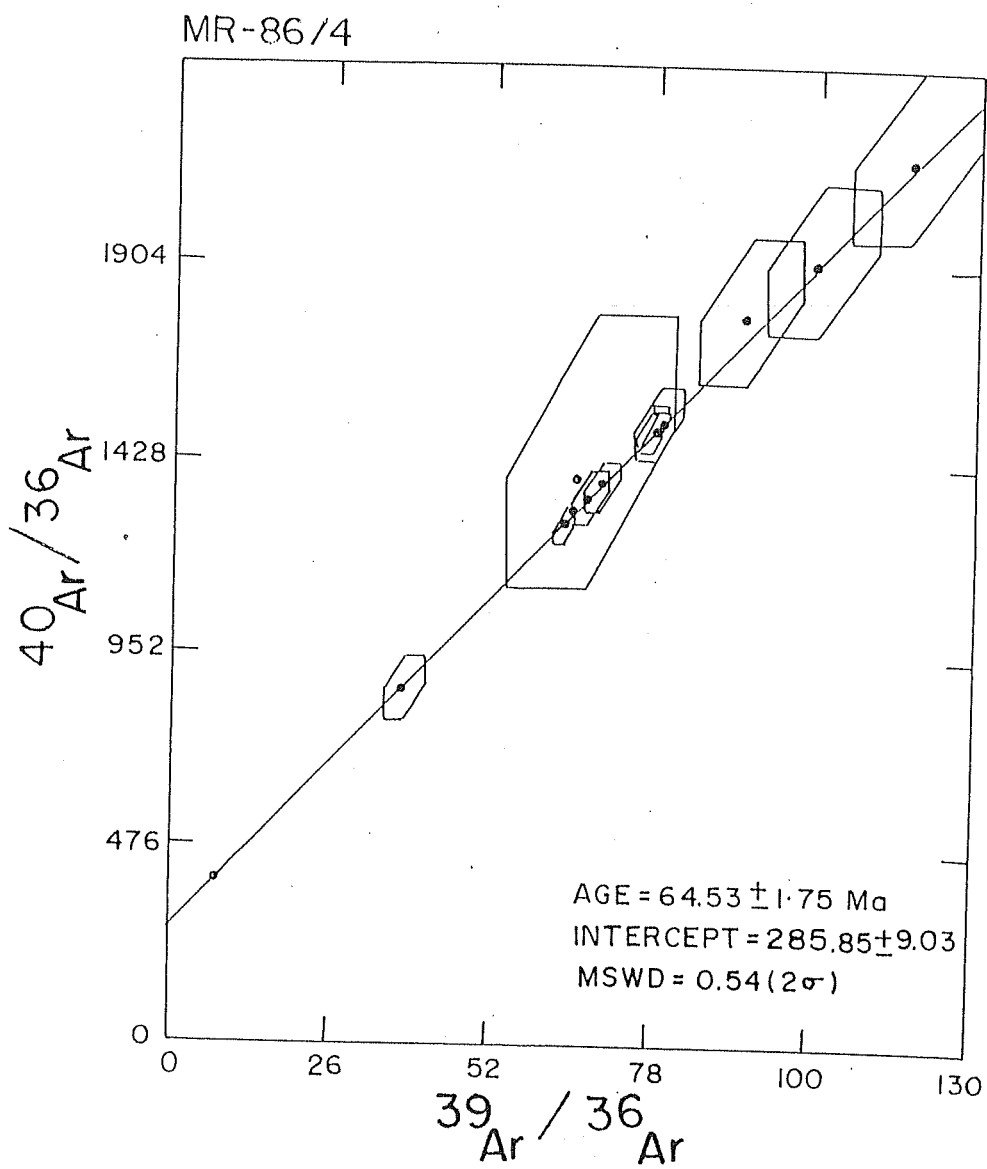


Fig. 4.37. $^{40}\text{Ar}/^{36}\text{Ar}$ vs. $^{39}\text{Ar}/^{36}\text{Ar}$ Isochron Plot for Musala Syenite (MR 86/4).

top of the Musala hill. The sample shows a saddle shaped spectrum (Fig. 4.38) indicating excess argon. The minimum age (three steps, 20.9% of total ^{39}Ar evolved) is 69.5 ± 0.9 Ma. Even though this age marks the upper boundary to the time of formation, the formation/emplacement age of this sample should be equal to that of the other syenite (MR 86/4) collected from the same hill, which is 64.1 ± 0.6 Ma.

The apparent K/Ca ratio does not vary systematically over the experiment and instead shows a double stage release pattern. The step-wise decrease in $^{39}\text{Ar}/^{37}\text{Ar}$ ratio indicates that argon is preferentially released from the Ca-dominant phase during the first four (i.e. upto 650°C) and the last five temperature steps (i.e. from 900 - 1200°C). The intermediate four temperature steps (700 - 850°C) do not produce any ^{37}Ar indicating that in these steps the argon is released solely from K-bearing phases.

4.5.1.B. MER HILL

Sample MR 86/7: This is a syenite collected from Mer hill. The sample shows a nine step plateau (Fig. 4.39) from 500 to 900°C constituting 54% of total ^{39}Ar released. The plateau age is 64.4 ± 0.8 Ma, while its isochron (Fig. 4.40) and total ages are 64.8 ± 1.7 Ma and 66.5 ± 1.7 Ma, respectively. The plateau and isochron ages of this sample are in good agreement, though the total age is slightly higher. The discordance in the total age is due to relatively higher ages obtained from the higher temperature steps. However, the concordance of plateau, isochron and total ages of this sample indicate that the syenite of Mer hill was also emplaced at about 64 Ma ago.

The behavior of argon release in this sample is different from that of MR 86/4 and MR 86/5. In the first ten steps i.e. up to 950°C , argon appears to be released from K-rich fraction while in the remaining steps, it is released from Ca-dominant phase.

4.5.1.C. TOA HILL

Sample MR 86/9: This is a gabbro which forms the most important rock type of Toa hill. This sample also shows a U-shaped spectrum (Fig. 4.41) like MR 86/1, MR 86/2

Table 4.25. Step heating argon isotopic compositions and apparent ages of sample
MR 86/5 (MUSALA SYENITE)
 $J=0.00236 \pm 0.00005$

Temp. (°C)	$^{36}\text{Ar}/^{39}\text{Ar}$	$^{37}\text{Ar}/^{39}\text{Ar}$	$^{40}\text{Ar}/^{39}\text{Ar}$	Age (Ma)	^{39}Ar (%)	$^{40}\text{Ar}^*$ (%)
500	0.1323 ± 0.0004	0.0547 ± 0.0001	61.48 ± 0.35	92.8 ± 3.4	5.7	36.4
550	0.0451 0.0002	0.1719 0.0008	32.16 0.19	78.4 2.4	5.5	58.6
600	0.0383 0.0002	0.6522 0.0041	30.07 0.17	78.0 2.4	5.1	62.3
650	0.0371 0.0003	0.9511 0.0026	28.45 0.17	73.0 2.2	5.4	61.5
700	0.0268 0.0001	-	24.42 0.14	68.8 2.0	7.4	67.5
750	0.0376 0.0002	-	27.87 0.16	69.8 2.2	5.1	60.0
800	0.0585 0.0002	-	34.17 0.20	70.3 2.2	8.4	49.3
850	0.0521 0.0002	-	33.24 0.19	74.5 2.4	9.5	53.8
900	0.0387 0.0001	0.0568 0.0008	31.20 0.18	82.1 2.4	12.3	63.3
950	0.0356 0.0001	0.1265 0.0015	31.75 0.18	88.0 2.6	14.1	66.8
1000	0.0331 0.0001	0.3621 0.0031	32.70 0.19	94.9 2.8	10.9	70.0
1050	0.0273 0.0002	0.4345 0.0008	30.44 0.18	92.7 2.6	6.9	73.5
1200	0.0312 0.0016	0.9331 0.0168	32.70 1.40	97.1 3.4	3.8	71.8
TOTAL	0.0442 0.0001	0.2261 0.0008	32.80 0.08	82.0 2.0	100.0	60.1

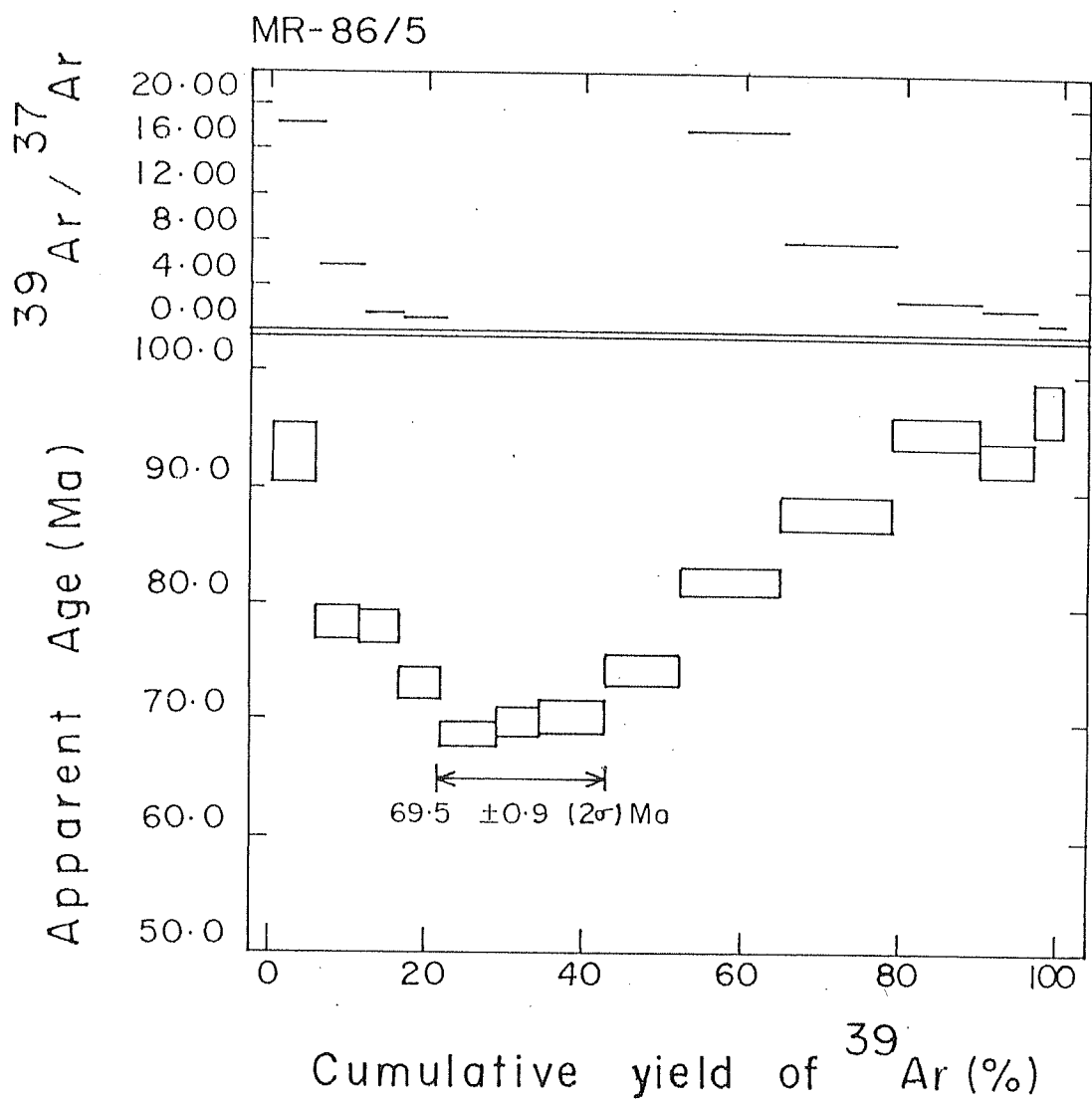


Fig. 4.38. ^{40}Ar - ^{39}Ar Age Spectrum for Musala Syenite (MR 86/5).

Table 4.26. Step heating argon isotopic compositions and apparent ages of sample
MR 86/7 (MUNDWARA SYENITE)
 $J=0.00237 \pm 0.00005$

Temp. (°C)	$^{36}\text{Ar}/^{39}\text{Ar}$	$^{37}\text{Ar}/^{39}\text{Ar}$	$^{40}\text{Ar}/^{39}\text{Ar}$	Age (Ma)	^{39}Ar (%)	$^{40}\text{Ar}^*$ (%)
500	0.2711 ± 0.0014	0.4509 ± 0.0022	94.69 ± 0.56	61.3 ± 5.2	1.30	15.40
550	0.0474 0.0008	0.3417 0.0022	29.04 0.20	63.0 3.0	1.80	51.70
600	0.0297 0.0004	0.3421 0.0006	24.06 0.15	64.0 2.2	2.90	63.40
650	0.0235 0.0002	0.3251 0.0012	22.16 0.13	63.7 1.9	5.87	68.62
700	0.0104 0.0001	0.3147 0.0031	18.33 0.11	63.9 1.8	10.26	83.12
750	0.0107 0.0001	0.2417 0.0032	18.76 0.11	65.4 1.9	7.78	83.15
800	0.0168 0.0002	0.1931 0.0022	20.42 0.12	64.7 1.9	6.31	75.63
850	0.0218 0.0002	0.2271 0.0016	22.20 0.16	66.0 1.9	7.30	70.98
900	0.0199 0.0001	0.3153 0.0065	21.24 0.12	64.4 1.8	10.50	72.26
950	0.0181 0.0001	0.2478 0.0004	21.44 0.13	67.4 1.9	23.42	75.06
1000	0.0233 0.0001	0.6311 0.0012	23.61 0.15	69.9 2.0	14.40	70.80
1050	0.0364 0.0002	1.7526 0.0035	27.68 0.17	70.7 2.2	6.40	61.00
1100	0.0491 0.0013	4.0349 0.0101	32.49 0.28	75.2 4.2	1.80	55.40
TOTAL	0.0241 0.0001	0.4887 0.0009	22.98 0.05	66.5 1.7	100.00	69.11

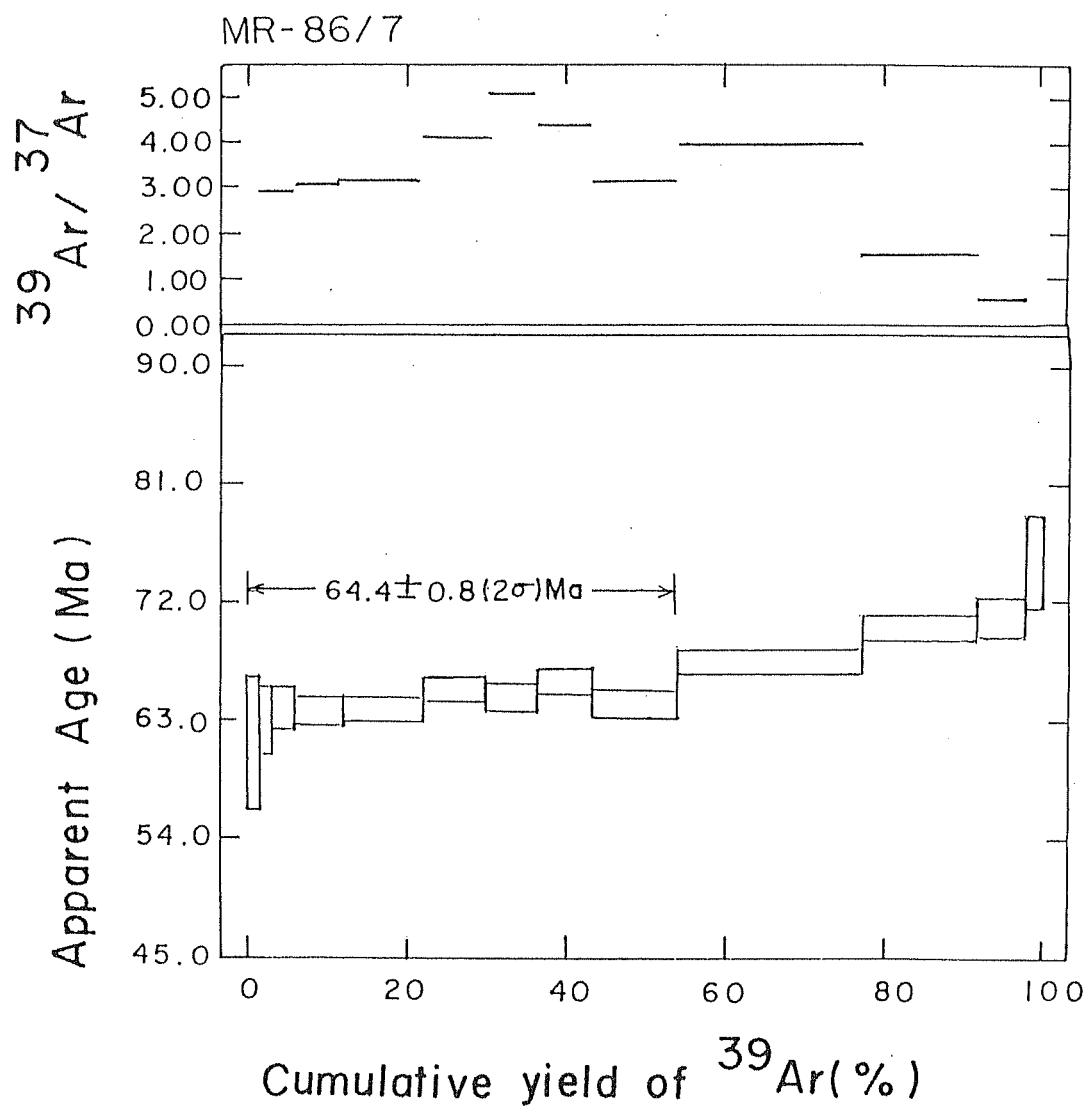


Fig. 4.39. ^{40}Ar - ^{39}Ar Age Spectrum for Mer Syenite (MR 86/7).

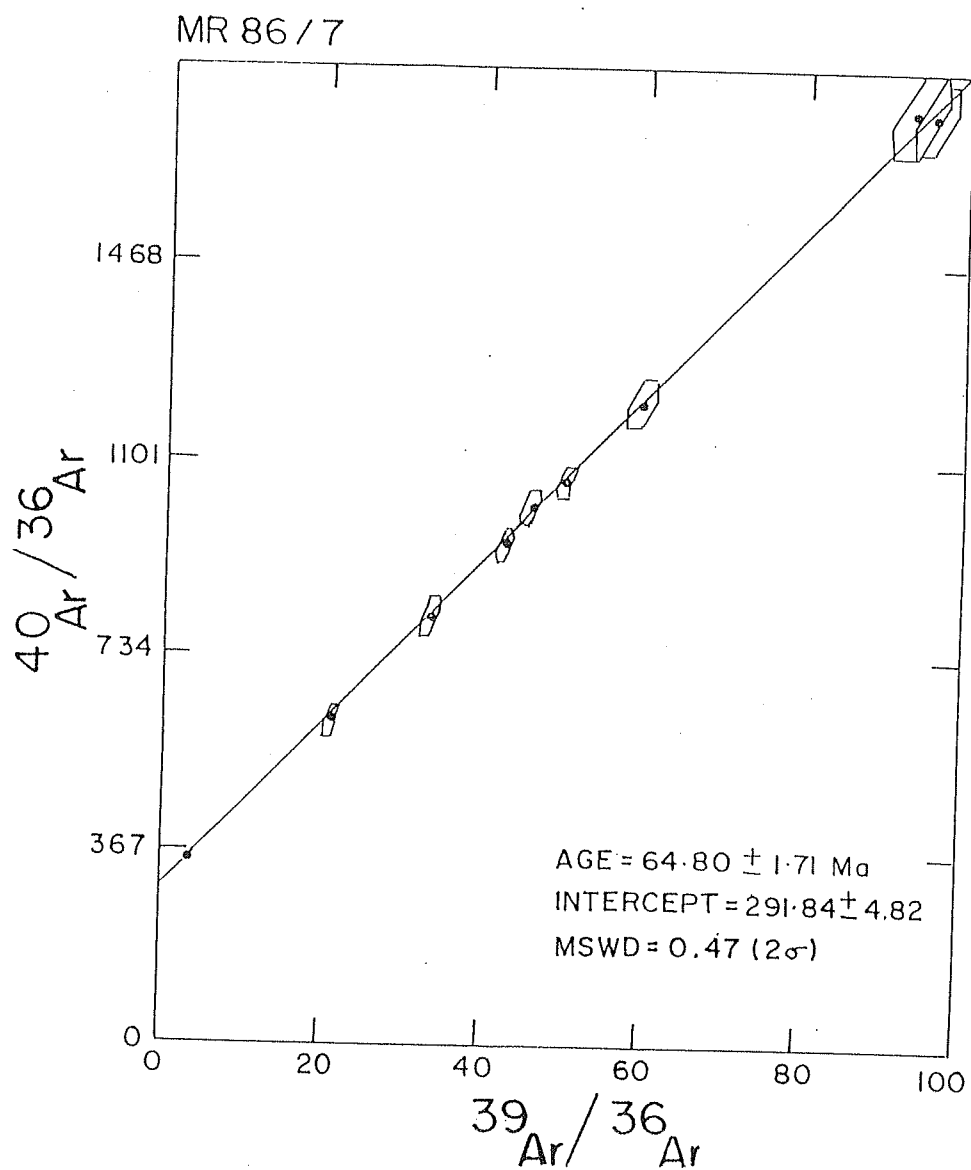


Fig. 4.40. $^{40}\text{Ar}/^{36}\text{Ar}$ vs. $^{39}\text{Ar}/^{36}\text{Ar}$ Isochron Plot for Mer Syenite (MR 86/7).

Table 4.27. Step heating argon isotopic compositions and apparent ages of sample
MR 86/9 (MUNDWARA GABBRO)
 $J=0.00232 \pm 0.00005$

Temp. (°C)	$^{36}\text{Ar}/^{39}\text{Ar}$	$^{37}\text{Ar}/^{39}\text{Ar}$	$^{40}\text{Ar}/^{39}\text{Ar}$	Age (Ma)	^{39}Ar (%)	$^{40}\text{Ar}^*$ (%)
550	1.0236 ± 0.0063	15.9721 ± 0.3865	422.50 ± 2.70	444.0 ± 22.0	1.0	28.0
600	0.4762 0.0055	19.3091 1.9066	254.10 3.20	422.0 22.0	1.0	45.0
650	0.3196 0.0022	15.7261 0.0488	173.00 1.10	302.2 11.0	2.7	45.4
700	0.1653 0.0015	8.0193 0.0243	74.08 0.52	102.7 5.6	4.8	34.0
750	0.0476 0.0007	4.2403 0.0084	37.09 0.28	93.9 3.6	8.2	62.0
800	0.0234 0.0005	2.6636 0.0053	28.94 0.21	90.0 3.0	12.9	76.1
850	0.0177 0.0005	2.7055 0.0054	24.45 0.20	78.8 2.8	13.7	78.6
900	0.0104 0.0006	2.6470 0.1937	20.44 0.16	71.2 2.6	12.8	84.8
950	0.0120 0.0006	3.5217 0.0071	21.68 0.19	74.4 2.8	17.4	83.6
1000	0.0241 0.0007	12.5711 0.0251	32.52 0.27	103.3 3.8	14.2	78.1
1050	0.0824 0.0028	83.3201 0.1666	61.77 0.72	150.3 9.2	4.6	60.6
1200	0.0855 0.0035	115.051 0.2301	73.16 0.93	190.3 11.2	6.2	65.5
TOTAL	0.0591 0.0003	16.7711 0.0391	44.62 0.12	110.3 3.0	100.0	60.8

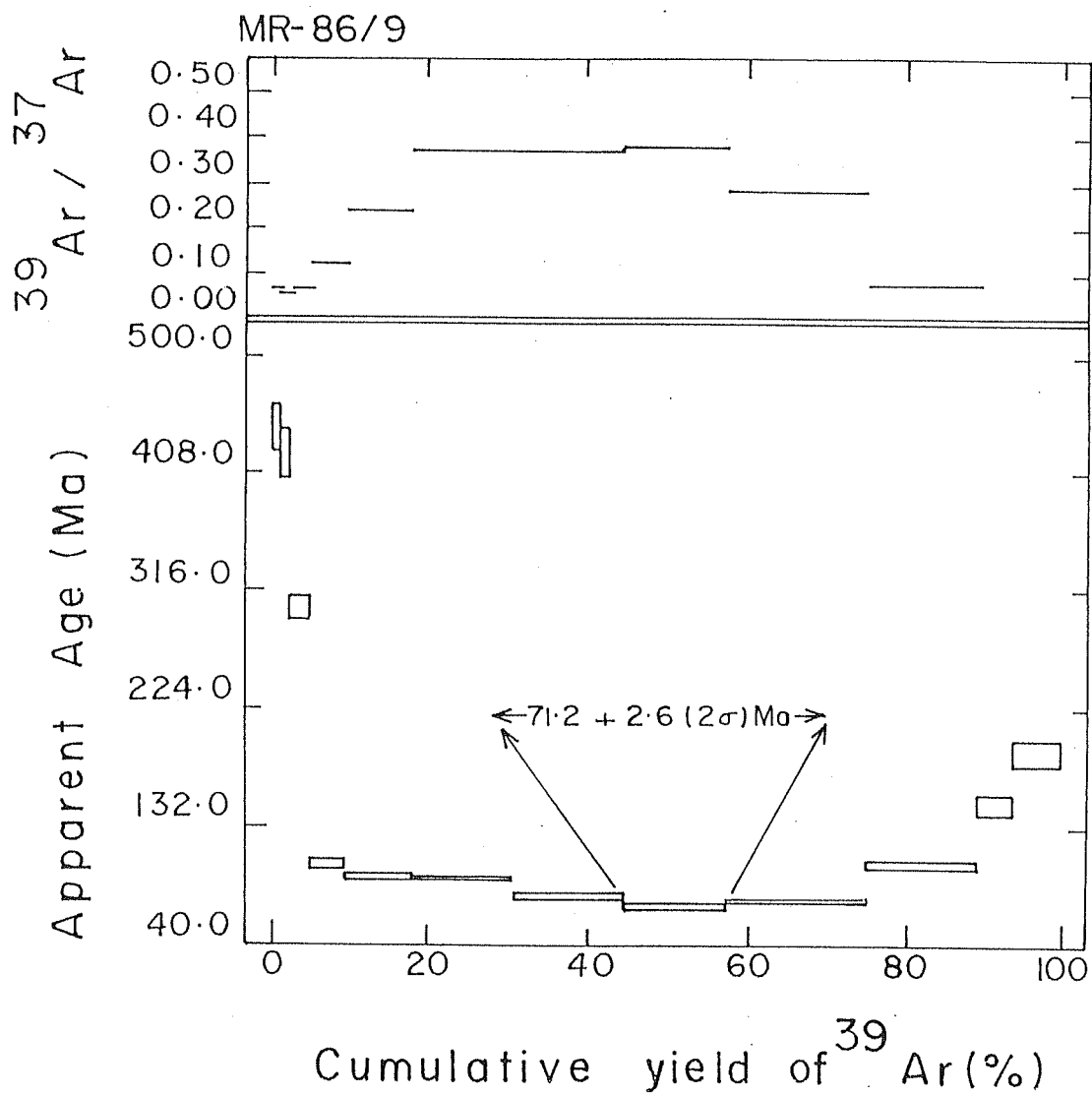


Fig. 4.41. ^{40}Ar - ^{39}Ar Age Spectrum for Toa Gabbro (MR 86/9).

and MR 86/5. The minima of the age spectrum is at 71.2 ± 2.6 Ma (12.8% of total ^{39}Ar release), which again marks the upper limit to the time of formation. However, a $^{40}\text{Ar}/^{36}\text{Ar}$ vs. $^{39}\text{Ar}/^{36}\text{Ar}$ regression analysis of all the data points provide an age of 69.8 ± 2.1 Ma, which could be considered as its formation age.

From the results presented above it is clear that, out of six samples analyzed from the Mundwara complex, only two syenite samples viz. MR 86/4 and MR 86/7 have shown good plateaus, which are concordant at 64 Ma. This suggests that the syenites of Musala as well as Mer hills are contemporary and were emplaced about 64 Ma ago. The remaining samples viz. MR 86/1 (essexite), MR 86/2 (basalt), MR 86/5 (syenite) and MR 86/9 (gabbro) have, however, exhibited saddle shaped spectra with their minima at 74.8 ± 1.0 Ma, 73.9 ± 0.4 Ma, 69.5 ± 0.9 Ma and 71.2 ± 2.6 Ma, respectively.

Subsequent to reporting our results (Rathore and Venkatesan, 1991 and 1993; Venkatesan et al., 1990), Basu et al. (1993) have reported recently a ^{40}Ar - ^{39}Ar weighted mean age of 68.53 ± 0.16 Ma (2σ) for the biotites separated from alkali olivine gabbro of Toa hill of the complex. This confirmed the age obtained by regression analysis of sample MR 86/9. Further, these authors have also reported saddle shaped spectra for two hornblendes separated from melagabbro with their minima at 71 Ma, exactly similar to the minima of 71.2 ± 2.6 Ma obtained for the sample MR 86/9 (gabbro) of our study.

It is to mention here that the regression analysis of total data points of essexite (MR 86/1) has given an age similar to its minima of 74 Ma only. However, based on the above results of gabbro (MR 86/2) as well as that of Basu et al. (1993) it is presumed that the essexite, which is essentially a type of gabbro, is also formed about 70 Ma ago.

As the Mundwara complex exhibits a complete suite of differentiated rocks with the syenites representing the end member of differentiation (Bose and Das Gupta, 1973), therefore, in the light of recent publication of Basu et al. (1993) and the present study it is proposed that the igneous activity at Mundwara commenced about 70 Ma ago. The differentiation continued and the activity seems to have culminated about 64 Ma ago as indicated by the perfect plateaus of syenites from the Musala and Mer hills, suggesting a total span of about 6 Ma for the igneous activity.

4.5.2. Sr ISOTOPIC DATA

Strontium isotopic compositions together with Rb and Sr contents of six whole rock samples are given in Table 4.28. The Rb/Sr ratios in the Mundwara alkali igneous complex show variation from 0.021 to 0.230. The initial $^{87}\text{Sr}/^{86}\text{Sr}$ ratios calculated assuming an age of 64 Ma for the syenites and 69 Ma for the other rock types vary from 0.70384 to 0.70551 (Table 4.28). Similar variations in cogenetic rocks have also been observed from the Tertiary volcanics of South Arabia (Dickinson et al., 1969; Cox et al., 1970). According to these authors, if a fractionated magma freezes with different Rb/Sr ratios at different levels within its chamber and these different levels were later remelted and brought to the surface without mixing, isotopic variations would be observed in a suite of apparently cogenetic rocks, as has been observed at Mundwara.

The Mundwara complex displays initial $^{87}\text{Sr}/^{86}\text{Sr}$ ratios similar to those of the least contaminated Deccan tholeiitic lavas, such as those of the Ambenali, Mahabaleshwar and Panhala Formations of upper sequence (Mahoney, 1988). The average $^{87}\text{Sr}/^{86}\text{Sr}$ value of the complex is 0.70457 which is similar to 0.70484 obtained by Subrahmanyam and Leelanandan (1989) and is slightly less than the average value of 0.7063 for the Girnar complex (Paul et al., 1977).

When the initial $^{87}\text{Sr}/^{86}\text{Sr}$ ratios are plotted against Sr content (Fig. 4.42) they fall in a field of *oceanic island basalts* as defined by Faure and Powell (1972). The mean of initial $^{87}\text{Sr}/^{86}\text{Sr}$ ratio (0.70457) of Mundwara igneous complex lie in the '*source region of basalt*' on the Sr evolution diagram (Fig. 4.31), suggesting upper mantle origin of the magma (Faure and Hurley, 1963).

The mantle source has also been characterized by high $^3\text{He}/^4\text{He}$ ratio of 13.9 and 10.5 times the air ratio (R_A) for the pyroxene separates from two different rocks of the Mundwara complex (Basu et al., 1993). Further, the least differentiated carbonatites of Mundwara have given $\delta^{13}\text{C}$ and $\delta^{18}\text{O}$ values of -6.4 per mil (PDB) and +6.1 per mil (SMOW), respectively, which are also indicative of their mantle source (Sarkar and Bhattacharya, 1992).

Bose (1972, 1980) has suggested plume generated fracture zones responsible for

Table 4.28. Rb-Sr content and Sr isotopic ratios of Mundwara Alkali Igneous Complex.

Sample No.	Rock Type	Rb (ppm)	Sr	K/Rb	Rb/Sr	$^{87}\text{Sr}/^{86}\text{Sr}$ (normalized)	$^{87}\text{Sr}/^{86}\text{Sr}$ (initial)
MR 86/1	Essexite	56	751	425.43	0.075	0.70518	0.70497±0.00012
MR 86/2	Basalt	75	417	244.60	0.179	0.70436	0.70384±0.00014
MR 86/4	Syenite	118	960	434.75	0.132	0.70504	0.70471±0.00012
MR 86/5	Syenite	163	709	232.73	0.230	0.70486	0.70426±0.00014
MR 86/7	Syenite	149	857	403.35	0.174	0.70597	0.70551±0.00013
MR 86/9	Gabbro	16	777	798.97	0.021	0.70415	0.70409±0.00011

Note: Initial $^{87}\text{Sr}/^{86}\text{Sr}$ ratios have been calculated assuming an age of 64±1 Ma for syenites and 70±1.5 Ma for other rock types as indicated by $^{40}\text{Ar}/^{39}\text{Ar}$ studies.

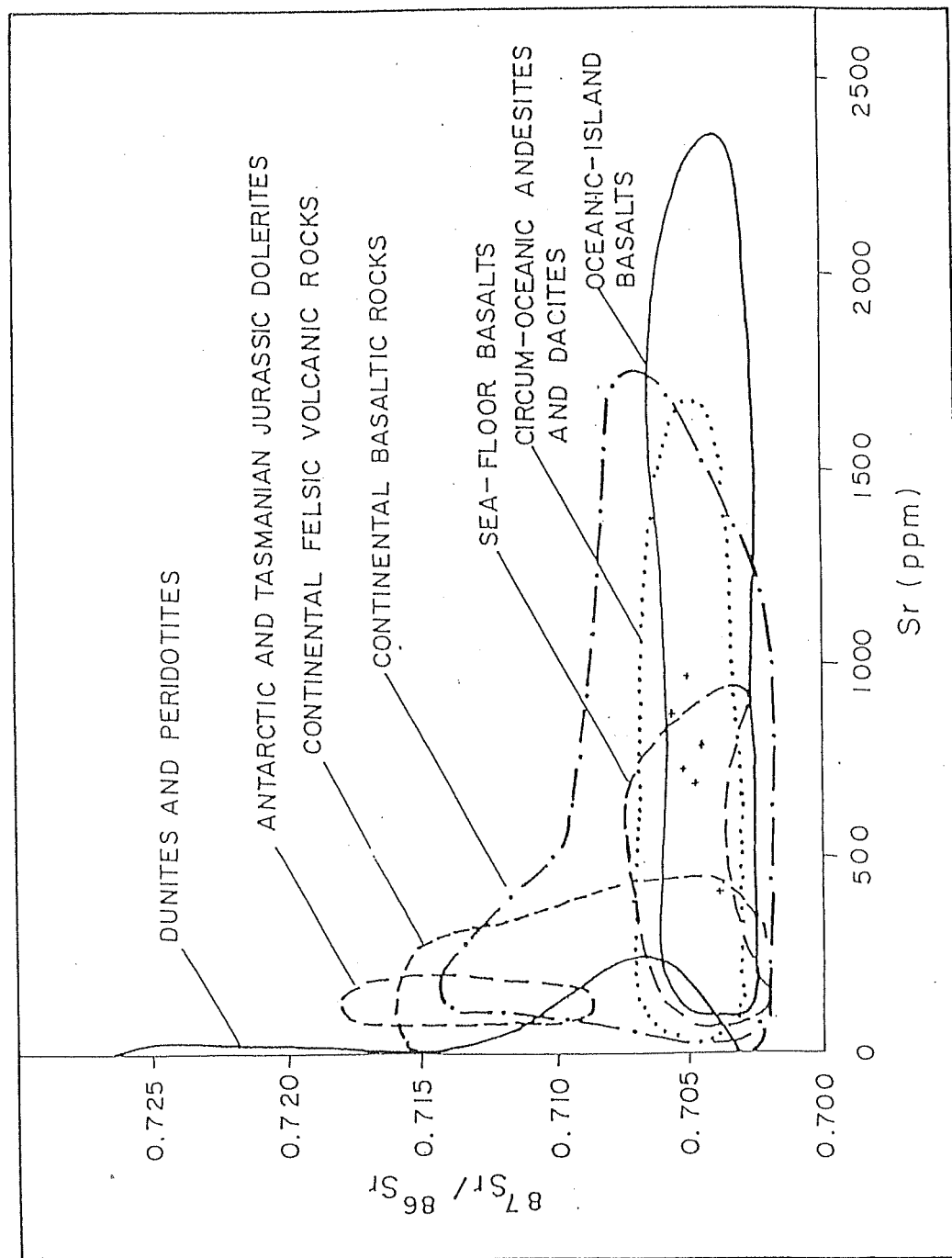


Fig. 4.42. Plot of Initial Sr Ratios Against Sr Content Of Mundwara Alkali Igneous Complex (after Faure and Powell, 1972).

the alkaline magmatism. Srivastava (1983, 1988) has suggested that the alkaline rocks associated with the Deccan volcanic province and those of the southwest Rajasthan belong to a Palaeocene igneous cycle. The reason of this Palaeocene activity was the northward drift of Indian plate which resulted in the reactivation of the ancient lineaments or faults.

Recently Basu et al. (1993) have also postulated a mantle plume origin for the Deccan volcanism and that of Mundwara complex. These authors have envisaged that the alkali magmatism began 3.5 Ma before the main pulse of Deccan volcanism at 65 Ma. They, further, suggested that the spatial-temporal relation between the Mundwara complex and the Deccan flood basalt, centered 600 km to the south, is consistent with northward motion of the Indian plate at 10-15 cm/yr over a nascent Reunion hotspot. Their observation indicates that the Cambay Graben was active 3.5 Ma before the rapid eruption of the bulk of the Deccan traps.

However, the present study indicates that at Mundwara the magmatic activity was not short spanned and instead continued for about 6 Ma from 70 to 64 Ma, which is not in keeping with the model postulated by Basu et al. (1993). Keeping in view the mantle plume theory of Basu et al. (1993) and the present studies, it is proposed that the igneous activity at Mundwara might have been triggered by the mantle plume, which might be responsible for the Deccan volcanism at 67 Ma (Venkatesan et al. 1993), at about 70 Ma ago and then the magma was residing at some depth to give pulsatic magmatic activity, supported by Subrahmanyam and Leelanandam (1989), and the activity seems to have culminated about 64 Ma ago with the emplacement of syenites.

CHAPTER V

SUMMARY AND CONCLUSIONS

The data presented and discussed in this thesis represent the first systematic geochronological effort, using K-Ar, ^{40}Ar - ^{39}Ar and Rb-Sr systematics, on Malani volcanics and associated igneous rocks from southwest Rajasthan, India. The study was undertaken with a view to understand the evolution of Malani igneous province (*MIP*). Also we report for the first time reliable ^{40}Ar - ^{39}Ar age data for the events related to the Deccan volcanism in Rajasthan. This chapter brings out the main findings and discusses the aspects which need further probe.

The present study indicates that the continental crust of this part of Indian sub-continent incorporates a number of volcanic and plutonic associations whose emplacement time spanned from about 780 to 670 Ma. Besides, the region has received wide spread thermal imprint between 500-550 Ma ago. Since then tectonically the region remained undisturbed until the youngest plutonic/volcanic events between 70 to 64 Ma, which emplaced differentiated igneous rocks at Mundwara and Tavidar of Sirohi and Jalore district, respectively.

The initial idea of La Touche (1902), Coulson (1933) and Heron (1953) that the Jalore and Siwana type granites represent the parent stock of the Malani rhyolites and all the different igneous rocks of the province including the basic rocks belong to a single Proterozoic magmatic event at 745 ± 10 Ma, supported in recent years by Pareek (1981), Kochhar (1984) and Bhusan (1984, 1985 and 1989), is belied by the present geochronological studies. This study gives new age determinations to felsic volcanics (Malani volcanics), peraluminous (Jalore) granites, peralkaline (Siwana) granites and rhyolites, mildly alkaline and alkaline rocks from different parts of the volcanic province.

The study clearly proves that the so called Malani igneous suite (i.e. *MIP*) does not represent a single magmatic event and instead represent a polyphase igneous activity.

The felsic volcanics of Gurapratap Singh, Dirí and Manihari belonging to basalt-andesite-dacite-rhyolite association constitute the oldest rock group in the province. These rocks were formed about 779 ± 10 Ma ago with initial $^{87}\text{Sr}/^{86}\text{Sr}$ ratio of 0.70612 ± 0.00046 indicating their crustal origin. The basalts, whose occurrences are confined to a small isolated outcrop, are contemporary to the other associated felsic volcanics but have different source (initial Sr ratio = 0.70385 ± 0.00062) and presumably have come from much deeper level in the mantle.

A few flows of ultrapotassic rhyolites are also found at Dirí, Gurapratap Singh and Manihari alongwith other felsic volcanics. These ultrapotassic rhyolites do not conform to the main trend and presumably mark a different phase of magmatic activity (Srivastava et al., 1989a). The present study shows that these rocks were formed about 681 ± 15 Ma ago with an initial Sr ratio of 0.7135 ± 0.0025 and are, thus, nearly 100 Ma (at least 73 Ma) younger than the associated felsic volcanics, indicating a different magmatic episode. The high initial Sr ratio of these rocks indicates incorporation of radiogenic ^{87}Sr from the country rock into the residual fraction of the magma.

The granites and associated rhyolites (normal as well as peralkaline) constitute most important rock types of the complex. These rocks are mainly exposed around Jalore and Siwana area of the province. The Jalore granite is peraluminous, while the Siwana granite is peralkaline in nature. The peralkaline granites and rhyolites which occur as sub-volcanic ring complex within the *MIP* are very important because of their tectonic significance and mode of occurrence. The ring structure of these rocks has been attributed to cauldron subsidence and vertical intrusion of granites along the periphery of collapse structure (Murthy, 1962). These granites have been considered cogenetic and coeval (ca. 745 ± 10 Ma) to the Malani rhyolites (La Touche, 1902; Coulson, 1933; Heron, 1953, Kochhar, 1984, Bhusan, 1984, 1985 and 1989). However, the present study indicate, that these granites represent two different magmatic events and were emplaced about 727 ± 8 Ma and 698 ± 10 Ma ago, respectively. The initial Sr ratios of these granites are 0.70559 ± 0.00037 and 0.7067 ± 0.0041 respectively, which though indistinguishable, suggest lower crustal derivation of the magma. Further, the Siwana granite and associated peralkaline rhyolites (pantellerites) are coeval and cogenetic.

At the southern extremity of the ring structure around villages Kundal, Mubari, Jimpur, Mangi and Dhiran southwesterly dipping normal rhyolites are exposed which are generally referred to as the outer rhyolites of Siwana (Srivastava et al. 1988 and Yadav, 1988). These rhyolites represent the youngest activity at Siwana at 674 ± 25 Ma with a high initial $^{87}\text{Sr}/^{86}\text{Sr}$ ratio of 0.7110 ± 0.0066 .

However, the age as well as initial Sr ratio of outer rhyolites are remarkably similar to that of the ultrapotassic rhyolites of Manihari, Pali district. The pooled isochron of these rocks give an age of 670 ± 11 Ma with an initial Sr isotopic ratio of 0.7145 ± 0.0021 . This age and initial Sr isotopic ratio are similar to the age and initial ratio obtained for ultrapotassic and outer rhyolites separately.

This exercise indicates that the outer rhyolites and ultrapotassic rhyolites were probably, derived from the same magma and crystallized at about 670 Ma ago. It may, also, be possible that the outer rhyolites are cogenetic with the peralkaline rocks and probably represent the end phase of the peralkaline activity, as suggested by Jacobson et al. (1958) and Bowden and Kinnaird (1978) for the Nigerian younger granitic province. According to these authors the peralkaline magma at the start of the magmatic cycle may turn to metaluminous to peraluminous at the end, giving rise to close association of both the peraluminous and peralkaline rocks within a single ring complex, as observed at Siwana. However, in either of the cases, the high initial Sr ratios of outer as well as ultrapotassic rhyolites are attributed to crustal contamination of the residual magma.

The ^{40}Ar - ^{39}Ar studies of basalt, dacite and rhyolite of Diri and Gurapratap Singh did not yield plateau ages but showed the spectra typical of rocks which have been reheated at about 500- 550 Ma ago subsequent to their formation about 780 Ma ago (Rb-Sr studies). Earlier Rb-Sr mineral ages determined on different granite bodies from Sendra, Sadri, Ranakpur and Sai have, also, indicated thermal event to reset the mineral ages around 500-550 Ma ago, which otherwise have the whole rock pooled Rb-Sr age of 800 ± 50 Ma (Choudhary, 1984). The effect of this thermal event in the rocks exposed further west and southwest of Aravalli range in Rajasthan is clearly brought out by the ^{40}Ar - ^{39}Ar studies of these volcanics.

The thermal event between 500-550 Ma has also been elucidated by the ^{40}Ar - ^{39}Ar studies of Jalore granites which otherwise have the formation age of about 730 Ma.

After the thermal event, about 500-550 Ma ago, this part of Indian sub-continent seems to have remained dormant until about 70 Ma ago when the different plutonic/volcanic events, possibly related to Deccan volcanism, took place in this region. We report for the first time ^{40}Ar - ^{39}Ar age data for the events from Rajasthan which are coeval with the Deccan volcanism (Rathore and Venkatesan, 1991, 1993 and Venkatesan et al., 1990).

Mildly alkaline rocks of Tavidar, Jalore district constitute the younger association of trachy basalt-trachy andesite-trachyte and rhyolite. The K-Ar studies of these rocks gave an indication of younger magmatic event. The detailed ^{40}Ar - ^{39}Ar studies have however helped to construct high resolution chronology of these differentiated rocks. Eight samples were analyzed for ^{40}Ar - ^{39}Ar studies which included two potassic andesites, two trachytes, one rhyolite, one potassic rhyolite and two hawaiites.

All the analyzed samples yielded good plateaus consistent with the fractional crystallization model resulting in the formation of different rock types from the same magma. The earliest differentiated rocks i.e. andesites were formed about 65.9 ± 0.4 Ma ago while the end member of the differentiated sequence i.e. potassic rhyolites were formed about 63.8 ± 0.8 Ma ago, suggesting a total span of about 2 Ma (at least 1 Ma) for the igneous activity (i.e. differentiation) at Tavidar, which resulted in the formation of a cogenetic suite of mildly alkaline rocks of andesite-trachyte-rhyolite-potassic rhyolite.

In addition to the differentiated rocks, two hawaiites were also dated which gave a mean age of 64.4 ± 0.5 Ma, thus, suggesting their contemporaneity with the associated mildly alkaline rocks of Tavidar. Initial Sr ratios of these rocks, calculated assuming an average age of 65 Ma, are indistinguishable, mainly because of large errors associated with the K-rhyolites. However, the mean initial $^{87}\text{Sr}/^{86}\text{Sr}$ ratio of differentiated rocks is 0.70525 which is different from the mean of 0.70441 obtained for the hawaiites, suggests generation of magma at different levels in the upper mantle.

The Mundwara alkali igneous complex is one of the plug like bodies occurring in

the western and northwestern part of the Indian shield from the Deccan volcanic province. The complex exhibits a complete suite of differentiated rocks with the syenites representing the end member of differentiation. Six whole rock samples were analyzed by ^{40}Ar - ^{39}Ar method to constrain the emplacement time of the Mundwara alkali igneous complex. The dated samples include four from Musala hill and one each from Mer and Toa hills of the complex. Out of the six samples analyzed, only two syenites one each from Musala and Mer hills yielded good plateaus which are concordant at 64 Ma. This suggests that these syenites are contemporary and were emplaced about 64 Ma ago. The remaining samples, however, have exhibited saddle shaped spectra owing to the presence of excess argon with their minima ranging from 70 to 74 Ma. These minima mark the upper limit to the time of their formation. However, least square regression analysis of all the data points of a gabbro and a basalt sample, having excess argon signatures, yielded ages of 69.8 ± 2.1 Ma and 69.7 ± 0.8 Ma, respectively, which can be considered as their formation ages.

Recently Basu et al. (1993) have reported laser heating ^{40}Ar - ^{39}Ar weighted mean age of 68.53 ± 0.16 (2σ) Ma for the biotites separated from alkali olivine gabbro of Toa hill of the complex. Further, these authors have also reported saddle shaped spectra for two hornblendes separated from melagabbro of Toa hill with their minima at 71 Ma, exactly similar to the minima of 71.2 ± 2.4 Ma obtained for the gabbro from the same hill in the present study.

In view of the above observations, it is proposed that the igneous activity at Mundwara started around 70 Ma ago. The differentiation continued and the activity seems to have culminated at 64 Ma ago, as indicated by concordant plateaus of syenites from Musala and Mer hills, suggesting a total span of about 6 Ma for the igneous activity. The initial $^{87}\text{Sr}/^{86}\text{Sr}$ ratios, calculated assuming an age of 64 Ma for the syenites and 70 Ma for the other rock types, vary from 0.70384 to 0.70551. The variation in the initial ratios may probably be due to freezing of fractionated magma, with different Rb/Sr ratios, at different levels within its chamber and subsequent remelting and extrusion onto the surface without mixing.

The average initial $^{87}\text{Sr}/^{86}\text{Sr}$ ratio for the Mundwara complex is 0.70457, which lies

in the '*source region of basalt*' on the Sr evolution diagram, suggesting an upper mantle origin of the magma.

The initial Sr isotopic ratios of Tavidar volcanics as well as that of Mundwara complex are similar to those of the least contaminated Deccan tholeiitic lavas, such as those of the Ambenali, Mahabaleshwar and Panhala Formations of the upper sequence (Mahoney, 1988). The genetic relationship between Mundwara, Tavidar and Deccan volcanism cannot be ascertained from Sr isotopic studies alone. However, based on present geochronological studies it can only be construed that these are coeval events.

The main conclusions arrived at based on the present studies are as follows:

- (i) *The Malani igneous province (MIP) of southwest Rajasthan does not represent a single magmatic event as hitherto believed and instead represents a polyphase igneous activity.*
- (ii) *Basalt-andesite-dacite-rhyolite association of Pali district are the oldest one in the Malani province. These rocks were formed about 780 Ma ago from the magma generated in the lower crust. The basalts, though contemporary to other associated felsic volcanics, have different source and presumably have come from much deeper level in the mantle.*
- (iii) *The Jalore and Siwana granites represent two different magmatic events and were emplaced about 730 and 700 Ma ago, respectively. The initial Sr ratios are indistinguishable but indicate derivation of the magma from the lower crust. Further, the Siwana granites and associated peralkaline rhyolites (pantellerites) are coeval and cogenetic.*
- (iv) *The outer rhyolites exposed south of the Siwana ring structure represent the youngest activity at Siwana about 670 Ma ago. These rocks have a very high initial $^{87}\text{Sr}/^{86}\text{Sr}$ ratio of 0.7110 due to incorporation of radiogenic ^{87}Sr in the residual magma.*
- (v) *The ultrapotassic rhyolites exposed at Manihari of Pali district have similarity in the age and initial Sr ratio with those of the outer rhyolites of Siwana, suggesting possible derivation of these rocks from the same residual magma.*
- (vi) *^{40}Ar - ^{39}Ar studies of basalt, dacite and rhyolite from Diri and Gurapratap Singh as well as of Jalore granites have indicated existence of a thermal event around 500-550 Ma ago.*

- (vii) ^{40}Ar - ^{39}Ar studies of mildly alkaline rocks of Tavidar have indicated a span of 2 Ma from 66 to 64 Ma for the differentiated rocks, ranging in composition from andesite to potassic rhyolites. Less voluminous basic rocks (hawaiites) are contemporary to the mildly alkaline rocks but have low initial Sr ratio of 0.70441 as compared to an average of 0.70525 for the latter and indicate derivation of the magmas at different levels in the mantle.
- (viii) At Mundwara, the igneous activity commenced around 70 Ma ago and culminated about 64 Ma ago. The average initial Sr ratio of the complex is 0.70457, suggesting an upper mantle origin of the magma.

It is very important to explore the source of heat which caused wide spread secondary isotopic equilibration in the Malani volcanics as well as granites around 500-550 Ma ago, as revealed by ^{40}Ar - ^{39}Ar studies from the province as well as by mineral Rb-Sr ages from central and southern extremity along the axial zone of Aravalli mountain chain by Choudhary (1984). This thermal imprint does not seem to be a localized event, instead it is probably related to a some large scale tectonic episode.

However, none of the rocks analyzed so far in Rajasthan have yielded primary crystallization time in the range of 500-550 Ma but the formation ages in this time band have been recorded from several granitoid plutons in the north from a long linear belt parallel to the Himalayan strike (Jager et al., 1971; Mehta, 1977; Le Fort et al., 1980, 1981, 1983; Trivedi et al., 1984 and Trivedi, 1990) and in south from southwest coast in Kerala (Nair et al., 1985; Santosh et al., 1989 and Santosh et al., 1994).

The emplacement of these younger granites in south have been correlated with the Pan-African thermo-tectonic episode (Santosh et al., 1994), which has resulted in wide spread crustal accumulation throughout Gondwana land prior to fragmentation and drifting (Kennedy, 1964). The thermal imprint as observed in southwest Rajasthan may also probably be related to the same Pan-African tectonic episode and the magma which caused resetting of Rb-Sr and ^{40}Ar - ^{39}Ar clocks might have crystallized at certain depth to form early Paleozoic granites and might not have been exposed so far in Rajasthan. However, this enunciation needs further probe.

REFERENCES

- Agrawal, V. (1984) Geochemistry of the volcanic rocks around Tavidar, district Jalore, Rajasthan. *Ph.D. thesis, Submitted to University of Rajasthan, Jaipur*, pp. 111.
- Bailey, D. K. (1974) Continental rifting and alkaline magmatism. In H. Sorenson (ed.) 'The alkaline rocks'. John Wiley and Sons, London, pp. 148-159.
- Barberi, F., Borsi, S., Ferrara, G., Marinelli, G. and Varet, J. (1970) Relations between tectonics and magmatology in the northern Danakil Depression (Ethiopia). *Phil. Trans. R. Soc. Lond., A* **267**, 293-311.
- Barth, T. F. W. (1966) Aspects of crystallization of the quartzo-feldspathic plutonic rocks. *Tscheron. Mineral. Petrol. Mitt.*, **11**, 209-222.
- Basu, A. R., Renne, P. R., Das Gupta, D. K., Teichmann, F. and Poreda, R. J. (1993) Early and Late Alkali Igneous Pulses and a High- ^3He Plume Origin for the Deccan Flood Basalts. *Science*, **261**, 902-906.
- Berger, G. W. and York, D. (1981) Geothermometry from $^{40}\text{Ar}/^{39}\text{Ar}$ dating experiment. *Geochem. Cosmochem. Acta.*, **45**, 795-811.
- Bevington, P. R. (1969) *Data reduction and error analysis for the physical sciences*. Mc Graw Hill Co. New York.
- Bhusan, S. K. and Sengupta, R. (1979) The Malani project: Geological Survey of India, Western Region, *Annual programme for 1979-80*, pp. 57-66.
- Bhusan, S. K. and Yagi, K. (1981) Malani volcanism of the Proterozoic in the western Rajasthan, India. *IAVCEI Symp., Tokyo*.
- Bhusan, S. K. (1984) Classification of Malani Igneous Suite. Symposium on Three decades of developments in Petrology, Mineralogy and Petrochemistry in India. *Geol. Surv. Ind., sp. pub.*, **12**, 199-205.
- Bhusan, S. K. (1985) Malani volcanism in western Rajasthan. *Ind. Jour. Earth Sci.*, **12** (1), 58-71.
- Bhusan, S. K. and Mohanty, M. (1988) Mechanics of intrusion and geochemistry

- of alkaline granites from Siwana, Barmer district, Rajasthan. *Ind. Jour. Earth Sci.*, **15** (2), 103- 115.
- Bhusan, S. K. (1989) Mineral chemistry and petrogenetic aspects of Malani volcanics, Western Rajasthan. *Ind. Miner.*, **43** (3 & 4), 325-338.
- Bhusan, S. K. (1991) Granitoids of Malani igneous complex, western Rajasthan, India. *Jour. Earth Sci.*, **18** (3-4), 184-194.
- Blanford, W. T. (1877) Geological notes on the Great Indian Desert between Sind and Rajputana. *Rec. Geol. Surv. India.*, **10**, 10-21.
- Bose, M. K. (1972) Deccan basalts. *Lithos*, **5**, 133-147.
- Bose, M. K. and DasGupta, D. K. (1973) Petrology of the alkali syenites of the Mundwara magmatic suite, Sirohi, Rajasthan. *India. Geol. Mag.*, **110**, 457-466.
- Bose, M. K. (1980) Alkaline magmatism in the Deccan volcanic province. *Jour. Geol. Soc. India*, **21**, 317-329.
- Bowden, P. (1974) Oversaturated alkaline rocks: granites, pantellerites and commendites. In H. Sorenson (ed.) 'The alkaline rocks'. John Wiley and Sons, London, pp. 109- 123.
- Bowden, P. and Kinnaird, J. A. (1978) Younger granites of Nigeria - a zinc rich province. *Trans Section B. Inst. Min. Metall.* **87**, 66-69.
- Brereton, N. R. (1970) Corrections for interfering isotopes in the $^{40}\text{Ar}/^{39}\text{Ar}$ dating method. *Earth Planet Sci. Lett.*, **8**, 427-433.
- Brooks, C., Wendt, I. and Herre, W. (1968) A two-error regression treatment and its application to Rb-Sr and initial $^{87}\text{Sr}/^{86}\text{Sr}$ ratios of younger variscan granitic rocks from the Schwarzwald Massif, South-West Germany. *J. Geophys. Res.*, **73**, 6071.
- Brooks, C, Hart, S. R., and Wendt, I. (1972) Realistic use of two-error regression treatments as applied to Rb-Sr data. *Rev. Geophys. and Space Physics*, **10** (2), 551-577.
- Carmichael, D. M. (1963) Crystallisation of feldspar in volcanic acid liquids. *Q. J. Geol. Soc. London*, **119**, 95- 131.
- Chakraborty, M. K. and Bose, M. K. (1978) Theralite-meltigite-carbonatite

- association in Mer ring of Mundwara suite, Sirohi district, Rajasthan. *Jour. Geol. Soc. India*, **19** (10), 454-463.
- Chakraborty, M. K. (1979) On the alkali syenites of Mundwara suite, Sirohi district, Rajasthan. *Proc. Ind. Nat. Sci. Acad.*, **45**, 284-292.
- Chakraborty, M. K. (1984) Petrology of the Mundwara sub-volcanic suite, Sirohi district, Rajasthan. *Proc. Ind. Nat. Sci. Acad.*
- Chandrasekaran, V. and Srivastava, R. K. (1992) Multivariate Statistical Analysis of Polyphase Igneous Rocks of the Malani Igneous Province with Special Reference to Sarnu Dandali Area, Western Rajasthan. *Jour. Geol. Soc. India*, **40**, 217-233.
- Chayes, F. (1960) On correlation between variables of constant sum. *Jour. Geophys. Res.*, **65**, 4185-4193.
- Choudhary, A. K. (1984) Precambrian geochronology of Rajasthan, Western India. *Ph.D. thesis, PRL, Ahmedabad, Submitted to Gujarat University, Ahmedabad, pp. 182.*
- Choudhary, A. K., Gopalan, K. and Sastry, A. (1984) Present status of the geochronology of the Precambrian rocks of Rajasthan. *Tectonophysics*, **105**, 131-140.
- Coulson, A. L. (1933) The Geology of the Sirohi State, Rajputana. *Mem. Geol. Surv. Ind.* **63** (1), 83-94.
- Cox, K. G., Gass, I. G., Mallick, D. I. J. (1970) The peralkaline volcanic suite of Aden and little Aden, South Arabia. *J. Petrol.*, **11**, 433-462.
- Crawford A. R. and Compston, W. (1970). The age of Vindhyan System of Peninsular India. *Quart. Jour. Geol. Soc., Lond.*, **125** (1), 351-372.
- Crawford, A. R. (1975) Rb-Sr age determinations for the Mount Abu granite and related rocks of Gujarat. *Jour. Geol. Soc. India*, **16**, 20-28.
- Dalrymple, G. B. and Lanphere, M. A. (1971) $^{40}\text{Ar}/^{39}\text{Ar}$ technique of K-Ar dating: A comparison with the conventional technique. *Earth Planet. Sci. Lett.*, **12**, 300-308.
- Dalrymple, G. B., Alexander, E. C. Jr., Lanphere, M. A. and Kraker, G. P. (1981) Irradiation of samples for $^{40}\text{Ar}/^{39}\text{Ar}$ dating using the Geological Survey TRIGA

reactor. *U. S. Geol. Surv., Prof. Paper*, **1176**.

- Das Gupta, D. K. (1974) Mundwara alkalic suite and Deccan volcanicity. *Bull. Indian Geol. Assoc.*, **7**, 137-144.
- Das Gupta, D. K. (1975) On the alkaline gabbroic rocks and syenites from Musala hill, Mer Mundwara, Sirohi district, Rajasthan. *Quart. Jour. Geol. Min. Met. Soc. India*, **47**, 117-124.
- Dasgupta S. K. and Chandra M. (1978) Tectonic element of West Rajasthan shelf and their stratigraphy. *Quart. Jour. Geol. Min. Met. Soc. India*, **50**, 1-16.
- Dashora, R. S. (1981) Geological investigation of Karara fluorspar deposits, district Jalore, Rajasthan. *Ph.D. thesis, Submitted to University of Rajasthan, Jaipur*. pp. **111**.
- Davis, J. C. (1973) *Statistics and data analysis in Geology*. John Wiley and Sons, New York, pp. **550**.
- Dickinson, D. R., Dodson, M. H., Gass, I. G., and Rex, D. C. (1969) Correlation of initial $^{87}\text{Sr}/^{86}\text{Sr}$ with Rb/Sr in some late Tertiary volcanic rocks of south Arabia. *Earth Planet. Sci. Lett.*, **6**, 84-80.
- Faure, G. and Hurley, P. M. (1963) The isotopic composition of strontium in oceanic and continental basalt: Application to the origin of igneous rocks. *J. Petrol.*, **4**, 31-50.
- Faure, G. and Powell, J. C. (1972) In '*Strontium Isotope Geology*', Springer - Verlag, Berlin, pp. **28-42**.
- Frank, E. and Stettler, A. (1979) K-Ar and ^{39}Ar - ^{40}Ar systematics of white K-mica from an Alpine metamorphic profile in the Swiss Alps. *Schweiz Mineral. Petrog. Mitt.*, **59**, 375- 394.
- Gast, P. W. (1968) Trace element fractionation and origin of tholeiitic and alkaline magma types. *Geochim. Cosmochim. Acta*, **32**, 1059-1086.
- Gaur, C. M. (1984) Geochemistry of acid volcanics of Manihari, Pali district, Rajasthan. *Ph.D. thesis, Submitted to University of Rajasthan, Jaipur*, pp. **111**.
- Gillespie, A. R., Huneke, J. C., and Wasserburg, G. J. (1982) An assessment of ^{40}Ar - ^{39}Ar dating of incompletely degassed xenoliths. *J. Geophys. Res.*, **87**, 9247-9257.

- Gopalan, K., Macdougall, J. D., Roy, A. B. and Murali, A. V. (1990) Sm-Nd evidence for 3.3 Ga old rocks in Rajasthan, northwestern India. *Precambrian Research*, **48**, 287-297.
- Greenburg, J. K. (1981) Characteristics and origin of Egyptian younger granites. *Summ. Bull. Geol. Soc. Amer.*, **92** (1), 63-67.
- Hanson, G. N., Simmons, K. R. and Bence, A. E. (1975) $^{40}\text{Ar}/^{39}\text{Ar}$ spectrum ages for biotite, hornblende and muscovite in a contact metamorphic zone. *Geochim. Cosmochim. Acta.*, **39**, 1269-1297.
- Harrison, T. M. and Mc Dougall, I. (1981) Excess ^{40}Ar in metamorphic rocks from Broken Hill, New south Wales: Implications for $^{40}\text{Ar}/^{39}\text{Ar}$ age spectra and the thermal history of the region. *Earth Planet. Sci. Lett.*, **55**, 123-149.
- Heier, S. and Adams, J. A. S. (1964) The geochemistry of the alkali metals. *Phys. Chem. Earth*, **5**, 255-380.
- Heron, A. M. (1917) The Geology of North - Eastern Rajputana and Adjacent Districts. *Mem. Geol. Surv. India*, **41**, Pt. I.
- Heron, A. M. (1953) The Geology of Central Rajputana. *Mem. Geol. Surv. India*, **79**, 1-339.
- Jacobson, S., Macleod, W. N. and Black, R. (1958) Ring complexes in the younger granite province of northern Nigeria. *Geol. Soc. London. Mem.* **1**, 72.
- Jager, E., Bhandari, A. K., and Bhanot, V. B. (1971) Rb-Sr age determinations on biotites and W. R. samples from the Mandi and Chor granites, Himachal Pradesh, India. *Eclogae Geol. Helv.*, **64** (3), 521-527.
- Kaneoka I. (1974) Investigation of excess argon in ultramafic rocks from the Kola Peninsula by the $^{40}\text{Ar}/^{39}\text{Ar}$ method. *Earth Planet. Sci. Lett.*, **22**.
- Kennedy, W. Q. (1964) *Univ. Leeds, Inst. African. Geology, 8th Report*, 48-49.
- Kochhar, N. (1984) Malani igneous suite: Hot spot magmatism and cratonization of the northern parts of the Indian shield. *Jour. Geol. Soc. India*, **25** (2), 155-161.
- Kochhar, N., Pande, K., and Gopalan, K. (1985) Rb-Sr age of the Tosham ring complex, Bhiwani, India. *Jour. Geol. Soc. India*, **26**, 216-218.

- Kochhar, N. (1989) High heat producing granites of the Malani igneous suite, northern peninsular India. *Ind. Minerals*, **43**, 339-346.
- Lanphere, M. A., Wasserburg, G. J., Albee, A. L. and Tilton, G. R. (1964) Redistribution of Sr and Rb isotopes during metamorphism, World Beater Complex, Panamint Range, California. *Isotopic and Cosmic Chemistry, North Holland Publishing Company, Amsterdam*.
- Lanphere, M. A. and Dalrymple, G. B. (1971) A test of the $^{40}\text{Ar}/^{39}\text{Ar}$ age spectrum technique on some terrestrial materials. *Earth Planet. Sci. Lett.*, **12**, 359-372.
- Lanphere, M. A. and Dalrymple, G. B. (1976) Identification of excess ^{40}Ar by the $^{40}\text{Ar}/^{39}\text{Ar}$ age spectrum technique. *Earth Planet. Sci. Lett.*, **32**, 141-148.
- Lanphere, M. A. and Dalrymple, G. B. (1977) Reply to comment by E. K. Jessberger. *Earth Planet. Sci. Lett.*, **37**, 169-172.
- La Touche, T. D. (1902) Geology of Western Rajputana. *Mem. Geol. Surv. India*, **35**, 1-16.
- Le Bas, M. J. (1971) Peralkaline volcanism, crustal swelling and rifting. *Nature*, **230**, 85-86.
- Le Bas, M. J. and Srivastava, R. K. (1989) The mineralogy and geochemistry of the Mundwara carbonatite dykes, Sirohi district, Rajasthan, India. *N. Jb. Miner. Abh.*, **160**.
- Le Fort, P., Debon, F. and Sonet, J. (1980) The lesser Himalayan Cordierite granite belt. Typology and age of the Pluton Manserah, Pakistan. *Proc. Int. Commit. Geodynamics. Corp. 6. Mfg. Peshawar Nov. 23-29, 1979. Spl. Issue Geol. Bull. Univ. Peshawar*.
- Le Fort, P., Debon, F. and Sonet, J. (1981) Lower Palaeozoic emplacement for granites and granitic gneisses of the Kathamandu Nappe (Central Nepal). *Terra Cognita, Spl. issue*, **30**, 72.
- Le Fort, P., Debon, F. and Sonet, J. (1983) The lower Palaeozoic lesser Himalayan granitic belt: emphasis on the Simchar Pluton of central Nepal granites of Himalayas, Karakorum and Hindu Kush. (ed) Sham, F. A., *Institute*

of *Geology, Punjab Univ., Lahore, Pakistan*, 235-255.

Le Maitre, R. W. (1968) Chemical variation within and between volcanic rock series - a statistical approach. *J. Petrol.*, **9**, 220-252.

Le Maitre, R. W. (1982) *Numerical Petrology*. Elsevier Sci. Pub. Co., Amsterdam, pp. 281.

Maheshwari, A. (1983) Geochemistry of volcanic rocks of Gura pratap Singh and Diri, Pali District, Rajasthan, India. *Ph.D. thesis, Submitted to University Of Rajasthan, Jaipur*, pp. 99.

Mc Intyre, G. A., Brooks, C., Compston, W. and Turek, A. (1966) The statistical assessment of Rb-Sr isochrons. *J. Geophys. Res.*, **71**, 5459-5468.

Mahoney, J. J. (1988) Deccan Traps. In '*Continental Flood Basalts*, J. D. Macdougall (ed.)', Kluwer Academic Publishers, Dordrecht, Netherlands, 151-194.

Mehta, P. K. (1977) Rb-Sr geochronology of the Kulu Mandi Belt - its implications for the Himalayan tectogenesis. *Rund schau*, **66**, 156-175.

Merrill, C. and Turner, G. (1966) Potassium-argon dating by activation with fast neutrons. *J. Geophys. Res.*, **71**, 2852-2857.

Mitchell, J. G. (1968) The $\text{argon}^{40}/\text{argon}^{39}$ method for potassium-argon age determination. *Geochim. Cosmochim. Acta.*, **32**, 781-790.

Mohr, P. A. (1970) Volcanic composition in relation to tectonics in the Ethiopian rift system: a preliminary investigation. *Bull. Volcan.*, **34**, 141-157.

Mukherjee, A. B. (1958) Structure of Malani Rhyolite and a part of the Siwana Granite around Siwana, Western Rajasthan. *Quart. J. Geol. Min. Met. Soc. Ind.*, **30**, 158-161.

Murthy, M. V. N. (1962) The significance of the ring pattern of Siwana granite bosses in Western Rajasthan. *Ind. Minerals*, **16** (2), 297-298.

Murthy, V. R. and Compston, W. (1965) Rb-Sr ages of chondrules and carbonaceous chondrites. *J. Geophys. Res.*, **70**, 5297.

Nair, N. G. K., Soman, K., Santosh, M., Arkelyants, M. H. and Golubyev, V. N. (1985) K-Ar ages of three granite plutons from north Kerala. *Jour. Geol., Soc.*

India, 26, 674-676.

- Narayan Das, G. R., Bagchi, A. K., Chaub, D. N., Sharma C. V. and Navaneethan, K. V. (1978) Rare metal content, geology and tectonic setting of the alkaline complexes across the Trans-Aravalli region, Rajasthan. *Recent Researches in Geology*. 7, Hindustan Publishing Corpn.,
- Nicolaysen, L. O. (1961) Graphic interpretation of discordant age measurements of metamorphic rocks. *N. Y. Acad. Sci.*, **91**, 198-206.
- Pande, K., Venkatesan, T. R., Gopalan, K., Krishnamurthy, P. and Macdougall, J. D. (1988) ^{40}Ar - ^{39}Ar Ages of Alkali Basalts from Kutch, Deccan Volcanic Province, India. *Mem. Geol. Soc. India*, **10**, 145-150.
- Pankhurst, R. J., Moorbath, S., Rex, D. C. and Turner, G. (1973) Mineral age patterns in Ca. 3700 my old rocks from West Greenland. *Earth Planet. Sci. Lett.*, **20**, 157-170.
- Papanastassiou, A. and Wasserburg, G. J. (1971) Lunar chronology and evolution from Rb-Sr studies of Appolo 11 and 12 samples. *Earth Planet. Sci. Lett.*, **11**, 37-62.
- Pareek, H. S. (1981) Petrochemistry and Petrogenesis of the Malani Igneous Suite, India. *Geol. Soc. Amer. Bull.*, **92** (2), 206-273.
- Pareek, H. S. (1986) Petrography and Geochemistry of Tosham hill felsic volcanics, Haryana. *Jour. Geol. Soc. India*, **27**, 254-262.
- Pascoe, E. H. (1960) A manual of geology of India and Burma. *Manager of Publication Govt. of India, New Delhi*, pp. 480-482.
- Paul, D. K., Potts, P. J., Rex, D. C. and Beckinsale, R.D.(1977) Geochemical and petrogenetic study of the Girnar igneous complex, Deccan volcanic province, India. *Bull. Geol. Soc. America*, **88**, 227-234.
- Phillips, D. and Onstott, T. C. (1986) Application of $^{36}\text{Ar}/^{40}\text{Ar}$ versus $^{39}\text{Ar}/^{40}\text{Ar}$ correlation diagram to the $^{40}\text{Ar}/^{39}\text{Ar}$ spectra of phlogopites from southern African Kimberlites. *Geophys. Res. Lett.*, **13**, 689-692.
- Provost, A. (1990) An improved diagram for isochron data. *Chem. Geol. (I. Geosci. Sect.)*, **80**, 85-99.

- Ranawat, P. S. and Dashora, R. S. (1984) Geology of Karara volcanic vent, Rajasthan. *Jour. Geol. Soc. India*, **25** (11), 728-734.
- Rathore, S. S. and Venkatesan, T. R. (1991) ^{40}Ar - ^{39}Ar age of essexite from Mundwara alkaline complex, Rajasthan. In *5th Natio. Symp. Mass Spectro.*, PRL, Ahmedabad, **EPS-11**.
- Rathore, S. S. and Venkatesan, T. R. (1993) ^{40}Ar - ^{39}Ar age of syenites from Mundwara alkali igneous complex, Rajasthan, India. In *6th Natio. Symp. Mass Spectro.*, IIP, Dehradun, **420-422**.
- Roddick, J. C., Cliff, R. A., and Rex, D. C. (1980) The evolution of excess argon in alpine biotites - A ^{40}Ar - ^{39}Ar analysis. *Earth Planet. Sci. Lett.*, **48**, 185-208.
- Samson, S. D. and Alexander, E. C. Jr. (1987) Calibration of the interlaboratory ^{40}Ar - ^{39}Ar dating standard MMhb1-1. *Chem. Geol. (I. Geosci. Sect.)*, **66**, 27-34.
- Santosh, M., Iyer, S. S., Vasconcellos, M. B. A. and Enzweiler, J. (1989) Late Precambrian alkaline plutons in south west India: geochronologic and rare-earth element constraints on Pan-African magmatism. *Lithos*, **24**, 65-79.
- Santosh, M., Suzuki, K. and Masuda, A. (1994) Re-Os dating of molybdenite from southern India: Implication for Pan-African metallogeny. *Jour. Geol. Soc. India*, **43**, 585-590.
- Sarkar, A. and Bhattacharya, S. K. (1992) Carbonates from Rajasthan indicate mantle carbon-and-oxygen-isotopic composition. *Curr. Sci.*, **62**, 368-370.
- Schairer, J. F. and Yoder, H. S. Jr. (1961) Crystallization in the system nepheline-forsterite-silica at 1 atm. *Yb Carnegie Instn. Washington*, **60**, pp. 141.
- Schimizu, N. (1964) An experimental study of the partitioning of K, Rb, Sr, Cs and Ba between clinopyroxenes and liquids at high pressures. *Geochim. Cosmochim. Acta*, **38**, 1789-1798.
- Seidemann, D. E. (1976) An $^{40}\text{Ar}/^{39}\text{Ar}$ age spectrum for a cordierite-bearing rock: isolating the effects of excess radiogenic ^{40}Ar . *Earth Planet. Sci. Lett.*, **33**, 268.
- Sharma, T. R. (1967) Petrochemistry of the Mundwara igneous complex, Sirohi, district, Rajasthan. *Jour. Indian Geosci. Assn.*, **7**, 35-45.

- Sharma, T. R. (1969) Magmatic differentiation in the Mundwara igneous complex, Sirohi district, Rajasthan. *Jour. Indian Geosci. Assn.*, **11**, 79-84.
- Sinha Roy, S. (1984) Precambrian crustal interaction in Rajasthan, NW India. *Indian Jour. Earth Sci., CEISM Seminal Volume*, 84-91.
- Srivastava, R. K. (1983) Temporal status of alkaline rocks of Deccan volcanic province and S. W. Rajasthan. *Geol. Mag.*, **120** (3), 303-304.
- Srivastava, R. K. (1988) Magmatism in the Aravalli Mountain Range and its Environs. *Mem. Geol. Soc. India*, **7**, 77-93.
- Srivastava, R. K., Yadav, A., Ashiya, I. D. and Chawde, M. P. (1988) Geochemistry of the peralkaline silicic rocks from the Malani volcanic province, Rajasthan, India. *IGCP 217 Workshop on Proterozoic rocks of India, Calcutta*, 106-107.
- Srivastava, R. K., Agrawal, V., Ashiya, I. D., Chandrasekaran, M. P., Gaur, C. P., Maheshwari, A. and Yadav, A., (1988) Temporal status and chemical variability of the rocks of the Malani volcanic province of south western Rajasthan. In *Natio. Symp. Applica. Geochem.*, Shivaji University, Kolhapur, **pp. 101**.
- Srivastava, R. K. (1989) Alkaline and peralkaline rocks of Rajasthan. *Mem. Geol. Soc. India*, **15**, 3-24.
- Srivastava, R. K., Maheshwari, A. and Upadhyaya, R. (1989a) Geochemistry of Felsic Volcanics from Gurapratap Singh and Dir, Pali District, Rajasthan (Part-I, Major Elements). *Jour. Geol. Soc. India*, **34**, 467-486.
- Srivastava, R. K., Maheshwari, A. and Upadhaya, R. (1989b) Geochemistry of Felsic Volcanics from Gurapratap Singh and Dir, Pali District, Rajasthan (Part-II, Trace Elements). *Jour. Geol. Soc. India*, **34**, 617-631.
- Steiger, R. H. and Jager, E. (1977) Subcommittee on geochronology : convention on the use of decay constants in Geo-and-Cosmochronology. *Earth Planet. Sci. Lett.*, **36**, 359-362.
- Stettler, A. and Bochsler, P. (1979) He, Ne and Ar composition in a neutron activated sea-floor basalt glass. *Geochim. Cosmochim. Acta*, **43**, 157-169.
- Stoennner, R. W., Schaeffer, O. A. and Katcoff, S. (1965) Half-lives of argon-37, argon-39 and argon-42. *Science*, **148**, 1325-1328.

- Subrahmanyam, N. P. and Rao, G. V. U. (1972) Age of the Mundwara igneous complex, Rajasthan. *Current Science*, **41**, 388-391.
- Subrahmanyam, N. P. (1986) Petrology and geochemistry of the Mundwara alkali igneous complex, Rajasthan. *Ph.D. thesis, Submitted to Osmania University, Hyderabad*.
- Subrahmanyam, N. P. and Leelanandam, C. (1989) Differentiation due to probable initial immiscibility in the Musala pluton of the Mundwara alkali igneous complex, Rajasthan, India. *Mem. Geol. Soc. India*, **15**, 25-46.
- Subrahmanyam, N. P. and Leelanandam, C. (1991) Geochemistry and petrology of the cumulophyric layered suite of rocks from the Toa pluton of the Mundwara alkali igneous complex, Rajasthan. *Jour. Geol. Soc. India*, **38**, 397-411.
- Tazieff, H., Marinelli, G., Barberi, F. and Varet, J. (1969) Geologie de l'Afar Septentrional. Premiere expedition du CNRS-France et du CNR-Italie (Decembre 67 - Fevrier 68). *Bull. Volcan.*, **33**, 1039-72.
- Tetley, N., Mc Dougall, I. and Heydegger, M. R. (1980) Thermal neutron interferences in the $^{40}\text{Ar}/^{39}\text{Ar}$ dating technique. *J. Geophys. Res.*, **85** (1312), 7201-7205.
- Till, R. and Colley, H. (1973) Thoughts on the use of principal component analysis in petrogenetic problems. *J. Int. Assoc. Math. Geol.*, **5**, 341-350.
- Trivedi, J. R., Gopalan, K. and Valdiya, K. S. (1984) Rb-Sr ages of granitic rocks within the lesser Himalayan nappes, Kumaon, India. *Jour. Geol. Soc. India*, **25** (10), 451-464.
- Trivedi, J. R. (1990) Geochronological studies of Himalayan Granitoids. Ph.D. thesis, PRL, Ahmedabad, Submitted to Gujarat University, Ahmedabad, pp.170.
- Turner, G. (1968) The distribution of potassium and argon in chondrites: In 'L. H. Ahrens (eds.), *Origin and Distribution of the Elements*. Pergamon, Oxford, pp. 387-398.
- Turner, G. (1971) Argon-40-argon-39 dating: The optimization of irradiation parameters. *Earth Planet. Sci. Lett.*, **10**, 227-234.

- Tuttle, O. F., Bowen, N. L. (1958) Origin of granite in the light of experimental studies in the system $\text{NaAlSi}_3\text{O}_8\text{-SiO}_2\text{-H}_2\text{O}$. *Mem. Geol. Soc. Amer.*, 74-153.
- Upadhyaya, R. and Srivastava, R. K. (1987) Clustering as an aid to evaluation of mode of genesis of the multiple intrusive body at Mundwara, Rajasthan. *Indian Jour. Geol.*, **59**, 117-125.
- Upadhyaya, R., Srivastava, R. K. and Agrawal, V. (1988). A statistical approach to the study of an igneous suite - a case history of Tavidar volcanics. *N. Jb. Miner. Abh.*, **159**, 311-324.
- Venkataraman, P. K., Sensharma, R. N. and Xavier, J. (1964) Petrology of some peralkaline granites of Barmer district, Rajasthan. *Geol. Surv. Ind. Misc.*, **8**, 57-72.
- Venkatesan, T. R., Pande, K. and Gopalan, K. (1986) $^{40}\text{Ar}\text{-}^{39}\text{Ar}$ Dating of Deccan Basalts. *Jour. Geol. Soc. India*, **27** (1), 102-109.
- Venkatesan, T. R., Rathore, S. S. and Srivastava, R. K. (1990) Ar-Ar studies of Malani Complex in Rajasthan, India: Evidences for different magmatic episodes. *Jour. Geol. Soc. Australia*, **27**, 106.
- Venkatesan, T. R., Pande, K. and Gopalan, K. (1993) Did Deccan volcanism pre-date the Cretaceous/Tertiary transition ?. *Earth Planet. Sci. Lett.*, **119**, 181-189.
- Vincent, P. M. (1970) The evolution of the Tibesti volcanic province, eastern Sahara. In 'African Magmatism and Tectonics (T. N. Clifford and I. G. Gass. eds.), Oliver and Boyd, Edinburgh', pp. 301-319.
- Widenbeck, M. and Goswami, J. N. (1994) High precision $^{207}\text{Pb}/^{206}\text{Pb}$ zircon geochronology using a small ion microprobe. *Geochim. Cosmochim. Acta* (in press).
- Wijbrans, J. R. (1985) Geochronology of metamorphic terrains by the $^{40}\text{Ar}/^{39}\text{Ar}$ age spectrum method. *Ph.D. Diss, Australian National University, Canberra*.
- Williamson, J. H. (1968) Least square fitting of a straight line. *Can. Jour. Phys.*, **46**, 1845-1847.
- Yadav, A. (1988) Geochemistry of Siwana granites and associated Rhyolites. *Ph.D. thesis, Submitted to University of Rajasthan, Jaipur*, pp. 114.
- Yadav, H. (1991) Geochemistry of the Jalore granites and associated Rhyolites.

- Ph.D. thesis, Submitted to University of Rajasthan, Jaipur, pp. 147.
- Yadava, B. R. and Karkare, S. G. (1976) Geochemistry of Mundwara igneous complex, District Sirohi, Rajasthan, India. *The Journal of Scientific Research, Banares Hindu University*, 26, 1-105.
- York, D. (1966) Least square fitting of a straight line. *Can. Jour. Phys.*, 44, 1079.
- York, D. (1969) Least square fitting of a straight line with correlated errors. *Earth Planet. Sci. Lett.*, 5, 320-324.
- Zeitler, P. K. (1987) Argon diffusion in partially degassed alkaline feldspar: Insights from $^{40}\text{Ar}/^{39}\text{Ar}$ analysis. *Chem. Geol. (I. Geosci. Sect.)*, 65, 167-181.